Vascular function prior to the development of overt atherosclerosis

A thesis submitted to the University of Manchester for the degree of Doctor of Philosophy in the Faculty of Medical and Human Sciences

Christopher John Cobb

School of Medicine
University of Manchester

2013

Contents

Final word count (inc. figure legends): 39,183

List of Figures

List of Tables

List of abbreviations

α-SMA	alpha smooth muscle actin
$ApoE^{-/-}$	apolipoprotein-E knockout
BK_{Ca}	large-conductance calcium-activated potassium channel
$[Ca^{2+}]_i$	intracellular calcium concentration
CAD	coronary artery disease
CaM	calmodulin
CaM_{Ca2+}	calcium bound calmodulin
CaMKII	calcium/calmodulin-dependent kinase isoform II
CCD	charge-coupled device
CICR	calcium induced calcium release
CVD	cardiovascular disease
DAB	3,3'-diaminobenzedine
DAG	diacylglycerol
DAPI	4',6-diamidino-2-phenylindole
DMSO	dimethylsulphoxide
ECM	extracellular matrix
F_{405}	405nm emitted fluorescence
F_{500}	500nm emitted fluorescence
FITC	fluorescein isothiocyanate
FOV	field of view
GPCR	g-protein coupled receptor
H&E	haematoxylin & eosin
HDL	high density lipoprotein
IHC	immunohistochemistry
IP_3	inositol 1,4,5-trisphosphate
IP_3R	inositol 1,4,5-trisphosphate receptor
LDL	low density lipoprotein
$LDLR^{-/-}$	low density lipoprotein receptor knockout
MLC	myosin light chain
MLCK	myosin light chain kinase
NCX	sodium-calcium exchanger
oxLDL	oxidised low density lipoprotein
PCNA	proliferating cell nuclear antigen
PFA	paraformaldehyde
PIP_2	phosphatidylinositol 4,5-bisphosphate
PKC	protein kinase C
PLC	phospholipase C
PMCA	plasma-membrane calcium ATPase
PMT	photomultiplier tube
PSS	physiological salt solution
ROC	receptor-operated calcium channel

RyR	ryanodine receptor
SERCA	sarco-/endoplasmic reticular ATPase
SMC	smooth muscle cell
smMHCII	smooth muscle myosin heavy chain isoform II
SOCE	store-operated calcium entry
SR	sarcoplasmic reticulum
STIM1	stromal interacting molecule 1
STOC	spontaneous transient outward current
TRP	transient receptor potential
TRPC	transient receptor potential canonical
VLDL	very-low density lipoprotein
VSMC	vascular smooth muscle cell
WT	wild-type

Abstract

Christopher John Cobb
University of Manchester
Doctor of Philosophy
Vascular function prior to the development of overt atherosclerosis
September 2013

The formation of atherosclerotic plaques is linked to a change in vascular function, with evidence of endothelial dysfunction and the proliferation of the underlying vascular smooth muscle cells (VSMCs). Prior to plaque development, risk factors are present that are capable of altering vascular function and promoting disease progression. These risk factors include hypercholesterolaemia, obesity and inflammation. The specific mechanisms of these risk factors in the early stages of atherosclerotic disease development have yet to be fully explored and are likely to be closely interwoven. The aim of this thesis was to assess the effects of these atherosclerotic risk factors, with a primary focus on the direct action of hypercholesterolaemia, on vascular function prior to the development of overt atherosclerosis.

After acute *ex vivo* cholesterol depletion and enrichment, a range of contractile and relaxant stimuli were applied to thoracic aortic rings of wildtype C57BL/6 mice. Cholesterol depletion significantly reduced contractility to phenylephrine ($p<0.05$) and serotonin ($p<0.01$). Acute cholesterol enrichment had no effect on vascular contractility, however, acetylcholine stimulated endothelial-dependent relaxation was significantly reduced ($p<0.05$). Feeding with either a standard chow or a high fat 'western' diet was undertaken for eight weeks in both $ApoE^{-/-}$ and C57BL/6 mice. The extent of atherosclerotic disease development was measured through *en face* lipid staining and histological analysis of aortae. Atherosclerosis was present in the aortic root and intercostal branches of chow and high fat fed $ApoE^{-/-}$ mice but not in diet-matched C57BL/6 mice. No atherosclerotic lesions were observed in the thoracic aortae. In addition, to allow the possibility for direct associations to be made between the associated risk factors of hypercholesterolaemia, obesity and inflammation, and vascular function, a phenotypic assessment of these characteristics was conducted.

Wire myography was employed to assess the vascular function of thoracic aortic rings from chow and high fat diet fed $ApoE^{-/-}$ mice and their age and diet matched wildtype C57BL/6 controls. It was found that contractility to both phenylephrine and serotonin was significantly increased in chow fed $ApoE^{-/-}$ mice (both $p<0.05$). Further investigation into the mechanism, using intracellular calcium imaging and the indo-1 dye, concluded that VSMC store-operated calcium entry was not altered. The exact mechanism behind this increase in contractility is therefore still unknown and there was no clear relationship to the atherosclerotic risk factors assessed. In addition to altered contractility, endothelial-dependent relaxation was shown to be significantly enhanced in high fat fed C57BL/6 ($p<0.01$) and $ApoE^{-/-}$ mice ($p<0.001$). Enhanced endothelial-dependent relaxations were transient and sensitive to specific inhibition of cyclooxygenase-2 but not nitric oxide synthase. These changes were hypercholesterolaemia-independent but correlated with signs of obesity and inflammation.

In summary, this investigation has demonstrated that vascular function was altered in the murine thoracic aorta prior to overt atherosclerotic plaque development. The implications for these observations relate to the possibility of masked early signs of vascular dysfunction and also the induction of compensatory mechanisms which may have amplified effects over a longer time course; possibly promoting the development and advancement of atherosclerotic disease.

Declaration

No portion of this thesis has been submitted in support of an application for any degree or qualification of the University of Manchester or any other University or Institute of learning.

Copyright

i. The author of this thesis (including any appendices and/or schedules to this thesis) owns certain copyright or related rights in it (the "Copyright") and s/he has given The University of Manchester certain rights to use such Copyright, including for administrative purposes.

ii. Copies of this thesis, either in full or in extracts and whether in hard or electronic copy, may be made only in accordance with the Copyright, Designs and Patents Act 1988 (as amended) and regulations issued under it or, where appropriate, in accordance with licensing agreements which the University has from time to time. This page must form part of any such copies made.

iii. The ownership of certain Copyright, patents, designs, trade marks and other intellectual property (the "Intellectual Property") and any reproductions ofcopyright works in the thesis, for example graphs and tables ("Reproductions"), which may be described in this thesis, may not be owned by the author and may be owned by third parties. Such Intellectual Propertyand Reproductions cannot and must not be made available for use without the prior written permission of the owner(s) of the relevant Intellectual Propertyand/or Reproductions.

iv. Further information on the conditions under which disclosure, publication and commercialisation of this thesis, the Copyright and any Intellectual Property and/or Reproductions described in it may take place is available in the University IP Policy (see http://www.campus.manchester.ac.uk/medialibrary/policies/intellectualproperty.pdf) , in any relevant Thesis restriction declarations deposited in the University Library, The University Library's regulations (see http://www.manchester.ac.uk/library/aboutus/regulations) and in The University's policy on presentation of Theses.

Acknowledgements

I would firstly like to thank the British Heart Foundation for funding this work. I have learnt so much from the four year programme; I am very happy and proud to have been part of the first cohort at the University of Manchester.

Enormous gratitude goes to my supervisors; to Cathy Holt whose constant positivity and sound advice has given me the boosts I have needed along the way. I'm also grateful for being invited to your house for dinner, so thanks to you, Nadim and the kids as well for making me feel welcome in the lab. I would like to thank Clare Austin for putting up with me when I have moments of uncertainty and for always being able to get me back on track. Thanks also go to David Eisner who helped me early on to try and understand the inner workings of a calcium imaging rig.

I am thankful to have had a very supportive advisor in Jaqui Ohanian, who has been willing to listen to me and offer help if it was needed. Thanks to all the support staff in the BSF for their help, in particular Mike Jackson and Allison Hallworth have been fantastic. I would like to thank Yifen Li of the lipid research group for performing the analysis of serum lipids, and also Emily Clark for her painstaking blinded analysis of the perivascular adipocytes.

I have been fortunate to have worked in such a friendly environment; I will have fond memories of my time in the department and would like to thank everyone that has contributed to that. However, I must give a special thank you to Carmine Circelli for endless debates and arguments that have kept me on my toes and helped to compound and increase my knowledge of science and many other areas along the way. Also, a very special thank you goes to Elizabeth Wright. She's been my all round entertainer and motivator for the last few years and it's been an absolute pleasure. This process would have been much harder without you being there.

Finally, I want to thank my family. Their constant support before and throughout my PhD has made me who I am and I will be eternally grateful to them. I love you all.

"I am an optimist. It does not seem too much use being anything else."

-Winston Churchill

1. Introduction

1.1. Overview

Cardiovascular disease (CVD) was responsible for 34% of deaths in the UK in 2007. The main cause of mortality is atherosclerosis, particularly in the coronary and carotid arteries, leading to myocardial infarction and ischaemic stroke [1]. Atherosclerosis is strongly associated with risk factors including hypercholesterolaemia, hypertension, obesity, inflammation and diabetes and is particularly evident in the developed world where the incidence is increasing rapidly [2]. This investigation will focus on the effects of hypercholesterolaemia, in the early stages of disease development prior to the development of overt atherosclerotic plaques, on vascular function; however, assessment of concomitant risk factors will also be employed. The development and progression of atherosclerosis has been studied for many years now due to its causative role in coronary artery disease and ischaemic stroke, however, our knowledge of the factors which drive these processes is currently limited. Therefore, the aim of the current project is to advance the understanding of these mechanisms, hopefully enabling the future development of new preventative or regressive treatments for atherosclerosis.

1.2. Atherosclerosis

1.2.1. Atherosclerotic disease development and progression

The development and progression of atherosclerotic plaques within arteries is a complex and multifaceted process which involves many signalling pathways and cell types (for a review see Douglas & Channon (2010) [3]). At present it is accepted that atherosclerotic lesion formation is linked to endothelial dysfunction, defined as a decrease in the bioavailability of nitric oxide, causing an increase in oxidative stress; leading to the expression of adhesion molecules and subendothelial infiltration of inflammatory monocytes. The integrity of the endothelial layer is compromised and monocytes become macrophages capable of scavenging oxidised lipids; most commonly oxidised low density lipoprotein (oxLDL), a form of cholesterol which is found in increasingly high concentrations in modern diets of the developed world [4]. These cholesterol laden macrophages, known as foam cells, form the first presentation of atherosclerosis which occurs at as young as ten years old, and is named a fatty streak [3].

This process occurs primarily in areas of low and oscillatory blood flow, such as the inner curve of branches or bifurcations, with areas of blood vessels experiencing high shear stress being largely resistant to lesion formation [5–7]. The progression to the formation of an advanced atherosclerotic plaque involves neointimal hyperplasia and the deposition of ECM components, such as collagen, dictated by the proliferative vascular smooth muscle cells. This forms a fibrous cap intended to stabilise the plaque and prevent rupture. Plaque rupture may lead to thrombosis and occlusion of the vessel lumen, the cause of both ischaemic stroke and myocardial infarction depending on the location of the vessel. Plaque rupture is the atherosclerotic end-point and is the cause of all atherosclerosis related deaths (Figure 1.1.). As described above the function of endothelial and vascular smooth muscle cells play an integral role in plaque development.

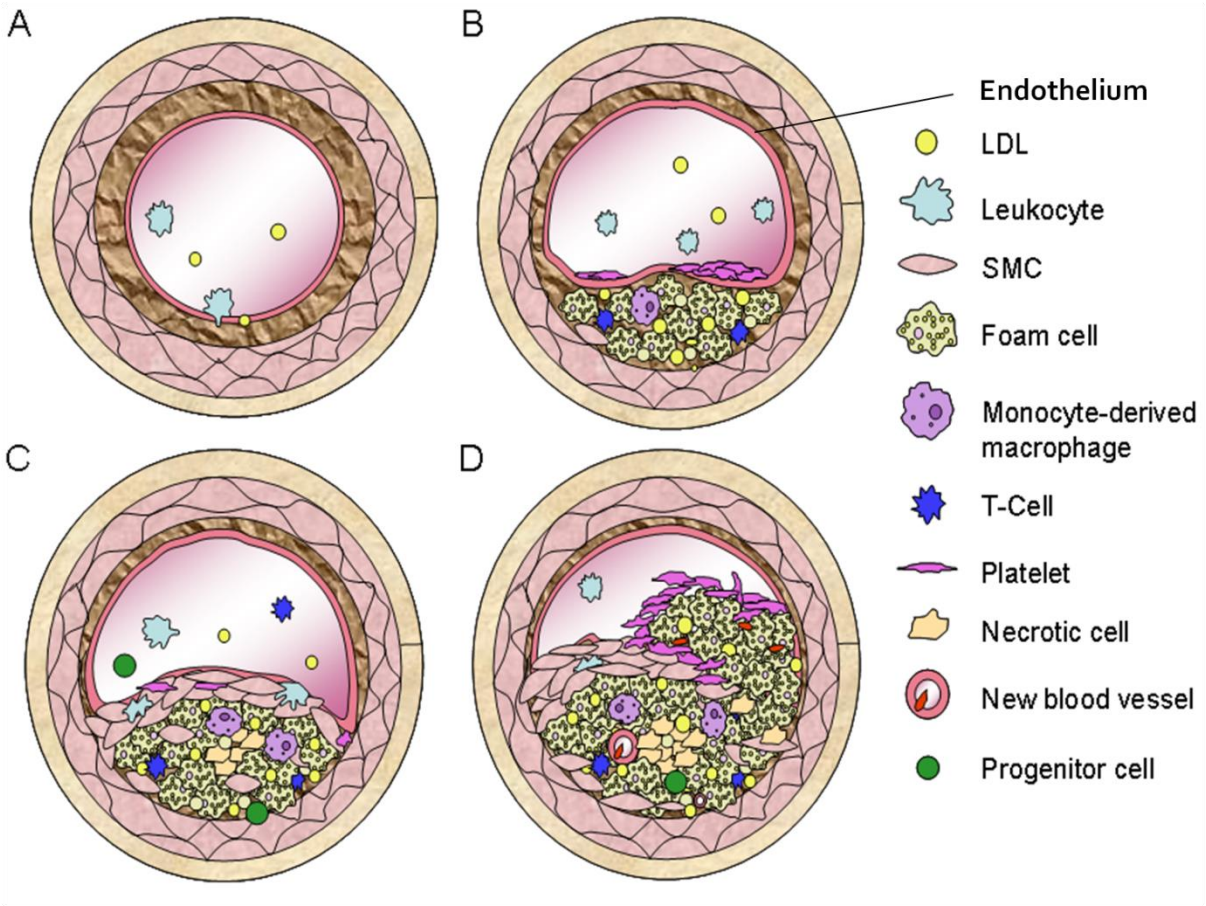

Figure 1.1. Development of an atherosclerotic plaque. A) Endothelial dysfunction is initiated by the uptake of excess plasma LDL and its subsequent oxidation (oxLDL); eventually stimulating an immune response. Inflammatory monocytes adhere to receptors on the endothelial surface and migrate into the intima where they are transformed into macrophages. **B)** The macrophages take up oxidised LDL in an unregulated fashion producing foam cells. More macrophages are recruited and are converted to foam cells leading to the formation of a fatty streak. **C)** Factors released by fat laden macrophages stimulate smooth muscle cell (SMC) migration and proliferation; this process along with the recruitment of other inflammatory cells (T-cells, neutrophils etc.) is the cause of intimal hyperplasia and the production of an advanced plaque. A complex plaque is the final stage of plaque progression which is characterised by a fibrous cap and a necrotic core. The complex plaque may be stable, restricting the lumen but allowing sufficient flow, or may be prone to rupture. **D)** If plaque rupture occurs, platelet aggregation will occur leading to formation of a thrombus and total occlusion of the lumen with cessation of flow. This is the cause of all atherosclerotic mortality and will lead to myocardial infarction or ischaemic stroke dependent on the plaque location (*Image produced by E.J. Wright and included with permission).*

1.2.1.1. The role of the endothelium in atherosclerotic disease progression

Endothelial cells line the lumen of all blood vessels. This one cell thick layer is of vital importance primarily as a barrier, regulating the exposure of the underlying medial smooth muscle to molecules in the plasma, and also by releasing vasoactive and anti-inflammatory factors, such as nitric oxide and prostacyclin [8]. Dysfunction of the endothelium is thought to be a key contributor to the initiation of atherosclerotic disease [9]. Dysfunction typically manifests as a reduction in nitric oxide bioavailability [10]. In addition to the reduction in paracrine signalling the barrier function of the endothelial cells can also be disrupted [11].

Endothelial cells have been identified in the regulation of vascular tone and also are known to secrete a number of cytokines and growth factors. These factors, including tumor necrosis factor-α (TNFα), interleukin-1 (IL-1) and monocytes chemoattractant protein-1 (MCP1), all of which have been implicated in the development and progression of atherosclerotic disease [9]. One of the most important effects of these inflammatory mediators is the increase in production of free radicals and the super oxide ion (O_2^-). This highly unstable ion is capable of scavenging nitric oxide and therefore reducing its bioavailabilty [12].

In response to an increase in circulating cholesterol low-density lipoprotein (LDL) concentrations are increased [13], endothelial cells have the capacity to take up LDL through scavenger receptors, such as CD36, expressed on the cell surface [9]. Within the endothelium LDL is converted to oxLDL. The endothelial response to oxLDL is to increase the expression of vascular adhesion molecule-1 (VCAM-1) and intracellular adhesion molecule-1 (ICAM-1) [14]; these adhesion molecules facilitate the transmigration of monocytes into the intimal space where they are transformed into macrophages. Scavenging of oxLDL by macrophages leads to the production of foam cells and the development of primary fatty lesions [9]. In addition, oxLDL is able to promote apoptosis of endothelial cells. The disruption of the endothelial barrier by apoptotic cell death is thought to increase thrombosis, through platelet activation, and also increase medial inflammation, due to the increased movement of inflammatory cells into the tissue [9,11].

1.2.1.2. The role of vascular smooth muscle cells in atherosclerotic disease progression

VSMCs are spindle-shaped cells arranged in concentric layers forming the *tunica media* of a blood vessel; they are responsible for maintaining the integrity of the vasculature and setting vascular tone; thus controlling the flow of blood. However, smooth muscle cells unlike cardiac or skeletal myocytes are not terminally differentiated and within arterial walls there is a heterogeneous population of smooth muscle cells [15]. In response to stress and injury VSMCs are able to adapt and differentiate into a proliferative phenotype stimulating extracellular matrix (ECM) deposition and growth as seen in other vascular diseases such as restenosis after stenting or hypertension [16–18]. In the case of atherosclerosis, endothelial dysfunction is able to promote the release of mitogens such as vascular endothelial growth factor (VEGF) and transforming growth factor-α (TGF-α) [19]. In addition, macrophages accumulated in the subendothelial space during fatty lesion formation are activated when taking up oxLDL. Upon activation the macrophages release growth factors, such as platelet-derived growth factor (PDGF) and fibroblast growth factor (FGF), directly onto the medial smooth muscle layer simulating a response to injury [19–21].

In summary, dysfunction of the endothelium, through a reduction in NO bioavailability and a breakdown in barrier function, is able to initiate events leading to the stimulation of VSMC phenotypic differentiation and the migration of VSMCs into the intimal space. The resultant effect is atherosclerotic disease development and progression [22].

1.3. Vascular Function

The contribution of both vascular endothelial and smooth muscle cells to the development of atherosclerosis has been outlined. The aim of this thesis is to assess the effects of these changes through their impact on the contractile and relaxant responses of vessels. In order to identify changes in vascular function that may occur in the early stages of atherosclerosis, firstly we must consider the mechanisms contributing to these actions in healthy tissue.

1.3.1. Endothelial cells and vascular function

The role of the endothelial cells in the vasodilation of blood vessels was first described by Furchgott & Zawadzki (1980) [23], highlighting the relaxant effects of acetylcholine on aortic preparations with rather than without the endothelium present; thought to be produced by a relaxing factor released from the endothelium (EDRF) [24]. This acetylcholine induced relaxation was found to be accompanied by a hyperpolarisation of the smooth muscle cells, reducing the opening probability of L-type calcium channels, and also a reduction in the production of calcium release inducing second messengers. There have since been defined a plethora of endothelial-dependent relaxant and contractile factors mediating vascular smooth muscle function [8]. For the purposes of this investigation only nitric oxide and prostacyclin (PGI_2) will be considered due to their association with relaxation of large arteries in rodents [25] and the forearm and coronary circulation of humans [26,27]. This has particular relevance due to the involvement of these two factors in flow-mediated dilation (FMD) [28,29]; measurement of which, in the forearm, is one of the primary diagnostic tools employed to assess vascular function in cardiovascular diseases, including atherosclerosis [30,31].

1.3.1.1. Endothelium-mediated vascular relaxation

In addition to flow mediated dilations, endothelial-dependent relaxation can also be produced by endogenous ligands, including acetylcholine, bradykinin, substance P and extracellular calcium. These ligands all interact with G-protein coupled receptors (GPCRs) which then activate heterotrimeric G-proteins. For the purposes of the current investigation the activation of muscarinic acetylcholine receptors (mAChR; subtypes M1- M3), by acetylcholine, will be considered.

The mAChRs, linked to the the $G\alpha_q$-subunit, activate phospholipase C (PLC). Phosphatidylinositol bisphosphate (PIP_2) is then hydrolysed by PLC, specifically by PLCβ [32,33], producing inositol triphosphate (IP_3) and diacylglycerol (DAG). IP_3 interacts with its receptors (IP_3R) on the closely linked endoplasmic reticulum (ER) to induce the release of calcium ions (Ca^{2+}) from stores; thus increasing intracellular calcium levels ($[Ca^{2+}]_i$) [34]. The increase in $[Ca^{2+}]_I$ can then activate endothelial nitric oxide synthase (eNOS), which exists in caveolae in an inactive state due to interaction with the scaffold domain of caveolin [35–37]. Intracellular Ca^{2+} binds calmodulin associated with the caveolae [38] which then binds to eNOS

causing a conformational change and its dissociation from caveolin [39]. This soluble eNOS is then active and produces NO which can induce smooth muscle hyperpolarisations [10].

Nitric oxide (NO) was identified as the EDRF by Moncada *et al.* (1988) [40]. Its production is determined primarily by the activity of the endothelial nitric oxide synthase enzyme (eNOS) and the availability of the pre-cursor L-arginine [41]. Nitric oxide relaxation is associated with activation of large conductance calcium-sensitive potassium (maxi-K or BK_{ca}) channels, through a cyclic guanosine monophophate (cGMP) dependent mechanism, leading directly to smooth muscle cell hyperpolarisation [42].

The importance of DAG, the second product of PIP_2 hydrolysis, with regards to endothelium-mediated relaxation is through the production of arachidonic acids after its metabolism by DAG lipase [43]. Arachidonic acids (AAs) are subsequently metabolized by Cytochrome P450 (CYP) epoxygenases, specifically CYP2C [44,45]. The result of this metabolic process is the production of prostaglandins. The relaxant prostaglandin prostacyclin (PGI_2) was also first identified by Moncada and colleagues in 1976 [46]. This factor is produced through the actions of the cyclooxygenase (COX) and prostacyclin synthase enzymatic activity metabolising arachidonic acid. Prostacyclin relaxation is mediated through the phosphorylation of targets mediating a pro-relaxant response, such as myosin light chain phosphatase, via cyclic adenosine monophosphate (cAMP) dependent activation of protein kinase A (PKA) [47].

In addition to the relaxant activities of both NO and prostacyclin both factors have been shown to be involved in regulation of neutrophil adhesion, platelet aggregation, and smooth muscle proliferation. NO also has the capacity to act as an antioxidant, protecting against free radical production [8,48,49]. The contribution of these factors and the impact of atherosclerotic disease development will be explored later in this introduction.

1.3.2. Vascular smooth muscle cells and vascular function

The control of flow by the contractile phenotype and the intimal hyperplasia of proliferative VSMCs are key processes in the development and progression of atherosclerotic plaques. The regulation of intracellular calcium concentration ($[Ca^{2+}]_i$) in vascular smooth muscle is central to the processes of contraction; initiated through an increase in global $[Ca^{2+}]_i$ [50] and the downstream effects on the contractile machinery (Figure 1.2).

The ability of a single signalling process to regulate multiple cellular actions will be dictated by modulation of the signal strength, duration, the sensitivity of the downstream targets to the signal and where the signal is produced and/or compartmentalised. These processes will be highlighted below.

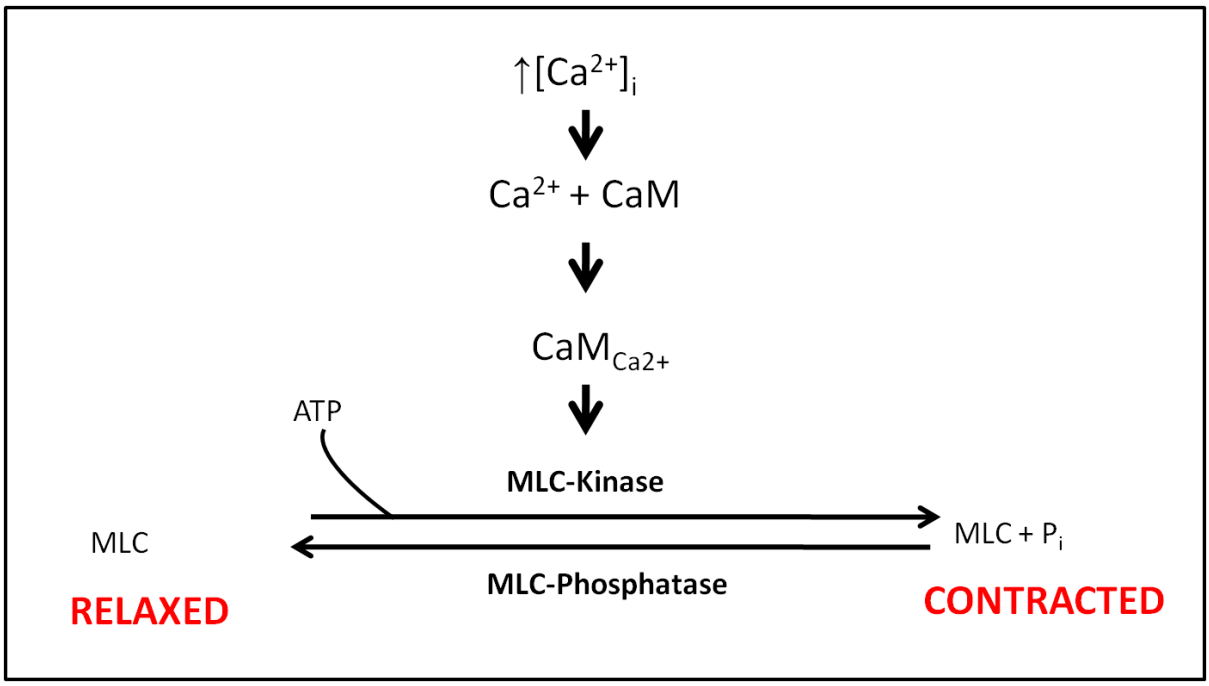

Figure 1.2. The mechanism of vascular smooth muscle contraction. An increase in intracellular calcium will increase the probability of binding to calmodulin (CaM). Activated calmodulin (CaM_{Ca2+}) is able to increase the activity of myosin light chain kinase (MLC-Kinase) promoting the phosphorylation of myosin light chain (MLC) protein. Phosphorylated MLC (MLC + P_i) is capable of binding to the actin cytoskeleton and initiating contraction. Relaxation is brought about by removal of this phosphorylation via MLC-Phosphatase. The balance between the activities of these two enzymes is involved in sensitisation of the contractile apparatus to calcium.

1.3.2.1. Vascular smooth muscle excitation-contraction coupling

The primary function of vascular smooth muscle is to contract and relax enabling control of blood flow; the initiation of contraction is dictated by $[Ca^{2+}]_i$ in a process termed excitation-contraction coupling. An increase in global $[Ca^{2+}]_i$ in VSMCs, the amplitude of which will determine the strength of the signal, can occur through many pathways; within large arteries such as the aorta this is primarily via G-protein coupled receptor (GPCR) activation or growth factor binding. However, to facilitate illustration of the primary mechanisms involved in raising global $[Ca^{2+}]_i$ in VSMCs, the activation of phospholipase C (PLC) will be

highlighted; a pathway which has been proven capable of initiating both contraction and proliferation of smooth muscle cells [50,51].

Upon binding of a specific ligand, both GPCRs ($G\alpha_q$-linked) and growth hormone receptors (protein tyrosine kinases), activate phospholipase C (isoforms β and γ, respectively [52–54]) enabling hydrolysis of phosphatidylinositol-4,5-bisphosphate (PIP_2) to inositol-1,4,5-trisphosphate (IP_3) and diacylglycerol (DAG). The Gβγ subunit of GPCRs is involved in transactivation of pro-proliferative signalling pathways, such as the mitogen-activated protein kinase (MAPK) pathway [55].

Upon generation, IP_3 will quickly bind to its receptor (IP_3R) on the sarcoplasmic reticulum (SR), the intracellular calcium store, causing a release of calcium into the cytoplasm. This calcium release may be augmented by a process termed calcium-induced calcium release (CICR) in which a second sarcoplasmic calcium release channel, the ryanodine receptor (RyR), is activated by the calcium from closely associated IP_3Rs; however, the involvement of this mechanism in vascular smooth muscle is currently unclear [56]. Activation of Ca^{2+}-sensitive chloride channels depolarises the cell further reaching the threshold for activation of voltage-sensitive Ca^{2+} channels [50], predominantly L-type calcium channels which are facilitated by the presence of Ca^{2+}.

The second metabolite of PIP_2 hydrolysis, DAG, acts to maintain the $[Ca^{2+}]_i$ rise in two ways. Firstly, via an indirect manner; protein kinase C (PKCδ) translocates to the plasma membrane in response to Ca^{2+} where it can be activated by DAG. Activated PKC is able to phosphorylate L-type Ca^{2+} channels and modulate their activity; mixed results have been described as to the effect of this phosphorylation, although in the case of muscarinic acetylcholine signalling, inhibition of PKC reduced carbachol induced contractions of bladder smooth muscle [57]. This positive effect of L-type Ca^{2+} channel phosphorylation on Ca^{2+} influx is supported as Ca^{2+}/calmodulin-dependent kinase (CaMKIIδ) is able to increase the calcium facilitation of L-type Ca^{2+} channels via phosphorylation [58].

The second and direct activity of DAG is as a ligand for receptor operated Ca^{2+} channels (ROCs). These channels have now been highlighted as members of the transient receptor potential (TRP) family of ion channels (for review see Clapham *et al.*(2001) [59]). The TRPC subgroup of this family (TRPC1-7), are all expressed in the vasculature [60,61], with TRPC3,

TRPC6 and TRPC7 having shown evidence of receptor activated opening in response to DAG [62–64]. It was then shown specifically that TRPC6 channels are activated by DAG allowing the influx of extracellular Ca^{2+} during agonist induced contraction of smooth muscle [65].

There is contention based around the principle of store-operated Ca^{2+} entry, a process which in non-excitable cells was shown to be driven by a complex of stromal interacting molecule 1 (STIM1) and Orai1 [66], however, in contractile vascular smooth muscle STIM1 and Orai1 were shown not to be expressed [67]. At present TRPC1, TRPC4 and TRPC5 are have all been suggested as putative mediators of SOCE in smooth muscle [68–70] but the true picture is far from clear.

1.3.2.2. $[Ca^{2+}]_i$-dependent vascular smooth muscle relaxation

There are four main mechanisms through which the Ca^{2+} is removed from the cytoplasm; these involve extrusion out of the cell via the sodium calcium exchanger (NCX) and the plasma membrane calcium ATPase (PMCA) as well as sequestration into intracellular stores through the sarco-endoplasmic reticular calcium ATPase (SERCA) and the mitochondrial uniporter. The goal of these mechanisms is to reduce the $[Ca^{2+}]_i$ down towards the resting level of around 200nM [71,72] and to load the intracellular stores ready for another activation; $[Ca^{2+}]$ in the SR of smooth muscle cell is approximately 160μM [73]. The accuracy of the stated $[Ca^{2+}]$ may be limited by the fact that both were calculated in cultured smooth muscle cells, the reasons for which will be discussed later. The majority of Ca^{2+}, around 60%, is removed out of the cell via the NCX (mainly NCX1.3) [74]. This is a high capacitance exchanger with relatively low affinity for Ca^{2+} ($K_d \approx 1\mu M$); it passively transports three sodium ions (Na^+) in for every Ca^{2+} extruded [75,76] and therefore relies on the activity of sodium potassium ATPases (Na^+K^+ATPases) to maintain the Na^+ gradient (specifically the α2 isoform) [77,78].

The remaining Ca^{2+} is extruded out of the cell in an active process by PMCAs, isoforms PMCA1 and PMCA4 being present on smooth muscle, or into intracellular stores via SERCA2b. These P-type ATPases have a higher affinity for Ca^{2+} ($K_d \approx 0.1\text{-}0.3\mu M$) but have a lower capacity for transport [79–81]. There is thought to be a contribution of the mitochondria in calcium handling particularly through the mitochondrial uniporter, however, this low affinity Ca^{2+} pump ($K_d \approx 10\text{-}20\mu M$) [82] is less well characterised. The role of mitochondria in

smooth muscle calcium handling is not clearly defined at the present time, the mitochondrial uniporter along with the mitochondrial NCX have been implicated in calcium buffering as well as calcium removal (for review see Szabadkai & Duchen (2008) [83]).

1.3.2.3. Calcium sensitivity

The concept of smooth muscle contractile machinery being sensitised to calcium was initially described in relation to the differential $[Ca^{2+}]_i$-force curves yielded by depolarisation and GPCR activation, observed in rat aortic smooth muscle [72,84,85]. These observations were developed further in permeabilised cells in which $[Ca^{2+}]_i$ was maintained at a fixed level. The addition of cyclic nucleotides produced relaxation which was found to be linked to reduced phosphorylation of the myosin light chain (MLC; Figure 1.2) [84,86]. Activation of GPCRs using the same permeabilised cell system showed an increase in force and MLC phosphorylation [87,88].

The mechanism at work in this process relies on the activity and phosphorylation status of a number of key proteins. Activation of GPCRs results in the inhibition of MLC phosphatase activity, responsible for dephosphorylating MLC, therefore promoting contraction (Figure 1.2); this occurs directly via phosphorylation of MLC phosphatase's regulatory subunit MYPT1 via RhoA kinase and indirectly through the PKC activated phosphatase inhibitor CPI-17 [89–93]. The contrasting effect promoting relaxation can be brought about by the activity of CamKII. Phosphorylation of MLC kinase by CaMKII reduces its affinity for calcium/calmodulin therefore reducing the phosphorylation of MLC [94]. The role of vascular smooth muscle cell $[Ca^{2+}]_i$ sensitisation in atherosclerosis has yet to be investigated, however, there is evidence of RhoA and Rho-associated kinase stimulating proliferation of rat aortic smooth muscle cells [95].

The mechanisms of calcium handling described above are set in the classical context of Ca^{2+} regulation on a global intracellular scale; however, this seems to be a simplification of the true nature of calcium signalling. Advancements in cellular imaging, fluorescent probes and molecular biology have highlighted the concept of signalling compartmentalisation and microdomains. These areas are now the focus of intense research and have been shown to be particularly important in Ca^{2+} signalling.

1.3.3. Vascular signalling compartmentalisation

Small omega (Ω) shaped, 50 – 100nm invaginations of the plasmalemma were first described in epithelial cells by Yamada in 1955 using electron microscopy [96]. It was he who named them "*caveolae intracellulares*" which translated from latin means intracellular caves. Further investigation led to the discovery that the level of invagination and density of caveolae was variable [97], and that they existed in a diverse range of tissues including endothelial cells; adipocytes; cardiac, smooth and skeletal myocytes; and epithelial cells [97,98]. The functional role of caveolae was explored further after the discovery of the proteins which coat them, namely the caveolins. As a result the functional significance of these morphologically unique structures has been recognised and subsequently investigated. The roles attributed to caveolae thus far include endocytosis, potocytosis, transcytosis, cholesterol homeostasis, signal transduction and the scaffolding of channels and receptors into micro-domains [99–102]. The compartmentalisation of signalling molecules into localised domains is thought to be of importance in both vascular endothelial and smooth muscle cell signalling and the subsequent vasoconstriction or vasodilation. The importance of this process is not completely understood as yet, although the possibility of its involvement in atherosclerosis and other vascular diseases is thought to be likely [103,104].

1.3.3.1. Caveolae and caveolins

Caveolae are a form of lipid raft and thus are enriched with cholesterol, sphingomyelin and glycosphingolipids. The ability to discern between the caveolae and lipid rafts is down to the protein coat which lines caveolae; this is a specialised coat protein known as caveolin [105]. This protein was subsequently found to be part of a larger family containing three genes encoding for caveolins including several isoforms. The three genes were named Cav- 1, 2 and 3 and the proteins they encoded identified as Caveolin-1 (α and β), Caveolin-2 (α, β and γ) and Caveolin-3. Caveolin-1 and caveolin-2 exhibit ubiquitous expression in comparison to caveolin-3 which is expressed exclusively on myocytes [103,106–108]. Recombinant expression of caveolin-1 or caveolin-3, but not caveolin-2, is sufficient to promote the formation of caveolae [109–111].

1.3.3.2. Endothelial signalling compartmentalisation

The muscarinic acetylcholine receptors (mAChR; subtypes M1- M3) have been shown to contain the caveolin binding motif but are not thought to be constitutively present in caveolae [112]. Both M2 and M3 subtypes have been shown to play a role in the production of endothelium-dependent smooth muscle relaxation [113,114] but there is no evidence as yet proving their localization to vascular endothelial caveolae. However, in studies using cardiac myocytes and airway smooth muscle both M2 and M3 receptors, respectively, have been proven to interact with caveolin after activation with an agonist [115,116]. The muscarinic pathways of the bladder have also been shown to be functionally affected by cav-1 knock-out mice; this evidence reinforces the mAChR link to caveolae. The mechanism of GPCR/G-protein interaction is suggested to be dynamic through a post-activation translocation of the receptor to caveolae [117]. This same mechanism has been shown to be used by other GPCRs involved in endothelial-dependent relaxation.

In addition to the receptor localization, interaction of the Gα-subunit with the caveolin scaffolding site was shown to have activity similar to a GDP dissociation inhibitor [118] and thus the localization of $G\alpha_q$ to caveolae maintains it in a GDP-bound inactive state. It will remain in this state until activation by a GPCR; causing dissociation from the scaffolding site and enabling GTP binding.

The stimulation of vascular relaxation in response to the increase in endothelial $[Ca^{2+}]_i$ is also coordinated by localization to caveolae. eNOS is targeted to caveolae and is held in an inactive state due to interaction with the scaffold domain of caveolin-1 [35–37]. A rise in $[Ca^{2+}]_i$ causes an activation of calmodulin, also shown to be associated with the caveolae [38]. Activated calmodulin binds to eNOS causing a conformational change and its dissociation from caveolin [39]. Thus the efficiency of this activation is enhanced through spatial association.

1.3.3.3. Vascular smooth muscle signalling compartmentalisation

The importance of lipid rafts and caveolae in the regulation of calcium microdomains is thought to derive from the nature of their shape. The flask-like invagination enables the immediate extracellular environment to be controlled with much more precision, the ranges

of [Ca^{2+}] able to be produced in this microdomain are able to modulate smooth muscle function [119]. With specific reference to vascular contractility it has been demonstrated that $G\alpha_q$ and $G\alpha_{11}$ linked GPCRs, including the α_1-adrenergic receptor and the 5-HT_{2A} receptor, as well as TRPC channels associate with cholesterol-rich caveolae or the caveolins [120–123].

In addition to organisation of contractile signalling, caveolar compartmentalisation is involved in the activation of a vascular smooth muscle cell relaxation mechanism. A Ca^{2+} spark is a spontaneous calcium release event from the RyR in response to SR overload and was first observed and characterised in cardiac myocytes by Cheng *et al.* (1993) [124]. In the cardiac myocyte, calcium sparks are seen to summate and form waves of calcium leading to an increase in global $[Ca^{2+}]_i$ integral to excitation-contraction coupling. The involvement of calcium sparks in smooth muscle excitation-contraction coupling has been a matter of great debate; Ca^{2+} sparks have been recorded in vascular smooth muscle cells [125]; however, their activity promotes relaxation rather than contraction as seen in the cardiac myocyte.

Sparks are released from clusters of RyRs on the SR, known as frequent discharge sites (FDS) [126,127]. The FDSs are thought to be spatially aligned with large-conductance Ca^{2+}-activated potassium channels (BK_{Ca}); evidence for the localisation of BK_{Ca} channels to caveolae in the myometrium support this suggestion [128,129]. The short burst of Ca^{2+} release into the low volume of the PM-SR microdomain is sufficient to raise the [Ca^{2+}] in the microdomain by 10-100µM. The change in global $[Ca^{2+}]_i$ is very low at around 2nM due to the effects of calcium buffers, such as calreticulin, preventing diffusion out of the junctional space [130,131]. The rapid increase in [Ca^{2+}] activates BK_{Ca} channels leading to a spontaneous transient outward current (STOC). The STOC hyperpolarises the smooth muscle cell leading to relaxation [132,133]. However, the role of this mechanism in larger arteries such as the aorta is currently unknown.

1.4. Studying vascular function during atherosclerotic disease development

Having outlined vascular function in health, the effects of atherosclerotic disease will now be explored. It is the aim of the present investigation to assess the effects on vascular function of atherosclerotic risk factors, predominantly hypercholesterolaemia, during early atherosclerotic development. Investigation into the molecular development and progression of atherosclerosis within the coronary arteries of humans is all but impossible at this time due

to the late stage at which the disease is currently identified and the limited availability of tissue. Human samples available are usually obtained post-mortem from patients who have undergone various diets and drug treatments. Therefore, the use of an animal model of atherosclerosis is an attractive alternative as age and diet can be carefully controlled allowing investigation into the early progression of the disease.

1.4.1. Animal models of atherosclerosis

The most effective way of producing an animal model of atherosclerosis is through genetic modification of lipid metabolism; due to hypercholesterolaemia being the only risk factor directly associated with development of atherosclerotic plaques [134]. There are two models of atherosclerosis used in the majority of investigations at present; the low density lipoprotein receptor knockout mouse ($LDLR^{-/-}$) and the apolipoprotein E knockout mouse ($ApoE^{-/-}$).

The LDLR is responsible for export of low density lipoproteins out of the blood stream into the liver where they are broken down and excreted [135]. The $LDLR^{-/-}$ mouse was created via targeting of the LDLR gene in embryonic stem cells. The subsequent mice were found to develop a serum-cholesterol concentration two-fold greater than wild type mice when both were fed a high fat diet. The lipid levels in the plasma were found to be similar to those found in human hyperlipidaemia and fatty streaks were observed in the aorta, coronary arteries and around the aortic valve [136].

ApoE is a high affinity ligand for the LDLRs; it is produced by the liver and macrophages and is integral for the efficient removal of lipids from the plasma. The $ApoE^{-/-}$ mouse, first created in 1992 [137], is now widely used in the study of atherosclerosis. These mice are spontaneously hypercholesterolaemic and develop atherosclerotic lesions, a process which can be accelerated by feeding with a high fat 'Western' diet [138] . Lesions within the coronary arteries, which are often the cause of mortality in humans, cannot be studied in these mice as they do not tend to develop [139]; however, lesions within the aortae of $ApoE^{-/-}$ mice are regularly used in the study of atherosclerosis as they have been shown to have a similar composition to those seen in human coronary arteries [140]. Lesions initially form in the aortic arch and subsequently along the thoracic aorta with enhanced distribution at branch points [138]. Fatty streaks are observed in these mice at around 10 weeks after feeding with normal chow; advanced plaques form at around 15 weeks and complex fibrous plaques are observed after

approximately 20 weeks. When a high fat diet is administered this process is accelerated with visible lesions being formed at around eight weeks [141].

At present there are few known advantages for choosing either model over the other. Initially the question being addressed needs to be considered as the lipid profiles of the two models differ; in ApoE$^{-/-}$ mice the main cholesterol carrier is very low density lipoprotein (VLDL) rather than LDL as seen in humans and LDLR$^{-/-}$ mice [142]. Quantification of the lesion size produced in each model was found to be very similar [143]. The main differences between the two models are, firstly, the speed at which lesions develop. ApoE$^{-/-}$ mice produce lesions of all types at a faster rate and to a greater extent [144]. Secondly, ApoE$^{-/-}$ mice appear to be more resistant to the development of obesity and diabetes when compared to LDLR$^{-/-}$ mice [145,146]; this may therefore suggest that the ApoE$^{-/-}$ model of atherosclerosis is the most favourable choice for the assessment of the specific changes induced by hypercholesterolaemia.

1.4.2. Apolipoprotein function

The role of apolipoproteins is to maintain the structure of cholesterol carrying particles; the combination of lipids and apolipoprotein create particles of different densities including chylomicrons, very low density lipoprotein (VLDL), low-density lipoprotein (LDL) and high-density lipoprotein (HDL). In addition, apolipoproteins also contribute to the activation of lipid metabolising enzymes and can act as ligands for cell surface receptors in the process of cellular cholesterol homeostasis which will be discussed later. There are four main classes of apolipoprotein that have been observed in mammals, ApoA, ApoB, ApoC and ApoE. Within these classes there are a number of isoforms, the function of these apolipoproteins in human lipid transport will now be discussed.

1.4.2.1. ApoA

ApoA proteins are primarily associated with the formation of HDL particles and are synthesised in the liver. The interaction of lipid laden ApoA-I with the scavenger receptor class B member 1 on the surface of cells promotes internalisation [147]. In contrast, when ApoA-I lipid content is low its conformation is changed and its function appears to be that of a lipid acceptor through close association with the ATP-binding cassette transporter A1 (ABCA1) [148]. In addition to the transport of cholesterol ApoA-I is able to activate the

cholesterol esterifying enzyme lecithin cholesterol acyltransferase (LCAT) enabling the conversion of free cholesterol into a more hydrophobic form [149]. ApoA-II is the second most common contributor towards the formation of HDL particles and is able to displace ApoA-I. The presence of ApoA-II has been shown to reduce the ability of cholesterol to be removed from cells [150].

1.4.2.2 ApoB

ApoB is responsible for the formation of chylomicrons and VLDL particles. There are two isoforms of ApoB; ApoB-48 is generated by intestinal cells and is required for the creation of chylomicrons. These particles are necessary for the transport of triglycerides after absorption in the intestines to the necessary targets such as the liver, adipose tissue and muscles . ApoB-100 is released from hepatocytes into the plasma and is involved in the formation of VLDL particles capable of transporting triglycerides stored in the liver to peripheral tissues where they can be hydrolysed to provide free fatty acids. ApoB-100 is also a ligand for the LDL receptor promoting the internalisation of lipoproteins through endocytosis. The primary role of ApoB derived particles is to promote absorption and transport of fats and fat soluble vitamins [151,152].

1.4.2.3. ApoC

There are three isoforms within this class of apolipoprotein, ApoC-I, ApoC-II and ApoC-III, which are capable of inhibitive or catalytic activity on several of the key lipid modifying enzymes. ApoC-I is thought to increase the activity of LCAT leading to a greater level of cholesterol esters [149]. ApoC-II is able to increase the activity of lipoprotein lipase (LPL), a critical enzyme in the metabolism of chylomicrons and VLDL particles; promoting the availability of free fatty acids [153]. In contrast, ApoC-III appears to reduce the activity of LPL, possibly by direct inhibition of ApoC-II activity [154] and also has been shown to block hepatocyte uptake of ApoE-containing lipoproteins [155], which will be outlined next.

1.4.2.4. ApoE

The ApoE class of apolipoproteins has three isoforms, E2, E3 and E4. ApoE3 is the most important of this class of proteins as it acts as a ligand for the LDL receptor and the ApoE receptor enabling the hepatic internalisation of ApoE3-containing lipoprotein particles; ApoE3 is not specific to a certain type of lipoprotein and can be found on VLDL, LDL and HDL particles. Therefore, ApoE3 is one of the key proteins in the maintenance of cholesterol homeostasis [156,157]. In addition to its role in lipid metabolism ApoE apolipoproteins are known to act as antioxidants [158], modulate inflammatory responses [159] and inhibit cellular proliferation [160], factors which are all involved in the development and progression of atherosclerotic disease. It is for these reasons that the $ApoE^{-/-}$ mouse has become a prevalent model for the study of atherosclerotic disease.

1.5. Modifications of vascular function during atherosclerotic disease development

The development of atherosclerotic disease involves the actions of closely associated risk factors, including hypercholesterolaemia, obesity and inflammation. Investigations into the direct relationship between individual risk factors and vascular function, in the context of atherosclerotic disease development, are limited at present due to their inter-relatedness. However, the current knowledge around this topic will now be explored.

1.5.1. Hypercholesterolaemia and vascular function

1.5.1.1. Cholesterol homeostasis

Cholesterol is a key component of all cell membranes involved in the maintenance of biological membranes. Cellular cholesterol homeostasis is regulated tightly. There are two predominant mechanisms through which cholesterol can be made available for the production of substrates able to be employed by the body's cells, such as components for membrane formation, steroid hormones. The first mechanism is through the de novo synthesis of cholesterol; this is a multi-step process of which the rate limiting step is catalyzed by HMG-CoA reductase. This enzyme is the target for cholesterol reducing statin therapies [161]. The second mechanism is through endocytosis of cell surface receptors, including LDL receptors (LDL and VLDL uptake) and scavenger receptor class B member 1 (HDL uptake). Inside the

cell the esterified cholesterol is hydrolyzed so that it is able to be used to create and maintain plasma, nuclear, reticular and mitochondrial membranes and in the formation of steroid hormones [162,163]. Cholesterol is able to be removed from cells through a process known as reverse cholesterol efflux. This process involves cholesterol being removed from cells via the ATP-binding cassette transporter A1 (ABCA1) [164] to be carried to the liver via HDL particles for excretion as bile salts [165] (Figure 1.3.)

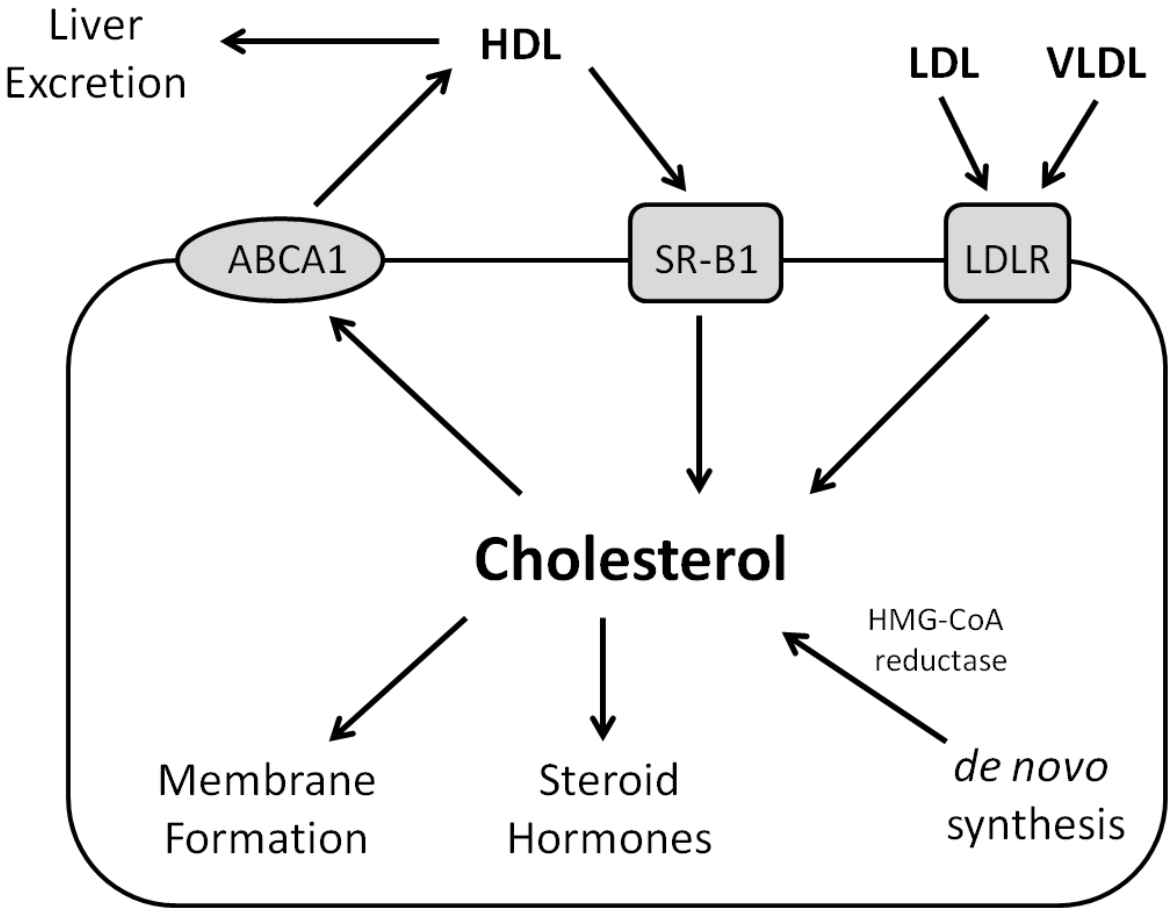

Figure 1.3. Cellular cholesterol handling. Cholesterol homeostasis is maintained by a balance between intracellular synthesis, influx of cholesterol from lipoprotein particles and efflux to the liver for excretion. De novo synthesis of cholesterol is performed from the pre-cursor acetate and is limited by the activity of the enzyme HMG-CoA reductase. Esterified cholesterol is carried in the plasma by lipoproteins which are then able bind to cell surface receptors. Very low and low density lipoproteins (VLDL and LDL) bind to the LDL receptor (LDLR) and high density lipoproteins (HDL) bind to the scavenger receptor class B member 1 (SR-B1). After hydrolysis, intracellular cholesterol can be employed to create membranes and steroid hormones. Efflux of excess cholesterol is performed by the ATP-binding cassette transporter A1 (ABCA1), it is transferred primarily to HDL particles and transported to the liver for excretion.

1.5.1.2. The role of cholesterol in vascular function

In vascular endothelial and smooth muscle cells function is linked to membrane cholesterol, firstly through regulation of the plasma membrane lipid bilayer width [166]. In response to hypercholesterolaemia the plasma membrane cholesterol content of arterial smooth muscle, isolated from high fat diet fed rabbits, was demonstrated to increase over time up to 13 weeks [166]. After eight weeks of high fat feeding the free cholesterol content of the rabbit thoracic aorta was shown to increase by 67% [167]. Cholesterol enrichment of plasma membranes increases the width of the phospholipid bilayer [166,167], a process which is capable of modifying the function of ion channels and receptors through the physical interactions with the protein structure [168,169]. Secondly, cholesterol is a key component of lipid rafts and caveolae, discrete domains within the lipid bilayer which are involved in the organisation of signalling domains. The importance of these domains in the compartmentalisation of vascular signalling has been highlighted previously. Exposure to hypercholesterolaemia has been shown to increase the number of caveolae and the expression of caveolin-1 in saphenous arteries of rats; this was observed on both endothelial and smooth muscle cells after high fat feeding for 16 weeks [170].

1.5.1.3. The effect of hypercholesterolaemia on endothelial dysfunction

Endothelial dysfunction, defined as the reduction in the relaxant response to acetylcholine, has been observed in response to hypercholesterolaemia in the rabbit corpus cavernosum [171], pulmonary artery [172] and thoracic aorta [173] and also in the thoracic aorta of chow [174] and high fat 'western' diet fed ApoE$^{-/-}$ mice[175,176] ApoE$^{-/-}$. Each of these studies highlighted a reduction in the response to nitric oxide signalling as the cause for the decrease in relaxation; Azadzoi *et al.* (1991) also noted that cyclooxygenase products e.g. prostacyclin were not affected by hypercholesterolaemia [171]. However, whether the development of endothelial dysfunction can be linked directly to the actions of hypercholesterolaemia is currently unclear. In hypercholesterolaemic rabbits and chow diet fed ApoE$^{-/-}$ mice the appearance of endothelial dysfunction appears to be correlated to the presence of atherosclerotic plaques [172,174]. This association is supported by the fact that endothelial-dependent relaxations in ApoE$^{-/-}$ mice, after exposure to acetylcholine, have been shown to be unchanged prior to plaque development; although basal nitric oxide was shown to be reduced, possibly signalling a very early trend towards dysfunction [177,178]. Acute exposure to high cholesterol for three hours also

had no effect on endothelial-dependent relaxation in rabbit femoral arteries [179]. In contrast to this, D'Uscio *et al.* (2001) [180] observed no plaque formation in the carotid arteries of $ApoE^{-/-}$ mice fed a high fat 'western' diet for 26 weeks but did observe endothelial dysfunction derived from the reduced activation of eNOS and an increase in superoxide ion production.

1.5.1.4. The effect of hypercholesterolaemia on contractility and smooth muscle calcium handling

The responses to contractile stimuli in a range of hypercholesterolaemic models, similarly to the above described endothelial responses, demonstrate some variability. In response to three hours exposure to high cholesterol, rabbit femoral arteries exhibited an increase in sensitivity to α-adrenergic stimulation [179]. Fransen *et al.* (2008) [178] demonstrated an increase in contractility to phenylephrine in the chow fed $ApoE^{-/-}$ mouse thoracic aorta and augmented contractility to serotonin was observed in the aortae of chronic hypercholesterolaemic monkeys [181]. However, after chronic exposure to hypercholesterolaemia, contractions to α-adrenergic stimulation in the rabbit thoracic aorta were observed to be reduced but contractions to serotonergic stimulation were increased [172,182]. The alterations in contractility have been associated with smooth muscle calcium handling.

Enrichment of vascular smooth muscle membranes has been shown to increase the permeability of cells to extracellular calcium upon agonist stimulation and under basal conditions [183–185]. Van Assche *et al.*(2007) [186] observed raised resting global $[Ca^{2+}]_i$ and increased IP_3-mediated Ca^{2+} release, linked to augmented SOCE, in the thoracic aortae of hypercholesterolaemic $ApoE^{-/-}$ mice prior to lesion formation. A role for hyperactive IP_3-mediated signalling and SOCE in alteration of calcium handling in response to hypercholesterolemia is supported by evidence that cholesterol depletion reduces the effects of endothelin-1 (IP_3-mediated) and SOCE (via TRPC1) on endothelium-denuded rat caudal arteries [187].

1.5.1.5. Hypercholesterolaemia, vascular function and atherosclerotic disease pathogenesis

There are a number of variants that may explain the variation observed in endothelial dysfunction and the modification of contractility across the models of hypercholesterolaemia.

The diets employed and the feeding durations are likely to be important due to their relationship to the stage of atherosclerotic disease development. Hypercholesterolaemia in humans is able to promote atherosclerotic plaque development through upregulation of adhesion molecule expression on endothelial cells [14]. In addition, an increase in the expression of caveolin-1 and the formation of caveolae has been linked to increased inactivation of nitric oxide by caveolin-1 binding; therefore promoting reduced NO bioavailability and increased super oxide ion formation [188,189]. A final consideration is that a mechanism of promoting atherosclerotic disease progression by hypercholesterolaemia may involve the stimulation of smooth muscle proliferation. Enhanced basal $[Ca^{2+}]_i$ and an increase in SOCE, in agreement with evidence from an animal model of early atherosclerosis [186], is closely associated with smooth muscle proliferation in culture [190]. The prevalence of proliferative smooth muscle cells early in the development of atherosclerosis is also shown by Agianniotis & Stergiopulos (2012) who observed an increase in the number of smooth muscle cells in hypercholesterolaemic $ApoE^{-/-}$ mice [191].

1.5.1.5.1. Modulation of calcium handling during smooth muscle proliferation

There is much evidence that Ca^{2+} signalling is able to drive proliferation of smooth muscle cells (reviewed by Berridge (2012) [192]. Changes in calcium handling protein expression have been catalogued in a series of models such as cultured VSMCs or isolated VSMCs from models of vascular injury (reviewed by Owens *et al.* (2004) [21] and House *et al.* (2008) [193]); however, translation of these findings to the context of atherosclerosis has been limited. The specific changes in some of the proteins associated with vascular function will now be described.

1.5.1.5.2. Voltage-gated Ca^{2+} channels

L-type Ca^{2+} channels are highly expressed in the differentiated contractile phenotype [194]. Their activation is linked with the expression of smooth muscle specific genes such as smooth muscle α-actin and smooth muscle myosin heavy chain (SM-MHC) [195]. However, another voltage-sensitive Ca^{2+} channel is also expressed; known as the T-type. The role of this channel in smooth muscle excitation-contraction coupling is currently unknown, however, it is suggested to be involved in VSMC proliferation [196]. The low-voltage activation

of T-type Ca^{2+} channels is thought to facilitate calcium entry in proliferative VSMCs which exhibit hyperpolarised membrane potentials (-45 to -70mV); around 20-40mV lower than those recorded in differentiated VSMCs [197,198]. In evidence from both culture induced proliferative VSMCs and those derived after balloon injury the ratio between L- and T-type Ca^{2+} channels is modified with expression being reduced and increased respectively [198–202].

1.5.1.5.3. TRPC1

It is suggested that store operated or capacitative Ca^{2+} entry (SOCE) plays a role in stimulating VSMC proliferation [190] a process that, as earlier described, is thought to involve TRPC1 channels [69]. The expression of this channel has been studied in many models with protein expression being increased in proliferative VSMCs in culture [67,203] and also after balloon injury in rat cerebral arteries [204]. The upregulation of TRPC1 is linked to increased Ca^{2+} entry in response to store depletion. The involvement of this process in stimulating proliferation is supported by the work of Kumar *et al.* (2006) [205] in which pharmacological blockade of TRPC1 reduced neointimal hyperplasia in human saphenous vein after balloon injury. The process of SOCE in non-excitable cells is regulated by the Orai and STIM protein complex; it is therefore interesting that VSMCs express Orai2 and 3 only after being cultured [67].

1.5.1.5.4. Ryanodine receptors

There are three known isoforms of RyR (RyR1-3) [206], however, the expression pattern of RyRs in VSMCs is currently unclear although there is evidence of both RyR2 and RyR3 [67,200,207]. When VSMCs are cultured and undergo phenotypic change RyR2 protein expression decreases [67]. The change in RyR3 expression is more complex, Vallot *et al.* (2000) [200] describe a decrease in RyR3 mRNA after having presented a high protein expression in differentiated VSMCs. Contrastingly, Berra-Romani *et al.* (2008) [67] demonstrate no RyR3 protein in freshly isolated aortic VSMCs but an increase in RyR3 protein expression when VSMCs are cultured.

The two studies are in agreement with the observation that caffeine sensitivity is reduced in proliferative VSMCs; a fact that may clarify the previous contradiction. The RyR3 gene has two splice variants (RyR3-I and RyR3-II) [208]. It is possible that the increase in protein

expression detected by Berra-Romani *et al.* (2008) [67] is linked to an increase in the caffeine insensitive RyR3-I splice variant. This is supported by the reduction in RyR3-II mRNA detected by Vallot *et al.* (2000) [200]. The true picture of RyR expression and its role in VSMC proliferation remains unclear, however, due to the role RyRs play in the regulation of excitability through BK_{Ca} activation any changes in the channel activity is likely to have downstream effects on vascular relaxation and Ca^{2+} handling in general.

1.5.1.5.5. IP_3 Receptors

There are three isoforms of IP_3R with IP_3R1 being expressed in the highest abundance in VSMCs [34]. IP_3Rs have been indicated in vascular proliferation as their stimulation leads to outgrowth of cultured cerebral arteries; in addition, pharmacological blockade of IP_3Rs can prevent this outgrowth [209]. However, it must be considered that the selection of pharmacological agents in this study has come under some criticism due to the potential effects on TRP channels [210]. Expression and activation of IP_3R1 is increased in association with growth [211,212], and has been demonstrated in cultured VSMCs along with an increase in expression of IP_3R2 and IP_3R3 [67]. Increased expression of IP_3Rs is thought to contribute to the maintenance of high $[Ca^{2+}]_i$ perpetuating the transcriptional effects of GPCR signalling [211].

1.5.1.5.6. SERCA

There are three SERCA genes all of which undergo alternative splicing producing isoforms that have different affinities for Ca^{2+}. Contractile VSMCs predominantly express SERCA2a; the expression of which is reduced in culture [67,200,213]. Refilling of the SR is suggested to be maintained through increased expression of the lower Ca^{2+} affinity pump SERCA2b [81], although, this effect has not been observed in all studies [213]. Despite the lack of consensus on SERCA2b expression the importance of SERCA2a on the maintenance of a contractile phenotype has been well supported. Lipskaia *et al.* (2005) [213] provide evidence of neointimal hyperplasia inhibition after adenoviral overexpression of SERCA2a in rat carotid arteries and re-expression of SERCA2a when cell arrest their growth upon achieving confluence in culture. The loss of a Ca^{2+} efflux mechanism would prolong the rise in $[Ca^{2+}]_i$ after stimulation, however, the functional effects of replacing SERCA2a with the higher Ca^{2+} affinity SERCA2b are currently unknown.

1.5.1.5.7. PMCA

VSMCs express multiple splice variants of PMCA; predominantly PMCA1b, PMCA4a and PMCA4b. Culture of rat carotid artery cells provokes an increase in PMCA4a expression which has been linked to proliferation [214]. PMCA4a has a lower affinity for Ca^{2+} and therefore increased expression will facilitate maintenance of a higher $[Ca^{2+}]_i$ [74].

1.5.1.5.8. Ca^{2+}-activated potassium channels (K_{Ca})

BK_{Ca} is the main 'off switch' for Ca^{2+} influx via its ability to hyperpolarise VSMCs and inactivate amongst others L-type Ca^{2+} channels. In VSMCs in culture and after balloon injury BK_{Ca} expression is reduced, a process which coincides with an increase in expression of the intermediate-conductance Ca^{2+}-activated K^+ channel (IK_{Ca}) [215,216]. The expression of IK_{Ca} is proposed to be linked to the more hyperpolarised membrane potentials observed in proliferative VSMCs. Like the BK_{Ca} channel IK_{Ca} is voltage-sensitive; however, it is opened at lower membrane potentials. Its involvement in VSMC proliferation has been demonstrated through the effects of the specific inhibitor TRAM-34 which reduced neointimal hyperplasia after balloon injury in rats [217].

1.5.1.5.9. Ca^{2+}/Calmodulin-dependent protein kinase II (CaMKII)

Contractile VSMCs express both CaMKIIδ and CaMKIIγ, which are used to regulate the activity of a number of Ca^{2+} handling proteins such as L-type Ca^{2+} channels and SERCA via phospholamban [218]. In culture derived proliferative VSMCs CaMKIIγ expression is reduced with a concomitant rise in δ splice variants, specifically $CaMKII\delta_2$; a pattern that has also been observed in VSMCs after balloon injury [210,219]. The specific effects of this particular isoforms are currently unknown, however, its association with growth initiation is well supported [220,221].

As stated, the consequences of these changes on vascular function have not yet been demonstrated. However, they represent possible areas of exploration when assessing the effects of hypercholesterolaemia during atherosclerotic disease development. It is difficult to associate individual risk factors, such as hypercholesterolaemia, with function during the

atherosclerotic disease development. One of the main reasons for this is that there are several concomitant risk factors linked to atherosclerosis that are also able to modulate vascular function; the most relevant of these risk factors in association with hypercholesterolaemia is obesity and its subsequent role in the generation of inflammation.

1.5.2. Obesity and inflammation

Obesity is closely associated with a high fat, high cholesterol diet and has been shown to accelerate atherosclerotic disease development in adolescent male patients [222]; demonstrating its ability to have an impact in the early stages of disease development. Obesity is characterised by an excessive increase in deposited adipose tissue [223]. Central obesity and a high body mass index correlate highly with an increase in the levels of inflammatory biomarkers observed in the presence of cardiovascular disease [224]. The measurement of these biomarkers has been used to predict the risk of future cardiovascular events, even in relatively healthy patients. Increased basal levels of interleukin-6 (IL-6)[225], tumor necrosis factor α (TNFα)[226] and C-reactive protein (CRP) [227,228] have been shown to exist in patients that went on to suffer from cardiovascular disease.

1.5.2.1. Adipose tissue

Adipose tissue is generally divided into two types; white adipose tissue (WAT) and brown adipose tissue (BAT). Definition between the two types of fat is based on the size of the lipid droplets within the tissue and the number of mitochondria [229]; WAT is comprised of a single, large lipid droplet whereas BAT is made up of a number of smaller deposits. The different morphology and mitochondrial density correlate to the function of the adipose tissue; the primary role of WAT is in the storage of lipids whereas BAT is more metabolically active and is associated with thermogenesis. WAT is also less vascularised and innervated than BAT [230,231].

1.5.2.2. Perivascular adipose tissue

Perivascular adipose tissue (PVAT) surrounds most blood vessels in close association to the adventitia. Previously considered to solely offer structural support it has recently been described as a paracrine organ capable of modulating vascular function and has been

suggested to contribute to the development of cardiovascular disease, including atherosclerosis [230,232]. The amount of PVAT surrounding blood vessels has been shown to correlate closely with overall adiposity and can therefore be used as an indicator of obesity [233]. PVAT has been shown to vary in its morphology and function with characteristics of both WAT and BAT being observed from different vascular beds. Gene expression analysis of the PVAT around the thoracic aorta of mice identified specific BAT markers [234] wheras morphological characterisation of human mesenteric [235] and internal thoracic artery [236] identified the presence of WAT. However, full characterisation of the prevalence of WAT and BAT in human PVAT of different vascular beds has not been conducted.

1.5.2.3. PVAT and atherosclerosis

A link between atherosclerosis and PVAT was first suggested due to the ability of PVAT to modulate vascular function; the presence of PVAT around the human internal thoracic artery was demonstrated to reduce vascular contractility [236]. The factors released from PVAT have been termed adipokines and can act via both endothelial-dependent and independent mechanisms to alter vascular function [236–238]. The vasoactive activity of PVAT will not form part of the present investigations; however, the role of PVAT in oxidative stress and inflammation associated with several disease states, including atherosclerosis, will be examined [229,239].

The most prevalent adipokine is adiponectin; demonstrated to act as a vasodilator but also as an anti-inflammatory mediator [230] the release of adiponectin is thought to protect against inflammation, insulin resistance and atherosclerotic plaque formation [240]. In response to the increase in adipose tissue observed in obesity, the size of individual adipocytes is increased as more lipids are stored. This increase in size of adipocytes is associated with a reduction in the release of adiponectin and an increase in the release of inflammatory cytokines; thought to be due to a hypoxic response within the centre of the cell [241]. An increase in adipocyte size has been observed in the aortic and mesenteric perivascular adipose tissue (PVAT) of high fat diet-induced obese rats and mice [242,243]. The local release of inflammatory cytokines from enlarged, hypoxic adipocytes have been linked with endothelial and overall vascular dysfunction through the increased production of superoxide ions [244]; leading to accelerated atherosclerotic plaque formation [229,243,245,246].

1.5.3. Vascular function and inflammation

Associated with an increase in local inflammation and the development of obesity is an increase in cyclooxygenase enzyme expression within the vascular wall [247]. The products of cyclooxygenase isoforms 1 and 2, thromboxane A_2 and prostacyclin, respectively, have been described to influence the process of atherosclerotic disease development and alteration of vascular function [248]. Cyclooxygenase isoform 1 (COX-1) is constitutively expressed; its activity has been shown to accelerate atherosclerosis in the $LDLR^{-/-}$ mouse model [249] and genetic ablation of the thromboxane A_2 receptor has been linked to retardation of disease development [250]. Cyclooxygenase isoform 2 (COX-2) is not expressed in healthy vascular tissues. There is a clear link between inflammation, inflammatory cytokines and an inducement of COX-2 expression [251,252], however evidence for the role of cyclooxygenase-2 (COX-2) and prostacyclin in atherosclerosis is a little less clear. Specific inhibition of the COX-2 enzyme has been demonstrated to inhibit early atherogenesis in mice [253–255], however, in female mice COX-2 activity has been described as atheroprotective [256] and genetic ablation of the prostacyclin receptor was shown to enhance atherosclerosis [250]. An increase in the number of cardiovascular events and the subsequent market withdrawal of the selective inhibitor Rofecoxib (Vioxx, Merck) [257] suggests that in humans COX-2 activity is anti-atherogenic. Obesity and the associated inflammation are therefore able to modulate vascular function, however, the highlighted studies have all assessed this parameter at advanced time points; the early actions of possible changes in perivascular adipocyte morphology, inflammation and cyclooxygenase activity are less well understood at this time.

Table 1. A summary of relevant literature relating to the assessment of lipidaemic profiles and obesity in C57BL/6 and ApoE$^{-/-}$ mice after feeding on a chow or high fat (HF) diet.

Strain and diet	Duration (weeks)	Cholesterol (mmol/L)	Triglycerides (mmol/L)	Body weight (g)	References
C57BL/6 Chow	2.5	1.6	1.7	-	Plump *et al.* (1992)[138]
	12	-	-	24.7	Fransen *et al.* (2008)[178]
	12	2.2	-	-	Shimano *et al.* (1995)[258]
	16	-	-	30.0	Schreyer *et al.* (2002)[145]
	78	1.6	-	-	Crauwels *et al.* (2003)[174]
C57BL/6 HF	2.5	3.4	2.1	-	Plump *et al.* (1992)[138]
	12	3.7	-	-	Shimano *et al.* (1995)[258]
	16	-	-	44.9	Schreyer *et al.* (2002)[145]
	28	2.8	1.1		Jiang *et al.* (2001)[259]
ApoE$^{-/-}$ Chow	2.5	12.8	2.8	-	Plump *et al.* (1992)[138]
	8	11.5	1.9	-	Burleigh *et al.* (2002)[254]
	8	15.2	-	-	Ali *et al*. (2005)[260]
	12	-	-	22.5	Fransen *et al.* (2007)[178]
	78	11.8	-	-	Crauwels *et al.* (2003)[174]
ApoE$^{-/-}$ HF	2.5	47.1	2.8	-	Plump *et al.* (1992)[138]
	8	23.3	-	-	Bjorkbacka *et al.* (2004)[261]
	10	27.1	-	-	Bjorkbacka *et al.* (2004)[261]
	16	-	-	35.2	Schreyer *et al.* (2002)[145]
	28	27	3.8	-	Jiang *et al.* (2001)[259]

1.6. Hypothesis and aims

The hypothesis of this study is that vascular function is modified by the presence of atherosclerotic risk factors, prior to the development of overt atherosclerosis.

The specific aims and objectives of this project are as follows:

1. **To assess the effects of acute cholesterol modulation on *ex vivo* murine thoracic aortic function.**

   The direct effects of membrane cholesterol modulation will be assessed in the thoracic aortae of wildtype C57BL/6 mice. Methyl-β-cyclodextrin will be employed to deplete membranes of cholesterol and water-soluble cholesterol will be employed to increase extracellular cholesterol and promote enrichment of vascular membranes. Both removal and enrichment of membrane cholesterol will be carried out. Vascular function including contractility to depolarisation, contractility to pharmacological agonists and endothelial-dependent and independent relaxation will be assessed using wire myography.

2. **To assess the effect of high fat feeding and/or ApoE gene deletion on the phenotype of mice in the early stages of atherosclerosis.**

   C57BL/6 and ApoE$^{-/-}$ mice will be fed on either a standard chow or a high fat diet for eight weeks post-weaning. As the focus of the present investigation is vascular function prior to the development of atherosclerotic plaques the extent of plaque formation will be assessed in the aorta as a whole and specifically within the thoracic aorta. The aim of the four described experimental groups is to generate a gradient of cholesterol concentrations, as shown previously by Plump *et al.* (1992) [262], allowing concentration-dependent effects and a direct link to serum cholesterol to be made in relation to vascular function. In addition, the specific effects of high fat feeding and ApoE gene deletion will be able to be defined. Assessing the lipidaemic profile to confirm the gradient of serum cholesterol concentrations is of great importance. However, as described previously, there is a need to explore the effects of other

atherosclerotic risk factors. To this end, total weight characteristics and visceral and perivascular adiposity will be measured to assess the development of obesity. Markers of systemic and local inflammation, namely spleen weight and perivascular adipocyte size, will also be investigated. Finally, fasting blood glucose will be measured to deduce the existence of diabetes and markers of smooth muscle proliferation will be assessed via immunohistochemistry as further evidence of the stage of disease development.

3. **To investigate alterations in vascular function prior to the development of atherosclerosis.**

   Using the same approach to the assessment of vascular function as in the first objective, the responses of thoracic aortic rings from the previously described four experimental groups will be determined. Alterations in vascular function will be highlighted and further examined mechanistically through the use of pharmacological antagonists of selected contributors, such as eNOS or COX activity. In addition, intracellular calcium imaging with the calcium-sensitive dye indo-1 will be used to assess smooth muscle calcium handling; in particular SOCE enabling a correlation to be made between possible changes in proliferation and contraction in vascular tissues. In order to achieve this aim a calcium imaging system will have to be set up and optimised prior to data generation.

Overall, through the achievement of these aims and objectives, and collation of the results as a whole, this study hopes to identify and explore the source of early changes in vascular function and how this may contribute to atherosclerotic disease development.

2. Materials and Methods

Suppliers of materials and reagents are listed in Appendix I. Recipes for solutions and buffers are listed in Appendix II.

2.1. Animals

All experiments were conducted in accordance with the Animals (Scientific Procedures) Act 1986, within the constraints of the relevant Home Office project and personal licences.
Control wild type mice, C57BL/6 strain, were obtained from Harlan laboratories at a range of ages dependent on the experimental requirements. $ApoE^{-/-}$ mice were originally produced by Jackson Laboratories through backcrossing with C57BL/6 mice after homologous recombination in embryonic stem cells creating a mutation in the ApoE gene ($ApoE^{tm1Unc}$). The colony of $ApoE^{-/-}$ mice was maintained in the University of Manchester Biological Services Unit and they were provided with food and water *ad libitum*.

2.1.1. Diet modulation

$ApoE^{-/-}$ mice were weaned at 3-4 weeks dependent on their level of development, only male offspring were taken forward for experimentation with the females either being maintained for breeding purposes or sacrificed at this time. The males of each litter were housed together and either transferred onto a high fat 'western' diet containing 21% milk fat and 0.15% cholesterol or were designated as a non-high fat group and maintained on rat and mouse standard diet No.1 (Chow; 0.5% milk fat, 0.022% cholesterol).

Control C57BL/6 mice designated to be fed on the high fat 'western' diet were brought in at three weeks of age and maintained for at least eight weeks before experimentation. Control mice designated as being in a non-high fat group were brought in at 11 weeks of age and maintained for at least 1 week before experimentation to allow for acclimatisation.

2.1.2. Experimental groups

For the purposes of this investigation four primary experimental groups were generated as shown in Figure 2.1. below. At times during the investigation feeding of either C57BL/6 wild type or $ApoE^{-/-}$ mice for longer time periods was conducted. The use of these additional groups will be stated explicitly in the analysis.

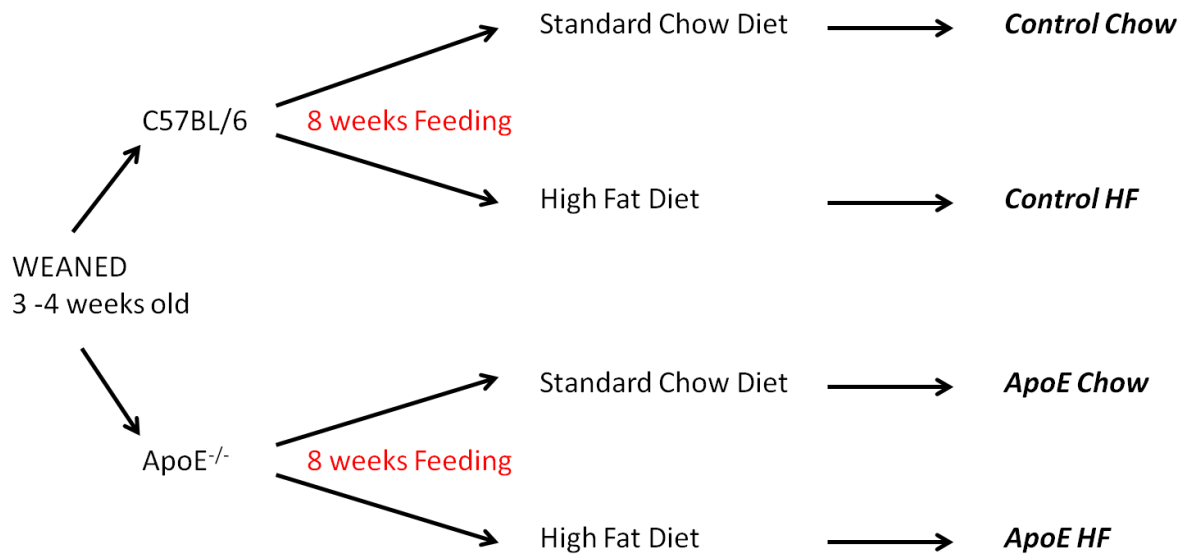

Figure 2.1. Generation of the experimental groups. All mice were fed either a standard chow diet (0.5% fat, 0.022% cholesterol) or high fat 'western' diet (21% fat, 0.15% cholesterol) and were experimented on after eight weeks feeding (post-weaning).

2.2. PCR genotyping of ApoE$^{-/-}$ mice

2.2.1. DNA isolation

Ear snips were obtained from ApoE$^{-/-}$ mice and stored at -20^{o}C prior to analyses. To each sample was added 200µl lysis buffer along with 10 µl proteinase K (1mg/ml). Samples were incubated overnight at 56^{o}C; the following morning they were centrifuged at 18,894g (13,00rpm) for 10 minutes. Supernatants were transferred to fresh tubes to which was added an equal amount of isopropanol (approximately 200 µl). After inverting 30 times, the samples were left on ice for 30 minutes. Samples were then centrifuged at 13,000rpm for five minutes before the supernatants were removed carefully and discarded without disturbing the pellets. The pellets were washed in 100 µl 70% ethanol by pipetting up and down prior to another centrifugation at 13,000rpm for 5 minutes. Pellets were air dried for approximately 10 minutes before being re-suspended in 25µl to 50µl of Tris-EDTA (TE) buffer.

2.2.2. PCR

A 25 µl PCR reaction was prepared by making a master mix with the following amounts of reagents: 3 µl 10X Buffer, 2.4 µl $MgCl_2$ (25mM), 2.4 µl dNTPs (2.5mM), 0.15 µl Taq Polymerase (5U/µl), 0.75 µl of each ApoE primer (20 µM):

oIMR180 (forward – 5'-GCCTAGCCGAGGGAGAGCCG);

oIMR181 (reverse – 5' TGTGACTTGGGAGTCTGCAGC);

oIMR182 (forward – 5'-GCCGCCCCGACTGCATCT).

Primer pair oIMR180 and oIMR181 were used to amplify the 155-bp wild type ApoE amplicon while the primer pair oIMR180 and oIMR182 were used to amplify a 243-bp vector-containing ApoE amplicon. Finally, 5 µl of DNA (or water for the negative control) was added.

The remainder of the reaction volume was made up using water before being subjected to the following cycling conditions in a Peltier PTC-2000 Thermal Cycler: 94^{o}C for 3 minutes, 94^{o}C for 20 seconds, 68^{o}C for 40 seconds, 72^{o}C for 2 minutes, 72^{o}C for 10 minutes, held at 4^{o}C.

Samples were loaded onto a 1.5% agarose gel containing 4 µl ethidium bromide (1mg/ml) with a DNA marker, Hyperladder V (5 µl). The samples were then run in 0.5X TAE buffer at 60 – 70mV for approximately two hours. The gel was observed using a Uvitech transilluminator and the image captured using Uvipro platinum software (Version 1.1).

2.3. ApoE$^{-/-}$ mouse phenotyping

2.3.1. Tissue sampling

Mice were weighed and then anaesthetised with an intraperitoneal injection of sodium pentobarbitone (Pentoject; 40mg per 30g body weight, overdose to induce death). Once fully anaesthetised, determined by the lack of reflex withdrawal to toe pinching, the animals were

pinned out and a midline incision was made followed by blunt dissection to expose the peritoneum. The peritoneum was cut down the midline, exposing the inner organs, and the rib cage was cut either side of the sternum. After cutting the diaphragm the ribs were opened out laterally, held by surgical grips, exposing the heart. The left ventricle was cannulated and perfused with Hepes-PSS for five minutes at a rate of approximately 3mls per minute using a peristaltic pump (Minipuls 3, Gilson, UK) connected to a needle (23G Microlance3; BD Medical, NJ, USA) (Figure 2.2)

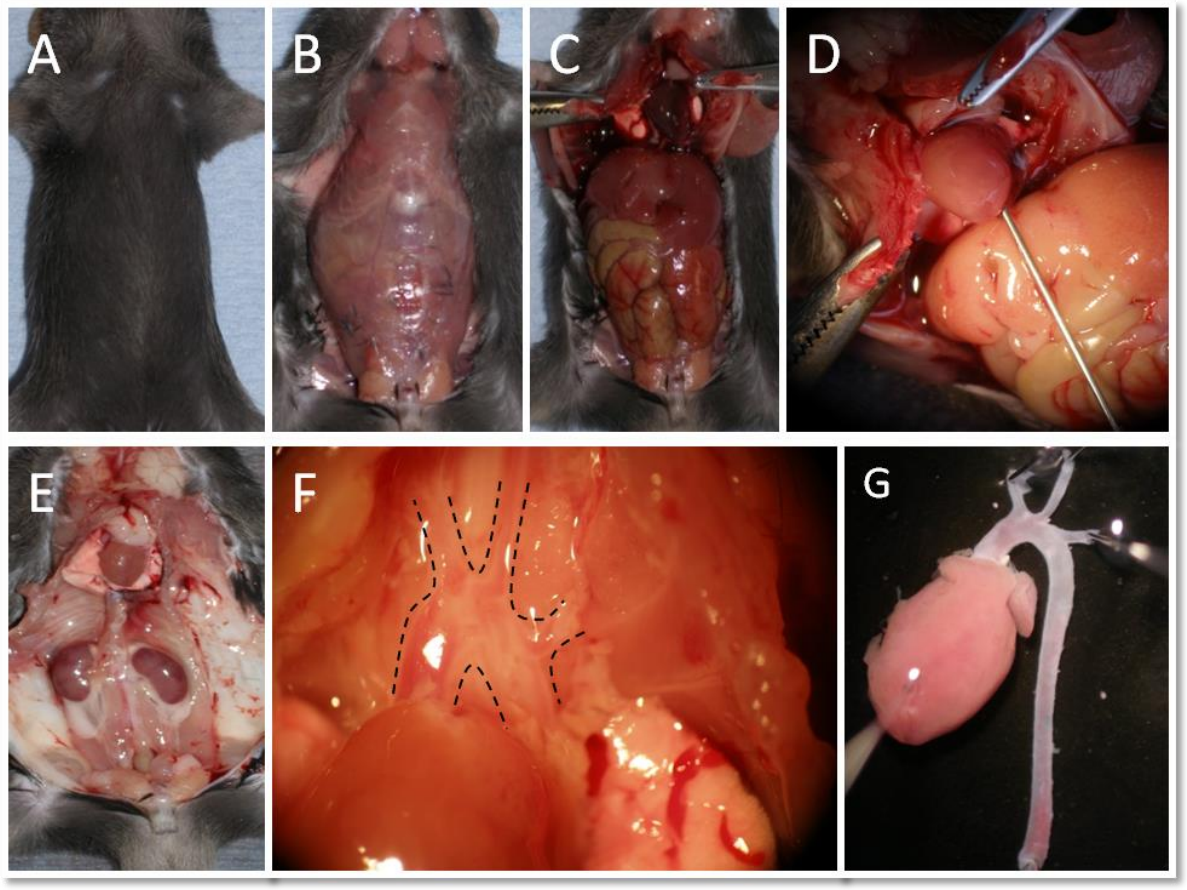

Figure 2.2. Dissection of the murine aorta. The heavily anaesthetised animal was secured on its back (**A**) before the peritoneum was exposed with an incision down the midline using blunt dissection to remove the skin (**B**). The peritoneum and the rib cage were then opened up to reveal the internal organs of the abdomen and expose the heart (**C**). The heart was cannulated and perfused at a rate of 3ml/min with ice cold HEPES-PSS for five minutes (**D**). The organs of the abdomen were removed; liver, stomach, pancreas, spleen, intestines (**E**). The aortic arch and its branches (dashed lines) were visualised, and along with the rest of the aorta, dissected out (**F**). The dissected aorta, still attached to the heart was then removed from the animal and placed in a petri-dish containing ice cold HEPES-PSS for isolation of the thoracic aorta and depending on the necessary preparation, removal of the remaining adventitial tissue (**G**).

The aortic arch and thoracic aorta, still attached to the heart, were then dissected away from the rear of the thoracic cavity, removed, and placed in ice-cold phosphate-buffered saline (PBS). This preparation was later pinned out on a silicone coated petri dish to allow for isolation of the thoracic aorta, the perivascular adipose tissue was left intact. In addition to the heart and thoracic aorta, the spleen and epididymal fat pads were also removed from each animal. The thoracic aorta was taken for further processing, dependent on the technique to be employed, the details of which will be outlined later in Section 2.3.2. The heart, spleen and epididymal or peri-gonadal fat pads were weighed, wet weight after removal of excess fluid from transport, for future comparisons.

2.3.2. Histology

2.3.2.1. Preparation of thoracic aortic tissue for histology

Thoracic aortae were stored in 4% PFA at 4^{o}C for 48hrs. These aortae were then placed into plastic histology cartridges; the tissue was wrapped in thin rolling paper to prevent it being washed out of the cartridge, and suspended in 50% industrial methylated spirits (IMS). The samples were subjected to a process of dehydration followed by infiltration of paraffin wax in a 60^{o}C vacuum oven using a Shandon Citadel 2000 tissue processor. Samples were then removed from the rolling paper and embedded vertically, to allow transverse cross-sections of the vessel to be taken, in a mould filled with molten paraffin wax. The wax was allowed to cool slightly before the labelled cassette lid was placed on top and the molten wax topped up. Once the wax had set hard, the blocks were removed from the moulds and stored at room temperature.

Wax blocks were sectioned using a Leica RM2145 microtome. Sections, 5µm in thickness, were floated onto the surface of a water bath at 45^{o}C before being placed onto poly-l-lysine coated microscope slides. These slides were dried vertically overnight at 37^{o}C to allow any water to run off and then were melted at 60^{o}C and allowed to cool prior to storage at room temperature.

2.3.2.2. Haematoxylin and Eosin (H&E) staining for identification of atherosclerotic plaque development

Sections, prepared as above, were de-waxed in xylene and rehydrated through a series of graded alcohols (100%, 90%, 75%, 50%; diluted in distilled water), before being washed in distilled water for five minutes. Mayer's haematoxylin, diluted 2:3 with distilled water, was applied for two minutes and then sections were washed for five minutes in warm tap water. The slides were then placed in 1% eosin Y solution for 30 seconds, dipped in distilled water two to three times, and dehydrated back through the graded alcohols (50%, 75%, 90%, 100%). The sections were mounted under glass coverslips using DPX mounting medium and left overnight to dry before observation. Sections were visualised using bright-field microscopy under a Leica DM 5000 B microscope; images were captured using a Leica DFC 320 camera and Leica Imaging software.

2.3.2.3. Quantification of atherosclerotic plaque development

As defined previously in our lab, quantification of lesion development was carried out using five sections at 25μm intervals (Kelly Farrell, PhD Thesis, 2009) from the proximal end of the thoracic aortae, defined by the first intercostal artery branch. After staining with Millers Elastin van Gieson to stain the elastic laminae images were taken for quantification. Using Image J software the internal lumen area was defined. The internal elastic lamina was then traced and the previous lumen area was subtracted to leave only the area of the intima. The intimal area was used as a measure of atherosclerotic plaque development [263].

2.3.2.4. *en face* Oil Red O staining for visualising intravascular fat deposition

Thoracic aortae were dissected as previously described. Extra care was taken to remove the adventitia completely; the adventitia is stained by Oil Red O and would result in background noise. The entire aorta was then cut longitudinally between the intercostal arteries. The tissue was dipped into 60% (v/v) aqueous triethyl phosphate for 2 – 3 seconds before being treated with the Oil Red O working solution for 20 minutes on a shaking platform. After incubation the vessel was removed from the Oil Red O and dipped once again in 60% (v/v) triethyl phosphate for two to three seconds. The tissue was then washed in distilled water before being pinned down flat on a silicone coated petri dish. This enabled visualisation of the inner

surface of the aorta and in this position it was photographed using an Olympus Camedia c-7070 wide zoom camera attached to a dissection microscope. Only a visual assessment was conducted with no formal measurement being applied.

2.3.3. Immunohistochemistry for the assessment of smooth muscle phenotype

Immunohistochemistry was used to assess the localisation of specific markers of contractile smooth muscle cells, namely α-smooth muscle actin (α-SMA), smooth muscle myosin heavy chain II (smMHCII) and smoothelin, within the thoracic aorta. The presence of both α-SMA and either smMHCII or smoothelin is indicative of a contractile phenotype. Proliferative smooth muscle cells will not express only α-SMA. Thoracic aortic samples were prepared as described previously in Section 2.3.2.1.

After de-waxing through xylene and rehydration through alcohols down to distilled water, as described previously (Section 2.3.2.2), endogenous peroxidase activity was inhibited by incubation for five minutes with 3% (v/v) hydrogen peroxide (H_2O_2). The tissue was then washed in PBS (3 x 5 minutes) and the sections were drawn around with a wax pen to allow individual sections on the same slide to be incubated with different solutions, if necessary. Non-specific binding of immunoglobulins was blocked by incubating sections with the appropriate serum for one hour at room temperature; 50µl of a 10% serum, 1% bovine serum albumin (BSA) solution was applied to each section.

The blocking solution was removed and without washing, the appropriate concentration of primary antibody, diluted in 1% BSA PBS, was applied for one hour at room temperature or 4^{o}C overnight. Negative control sections were produced by omitting the primary antibody and incubating with 1% BSA PBS alone. After washing with PBS (3 x 5 minutes) the appropriate secondary antibody was applied (50µl, diluted in 1% BSA PBS) for one hour (in the case of α-SMA no secondary antibody was necessary as a conjugated primary antibody was used). When using non-fluorescent secondary antibodies the slides were washed in PBS (3 x 5 minutes) before being incubated with Vectastain ABC (avidin-biotin conjugate) solution for 30 minutes at room temperature. After washing in PBS (3 x 5 minutes) a DAB (3,3'-diaminobenzedine) kit was applied, made up to the manufacturer's instructions, until a brown colour developed (5 – 10 minutes); the reaction was stopped by immersing the slides in distilled water. Slides were counterstained with Mayer's haematoxylin for one minute,

washed in warm tap water, dehydrated through graded alcohols and then mounted using DPX mounting medium. When using fluorescent secondary antibodies, the slides were washed in PBS (3 x 5 minutes) after incubation and mounted immediately using a mounting medium containing DAPI (4',6-diamidino-2-phenylindole) nucleic acid stain (Vectashield). Sections were again visualised using a Leica DM 5000 B microscope; images were captured using a Leica DFC 320/350FX camera (brightfield and fluorescence, respectively). See Appendix III for a full details of antibody optimisation.

2.3.4. Measurement of plasma glucose and lipids

Blood samples, 0.3 -0.5ml, were taken at sacrifice via cardiac puncture from animals that had been fasted overnight. Glucose measurements were made immediately whereas all lipid analyses were performed after the blood had been spun at 1700g (3000rpm), maintained at 4^{o}C, for 10 minutes to separate the plasma. Plasma was stored at -80^{o}C prior to use. Lipidemic profile analysis was performed by Yifen Liu of the Lipid Biology Research Group, Manchester University, UK.

2.3.4.1. Fasting blood glucose

Fasted blood glucose levels were measured via the glucose oxidase method. Glucose oxidase is combined with a peroxidase to colorimetrically assess the production of H_2O_2. This was achieved using the hand-held Contour® blood glucose monitoring system (Bayer, Germany). After installation of the test strip into the reader, it was placed into the blood sample for five seconds and the reading, expressed in mmol/L, on the monitoring system was recorded. A new strip was used for each sample [264].

2.3.4.2. Triglycerides

Plasma triglyceride measurements were performed using an automated colorimetric glycerol-3-phosphate Oxidase-PAP. Triglycerides are hydrolysed with lipases to produce glycerol and fatty acids. The activity of glycerol kinase produces glycerol-3-phosphate. Oxidation of glycerol-3-phosphate produces H_2O_2 which through the action of peroxidase can be measured through the formation of a quinoneimine based indicator [265]. The analysis was carried out using a bench top clinical chemistry analyzer (Cobas Mira, Roche). Plasma triglyceride concentrations are expressed in mmol/L.

2.3.4.3. Cholesterol

Total fasting plasma cholesterol concentrations were measured using an automated enzymatic end point assay (Randox Laboratories Ltd.). Cholesterol esters are enzymatically cleaved by cholesterol esterases to produce free cholesterol. The action of cholesterol oxidase on cholesterol produces H_2O_2 which can again be measured through the action of peroxidase and the formation of a quinoneimine based indicator [266]. Plasma HDL-cholesterol concentrations were measured using an enzymatic clearance assay (Randox Laboratories Ltd.). In an initial reaction other cholesterol components (LDL-, VLDL-cholestrol and chylomicrons) are removed through the actions of cholesterolase, cholesterol oxidase and catalase. A second treatment with cholesterolase and cholesterol oxidase allowed detection of the HDL concentration through the peroxidation of H_2O_2 to produce the quinoneimine indicator. Both analyses were performed on a Cobas Mira automated bench top biochemical analyzer (Roche) [267,268].

2.3.5. Quantification of perivascular adipocyte size and number as a marker of obesity

Paraformaldehyde fixed, paraffin embedded mouse thoracic aortae with the perivascular adipose tissue (PVAT) intact were cut into 5µm sections and mounted onto poly-l-lysine coated microscope slides; whereupon they were stained with Mayer's haematoxylin and eosin Y (H&E) stain, as previously described (Sections 2.3.2.1 - 2.3.2.2) for the detection of adipocyte membranes.

Images were captured using a Leica DFC 320 camera attached to a Leica DM 5000 B microscope. PVAT was defined as being within 150µm of the vessel wall and the population was subdivided into small ($<5\mu m^2$) and large ($>5\mu m^2$) adipocytes. The area was calculated by drawing round the "adipocyte ghost", the membrane that remains after processing of the tissue through xylene and alcohols. This was performed using Image J software that was calibrated prior to taking measurements. The counting of adipocyte populations were also performed on Image J. All measurements were performed by an operator blinded to the experimental groups in order to reduce bias.

In order to produce results that were representative of the population, an initial analysis was conducted. Within a field of view (FOV) measuring 260x193µm a region of interest (ROI),

50x50µm, was randomly chosen and the small and large adipocyte area and number was calculated. Progressive mean values were obtained for each individual ROI, both cell number and area (e.g. mean of ROIs 1 + 2, mean of ROIs 1 + 2 + 3, etc.), to assess after which point the standard error of the mean became consistent. From this it was determined that all further sections were to be analysed using 3 separate FOVs. For quantification of adipocyte area it was determined that 4 ROIs per FOV were required and for quantification of adipocyte number 6 ROIs per FOV were required.

Data were represented as the mean ± standard error of the mean (SEM) for all measurements. Differences in mean adipocyte area and mean adipocyte number were assessed using a one way ANOVA with a post-hoc Tukey's multiple comparison test. All analyses used Prism software (GraphPad, USA). Probability values of $p<0.05$ were deemed significant.

2.4. Wire myography

2.4.1. Preparation of thoracic aortae

The aorta was removed as previously described in Section 2.3.1. It was then transported in ice cold HEPES-PSS and pinned down in a silicone lined dissection plate. Using a stereoscopic dissection microscope along with fine forceps and scissors the adventitial tissue, including connective and perivascular adipose tissue, was carefully removed. The thoracic aorta was separated from the aortic arch and four 3mm rings were cut from the proximal end starting from the origin first intercostal artery.

2.4.2. Mounting and normalisation

The thoracic aortic rings were placed into separate baths of a multi-chamber myograph (Danish Myo Technology, Arhaus N, Denmark), each containing 6ml of ice-cold HEPES-PSS. HEPES buffered solutions were employed due to their ability to maintain a stable pH; this was of great importance to the imaging of intracellular calcium (Section 2.5) due to the sensitivity of the indo-1 dye to pH. The rings were mounted into the jaws of the individual baths using two 40µm diameter tungsten wires. Upon completion of this mounting procedure, the bath solutions were immediately gassed with 100% oxygen and allowed to warm to 37^{o}C over the course of 20 minutes. During this time, no tension was applied to the vessel

segments. After this initial acclimatisation period, the tension on the aortic rings was increased incrementally over a 30 minute period until the tension was stable at 5mN, as described previously [269].

2.4.3. Assessment of viability and contractility

When stable at 5mN resting tension the HEPES-PSS was aspirated and replaced with HEPES-KPSS (100mM KCl isosmotically substituted for NaCl) to elicit contraction. Once a stable contraction was produced (3 – 5 minutes), the bath solution was aspirated and replaced three times with HEPES-PSS to remove the contractile stimulus completely and allow the vessel to relax to its resting tension. This process was repeated twice on every vessel segment prior to the addition of any other stimuli. This allowed for confirmation of vessel viability but also represented a standard contraction that all further contractions would be normalised against. Using this method of standardisation to compare across different vessels, the data in this thesis relating to agonist induced contractions will be presented as a percentage of the final HEPES-KPSS induced contraction, as used by studies on other large vessel preparations [270–272].

2.4.3.1. Agonist-induced contractions

Initial cumulative dose-response curves were constructed for phenylephrine and serotonin (5-HT) using a 1nM – 30µM range of concentrations (Figure 2.3.). From these data it was decided that a maximal dose for both agonists, to be used in future experiments, was 10µM. For both agonists, a 10mM stock solution was produced fresh at the start of each week and stored on ice during experiments and at 4^{o}C overnight to maintain the stability of the compounds. To achieve the desired final bath concentration, 10µM, 6µl of the stock solution was added into the 6ml bath volume.

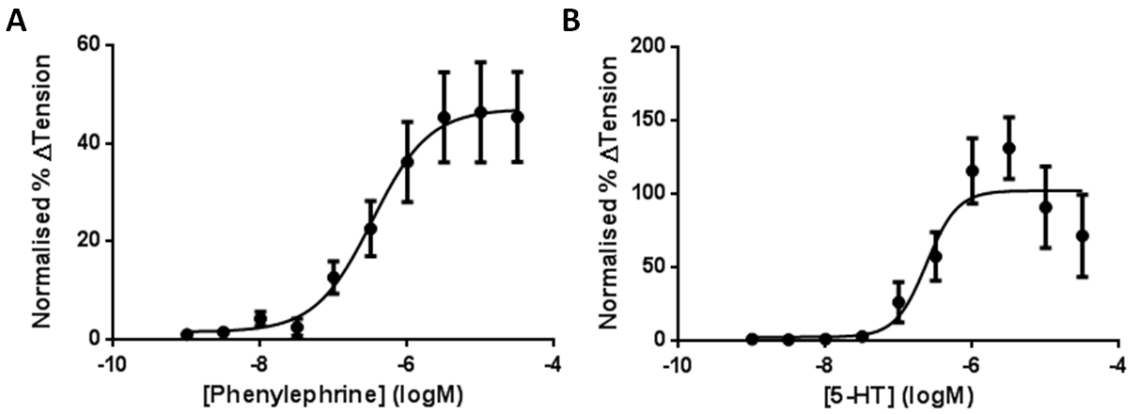

Figure 2.3. Cumulative dose-response curves in the presence of phenylephrine and serotonin to assess maximal contractile response. Thoracic aortic rings, mounted on a wire myograph and set to a resting tension of 5mN, were exposed to increasing concentrations of phenylephrine (**A**) and serotonin (5-HT; **B**). The concentration range employed was 1nM – 30μM. The contractile data were normalised to the relevant contraction to HEPES-KPSS and are expressed as mean ± SEM (n = 4 for each treatment). The maximal contractile response was defined on the plateau phase of the sigmoidal curve. For both agonists 10μM was taken forward as the concentration to be used in subsequent experiments.

2.4.4. Stimulating endothelium-dependent and independent relaxations

Aortic rings were firstly pre-constricted with 10μM phenylephrine until a steady contraction was produced. Maximal concentrations, 10μM, of both acetylcholine and sodium nitroprusside were used to induce endothelium-dependent and independent relaxation, respectively. A 10mM stock was made at the start of each week for both compounds and maintained on ice during the experimental protocol and at 4^{o}C overnight. After each exposure to both compounds the baths were aspirated three times and the bath fluid replaced with fresh HEPES-PSS before leaving the aortic rings to return to their baseline tension for at least 10 minutes.

2.4.5. *Ex vivo* modulation of cholesterol

2.4.5.1. Cholesterol removal

Methyl-β-cyclodextrin (MβCD) was employed to remove cholesterol from thoracic aortic rings, as previously described [128,187,273]. The entire bath volume was aspirated and replaced with HEPES-PSS containing 10mM MβCD. This solution was left to incubate for one hour. The same MβCD-containing solution was used for all subsequent washes and remained

present throughout the experiment. The total exposure time to MβCD-containing solution was approximately 120 minutes.

2.4.5.2. Cholesterol addition

Water-soluble cholesterol (≈40-45mg cholesterol/g of MβCD), as used in previous studies to increase membrane cholesterol [168], was dissolved in HEPES-PSS to a concentration of 5mM. Once again the bath was aspirated and the cholesterol-containing solution was used to replace it. The aortic rings were incubated with the raised level of extracellular cholesterol for one hour. Again this solution was used for all subsequent washes and was present for the remainder of the experimental protocol.

2.4.6. Pharmacological inhibitors of nitric oxide and prostaglandin signalling

Pharmacological inhibitors were used to assess the impact of several components on endothelium-dependent relaxation. Nitric oxide synthase was inhibited through the use of the Nω-nitro-L-arginine (L-NNA; 50μM [274]). Total cyclooxygenase activity was blocked through the use of indomethacin (10μM; dissolved in DMSO, final bath concentration 0.05% [275,276]). Specific activity of cyclooxygenase-2 was inhibited through the addition of celecoxib (5μM; dissolved in DMSO, final bath concentration 0.1% [277]). All inhibitors were made up to larger volumes in HEPES-PSS allowing for total exchange of the bath solution to promote even distribution across the tissue. Tissues exposed to the inhibitors were incubated for one hour. The inhibitor-containing solutions were used after incubation for all washes so as to be present throughout the experimental protocol.

2.4.7. De-endothelialisation thoracic aortic rings

In some experiments the endothelium was removed to enable its contribution to vascular function to be assessed. To achieve this, after checking the initial viability of the tissue with HEPES-KPSS at 5mN resting tension, the myographs were removed and placed under a stereoscopic dissection microscope. The tension on the aortic ring was reduced slightly and a single horse hair, due to its coarse exterior, was passed through the lumen. The horse hair was then rotated gently around the internal surface of the vessel segment for approximately one

minute. The tension was then completely removed and the bath solution replaced three times with fresh HEPES-PSS. The aortic rings were left, gassed with 100% oxygen and maintained at 37^{o}C, for 20 minutes. After this time the tension was again incrementally increased back to 5mN over the course of 20 minutes. When a stable baseline tension of 5mN had been achieved the aortic rings were exposed to HEPES-KPSS twice to check for damage to the contractile tissue. This was achieved through comparison to the initial viability testing; aortic rings which showed >20% reduction in HEPES-KPSS contractility were discarded from analyses. In the presence of an intact endothelium the response to acetylcholine after pre-constriction with 10μM phenylephrine is approximately 50% relaxation; therefore, endothelium removal was confirmed by the lack of response (<20% relaxation) to acetylcholine.

2.4.8. Inducing store-operated calcium entry in the thoracic aorta

In order to investigate the effect of store-operated calcium entry on thoracic aortic contractility, tissues were incubated in calcium free HEPES-PSS for 30 minutes; after the fore mentioned normalisation and viability assessment. After this time the bath solution was replaced with HEPES-PSS containing 10μM cyclopiazonic acid (CPA; dissolved in DMSO, final bath concentration 0.05% [186]). After 30 minutes incubation, the extracellular calcium was returned with CPA still present in the bath solution. After 20 minutes the tissues were washed with HEPES-PSS to remove the CPA. When a stable baseline had been achieved, the viability of the tissue was again assessed through exposure to HEPES-KPSS.

2.4.9. Data analysis and statistics

All recordings were made using LabChart (Version 7.; ADInstruments, Oxford, UK). All measurements were taken at the maximal stable level of contraction/relaxation. Contractions to HEPES-KPSS are represented as actual changes in tension (mN). Agonist induced contractions are normalised to the relevant HEPES-KPSS contraction and expressed as a % change in tension. Stimulations performed after exposure to pharmacological inhibitors are normalised to the post-incubation HEPES-KPSS. All relaxations are represented as a percentage reduction in tension from the peak tension prior to exposure (% relaxation).
All data are expressed as means ± standard error of the mean (SEM). All data were analysed using Prism analysis software (Version 6.; GraphPad, California, USA). Comparisons

between the experimental groups were made using a one-way analysis of variance (ANOVA) with a post-hoc Tukey's multiple comparisons test. A $p<0.05$ was considered significantly different

2.5. Intracellular calcium imaging for the assessment of store-operated calcium entry in the thoracic aorta

2.5.1. Tissue preparation and mounting

Thoracic aortae were dissected and the adventitia removed as previously described. Two to three aortic rings were taken and then cut longitudinally in between the intercostal arteries. The strips were incubated in HEPES-PSS containing the acetoxymethylester form of the calcium-sensitive fluorescent dye indo-1 (20μM; 1mM stock solution made up in DMSO containing 20% pluronic acid [278]) for three hours in the dark at room temperature. Following incubation with indo-1, a strip was mounted into a bespoke imaging chamber. The imaging chamber for mounting and visualising strips of mouse aortae was created in-house (Chemistry department workshop, Manchester University) to specifications allowing it to be fitted securely onto the existing Nikon Diaphot-TMD microscope. The imaging chamber was designed to have a bath volume of 1mL when a cover slip was secured to the underside, using high vacuum grease (Dow Corning, USA), enabling a fast bath volume exchange time. Glass capillary tubes were bent and cut to serve as inflow and outflow tubes before being secured to the imaging chamber with silicone rubber compound; these were then able to be connected to the existing inflow and outflow tubing of the pressure myograph. Insect pins were bent and secured to either side of the imaging chamber to create hooks on to which the tissue could be mounted; the smooth muscle layer was placed in the path of excitation as this was the tissue of interest (Figure 2.4).

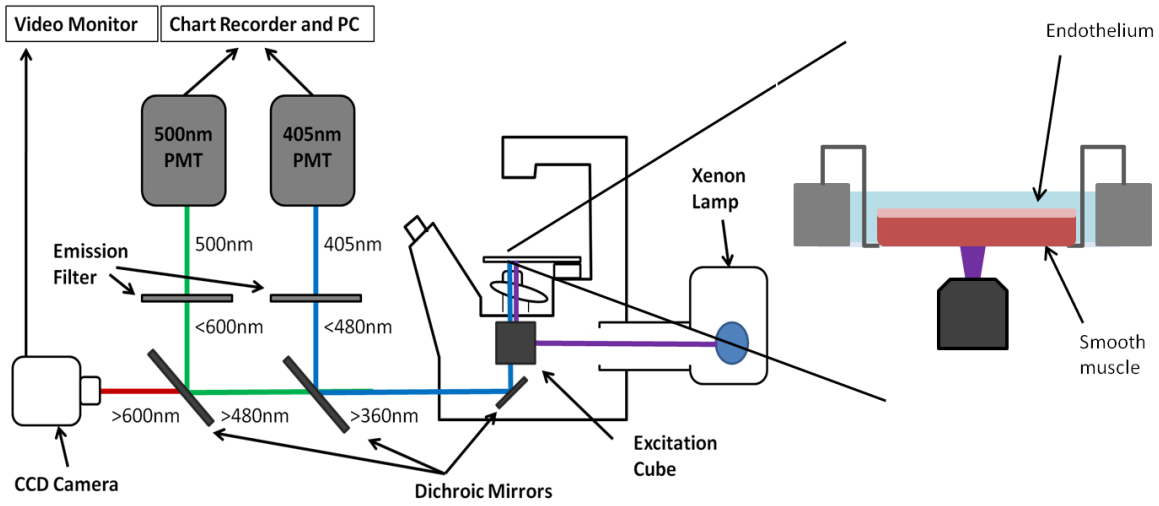

Figure 2.4. Imaging intracellular calcium. An inverted microscope was used to image an opened out section of thoracic aorta, pre-loaded with the calcium-sensitive fluorescent dye Indo-1 (20μM) for three hours at room temperature and mounted to allow imaging of the smooth muscle. UV light from the xenon lamp was filtered and directed towards the indo-1 loaded tissue by the excitation cube within the microscope. The tissue was excited at 340nm and the emitted light then filtered by a dichroic mirror, allowing only light >360nm to pass through towards the photomultiplier tubes (PMTs). A second dichroic mirror was used to direct light <480nm up, through a 405nm emission filter, to the PMT. Similarly, a third dichroic mirror was employed to reflect light <600nm up, through a 500nm emission filter, into another PMT. The remaining light >600nm was detected by a charge-coupled device (CCD) camera, allowing visualisation of the vessel on a monitor. The signals from PMTs were then transmitted to the pre-amplifiers and recorded via Lab Chart software on a PC.

2.5.2. Calcium imaging apparatus

Due to the light-sensitivity of indo-1 and the photo-recording instruments, all incubations and recordings of $[Ca^{2+}]_i$ were conducted in the dark using only the minimum amount of light necessary for mounting and adjustment of the system. The mounted and loaded tissue was visualised on a Diaphot-TMD microscope (Nikon, Japan) with a 10x Fluor objective (via a 600nm filter; 25nm bandpass, Cairn research, Kent, UK). Tissues were excited at 340nm using a high-intensity xenon light source (XPS-100; Nikon). Background fluorescence, observed when the tissue is removed from the field of view (FOV), was reduced by closing FOV to highlight only the section of vessel; this dramatically reduced the emitted signal intensity but enabled a true assessment of the fluorescence in the tissue. The emitted light was filtered using two dichroic mirrors deflecting the relevant wavelengths of light to two photomultiplier tubes (PMTs) with 405nm and 505nm bandpass filters in front of them, respectively (15nm bandpass, Cairn Research). The PMTs were powered by a variable power supply units (Cairn Research) set at 1000V for each PMT. The signals from these PMTs

were passed through pre-amplifiers (Cairn Research) and recorded on a PC running WinDaq acquisition software (Version 3.28; Dataq Instruments, USA) via a DI-720 data acquisition system (Dataq Instruments) (Figure 2.2). The calcium imaging apparatus was validated through the use of the free acid form of the indo-1 dye, pentopotassium salt, which is able to bind calcium without the need for enzymatic cleavage. Excitation was measured in calcium free HEPES-PSS and then in the presence of 5mM CaCl with both solutions containing 2µM indo-1 pentopotassium salt (Figure 2.4)

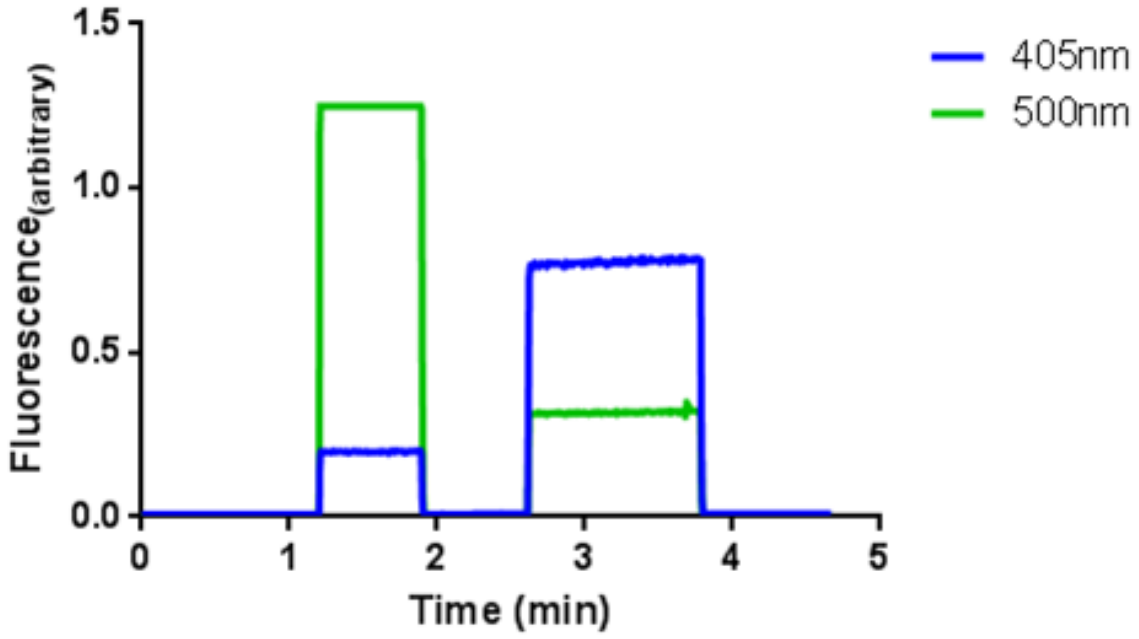

Figure 2.5. Validation of calcium imaging equipment. In the presence of 2µM Indo-1 pentopotassium salt, calcium free (2mM EGTA) and 5mM CaCl solutions were imaged on the calcium imaging setup. The above representative trace shows the signals recorded from the 405nm and 500nm photomultiplier tubes, representing the calcium bound and un-bound fluorescence, respectively. When imaging calcium free solution, the signal from the 500nm PMT is much higher than that of the 405nm PMT. Upon changing $[Ca^{2+}]$ to 5mM the proportion of calcium-bound to unbound increases; reflected in the fall in 500nm PMT signal and increase in 405nm PMT signal. The detection of these changing signals highlights the ability of the system to generate a usable ratio as a measure of $[Ca^{2+}]_i$ change.

2.5.3. Experimental protocol for inducing store operated calcium entry

Intracellular calcium imaging was employed to assess store-operated calcium entry in the thoracic aorta. All solutions were continuously superfused, maintained at 37^{o}C in a waterbath

and gassed with 100% oxygen. After an initial 15 minutes superfusion with HEPES-PSS to remove any excess or uncleaved indo-1 dye the tissue was excited. The following protocol was then applied; timings represent the superfusion time of each solution:

Calcium Free HEPES-PSS	5 minutes
HEPES-PSS	Allow to return to baseline
Calcium Free HEPES-PSS	10 minutes
Calcium Free HEPES-PSS + 10μM CPA	30 minutes
HEPES-PSS + 10μM CPA	15 minutes

At the end of each experiment the tissue was superfused with calcium free HEPES-PSS containing 20mM manganese chloride ($MnCl_2$; Mn-HEPES-PSS) for 30 minutes to quench the indo-1 dye. Through quenching of the indo-1 dye the calcium-dependent fluorescence is removed, the remaining signal is the intrinsic auto-fluorescence of the tissue. This auto-fluorescence is a product of the excitation and emission peaks, 240 and 470-490nm respectively, of pyridine nucleotides (NADH, NADP) which exist within the tissue. Their excitation and emission peaks overlap with the indo-1 spectrum [279,280].

2.5.4. Calcium imaging data analysis and statistics

Analysis of these data was performed by exporting the raw values from the 405nm and 500nm PMTs into a Microsoft Excel spreadsheet. The mean value of autofluorescence, taken from the plateau phase of quenching, was subtracted from the raw 405nm and 500nm signal data; a previous study in myometrium has shown that loading with indo-1 dye has no effect on autofluorescence [281]. The auto-fluorescence corrected values were then plotted against time and showed a rise in 405nm emission and a fall in 500nm emission. This allowed a ratio of 405:500nm emitted wavelengths to be calculated that would rise and fall in proportion to the level of $[Ca^{2+}]_i$ in a semi-quantitative manner. The use of a ratiometric $[Ca^{2+}]$ indicator reduced the effects of non-uniform dye distribution and the concentration of signal density, brought about during contraction, due to the equal effects on the individual 405nm and 500nm emitted wavelengths.

After analysis of these data, a 405:500nm emission ratio was calculated. This has been shown in a previous study, in which indo-1 signals were calibrated to absolute $[Ca^{2+}]$, to be an

appropriate indicator of $[Ca^{2+}]_i$ [282]. No calibration of indo-1 405:500nm emission ratio to absolute $[Ca^{2+}]$ was attempted during this study due to the uncertainty surrounding this practice [283,284].

Data are expressed as either the raw 405nm:500nm fluorescence ratio (F_{405}:F_{500}) or as the change in ratio (ΔF_{405}:F_{500}) represented as the mean ± standard error of the mean (SEM). Statistical analysis was carried out using Prism analysis software (Version 6; GraphPad). Comparisons were made using the Student's t-test with a $p<0.05$ being deemed to indicate a significant difference.

3. Can vascular function be altered by *ex vivo* cholesterol modulation?

3.1. Overview

Free cholesterol is a vital component of plasma membranes with an ability to alter their rigidity, permeability and organisation of signalling [285,286]. The functional levels of cholesterol required to balance degradation are met by cellular synthesis but are added to by dietary intake. Prolonged exposure to a high cholesterol diet can lead to an excess being carried in the blood stream. Hypercholesterolaemia is a well known key risk factor in the development of atherosclerotic disease [287].

The control of fluid dynamics within blood vessels is directly linked to the function of both the endothelial and smooth muscle cells and has been associated with increased susceptibility to atherosclerotic plaque formation [288,289]. Hypercholesterolaemia is associated with modification of caveolar compartmentalisation and has been shown to impact on calcium handling in vascular endothelial and smooth muscle cells [170,183]. Alterations in vascular function induced by such changes in vascular signalling will impact on the control of vascular tone and flow dynamics, therefore, cholesterol induced alterations in vascular function may be pro-atherogenic. Cholesterol depletion in rat tail arteries has been demonstrated to produce a reduction in vascular contractility [290], highlighting the necessity for cholesterol in normal vascular function. However, the acute effects of cholesterol depletion have not previously been observed in mouse aortae. Similarly, the effects of excess cholesterol have been studied on cultured vascular smooth muscle and endothelial cells and *ex vivo* smooth muscle membranes in several models [14,167,291,292], however, there is little literature highlighting the effects on overall vascular function in the murine aorta. The aim of this section of work was to assess the direct impact on vascular function of the atherosclerotic disease associated risk factor, cholesterol.

3.1.1. Methods

Male wild type mice (C57BL/6) at 12 weeks of age, fed *ad libitum* on a standard chow diet, were sacrificed with an anaesthetic overdose. The heart and aorta were removed and placed into a silicone coated petri dish containing ice-cold HEPES-PSS for isolation of the thoracic aorta. The vessel was cleaned of the perivascular adipose tissue and four aortic rings, approximately 3mm diameter, were cut from the proximal end of the isolated thoracic aorta.

Aortic rings were placed separately into the baths of a wire myograph (Danish MyoTechnology). Two 40µm wires were passed through the lumen of each ring before being secured tightly onto the myographs, taking care not to damage the endothelium. After an initial equilibration period the tension was increased incrementally over 30 minutes until a steady resting tension of 5mN was achieved.

The tissues were assessed for viability by exposure to HEPES-KPSS. This was repeated and the steady contractile response produced upon the second exposure was used as a reference for normalisation of future contractile data. Tissues were exposed to single maximal doses of the contractile agonists, phenylephrine (10µM) and serotonin (5-HT; 10µM; as determined by results described in Chapter 2.). The contributions of endothelial-dependent and –independent relaxations were assessed through the use of acetylcholine (10µM) and sodium nitroprusside (10µM), respectively.

Ex vivo modulation of cholesterol was achieved through the use of the cholesterol chelator methyl-β-cyclodextrin (MCD) and water soluble cholesterol. The contractile and relaxant function of the aortic rings was assessed after one hour incubation with the respective treatments, where possible. Statistical analysis was performed using Prism software (Version 6.) using a one-way ANOVA with a post-hoc Tukey's multiple comparisons test. Probability values of $p<0.05$ were considered significant. Full details of the experimental procedures can be found in sections 2.4.1 – 2.4.5 of Chapter 2.

3.2. Results

3.2.1. The effect of *ex vivo* cholesterol removal on vascular function

Cholesterol is an integral part of all plasma membranes and in particular is associated with the signalling domains, caveolae and lipid rafts. In order to demonstrate a role for membrane cholesterol in the function of vascular tissue we used the cholesterol chelator methyl-β-cyclodextrin (MCD) to remove it in an *ex vivo* setting. A range of MCD concentrations were employed to assess both maximal and submaximal effects.

3.2.1.1. The effect of *ex vivo* cholesterol removal on thoracic aorta contractility

Contractility was assessed by exposure of the aortic rings to three stimuli. The first was HEPES-PSS containing 100mM potassium chloride (KCl) to induce depolarisation; through manipulation of the smooth muscle electro-chemical gradients. The two other stimuli were pharmacological agonists dependent on membrane receptor binding to induce contraction. Phenylephrine and serotonin were employed as they act at different receptors; α_1-adrenoreceptors and 5-HT receptors, respectively. However, after binding to their individual receptor, the agonists activate the same downstream intracellular signalling pathway. Comparison responses to these three stimuli allowed identification of whether the removal of cholesterol had a global effect on the tissue or whether the receptors and/or their downstream mechanisms were affected disproportionately.

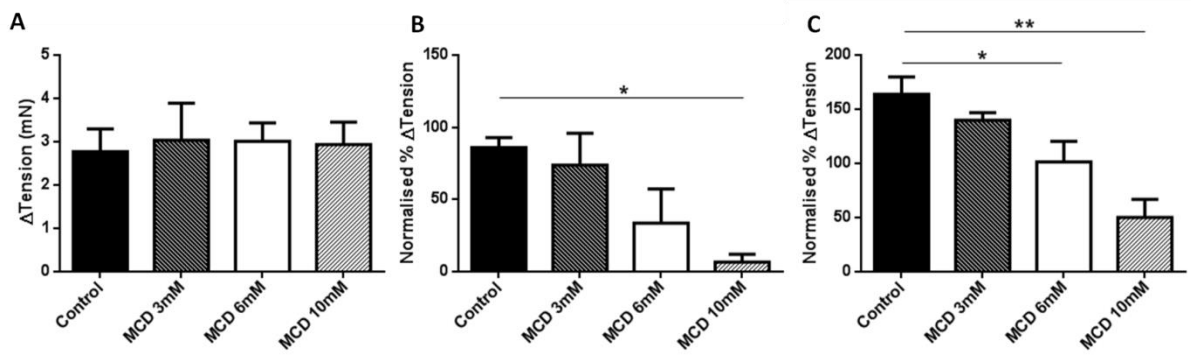

Figure 3.1. The effect of increasing methyl-β-cyclodextrin concentration on *ex vivo* murine thoracic aorta contractility. The contractility of murine thoracic aortic rings was measured after incubation (60 mins) with increasing concentrations of methyl-β-cyclodextrin (MCD; 3, 6, 10mM). **A**) Contractility to depolarisation (100mM KCl) was unaffected by removal of cholesterol by MCD. **B**) Contractility to the α_1-adrenoceptor agonist phenylephrine was significantly reduced at 10mM MCD only. **C**) Contractility to the 5-HT receptor agonist serotonin was significantly reduced at both 6 and 10mM MCD (n = 4,3,3,4 respectively; one-way ANOVA with post hoc Dunnett's multiple comparison test, * $p<0.05$, ** $p<0.01$).

Contraction to a depolarising stimulus was not significantly different from control after incubation with 3, 6 or 10 mM MCD (Figure 3.1 A; 2.8±0.5mN vs. 3.0±0.9mN, 3.0±0.4mN, 2.9±0.5mN, respectively p=ns). In contrast, contractions induced using phenylephrine produced a slight concentration dependent trend towards reduced contractility in the presence of MCD (Figure 3.1 B.). When compared to control (85.9±6.9%) mean contractility was reduced at 3mM MCD (73.8±22.1%) and 6mM MCD (33.7±23.5%). The reduction in

contractility was shown to be significant only after incubation with 10mM MCD (6.7±5.3%; $p<0.05$; Figure 3.1. and 3.2). There was a high degree of variability observed in the mean data. When looking at the individual data for contractility to phenylephrine after treatment with 3mM MCD (117.4%, 58.0%, 45.9%), 6mM MCD (80.6%, 12.9%, 7.7%) and 10mM MCD (17.2%, 0.1%, 3.0%), it can be seen that there is a pattern of one larger contractile response. The large contractile response was generated in aortic rings from the same animal. The large effect on the standard error of the mean is due to the small number of repeats. Contractions produced by exposure to serotonin also showed a concentration dependent trend (Figure 3.1 C.). When compared to control (163.8±15.9%) the mean contraction was reduced after treatment with 3mM MCD (139.8±7.0%) and was found to be significantly reduced at both 6mM (101.5±18.8%; $p<0.05$) and 10mM MCD (50.2±16.6%; $p<0.01$).

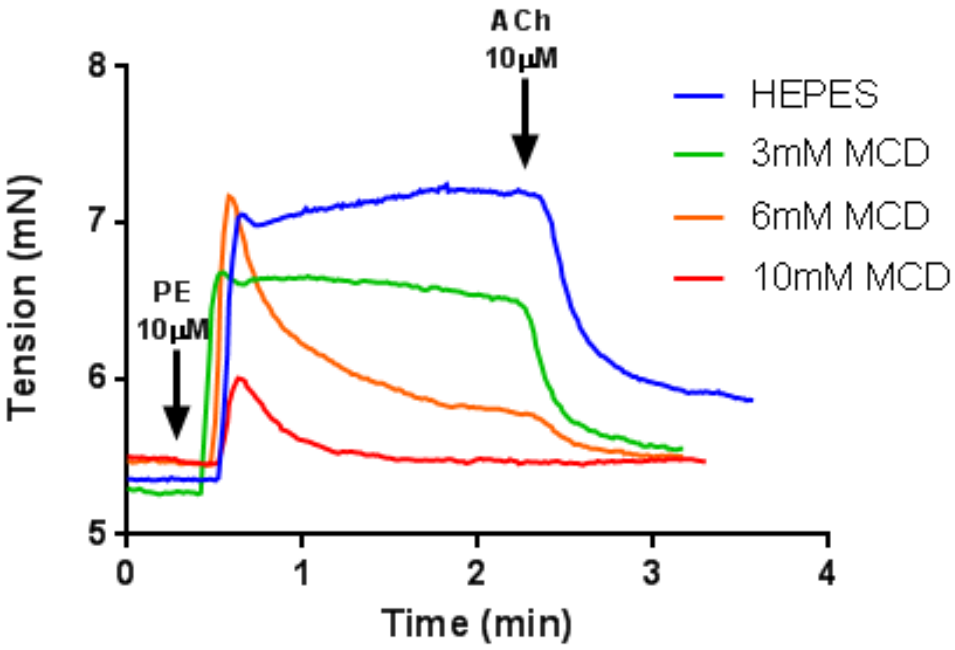

Figure 3.2. Representative traces showing the effect of methyl-β-cyclodextrin treatment on *ex vivo* murine thoracic aorta contractility. After incubation with increasing concentrations of MCD, the plateau phase of contractility to 10µM phenylephrine in thoracic aortic rings was measured. The response to stimuli inducing relaxation, such as acetylcholine (ACh), was unable to be measured after treatment with 10mM MCD due to its impact on contractility. At lower concentrations of MCD, although contractility appeared to be reduced, a relaxant response was able to be measured.

3.2.1.2. The effects of *ex vivo* cholesterol removal on thoracic aorta relaxation

The effects of cholesterol removal on endothelium-dependent and independent relaxation were assessed through the use of acetylcholine (ACh) and the nitric oxide donor sodium nitroprusside (SNP), respectively, after pre-constriction with phenylephrine. Due to the significant reduction in contractility seen following incubation with 10mM MCD relaxation data was not reliable (Figure 3.2).

When considering the mean data, exposure to increasing concentrations of MCD showed no significant effect on endothelium-dependent relaxation (Figure 3.3 A.; Control (74.2±3.6%) vs. 3mM MCD (84.6±3.5%) and 6mM MCD (78.0±13.0%)). These data must be considered in the context of the previously described variance in contractility to phenylephrine. If the raw data is considered after treatment with 6mM MCD (52.1%, 90.4%, 91.6%) it can be seen that in the animal previously described to show a greater contractility that the relaxation is lower, therefore, the relaxant effect observed is unlikely to be relative to the contractile response. However, when assessing the raw data after treatment with 3mM MCD (81.7%, 80.6%, 91.5%) there appears to exist relaxant responses relative to the contractility. Based on this observation we can suggest there is a trend towards increased endothelial-dependent relaxation after treatment with 3mM MCD. After consideration of the contractile variability it was concluded that no significant effect was seen after treatment with SNP to induce endothelium-independent relaxation (Figure 3.3 B.; Control (94.2±2.3%) vs. 3mM MCD (101.0±5.7%) and 6mM MCD (115.1±12.3%).

In summary, the removal of cholesterol using MCD was able to reduce contractility in response to receptor mediated pharmacological agonists but not a depolarising stimulus. Removal of cholesterol using a low concentration of MCD showed a trend towards increasing endothelial-dependent relaxation, however, no significant effect was observed. Endothelial-independent relaxation was shown to be unaffected after treatment with MCD.

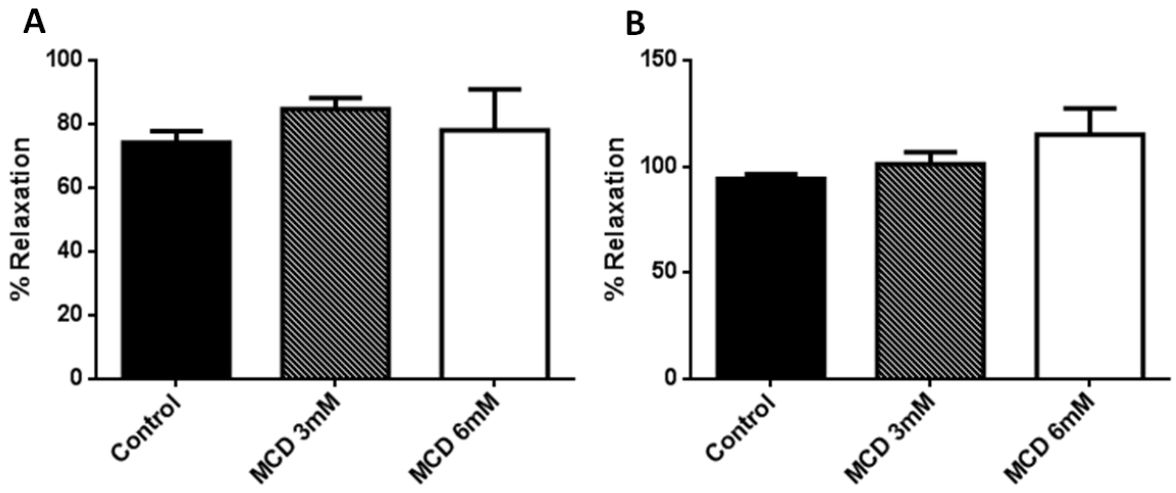

Figure 3.3. The effect of *ex vivo* cholesterol removal on endothelium-dependent and independent relaxation in the murine thoracic aorta. Thoracic aortic rings from C57BL/6 wild type mice were mounted onto a wire myograph and incubated with sub-maximal concentrations of MCD (3 and 6mM) for one hour. They were pre-constricted with phenylephrine (10µM) and then exposed to relaxant stimuli. Relaxation was measured as a percentage decrease from the level of stable contraction. **A**) Induction of endothelial-dependent relaxation was achieved by exposure to acetylcholine (10µM). There was no observed effect of 3 or 6mM MCD incubation when compared to time-matched HEPES-incubated controls (n = 4,3,3, respectively). **B**) Endothelial-independent relaxation was stimulated with SNP (10µM). There was no significant effect of incubation in either 3 or 6mM MCD when compared to control (n = 4,3,3, respectively).

3.2.2. The effects of *ex vivo* cholesterol addition on vascular function

Vascular tissues are able to take up cholesterol in the extracellular environment for a variety of uses. One of the destinations for this cholesterol is to be incorporated into the plasma membrane. Extracellular free cholesterol was increased to 5mM (194mg/dl) to assess the impact this might have on vascular function.

3.2.2.1. The effects of *ex vivo* cholesterol addition on thoracic aorta contractility

As described above in Section 3.2.1.1, contraction was induced using both a depolarising stimulus and pharmacological agonists; allowing an insight into the impact of cholesterol addition on the membrane as a whole, and then specifically on signalling domain-associated receptors and/or downstream messengers (Figure 3.4)

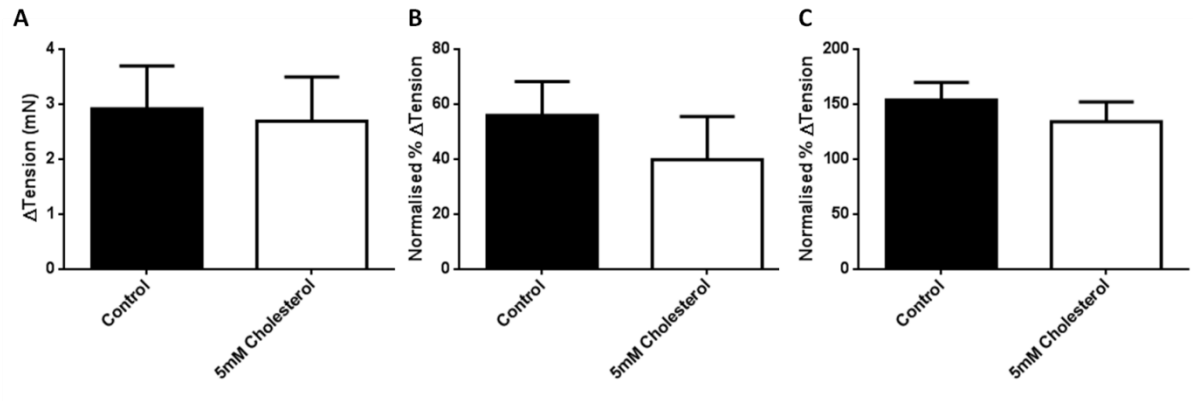

Figure 3.4. The effect of *ex vivo* cholesterol addition on contractility. The contractility of murine thoracic aortic rings was measured after incubation (60 mins) with cholesterol (5mM). Contraction was stimulated with (**A**) 100mM KCl, (**B**) 10μM phenylephrine and (**C**) 10μM serotonin. No significant effect of cholesterol incubation was observed in response to any of the stimuli (n = 4 in each group; unpaired Student's t-test).

After incubation for one hour with an extracellular free cholesterol concentration of 5mM, there was no change in contractility in response to a depolarising stimulus, when compared to control (Figure 3.4 A.; 2.9±0.8mN vs. 2.7±0.8mN, p=ns). The contractility to the pharmacological agonists phenylephrine (Figure 3.4 B.) and serotonin (Figure 3.4 C.) was also seen to be unchanged from control after incubation with 5mM cholesterol (56.0±12.3% vs. 39.8±15.8% and 153.8±16.0% vs. 134.1±17.9%, respectively p=ns).

3.2.2.2. The effects of *ex vivo* cholesterol addition on thoracic aorta relaxation

The effects of incubation with 5mM extracellular free cholesterol on the endothelial-dependent and independent components of thoracic aorta relaxation were again measured after pre-constriction with phenylephrine. The endothelium-dependent relaxation response induced by acetylcholine was shown to be significantly reduced after incubation with cholesterol, when compared to control (Figure 3.5 A.; 73.0±5.2% vs. 51.4±5.7%; $p<0.05$), however, there was no significant difference observed after stimulation of endothelium-independent relaxation (Figure 3.5 B.; 93.3±1.8% vs. 86.8±7.7%).

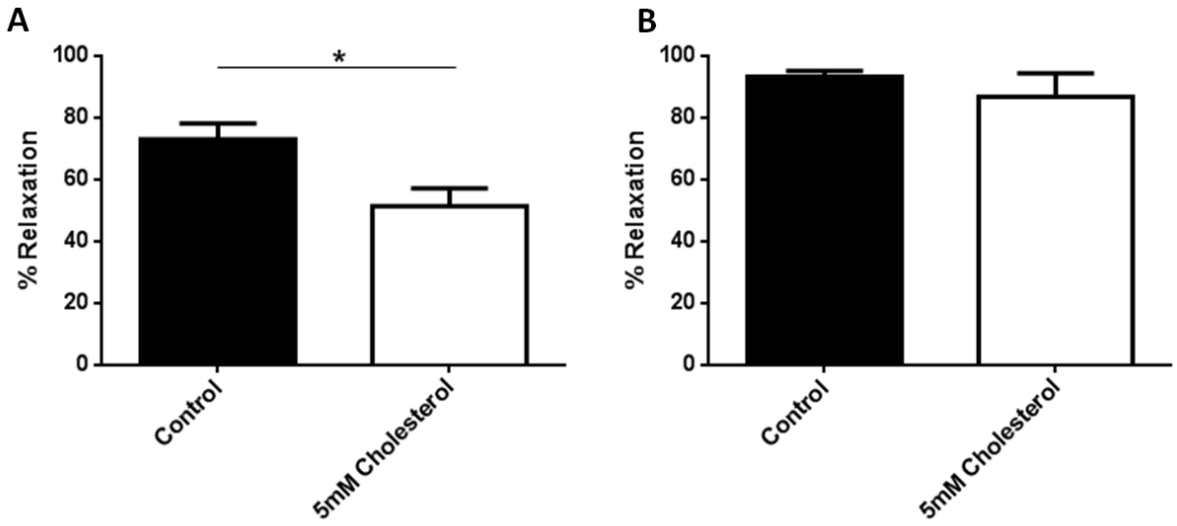

Figure 3.5. The effect of *ex vivo* cholesterol addition on endothelial-dependent and independent relaxation in the murine thoracic aorta. After incubation with 5mM cholesterol (60 minutes) thoracic aortic rings, pre-constricted with 10μM phenylephrine, were exposed to either 10μM acetylcholine (**A**) or 10μM sodium nitroprusside (**B**) to assess any effects on endothelial-dependent and independent relaxations, respectively. The acute addition of 5 mM cholesterol significantly reduced endothelial-dependent but not independent relaxation in the murine thoracic aorta (n = 4 in each group; Unpaired Student's t-test; * $p<0.05$).

In summary, incubation in 5mM extracellular free cholesterol for one hour had no significant effect on contractility, in response to both a depolarising stimulus and pharmacological agonists, or endothelium-independent relaxation to SNP. There was however, a significant reduction in endothelial-dependent relaxation as observed by the significant reduction in relaxation after exposure to acetylcholine.

3.3. Discussion

The aim of this chapter was to investigate the effects of *ex vivo* manipulation of extracellular cholesterol on vascular function in the murine thoracic aorta. Studies were conducted in which cholesterol was removed from intact vascular tissue or added into the extracellular media, to promote incorporation into the tissue; the contractility and relaxation of the vessel was then measured in response to a number of different agonists. These investigations have shown that in the murine thoracic aorta cholesterol extraction significantly reduced contractility to pharmacological agonists, phenylephrine and serotonin, but not to a non-receptor mediated depolarising stimulus. Depletion of cholesterol also had no significant effect on relaxation. In contrast, excess extracellular free cholesterol had no significant effect on contractility but was shown to reduce endothelial-dependent but not independent relaxation. The direct effects of cholesterol are linked to its importance in membrane organisation; specifically the maintenance of signalling domains, including caveolae and lipid rafts, which are abundant in vascular tissues [290,293,294]. The localisation of effectors of the contractile and relaxant stimuli within or distinct from these cholesterol rich domains is likely to be the reason for the observation of differing responses; the effects of both cholesterol depletion and addition on these effectors will be discussed below. The most recognisable limitation to the present investigation was the limited number of animals employed. This has restricted the strength of the conclusions able to be drawn from the subsequent data. In light of this, the data will be discussed within a broad context taking the limitations into consideration.

3.3.1. Cholesterol depletion

The use of MCD as a cholesterol extracting agent capable of disrupting caveolae has been validated in previous models using electron microscopy of rat ureter and tail arterial smooth muscle [290,295]. The expression of the caveolin-1 protein and the flask like shape of caveolae allow for the effects of cholesterol depletion to be directly measured, however, non-caveolin-1 expressing cholesterol rich domains known as lipid rafts have also been identified in plasma membranes and extraction of membrane cholesterol is thought to affect their structure equally [296,297]. The present investigation did not attempt to separate between the two types of signalling domain; therefore, to simplify the discussion reference will be made only to cholesterol-rich signalling domains. Although the effect of *ex vivo* cholesterol depletion of

these signalling domains has been shown to reduce smooth muscle contraction in other animal models, including vascular smooth muscle [187,290,298–301], there has been only a limited amount of research conducted on the murine thoracic aorta. This is an important factor due to the increase in the prevalence of murine models of vascular diseases, including atherosclerosis, in which cholesterol modulation is a key factor [144].

The present investigation has shown that contractions evoked by non-receptor mediated depolarisation were unaffected by cholesterol depletion, consistent with previous findings observed in the rat coronary artery. Contraction, after exposure to the depolarising stimulus, is elicited via a rise in $[Ca^{2+}]_i$ through opening of voltage-gated L-type calcium channels, this rise in $[Ca^{2+}]_i$ was also shown to be unaffected after cholesterol depletion by Prendergast *et al.* (2010)[302] and others previously [303]. Thus, the present data suggest that the L-type calcium channel is not associated with cholesterol-enriched signalling domains in murine aortic smooth muscle cells; this appears to be a tissue specific finding as functional evidence for caveolar localisation of the L-type calcium channel has been shown in cardiac myocytes [304].

Upon stimulation of tissues with receptor-mediated pharmacological agonists, it was shown in this investigation that contractility to both phenylephrine and serotonin was significantly reduced after cholesterol depletion with 10mM methyl-β-cyclodextrin. Mean contractility to phenylephrine was found to be variable. However, when the raw data was observed it was shown that the contractility in aortic rings from one individual was higher at all three concentrations of methyl-β-cyclodextrin. The high standard error is a product of the small n numbers and therefore it is hypothesised that if the number of animals was to be increased the concentration dependent reduction in contractility after methyl-β-cyclodextrin would be drawn out. However, the current data do not allow for firm conclusions to be made and this must be taken into consideration when discussing inferences.

Phenylephrine and serotonin bind to the α_1-adrenoreceptor and 5-HT_{2A} receptor, respectively, which are transmembrane receptors expressed in the vascular smooth muscle and both linked to the Gαq protein [305–309]. Contraction and the prerequisite rise in $[Ca^{2+}]_i$ is produced via the PLC-IP_3 signalling pathway [310,311]. The trend observed in the current data therefore suggests that both receptors are localised to cholesterol-enriched signalling domains and that extraction of cholesterol from the vascular smooth muscle membrane produces a disconnect

between the receptor and the intracellular signalling effectors. This is consistent with previous investigations in other animal models with respect to the 5-HT_{2A} receptor localisation, shown in glioma cells [121] and vascular smooth muscle cells [290], as well as the contractile response to serotonin stimulation in both the rat caudal and coronary arteries [290,302]. However, previous literature suggests a degree of tissue specific effectiveness of cholesterol with regards to the α_1-adrenoreceptor. In the rat coronary artery, cholesterol depletion was shown to have no effect on contraction or $[Ca^{2+}]_i$ signalling in response to phenylephrine [302]; whereas, in rat bladder and caudal artery smooth muscle, respectively, an increase in contractility [301] and the $[Ca^{2+}]_i$ response [290] to α_1-adrenoreceptor agonists was observed after treatment with MCD. The present data, as discussed previously, showed a trend towards a concentration dependent reduction in contractility to phenylephrine after treatment with MCD; although the small number of animals and a large standard error must be taken into account.

The differing responses between vascular beds observed in the same rat model, outlined above, allow only for the hypothesis that responses to agonists at α_1-adrenoreceptors and 5-HT_{2A} receptors are dependent on cholesterol-enriched signalling domains specifically in the murine thoracic aorta. The mechanism involved in cholesterol-dependency of receptor-mediated contractility is hypothesised to involve breakdown in the post-receptor signalling of the downstream PLC-IP_3 pathway. Further evidence for this hypothesis is shown by the reduced contractility to both angiotensin II [301] and endothelin-1 [187,290,302], agonists activating Gαq-PLC-IP_3 linked receptors, after MCD treatment. Although identification of the exact intracellular mechanism is yet to fully elucidated, cholesterol depletion is able to alter store-operated calcium entry [187] and the pharmacology of vascular calcium-activated chloride channels [298]; shown to be components of vascular smooth muscle contractility in their respective models.

Investigation of the effects of cholesterol depletion on relaxant mechanisms in the murine thoracic aorta has provided evidence to show that endothelial-independent relaxation, induced by stimulation with SNP, is not dependent on membrane cholesterol; in agreement with previous literature in the rabbit aorta [312]. Endothelial-dependent relaxation of vascular smooth muscle has three main components; the release of nitric oxide, prostacyclin or the endothelial-derived hyperpolarizing factor (EDHF) [47,313,314], each of which are altered in their relative contributions to the overall relaxant effect, when stimulated by agonists such as

acetylcholine, in different vascular beds. Within the thoracic aorta nitric oxide signalling is the primary contributor and its production, constitutively by endothelial nitric oxide synthase (eNOS), has been shown to be regulated by localisation to caveolae [189,315]. The present study has shown that in the murine thoracic aorta, cholesterol depletion with a low concentration of MCD (3mM) showed a trend towards increased endothelial-dependent relaxation; however, this was not shown to be a significant effect and may be limited by the small number of animals (n = 3). Previous discussions on the variance of contractile responses to phenylephrine must also be considered, but the raw data suggest that at this concentration the relaxant response is relative to the level of contraction, although once again confirmation of this relationship is limited by the small number of animals. If upon further examination of this response the trend was found to develop into a significant difference this may reflect a reduction in the number of caveolae and in turn dissociate nitric oxide synthase from caveolin-1 leading to an increase in the release of nitric oxide. This hypothesis is in contrast to the results of Darblade *et al.* (2001), who observed a reduction in endothelial-dependent relaxation in the rabbit aorta [312]; in addition, Blair *et al.* (1999) showed that treatment with MCD causes a translocation of eNOS from the plasmalemma to intracellular membranes in cultured porcine pulmonary artery cells [316], thought to reduce nitric oxide production. It is possible that there exists a degree of inter-vascular bed and inter-species heterogeneity in the endothelial-dependent relaxation response to cholesterol depletion. In addition, other methodological differences must also be considered, such as the use of a different cholesterol chelating agent, 2-hydroxypropyl-β-cyclodextrin (hp-β-CD), in the study of Darblade *et al* (2001).

3.3.2. Cholesterol addition

The addition of extracellular free cholesterol is capable of reversing the effects of MCD by promoting the reformation of cholesterol-rich signalling domains [290,312], in addition, incubation of cultured cells and *ex vivo* tissues with increased extracellular free cholesterol has been shown to alter smooth muscle function [185,292,317]. The present investigation employed the use of water-soluble cholesterol which has been previously described [290,317]; however, other methods of enriching membranes with free cholesterol are available, such as the use of free cholesterol and phospholipid containing liposomes or human low density lipoprotein (LDL) [183,185,259,292]. The results of the present study will be compared to these

methods to highlight the effects of cholesterol enrichment and possible methodological-dependent differences.

The present investigation has shown that acute incubation (one hour) with an excess of extracellular free cholesterol in an *ex vivo* tissue preparation has no effect on contractility in response to KCl or serotonin in agreement with previous literature employing a different methodology [259]. The present investigation also observed no change in the contractility to phenylephrine stimulation, however, after perfusion of pressurised rabbit femoral arteries with cholesterol and phospholipid containing liposomes Broderick *et al.* (1989) show evidence of increased contractility to the same stimulus [179]. This may be evidence of species or vascular bed differences, in agreement with the effects of cholesterol depletion, but there is also a temporal difference in the methodology of two investigations. The three hour incubation employed in the highlighted investigation, compared to one hour in the present study, suggests the need for longer incubation times to observe an effect of membrane cholesterol enrichment.

Observation of the effects of free cholesterol enrichment on endothelium-independent mechanisms of vascular relaxation produced results consistent with those observed after cholesterol depletion, namely no significant change; there was however, no supporting literature showing the effects of SNP after *ex vivo* cholesterol enrichment. In contrast, endothelial-dependent relaxation after stimulation with acetylcholine was significantly lower in mouse aortae after incubation with 5mM water-soluble cholesterol. Once again, there is scant literature outlining the effects of *ex vivo* cholesterol enrichment on endothelial-dependent relaxation. However, an investigation conducted by Jiang *et al.* (2001), in the same animal model employed in the present study, showed that overnight incubation with native human-LDL did not significantly change acetylcholine induced relaxation [259]. This may represent a concentration dependent effect of cholesterol as Jiang *et al.* (2001) employed LDL at a concentration of 5mg protein/ml, which, although the exact concentrations of free cholesterol were not quantified, will make available less free cholesterol than the 5mM concentration employed in the present investigation.

3.4. Conclusions

This chapter aimed to assess the effects of modulating cholesterol, an excess of which in the blood is a key risk factor for the development of atherosclerosis, on the vascular function in the murine thoracic aorta. It has been demonstrated that contractility to phenylephrine and serotonin is dependent on their receptor's localisation to cholesterol-rich signalling domains, most likely due to their organisational role in linking the receptor to the downstream intracellular signalling molecules. Cholesterol enrichment may be able to modulate receptor mediated contractions, however, this was not observed in the present study; possibly due to the concentration and temporal dependence of cholesterol incubations. Significant alterations in vascular relaxation were not observed after sub-maximal cholesterol depletion; however, cholesterol enrichment was able to reduce endothelial-dependent relaxations, simulating dysfunction, a widely reported early stage in the development of advanced atherosclerosis.

3.4.1. Summary of conclusions

- **Acute depletion of membrane cholesterol produced a significant reduction in contractility to phenylephrine and serotonin in the murine thoracic aorta.**

- **Acute enrichment of membrane cholesterol content did not alter vascular contractility in the murine thoracic aorta.**

- **Acute enrichment of membrane cholesterol produced a significant reduction in endothelial-dependent relaxation to acetylcholine.**

3.4.2. Limitations

As previously outlined, the primary limitation to the conclusions drawn from the above data is the low experimental numbers. This factor has been taken into consideration where necessary, with justifications from the raw data; however, to allow for firmer conclusions to be made and to draw out some of the observed trends an increase in the number of animals would be necessary. However, in addition to this there are further methodological limitations to the present conclusions; one of which is evidenced by the large degree of conflicting data available in previous literature; a product of differences between species and even between vascular beds within the same species. Therefore, the above conclusions are only applicable to the murine thoracic aorta and care should be taken when trying to extrapolate the present findings to other models. The basis of this investigation was based around the modulation of membrane cholesterol content. The present study was limited in the fact that no direct measure of membrane cholesterol was made to confirm the removal or addition of cholesterol from or into the membranes of vascular endothelial and smooth muscle cells.

Another limitation is the acute nature of the exposure to cholesterol and that only the effects of free cholesterol incorporation into membranes were investigated. In the setting of developmental atherosclerosis, hypercholesterolaemia is a chronic condition and the cholesterol is able to be modified, most relevantly by oxidation. Therefore, acute *ex vivo* modulation of cholesterol is unlikely to show the true effects of hypercholesterolaemia on vascular function due to the lack of the additional complementary and possibly detrimental systems. For further investigations an animal model is required, and it is this that will be addressed in the following chapter.

4. How does high fat feeding and ApoE gene deletion affect the phenotype of mice in the early stages of atherosclerotic disease development?

4.1. Overview

The study of atherosclerotic disease development has in the past been conducted on a wide variety of animal models including rabbits, pigs and monkeys [167,181,318] due to the difficulty in attaining relevant human tissue samples. However, over the last 20 years the use of genetically modified mouse models has increased dramatically. These models have centred on reducing or completely ablating the expression of key proteins in the lipid metabolism process. Although there are other mouse models available, including the LDL receptor knockout ($LDLR^{-/-}$), the most widely employed is the apolipoprotein E knockout mouse ($ApoE^{-/-}$) [144,319]. Apolipoprotein E (ApoE) is produced primarily by the liver, although extra-hepatic sources include the brain and macrophages, and plays an anti-atherogenic role by promoting absorption and excretion of dietary cholesterol [320]. Developed simultaneously by two research groups the ApoE knockout mouse develops hypercholesterolaemia when fed a standard chow diet; this can then be exacerbated by feeding with a high fat 'western' diet [138,140]. After high fat feeding $ApoE^{-/-}$ mice have been shown to develop advanced atherosclerotic plaques that express similar characteristics, in their constitution, to those found in humans [321]. However, the phenotype of the $ApoE^{-/-}$ mouse prior to the development of advanced plaques has not been extensively investigated.

This study aimed to identify phenotypical changes in mice attributable to high fat feeding and/or the deletion of the ApoE gene prior to the development of overt atherosclerosis. The stage of atherosclerotic disease development was assessed through histological analysis and through immunohistochemical staining to assess the prevalence of proliferative smooth muscle. The involvement of smooth muscle proliferation is well characterised in advanced atherosclerotic plaques [322], however, their contribution to the early stages of atherosclerotic disease development is currently unclear. Characteristics such as bodyweight and perivascular adipose tissue morphology will be measured in addition to serum lipid and glucose concentrations. The aim of these measurements is to build up a picture of the phenotype that exists in each of the experimental groups. Investigation into the presence of underlying atherosclerotic risk factors such as hypercholesterolaemia, obesity, inflammation and metabolic syndrome will allow for clearer interpretation of future investigations into vascular function.

4.1.1. Methods

Full details of the following procedures can be found in section 2.3 of Chapter 2. Male C57BL/6J and ApoE$^{-/-}$ mice (on a C57BL/6J background; bred in the University of Manchester Biological Sciences Facility) were fed on either a standard chow diet or a high fat 'western' diet for eight weeks. Processed aortic tissue, with the perivascular adipose tissue and adventia still intact, was sectioned and stained with haematoxylin and eosin to allow for analysis of the perivascular adipocytes and atherosclerotic lesion development.

Atherosclerotic lesion development in the thoracic aorta was quantified using Image J software analysis of H&E stained sections. There were five animals in each group; for lesion quantification 5 sections of thoracic aorta were measured from each animal (the sample size was defined by prior investigations highlighted in Chapter 2). The internal elastic lamina was identified and traced using the image analysis software. The internal lumen diameter was then measured in the same way. By subtracting the latter from the former we were left with a measure of the intimal thickness that would allow for comparison of atherosclerotic development.

Identification of the phenotype of smooth muscle cells within 5 μm sections of thoracic aortic tissue, from chow fed control mice only, was undertaken through immunohistochemical staining with antibodies targeted to α-smooth muscle actin (α-SMA; present in all smooth muscle cells), smooth muscle myosin heavy chain II (smMHCII; present only in contractile smooth muscle cells) and smoothelin (present only in contractile smooth muscle cells). During IHC optimisation, a number of different approaches were taken including alternative antigen retrieval and fluorescent and non-fluorescent detection methods. For each antibody a titration was performed to optimise the staining. Specific experimental conditions for each antibody are outlined in Appendix III.

Animals were fasted overnight and blood glucose concentrations were measured at sacrifice. Blood samples were taken via cardiac puncture and the serum isolated, using centrifugation, for measurement of cholesterol and triglyceride levels. At this point the aortae were dissected out, after perfusion with PBS, and fixed in 4% PFA before histological processing. In addition, fresh tissue was used for *en face* Oil Red O staining. The hearts, spleens and epididymal fat pads were taken to be weighed.

Analysis of the size and number of perivascular adipocytes was carried out under blinded conditions, once again using Image J software. Adipocyte ghosts where outlined in 3 fields of view from one section from each animal (the sample size was defined after prior investigation as described in Chapter 2). Within each field of view adipocytes from 4 and 6 random regions of interests were measured to assess adipocyte area and adipocyte number, respectively.

Mice were separated into four separate groups: C57BL/6J mice fed a standard chow diet (Control Chow) or a high fat 'western' diet (Control HF) and ApoE null mice fed a standard chow diet ($ApoE^{-/-}$ Chow) or a high fat 'western' diet ($ApoE^{-/-}$ HF). Statistical analysis was conducted using Prism software (Version 6) employing a one-way ANOVA with a post hoc Tukey's multiple comparisons test, unless otherwise stated. A probability value of $p<0.05$ was considered statistically significant.

4.2. Results

4.2.1. Genetic screening of $ApoE^{-/-}$ mice

Animals were routinely genotyped to confirm the deletion of the ApoE allele; litters were randomly selected. Control DNA for comparison was obtained from wildtype C57BL/6 mice. The genotyping protocol was performed in accordance with that from the Jackson Laboratory, where the $ApoE^{-/-}$ mice are reposited. The ApoE allele was amplified to 245bp corresponding to the, vector containing, exon 3. The wildtype DNA was amplified to 155bp, corresponding to the naive exon 3 containing the ApoE allele. DNA from a previously confirmed $ApoE^{-/-}$ mouse was used as a positive control. All the animals genotyped showed amplification to 245bp aligning well with the positive control. The negative control, water only, showed no bands (Figure 4.1).

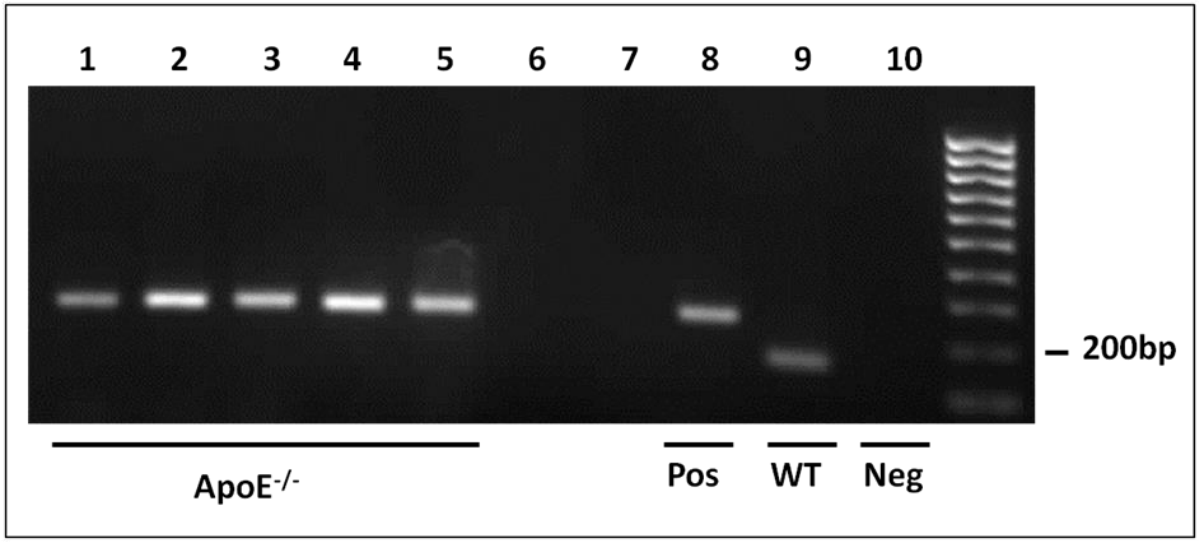

Figure 4.1. Genotyping of ApoE$^{-/-}$ mice. Lanes 1 – 5 show the DNA extracted from the current colony of ApoE$^{-/-}$ mice after amplification with primers oIMR0180, oIMR0181 and oIMR0182. The test DNA aligns well with the positive control DNA sample (Pos; lane 8) at around 245bp, the expected size of the ApoE allele containing the disruptive vector. There is no observable band at the same size as the WT ApoE allele (WT; lane 9) and the negative control (water only; Neg; lane 10) was clear.

4.2.2. The assessment of atherosclerotic disease development in the thoracic aorta

The focus of this investigation was on the phenotypical changes occurring prior to the development of overt atherosclerosis. C57BL/6 mice have been shown to be susceptible and ApoE$^{-/-}$ mice are known to develop complex lesions in the aortic root after 10-12 weeks of feeding on a standard chow diet; the speed of development can be increased through feeding with a high fat diet. Therefore assessment of atherosclerotic disease development was carried out, in the thoracic aortic region of interest, to confirm the extent of atherosclerotic plaque development in C57BL/6 (control) and ApoE$^{-/-}$ mice after eight weeks feeding on either a standard chow or a high fat 'western' diet. This was achieved firstly in a qualititative manner, using *en face* Oil Red O staining, to identify lipids within the entire aortic lumen (Figure 4.2). There was some staining of fatty deposits identified in the aortic arch and in the intercostal branches, however, there was no visible evidence of staining in the thoracic aortae of control mice after feeding with either a chow or a high fat diet for eight weeks. Some small areas of intravascular fat deposition were observed in the thoracic aortae of ApoE$^{-/-}$ mice, however, histological quantification did not confirm this as a population wide trend. Quantification of

atherosclerotic disease progression was attempted by measuring the intimal thickness from haematoxylin and eosin stained tissue sections. Quantitative data is not shown as there was no evidence of thoracic aortic intimal thickening observed in control or ApoE$^{-/-}$ mice after feeding on either diet (Figure 4.3). For comparison, images of *en face* Oil red O stained aorta and haematoxylin and eosin stained aortic sections from a 26 week old ApoE$^{-/-}$ mouse can be seen in Appendix IIII.

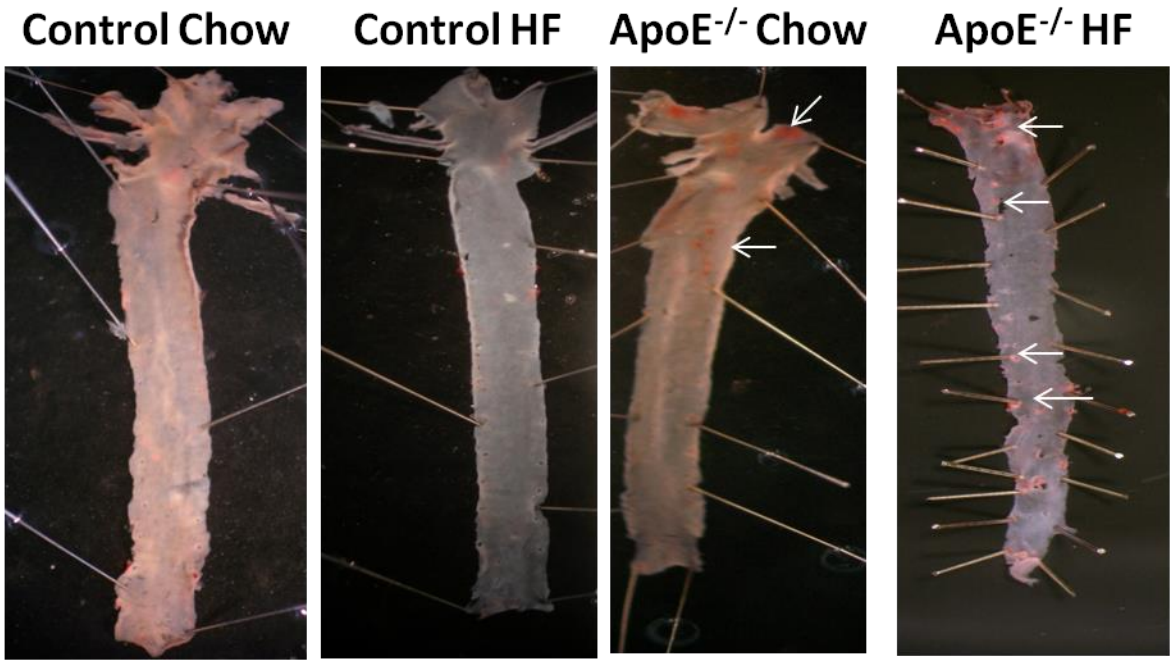

Figure 4.2. Qualitative assessment of atherosclerotic disease development. Aortae from ApoE$^{-/-}$ mice and their age and strain matched controls, fed either a chow or high fat diet for eight weeks were assessed for the presence of atherosclerotic plaques using *en face* Oil-red O staining. Control mice demonstrated no visible signs of fatty streak development. Positive staining of fatty streak development was observed in the aortic arch and intercostal arteries after eight weeks feeding in ApoE$^{-/-}$ mice (arrows), however, within the thoracic aorta there was very little staining observed. The extent of lesion coverage was not assessed, however, high fat feeding in ApoE$^{-/-}$ mice appears to increase the development of intravascular fat deposits.

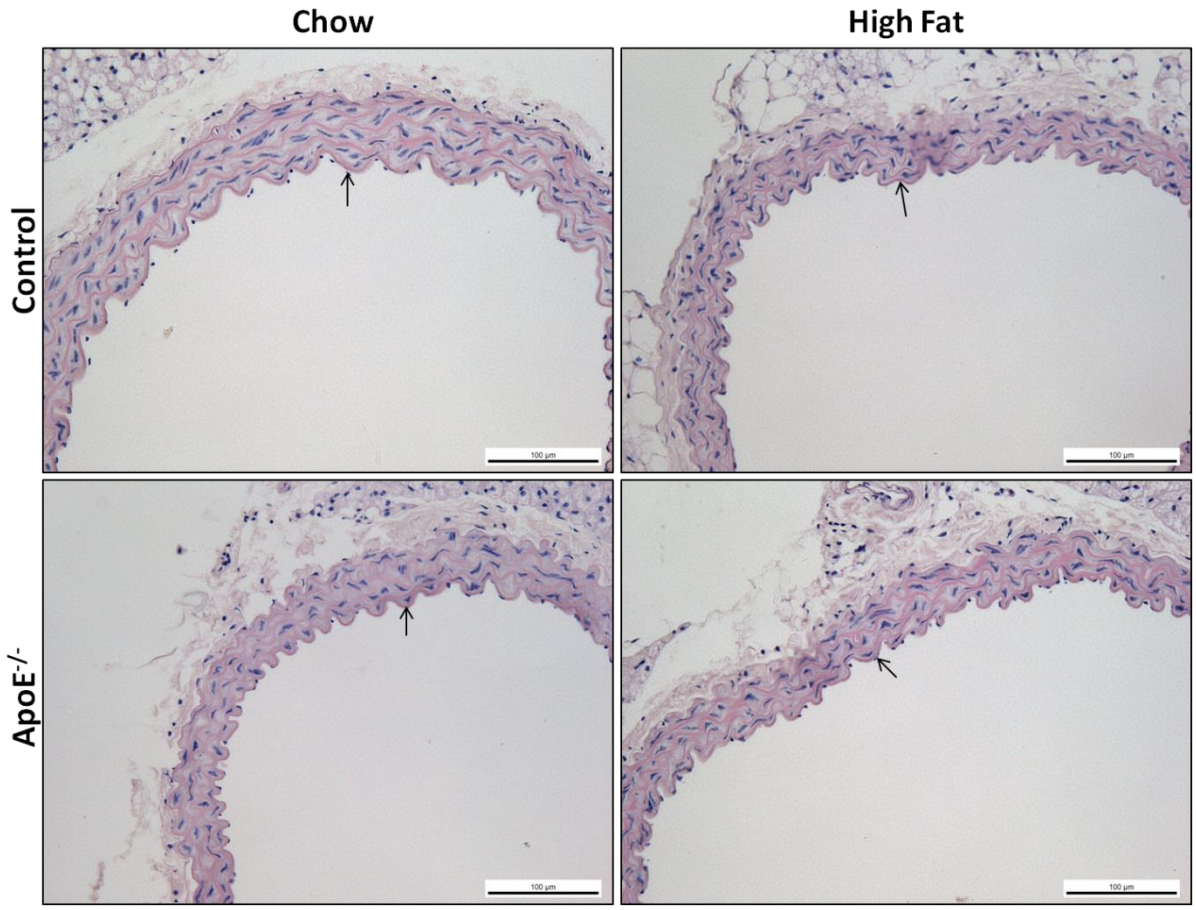

Figure 4.3. Representative images showing no intimal thickening present in chow or high fat fed control and ApoE$^{-/-}$ mice. Histological sections from the descending thoracic aorta were stained with haematoxylin and eosin. This enabled visualisation of the internal elastic lamina (indicated by the arrows). The distance from the internal elastic lamina to the lumen of the vessel (inclusive of the endothelial layer) is defined as the intima. No thickening was observed in chow or high fat 'western' diet fed control and ApoE$^{-/-}$ mice (Scale bar represents 100µm).

4.2.2.1. Immunohistochemical identification of proliferative vascular smooth muscle cells

The prevalence of proliferative smooth muscle cells is usually associated with the presence of atherosclerotic plaques, however, their involvement in the earlier stages of atherosclerotic disease development is currently unknown. Modifications in calcium handling proteins and a loss of expression of contractile proteins, such as smooth muscle myosin heavy chain II (smMHCII) and smoothelin, suggest that an increase in proliferative smooth muscle cells is able to alter vascular function. Firstly, immunostaining with an alkaline phosphatase-

conjugated primary antibody to α-SMA, present in all smooth muscle cells, was performed. This resulted in clear, bright staining of the smooth muscle cells within the aortic wall with no observable non-specific staining of the endothelium or adventitia (Figure 4.4). Secondly, identification of smooth muscle cells expressing smMHCII was attempted. An extensive optimisation of the smMHCII antibody was undertaken using both fluorescent and non-fluorescent secondary antibodies (Appendix III); however, no signal could be detected. Finally, the expression of smoothelin in the thoracic aorta was assessed. Smooth muscle specific staining was observed (Figure 4.4), however, the resolution of the staining appeared too diffuse; identification of individual smooth muscle cells was unreliable, therefore no further analysis was carried out.

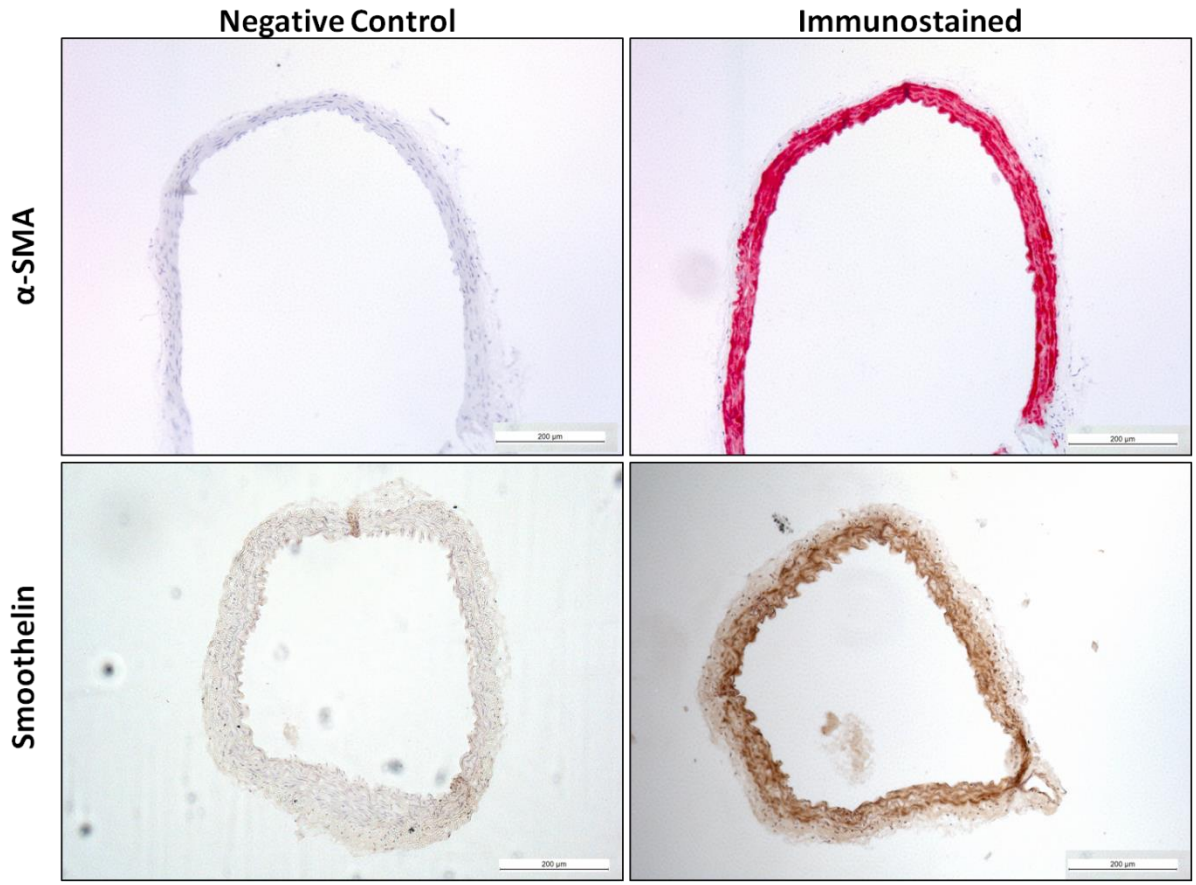

Figure 4.4. Immunohistochemical staining of contractile smooth muscle markers. Staining was undertaken to assess the prevalence of proliferative smooth muscle cells in the descending thoracic aorta of chow fed control mice. All smooth muscle cells express α-smooth muscle actin (α-SMA; Top), however, when smooth muscle cells start to proliferate the constitutive expression of smoothelin (Bottom) is lost. Medial staining correlating to smooth muscle cells was observed for both α-SMA and smoothelin when compared to their respective negative controls (primary antibody omitted). Expression within individual cells was unable to be identified due to the diffuse nature of the staining (scale bars represent 200μm).

4.2.3. The effect of high fat feeding and ApoE gene deletion on the phenotype of mice

High fat feeding with a 'western' diet is often used in studies to promote atherosclerosis in mice. This method is often combined with deletion of the ApoE gene to speed up and exacerbate the extent of hypercholesterolaemia and development of atherosclerotic disease. Here, mice were phenotyped to allow for an understanding of the effects of a high fat diet, and also the direct effects of ApoE gene deletion, on the phenotype of mice.

4.2.3.1. The effect of high fat feeding and ApoE gene deletion on the bodyweight of mice

All animals were weighed prior to sacrifice to determine their total bodyweight (Figure 4.5 A), in addition, the heart weight, after removal of the epicardial fat, was taken and its ratio to the bodyweight of each animal was calculated to ascertain if changes in body weight were due to a change in the overall size of the animal rather than just weight (Figure 4.5 B). Adipose or fat tissue, as a contributor towards bodyweight, was of interest in this investigation and so the epididymal fat pads were weighed as a representation of overall body fat content (Figure 4.6).

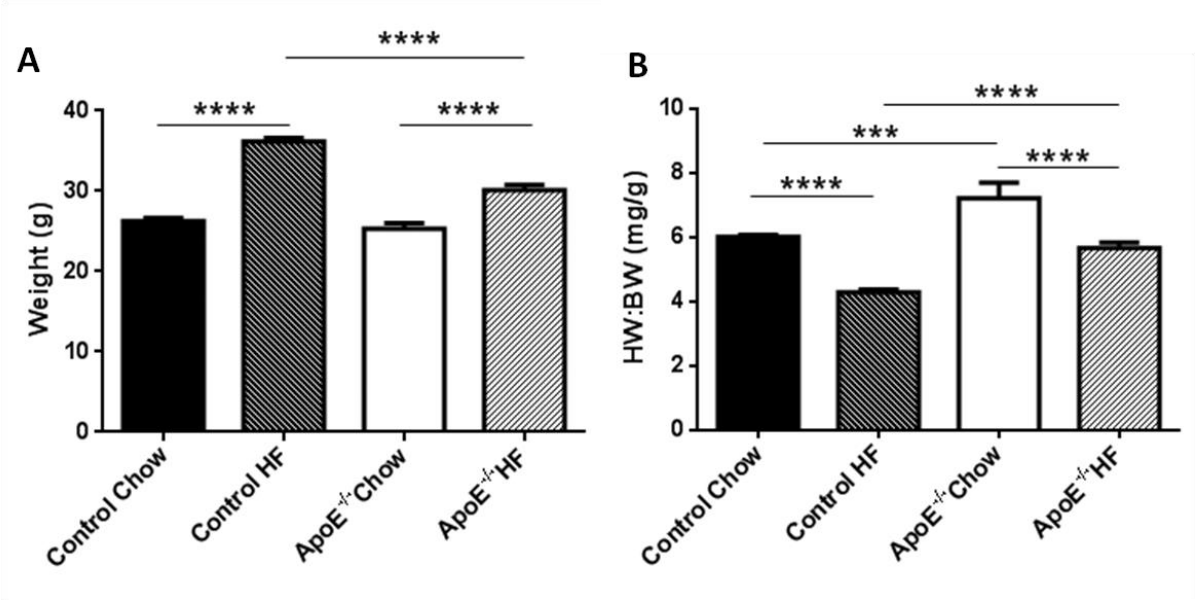

Figure 4.5. The effect of high fat feeding and ApoE gene deletion on the weight characteristics of mice. A) Feeding with a high fat diet caused a significant increase in body weight in both control and ApoE$^{-/-}$ mice compared to the respective chow-fed controls, however, ApoE$^{-/-}$ mice gained significantly less weight than their age, strain and 'western' diet matched controls (n = 30,35,19,20 respectively; one-way ANOVA with post hoc Tukey's multiple comparisons test, ****p<0.001). **B**) The heart weight to body weight ratio (HW:BW) was significantly increased in ApoE$^{-/-}$ mice fed a control diet when compared to their diet matched controls. After feeding for eight weeks on a high fat 'western' diet the HW:BW was significantly reduced in both control and ApoE$^{-/-}$ mice, although to a significantly greater extent in control mice (n = 13,15,5,9, respectively; one-way ANOVA with post hoc Tukey's multiple comparisons test, *** p<0.005, **** p<0.001).

After eight weeks feeding there was no significant difference in bodyweight observed between control and ApoE$^{-/-}$ mice when fed a standard chow diet (26.26±0.40g vs. 25.31±0.70g). Feeding of control C57BL/6 mice with a high fat diet led to a significant increase in body weight (26.26±0.40g vs. 36.16±0.47g; $p<0.001$). The same trend was seen when ApoE$^{-/-}$ mice were fed a high fat diet, when compared to chow fed ApoE$^{-/-}$ mice (25.31±0.70g vs. 30.12±0.65g; $p<0.001$). However, the overall bodyweight of high fat fed control mice was significantly greater than diet matched ApoE$^{-/-}$ mice (36.16±0.47g vs. 30.12±0.65g; $p<0.001$).

ApoE$^{-/-}$ mice fed a standard chow diet for eight weeks were shown to have a higher heart weight to bodyweight ratio (HW:BW) when compared to diet matched control mice (6.02±0.06mg/g vs. 7.22±0.48mg/g; $p<0.005$). High fat feeding in both control and ApoE$^{-/-}$ mice produced a significant decrease in the HW:BW when compared to their chow fed counterparts (Control chow vs. HF: 6.02±0.06mg/g vs. 4.29±0.10mg/g; $p<0.001$. ApoE chow vs. HF: 7.22±0.48mg/g vs. 5.67±0.17mg/g; $p<0.001$). The HW:BW was significantly smaller in control high fat fed mice when compared to diet matched ApoE$^{-/-}$ mice (4.29±0.10mg/g vs. 5.67±0.17mg/g; $p<0.001$), however, the average decrease in HW:BW induced by high fat feeding was not significantly different between control and ApoE$^{-/-}$ mice (1.69±0.10mg/g vs. 1.42±0.50mg/g).

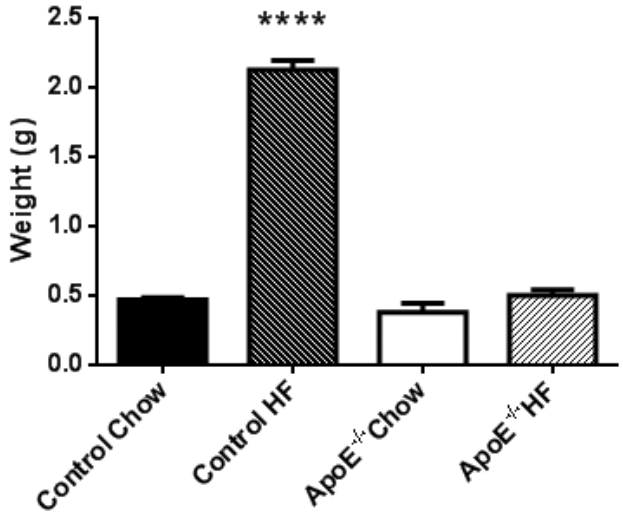

Figure 4.6. The effect of high fat diet and ApoE gene deletion on epididymal fat pad weight. Both epididymal fat pads were removed and weighed together. There was no observed difference between the control and ApoE$^{-/-}$ chow fed mice. After eight weeks high fat feeding control animals showed a significant increase in the weight of epididymal fat pads, however, this increase was not observed in the diet matched ApoE$^{-/-}$ mice (n= 13,15,5,9, respectively; one-way ANOVA with post hoc Tukey's multiple comparisons test, **** $p<0.001$).

After eight weeks of feeding on a standard chow diet the weight of the epididymal fat pads from control mice and ApoE$^{-/-}$ mice was not significantly different (0.47±0.01g vs. 0.38±0.07g). The feeding of a high fat diet for the same period produced a significant increase in epididymal fat pad weight in control animals (0.47±0.01g vs. 2.13±0.07g; $p<0.001$), however, there was no significant increase in weight observed in ApoE$^{-/-}$ mice (0.38±0.07g vs. 0.50±0.04g).

In summary, high fat feeding significantly increases body weight in both control and ApoE$^{-/-}$ mice, but the increase is to a lesser extent in ApoE$^{-/-}$ mice. The HW:BW is significantly larger in chow fed ApoE$^{-/-}$ mice when compared to diet matched controls. High fat feeding produces a reduction in HW:BW ratio in both control and ApoE mice. A significantly lower HW:BW is seen in ApoE$^{-/-}$ mice, however, the mean change in HW:BW is not significantly different. Finally, high fat feeding causes a significant increase in epididymal fat pad weight in control mice that is not seen in diet matched ApoE$^{-/-}$ mice.

4.2.3.2. The effect of high fat feeding and ApoE gene deletion on the lipidemic and glycemic profiles of mice

The high fat 'western' diet has a higher cholesterol content than the standard chow diet (0.15% vs. 0.022%) and one of the main activities of the ApoE lipoprotein is to facilitate the removal of cholesterol from the blood in the liver. It is for this reason that the lipidemic profile, including total cholesterol, HDL-cholesterol and triglycerides, was measured in serum samples obtained from cardiac puncture blood samples after overnight fasting (Figure 4.7 A – C). The fasted blood glucose concentrations of these samples were measured immediately. This was carried out to assess whether high fat feeding or the ApoE gene deletion would lead to the development of a glucose homeostasis disruption (Figure 4.7 D).

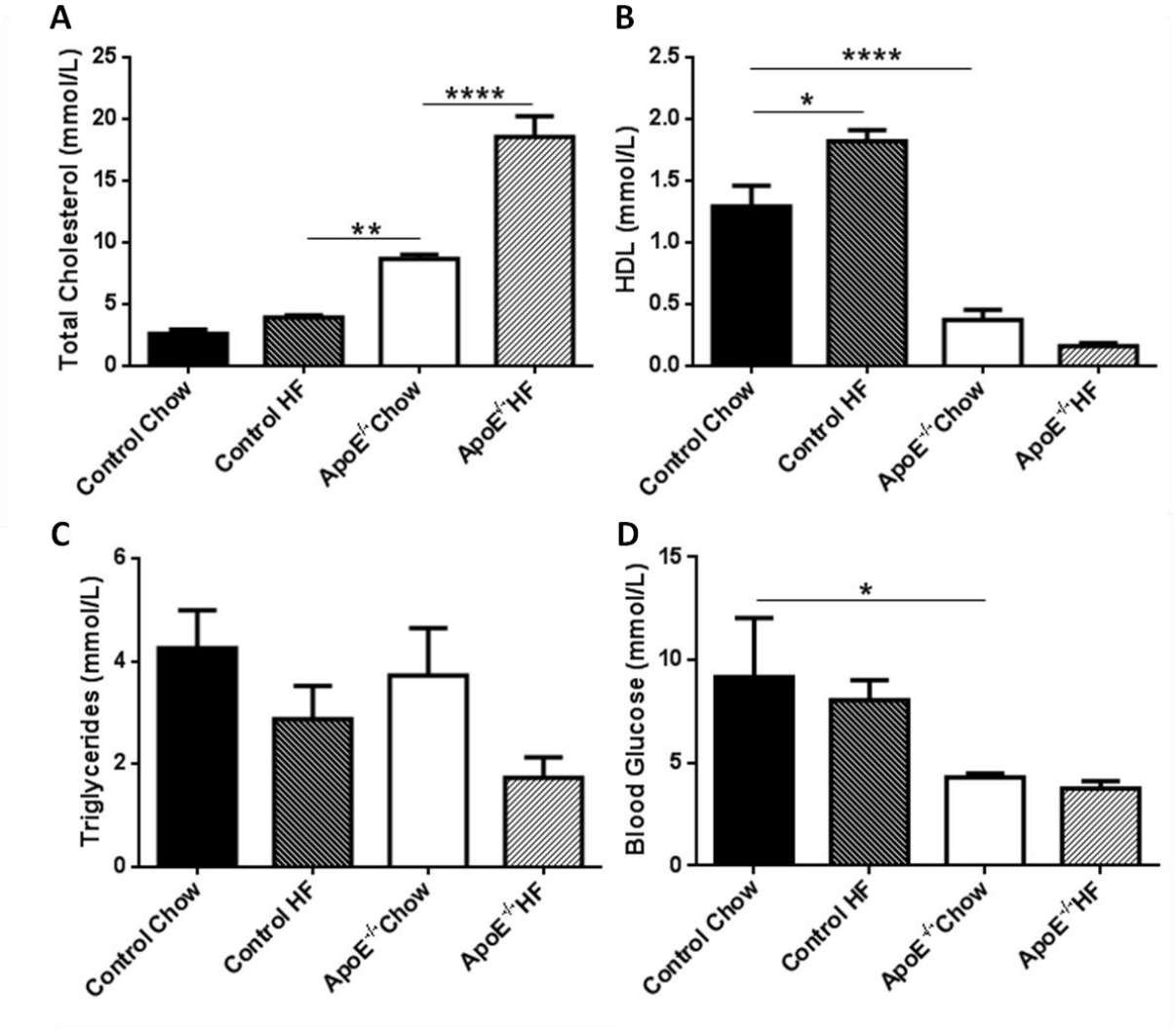

Figure 4.7. The effect of high fat feeding and ApoE gene deletion on the plasma lipidaemic and glycemic profile. Measurement of total cholesterol, HDL-cholesterol, triglycerides and blood glucose in ApoE$^{-/-}$ mice and their age and background strain matched controls after feeding with chow (1% fat) and high fat (21% fat) diets. **A**) Total serum cholesterol was significantly increased in ApoE$^{-/-}$ mice fed a chow diet and further increased through feeding with a high fat diet. **B**) The concentration of HDL increased significantly in response to high fat feeding in control mice. This response to high fat feeding was not observed in ApoE$^{-/-}$ mice, however, it was observed that when fed a normal chow diet ApoE$^{-/-}$ mice have a significantly lower HDL concentration. **C**) There was no significant change in triglyceride concentration between the groups. **D**) Fasting blood glucose levels were not significantly changed by high fat feeding in either control or ApoE$^{-/-}$ mice. However, it was observed that ApoE$^{-/-}$ mice did have a significantly lower blood glucose concentration when compared to chow fed controls (n = 5 per group; one-way ANOVA with a post hoc Tukey's multiple comparisons test, * $p<0.05$, ** $p<0.01$, **** $p<0.001$)**.**

After eight weeks feeding with a high fat diet, fasting total cholesterol was not significantly increased in control mice (2.62±0.34mmol/l vs. 3.91±0.21mmol/l). However, in ApoE$^{-/-}$ mice fed a standard chow diet for eight weeks there was a significant increase when compared to both chow (2.62±0.34mmol/l vs. 8.67±0.36mmol/l; $p<0.01$) and high fat diet fed control mice (3.91±0.21mmol/l vs. 8.67±0.36mmol/l; $p<0.01$). Feeding of ApoE$^{-/-}$ mice with a high fat diet significantly increased the total cholesterol level further (8.67±0.36mmol/l vs. 18.53±1.72mmol/l; $p<0.001$)

The high-density lipoprotein component of total cholesterol (HDL-cholesterol) after eight weeks feeding on a chow diet was found to be significantly lower in ApoE$^{-/-}$ mice compared to diet matched control mice (1.29±0.17mmol/l vs. 0.37±0.08mmol/l; $p<0.001$). When fed on a high fat diet a significant increase in HDL-cholesterol was observed in control mice (1.29±0.17mmol/l vs. 1.82±0.09mmol/l; $p<0.05$) but not in ApoE$^{-/-}$ mice. There was a trend towards a reduction in the level of HDL-cholesterol in these mice; however, it was not significant (0.37±0.08mmol/l vs. 0.16±0.02mmol/l p=ns).

Fasting triglyceride levels were not significantly different between control and ApoE$^{-/-}$ mice when fed on a standard chow diet for eight weeks (4.25±0.73mmol/l vs. 3.72±0.92mmol/l). The feeding of a high fat diet showed a trend towards reduced levels of triglycerides in control (4.25±0.73mmol/l vs. 2.87±0.64mmol/l p=ns) and ApoE$^{-/-}$ mice (3.72±0.92mmol/l vs. 1.73±0.40mmol/l p=ns), however, the reduction in both groups was found to not be significantly different.

Analysis of the fasting blood glucose concentrations highlighted that ApoE$^{-/-}$ mice have significantly lower blood glucose levels than control mice after feeding for eight weeks on a standard chow diet (4.30±0.19mmol/l vs. 9.17±2.88mmol/l, $p<0.05$). Feeding with a high fat diet for the same period did not induce any significant changes in blood glucose concentration in either control (9.17±2.88mmol/l vs. 8.05±0.96mmol/l) or ApoE$^{-/-}$ mice (4.30±0.19mmol/l vs. 3.76±0.35mmol/l).

In summary, total cholesterol is not significantly increased after high fat feeding for eight weeks in control mice but is increased significantly in ApoE$^{-/-}$ mice fed on a standard chow diet for the same time period. Feeding ApoE$^{-/-}$ mice on a high fat diet causes a further significant increase in total cholesterol. HDL-cholesterol increases after high fat feeding in

control mice, however, this trend is not seen in ApoE$^{-/-}$ mice which have significantly lower HDL-cholesterol serum concentrations when fed either the standard chow or high fat diets. Triglyceride levels are not significantly different between control and ApoE$^{-/-}$ mice but show a trend towards being reduced after high fat feeding. Finally, fasting blood glucose is significantly lower in chow fed ApoE$^{-/-}$ mice when compared to diet matched controls but feeding with a high fat diet has no significant effect in either group.

4.2.3.3. The effect of high fat feeding and ApoE gene deletion on spleen weight

Atherosclerosis is closely correlated with inflammation and therefore the spleen weights of C57BL/6 (control) and ApoE$^{-/-}$ mice were measured, after eight weeks feeding on either a standard chow diet or a high fat 'western' diet, as an indirect indicator [323]. There was no significant difference in spleen weight when control chow fed mice were compared to diet matched ApoE$^{-/-}$ mice (72.37±3.28mg vs. 84.97±6.01mg p=ns). After feeding with a high fat diet, however, there was a significant increase in spleen weight in both control (72.37±3.28mg vs. 102.6±2.55mg; $p<0.001$) and ApoE$^{-/-}$ mice (84.97±6.01mg vs. 115.8±6.26mg; $p<0.005$). The increase in spleen weight was not significantly different between high fat diet fed control and ApoE$^{-/-}$ mice.

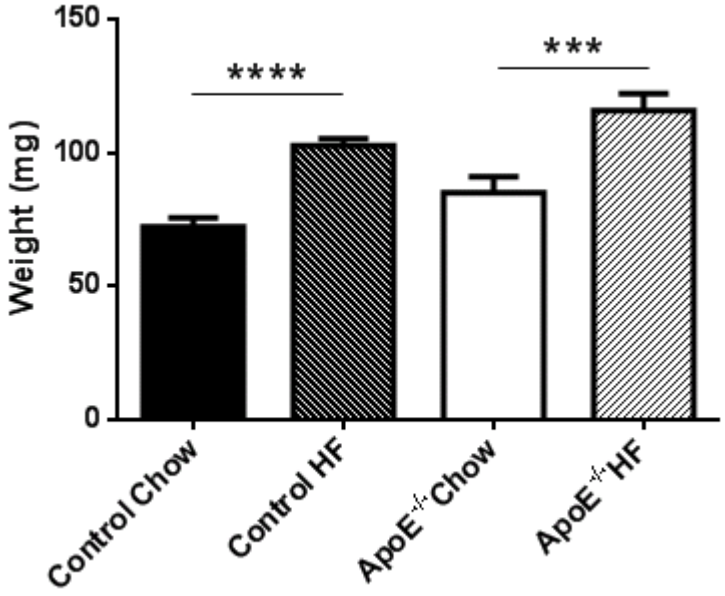

Figure 4.8. The effect of high fat feeding and ApoE gene deletion on spleen weight. There was no difference in spleen weight between control and ApoE$^{-/-}$ mice when fed on a chow diet. Feeding with a high fat diet for eight weeks showed a significant increase in spleen weight in both control and ApoE$^{-/-}$ mice. The increase in spleen weight was not significantly different between the control and ApoE$^{-/-}$ mice (n= 13, 15, 9, 12, respectively; one-way ANOVA with post hoc Tukey's multiple comparisons test, *** $p<0.005$, **** $p<0.001$).

4.2.3.4. The effect of high fat feeding and ApoE gene deletion on perivascular adipocyte morphology

PVAT has been identified as a source of anti-inflammatory and vasoactive factors, called adipokines. During the development of obesity, adipocytes increase their lipid deposits and become enlarged. These enlarged adipocytes then release less of the anti-atherogenic adipokines and start to produce inflammatory cytokines [324]. It is for this reason that the morphology of the perivascular adipocytes was measured, to assess the effects of high fat feeding and ApoE gene deletion on the signs of developing obesity. Initial qualitative assessment of the adipocyte morphology identified two distinct populations; small adipocytes ($< 5\mu m^2$) and large adipocytes ($> 5\mu m^2$) (Figure 4.9). These two populations were assessed individually for changes in their size (Figure 4.10 A and B) and number (Figure 4.10 C and D).

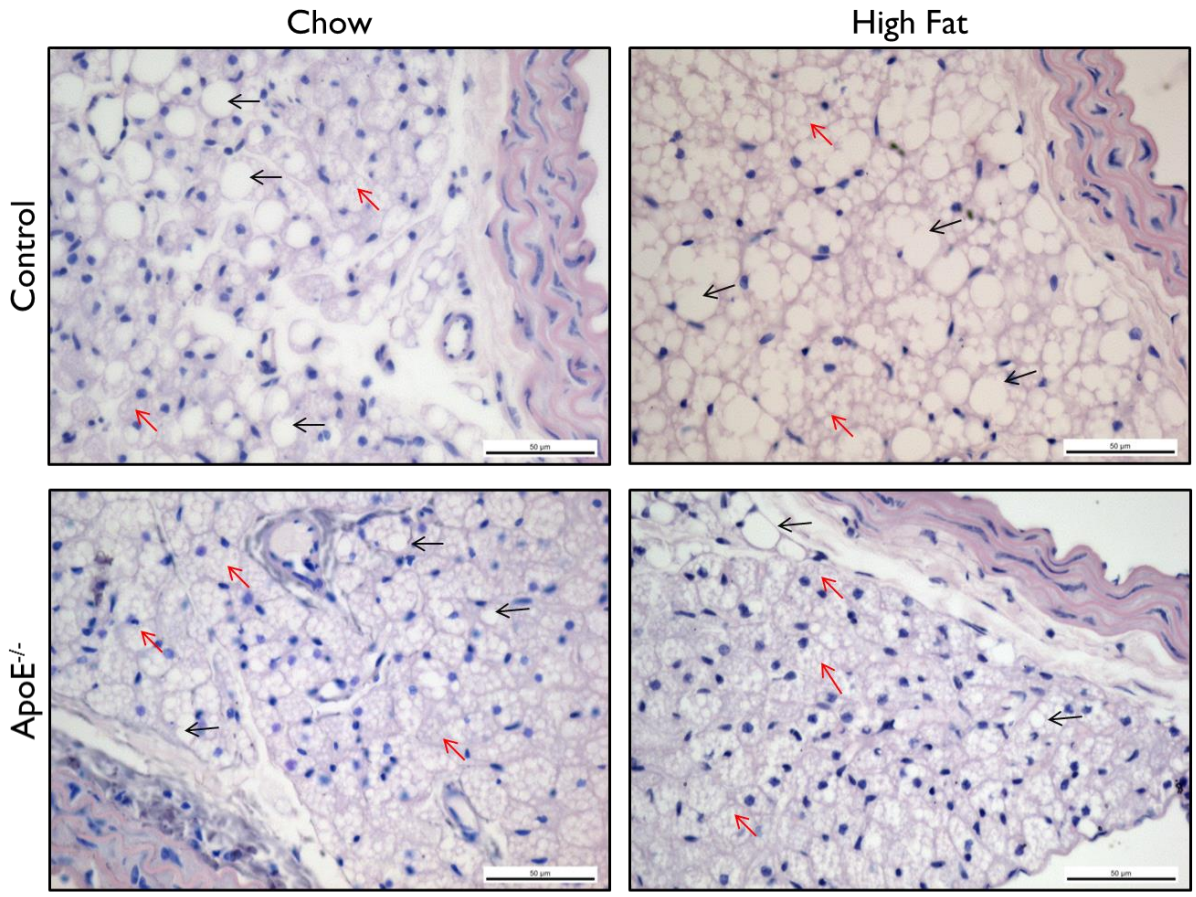

Figure 4.9. Representative images of murine thoracic aortic perivascular adipose tissue showing the effects of high fat feeding and ApoE deletion. Qualitative analysis of histological sections of thoracic aortic PVAT identified the presence of small (red arrows) and large (black arrows) adipocytes (Scale bar represents 50µm).

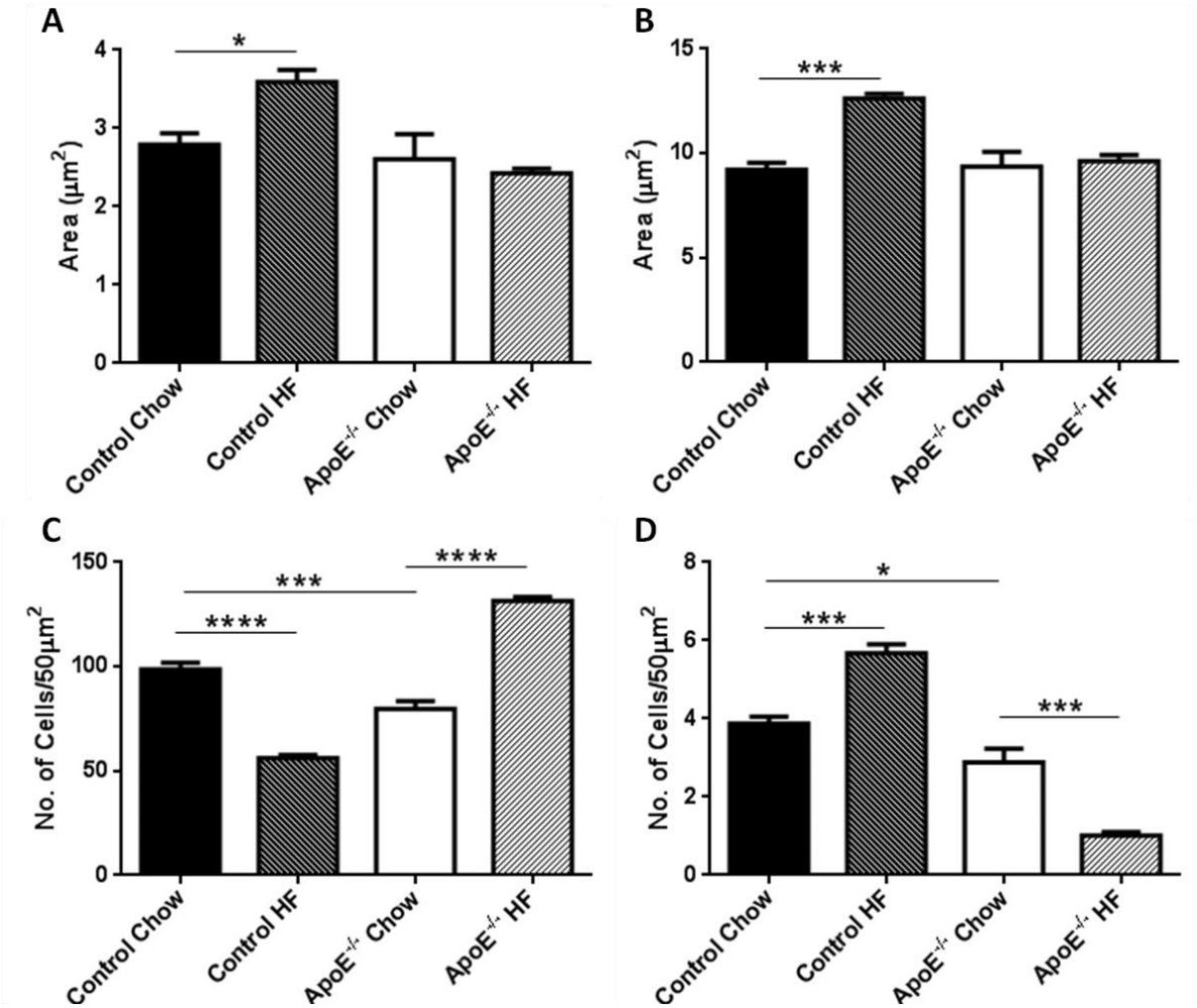

Figure 4.10. The effect of high fat feeding and ApoE gene deletion on perivascular adipocyte morphology. The area and number of adipocytes was measured in murine thoracic aortic PVAT as an indicator of early obesity. Two distinct populations of adipocytes were identified; according to their size these were defined as small (< 5 µm^2) and large (> 5µm^2) adipocytes. Analysis of the area of small (**A**) and large adipocytes (**B**) demonstrated that high fat feeding in control mice lead to hypertrophy of both adipocyte populations. No change was observed in ApoE$^{-/-}$ chow fed mice. However, ApoE gene deletion does appear to protect against high fat diet induced adipocyte hypertrophy as no change in adipocyte area was observed in high fat fed ApoE$^{-/-}$ mice. Assessment of the number of small (**C**) and large (**D**) adipocytes demonstrated that ApoE$^{-/-}$ mice have a lower overall level of adiposity; numbers of small and large adipocytes were significantly lower in chow fed ApoE$^{-/-}$ mice. In response to high fat feeding control mice demonstrated a significant increase in the number of large adipocytes and a reduction in the number of small adipocytes. The inverse of this relationship was observed in ApoE$^{-/-}$ mice (n=5 per group, one-way ANOVA with post hoc Tukey's multiple comparisons test, * $p<0.05$, *** $p<0.005$, **** $p<0.001$).

Upon analysis of the size of small adipocytes (< 5 μm^2) it was found that there was no significant difference between control or ApoE$^{-/-}$ mice when fed on a standard chow diet for eight weeks (2.79±0.14μm^2 vs. 2.60±0.32μm^2). After high fat feeding, for the same period, control animals exhibited a significant increase in small adipocyte area (2.79±0.14μm^2 vs. 3.59±0.16μm^2; $p<0.05$). This increase was not observed in ApoE$^{-/-}$ mice after eight weeks high fat feeding (2.60±0.32μm^2 vs. 2.42±0.06μm^2 p=ns). The same trend was observed when the area of large adipocytes (>5μm^2) was assessed. There was no difference between control and ApoE$^{-/-}$ mice on a standard chow diet (9.23±0.32μm^2 vs. 9.36±0.72μm^2) but after high fat feeding the size of the large adipocytes was significantly increased in control (9.23±0.32μm^2 vs. 12.63±0.23μm^2; $p<0.001$) but not in ApoE$^{-/-}$ mice (9.36±0.72μm^2 vs. 9.62±0.30μm^2).

The number of adipocytes was measured and revealed that, after feeding on a standard chow diet, control mice have a significantly higher number of small and large adipocytes compared to diet matched ApoE$^{-/-}$ mice (Small adipocytes: 98.73±3.2cells/50μm^2 vs. 79.74 ±3.78 cells/50μm^2; $p<0.001$. Large adipocytes: 3.88 ±0.18 cells/50μm^2 vs. 2.88 ±0.35 cells/50μm^2; $p<0.05$). After eight weeks on a high fat diet control mice showed a significant decrease in the number of small adipocytes (98.73 ±3.22 cells/50μm^2 vs. 56.08 ±1.61 cells/50μm^2; $p<0.001$) and a significant increase in the number of large adipocytes (3.88 ±0.18 cells/50μm^2 vs. 5.67 ±0.54 cells/50μm^2; $p<0.005$). The opposite trend was observed in high fat diet fed ApoE$^{-/-}$ mice with a significant increase in the number of small adipocytes (79.74 ±3.78 cells/50μm^2 vs. 131.50 ±1.94 cells/50μm^2; $p<0.001$) and a significant decrease in the number of large adipocytes (2.88 ±0.35 cells/50μm^2 vs. 1.01 ±0.09 cells/50μm^2; $p<0.005$).

In summary, after eight weeks feeding on a chow diet control mice have a larger number of small and large adipocytes compared to diet matched ApoE$^{-/-}$ mice. After high fat feeding, hypertrophy of small and large adipocytes was observed in control mice, however, this was not observed in ApoE$^{-/-}$ mice. High fat feeding induced an increase in the number of large adipocytes with a concomitant reduction in the number of small adipocytes in control mice. The opposite trend was observed in ApoE$^{-/-}$ mice.

4.3. Discussion

The aim of this chapter was to assess the phenotype of C57BL/6 (control) and ApoE$^{-/-}$ mice after feeding on either a standard chow diet or a high fat 'western' diet for eight weeks. To this end a number of parameters, associated with increased risk of atherosclerotic disease, were measured along with an assessment of the stage of development. It was noted by Nakashima *et al.* (2004) that ApoE$^{-/-}$ mice fed a high fat diet demonstrated foam cell deposition, an early stage of atherosclerotic plaque development, in the aortic root and pulmonary arteries after 10 weeks feeding [141]. However, in the present investigation it was found that after eight weeks of high fat feeding, although there was some evidence of fatty depositions in the aortic arch and intercostal branches of ApoE$^{-/-}$ mice, no fatty lesions were observed in the thoracic aorta itself. This was also confirmed in control mice after feeding on either diet. Plaque formation in the thoracic aorta occurs in both ApoE$^{-/-}$ mice and humans but is considered as a late-stage development [143,325,326] which increases the prevalence of strokes in human patients [327]. Our data are in agreement with these findings and confirm that after eight weeks feeding with a high fat 'western' diet there is no evidence of overt atherosclerotic disease in the descending thoracic aorta.

Obesity has been characterised as a risk factor for the development of cardiovascular diseases associated with atherosclerotic disease [328]. To assess the effects of high fat feeding and ApoE gene deletion on overall body weight, heart weight to body weight ratio (HW:BW; an indicator of growth rather than obesity), as well as sites of obesity associated fat deposition (epididymal fat pads and aortic perivascular adipose tissue), were compared between control and ApoE$^{-/-}$ mice. The present study has identified two major differences attributable to the effects of ApoE gene deletion. A larger HW:BW ratio was observed in ApoE$^{-/-}$ mice after eight weeks feeding on standard chow and high fat diet which is likely due to the presence of right ventricular hypertrophy [329], a previously identified phenomenon in these mice. In addition, using aortic PVAT adipocyte numbers as an indicator suggested an overall lower level of adiposity in ApoE$^{-/-}$ mice which is supported by previous evidence [330].

Following high fat feeding, there was a significant increase in the body weight of control and ApoE$^{-/-}$ mice, which when taken in conjunction with the lack of relative change in the HW:BW ratio, suggests an increase in fat deposition as the cause. However, in accordance with previous literature, there appeared to be a level of protection afforded by the deletion of

the ApoE gene against weight gain in response to feeding with a high fat diet [146,330]. This was additionally evidenced by the lack of increased epididymal fat pad weight and thoracic aorta PVAT adipocyte hypertrophy in ApoE$^{-/-}$ mice after high fat feeding. It has been suggested by Schreyer *et al.* (2002) that this protective role of ApoE deletion is conferred in its ability to promote lipoprotein secretion rather than fatty acid oxidation, which leads to adipose tissue deposition, from hepatic triglyceride stores [330].

The lipidaemic profiles of ApoE$^{-/-}$ mice have been recorded at a number of time points since their creation, however, a large proportion of the literature has focused on feeding for longer than 3 months [258,259,319,331] to allow the development of advanced atherosclerotic plaques. The present study was designed to assess the lipidemic phenotype prior to this level of disease development; therefore, feeding for only eight weeks was undertaken. Plump *et al.* (1992) showed that after just 2.5 weeks feeding on either a standard chow or a high fat 'western' diet total serum cholesterol levels were significantly increased in ApoE$^{-/-}$ mice, however, high fat feeding did not significantly increase total plasma cholesterol concentration in wildtype C57BL/6 mice; a pattern of results which correlates directly with those observed after eight weeks feeding in the present investigation. The levels of total cholesterol were also not significantly different between 2.5 and eight weeks feeding in any group (data not shown); suggesting that total cholesterol is raised quickly and plateaus within 2.5 weeks of feeding. The observed hypercholesterolaemia is due to the previously mentioned role of ApoE in the preferential production of lipoproteins from hepatic triglyceride stores [330] as well as its role in extra-hepatic tissues in promoting reverse cholesterol transport, demonstrated in a model of ApoE overexpression [258]. In addition to ApoE, high density lipoproteins are also linked to reverse cholesterol transport [332,333].

In human and murine models, the concentration of HDL is inversely correlated with atherosclerotic disease risk and HDL-mimetics are being assessed as possible future treatments for hypercholesterolaemia [334–337]. After high fat feeding the level of HDL cholesterol in C57BL/6 mice was increased. In contrast, the levels of HDL cholesterol observed in ApoE$^{-/-}$ mice were significantly lower after feeding on a standard chow diet and were not significantly altered in response to high fat feeding. These findings again are in accordance with those observed by Plump *et al.* (1992) after 2.5 weeks feeding [138] and suggests that the lipidemic profile responds rapidly to dietary modulation and subsequently plateaus. Laboratory mice are typically resistant to atherosclerotic disease due to the majority

of cholesterol being transported by anti-atherogenic HDL, however, Paigen *et al.* (1985) examined several inbred strains of mice and found that C57BL/6 mice typically have a lower concentration of HDL cholesterol, thus they are susceptible to developing atherosclerosis, although only after extended feeding [338,339]. The further reduction of HDL cholesterol concentration in ApoE$^{-/-}$ mice suggests that murine HDL is rich in ApoE rather than ApoA-I and ApoA-II observed in human HDL [337,340]. This reduction in the ability to carry cholesterol on HDL in the presence of an increased cholesterol burden will increase the prevalence of very low and low density lipoproteins (VLDL and LDL, respectively) which are pro- rather than anti-atherogenic and explain the exacerbated susceptibility of ApoE$^{-/-}$ mice to atherosclerotic disease.

Other atherosclerotic risk factors borne within the serum were then considered. The first being the concentration of plasma triglycerides. The results of the present investigation were inconclusive showing no significant alterations in the level of plasma triglycerides even in response to high fat feeding. This was surprising as in the same mouse model triglyceride concentrations were increased in both short- and long-term feeding with the high fat 'western' diet [138,259]. The present data show a trend towards a reduced triglyceride concentration after high fat feeding which is counter-intuitive, the method of measurement was therefore examined. One contributing factor may be that the assay employed was unable to measure free glycerol therefore producing an artificially lower concentration, in addition, a similar Cobas analyser was shown to be unable to accurately determine triglyceride concentrations in highly lipidemic samples due to the generation of an anaerobic environment interfering with the development of the colorimetrically analysed chromagen [341].

In addition to cholesterol, the glycemic profile was assessed due to its implications for insulin signalling and the presence of diabetes; a major co-morbidity of atherosclerotic disease [342–344]. Our investigations have shown that high fat feeding does not have a significant effect on fasting blood glucose concentrations in C57BL/6 or ApoE$^{-/-}$ mice. However, it was observed that ApoE$^{-/-}$ mice, in a similar fashion to adiposity, showed significantly lower blood glucose concentrations after eight weeks feeding on a standard chow diet; suggesting some level of protection against high fat diet induced hyperglycaemia. This has been suggested previously, however, the direct mechanism is yet to be elucidated [330]. As an assessment of the overall phenotype it is possible to compare the fasting blood glucose concentrations to those observed in a model of type II, diet induced, diabetes. The db/db mouse has a fault in leptin

signalling and develops a diabetic phenotype [345]; a comparison between the data from the present study and those measured in two studies using age matched db/db mice show fasting glucose levels of approximately 27mmol/L [346,347] which is 3 times as large as the highest blood glucose concentration, measured in high fat diet fed C57BL/6 mice. Therefore it is possible to conclude that high fat feeding for eight weeks in C57BL/6 mice does not produce a diabetic phenotype and that deletion of the ApoE gene confers a further protective effect.

Obesity, hypercholesterolaemia, and hyperglycaemia have all been discussed above. These are three key risk factors that have been theorised to contribute to the development of atherosclerosis. However, as the field of atherosclerotic disease research has developed over the past 20 years it has come to be widely accepted that these are co-risk factors all contributing together and that the origins of the disease may lie in the role of inflammation [3,348]. In order to assess the effects of high fat feeding and ApoE gene deletion we employed an indirect measure of inflammation; spleen weight [323,349–351]. The present study found that deletion of the ApoE gene in the absence of high fat feeding did not alter inflammation, however, in both C57BL/6 wildtype and $ApoE^{-/-}$ mice eight weeks feeding on a high fat 'western' diet significantly increased spleen weights; indicating an increase in overall inflammation. It has been shown that ApoE has an anti-inflammatory role independent of its effects on lipid metabolism [352,353], however, the present data show no significant difference in spleen weight between diet matched C57BL/6 and $ApoE^{-/-}$ mice. The reason for this may be, as previously stated, that the measurement of spleen weights, although commonly employed, is only an indirect measurement of inflammation. Therefore, further investigation into the specific levels of inflammatory cytokines may highlight previously described effects of ApoE gene deletion [260].

Atherosclerosis is a vascular disease and therefore vascular specific inflammation has been attributed as one of the primary triggers in the diseases progression. One such source of vascular inflammation, that has been shown to influence vascular function through modification of nitric oxide signalling, is perivascular adipose tissue (PVAT) [236,241,242,354]. The increase in inflammatory cytokine release from the adipose tissue has been linked to obesity and the increased size of individual adipocytes developing a hypoxic core [324,355]. The present study observed that deletion of the ApoE gene had no effect on the size of either the population of large or small adipocytes. Confirmation of the presence of brown adipose tissue within murine thoracic aorta PVAT has been described previously, however, in the present

investigation only morphological characterisation was employed which clearly identified two distinct populations; further characterisation would require the use of specific markers such as uncoupling protein 1 (UCP1) [234]. Analysis of the effects of high fat feeding showed that after eight weeks on the 'western' diet PVAT adipocytes in C57BL/6 mice, both large and small, were significantly larger. The same increase was not observed in ApoE$^{-/-}$ mice after high fat feeding. The increase in adipocyte size correlates to an increase in lipid deposition, therefore, as previously described, the role of ApoE in fatty acid oxidation, promoting fat deposition, is the likely mechanism behind this observation; again supported by the protection against obesity observed in ApoE$^{-/-}$ mice [330].

4.4. Conclusions

Overall, this chapter aimed to identify the phenotypical changes, associated with well characterised risk factors for atherosclerotic disease, that occur in mice due to the effects of high fat feeding and/or ApoE gene deletion. The use of diet matched controls, a methodological approach that is often over looked when studying the effects high fat feeding, with particular reference to vascular function [175,180,259,356], was employed to allow for the source of any observed changes to be attributed to genetic or dietary manipulation. In both C57BL/6 and ApoE$^{-/-}$ mice we have confirmed that after eight weeks of feeding on a standard chow diet or a high fat 'western' diet there is no evidence of overt atherosclerosis.

Total cholesterol was not significantly increased by high fat feeding in C57BL/6 mice; however, deletion of the ApoE gene produced hypercholesterolaemia which was then significantly exacerbated by high fat feeding. In addition, through comparison with specific animal models, we can conclude that there is no evidence for dysfunction of blood glucose homeostasis induced by high fat feeding or ApoE gene deletion. However, it was observed that deletion of the ApoE gene resulted in a significantly lower basal fasting glucose concentration. Investigation into markers of obesity demonstrated that in response to high fat feeding, both C57BL/6 and ApoE$^{-/-}$ mice gain weight, however, deletion of the ApoE gene results in a level of protection. During histological analysis of thoracic aortic PVAT it was observed that ApoE$^{-/-}$ mice have a lower level of basal adiposity and they are protected against high fat 'western' diet induced adipocyte hypertrophy. Adipocyte hypertrophy has been associated with increased inflammation. Spleen weight was assessed as an indirect

measure of systemic inflammation and was shown to be increased in response to high fat diet in both C57BL/6 and ApoE$^{-/-}$ mice.

Moving forward with this model to assess vascular function prior to the development of atherosclerotic disease in the following chapter will allow isolation of some of the main atherosclerotic risk factors; such as increased plasma cholesterol without the presence of obesity or inflammation in ApoE$^{-/-}$ mice after feeding on a standard chow diet. This approach may allow for an increased understanding in the contribution of risk factors in the early stages of atherosclerotic disease development.

4.4.1. Summary of conclusions

- **After eight weeks feeding on either a chow or high fat diet there was no evidence of atherosclerotic plaques or intimal thickening in the descending thoracic aorta of C57BL/6 or ApoE$^{-/-}$ mice.**

- **Total cholesterol is significantly increased in chow fed ApoE$^{-/-}$ mice after eight weeks; feeding with a high fat 'western diet' causes a further significant elevation.**

- **Fasting blood glucose was lower in ApoE$^{-/-}$ chow fed mice indicating a protective role for ApoE**

- **High fat feeding caused a significant increase in total body weight and perivascular adipocyte hypertrophy in C57BL/6 mice. Deletion of the ApoE gene appears to offer a degree of protection against weight gain and confers resistance to adipocyte hypertrophy.**

- **Spleen weight, indicative of systemic inflammation, is significantly increased after feeding on a high fat 'western' diet; observed in both C57BL/6 and ApoE$^{-/-}$ mice.**

5. Is vascular function altered prior to overt atherosclerotic disease development?

5.1. Overview

The effects on vascular function of atherosclerotic risk factors; such as hypercholesterolaemia, obesity and inflammation, have been studied in isolation, however, through the use of a animal models their combined function is able to be assessed. Contributing to vascular function are, primarily, the activities of endothelial and smooth muscle cells. Their responses to circulating factors and paracrine signalling, including nitric oxide and prostaglandins, along with the intracellular effector [Ca^{2+}], have previously been investigated in atherosclerosis however, largely after the development of atherosclerotic plaques [357]. Whether the activity of endothelial or smooth muscle cells is altered during the early development of atherosclerotic disease is an important question to consider. This is due to the fact that vascular function has become part of the diagnostic assessment of cardiovascular disease [31] and identification of early changes in vascular function may highlight potential early warning signs. However, the translation of vascular function from the mouse model to the clinic is difficult. There is still a necessity to identify and expand the current knowledge of early atherosclerotic pathogenesis and the role the vasculature can play in this with the hope of improving diagnosis and opening up new areas for possible treatments.

An increase in vascular contractility is considered a risk factor for atherosclerotic disease development. The contractile nature of vessels controls the flow dynamics of blood within the lumen and can allow for areas of disturbed flow; areas which are more susceptible to atherosclerotic lesion development [288]. Vascular smooth muscle cell proliferation may also be able to modulate vascular function. There is evidence for the migration and proliferation of smooth muscle cells in advanced atherosclerotic lesions [3] and these proliferative cells have altered intracellular calcium handling [67]. The tight control of $[Ca^{2+}]_i$ is of vital importance in the regulation of vascular contractility by vascular smooth muscle cells. In addition, the reduced activity of relaxant factors, particularly nitric oxide, is widely perceived to indicate dysfunction in the vascular endothelium. Thought to be brought about by increased reactive oxygen species production, the reduction of nitric oxide activity in the endothelium is also considered as a primary step in the development of atherosclerosis [358] due to effects on the vascular tone and also by promoting expression of adhesion molecules [359]. The latter of these processes promotes recognition and infiltration of inflammatory cells, a well established

phase of early plaque development [3,348]; however, this can also have downstream effects on vascular function via the activity of prostaglandin signalling [322].

Therefore, this investigation will focus on the early stages of atherosclerosis prior to the development of wide spread advanced atherosclerotic plaques, to identify the effects of risk factors such as hypercholesterolaemia, obesity and inflammation. The ability of the murine thoracic aorta to contract and relax at this early stage of development will be assessed; further investigation into intracellular mechanisms and signalling pathways, including $[Ca^{2+}]_i$, nitric oxide and prostaglandins, will also be carried out.

5.1.1. Methods

Full details of the methods employed can be found in sections 2.4 and 2.5 of Chapter 2. *Ex vivo* wire myography was performed on thoracic aortic rings from C57BL/6 (control) and $ApoE^{-/-}$ mice fed on either a standard chow or a high fat 'western' diet for eight weeks. Contractility was assessed through exposure to a depolarising stimulus as well as two pharmacological agonists, phenylephrine and serotonin. These agonists act at different receptors but share the same downstream intracellular second messengers. Alterations in the contractile activity of the thoracic aorta were investigated further using de-endothelialisation and intracellular calcium imaging. Imaging of intracellular calcium was performed using tissues loaded with the calcium sensitive dye Indo-1. Two mechanisms of vascular relaxation, endothelium-dependent and independent, were investigated using acetylcholine and sodium nitroprusside (SNP), respectively. Alterations in these two mechanisms were investigated further through pharmacological inhibition of the downstream effectors.

Contractile data are represented as changes in tension (ΔTension). Contractions to the depolarising stimulus were measured in absolute force (mN); contractions to pharmacological agonists were then normalised to this value as a percentage change (normalised % ΔTension). Intracellular calcium data are represented as a change in the autofluorescence-corrected 405nm:500nm fluorescence ratio ($\Delta F_{405}:F_{500}$). All relaxation data are represented as percent reduction from the stable peak contraction to phenylephrine (% relaxation). Data were analysed using Prism software (Version 6.) employing a one-way ANOVA with post hoc Tukey's multiple comparisons test or Student's t-test, as stated. Probability values of $p<0.05$ were considered to be significantly different.

5.2. Results

5.2.1. Vascular contractility during developmental atherosclerosis

Vascular contractility was assessed in response to different mediators of contraction. Firstly, high extracellular potassium chloride (KCl) produced contraction via direct electro-chemical induction of depolarisation (Figure 5.1). Pharmacological agonists to membrane bound α-adrenoreceptors (phenylephrine; Figure 5.2 A) and 5-HT receptors (serotonin; Figure 5.2 B), activators of the $G\alpha_q$-PLC-IP_3 second messenger cascade, were then employed.

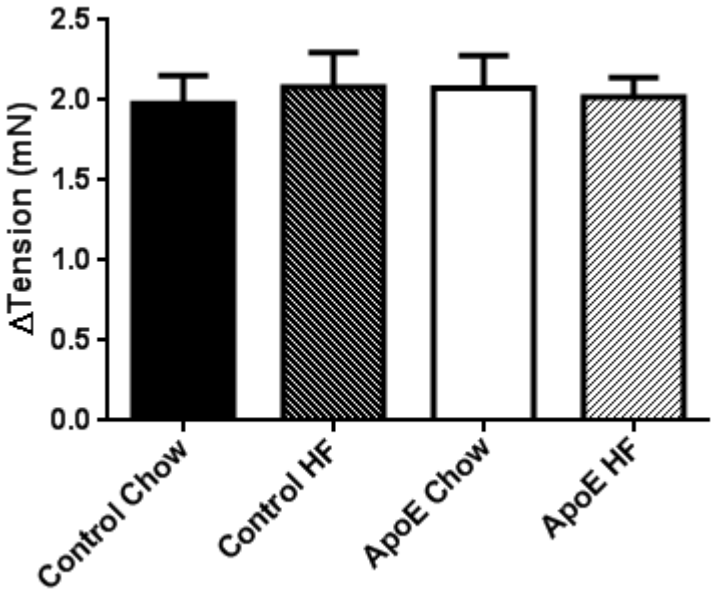

Figure 5.1. The effect of high fat feeding and ApoE gene deletion on contractility to a depolarising stimulus. Thoracic aortic rings in an *ex vivo* wire myograph were constricted with 100mM KCl containing HEPES-PSS. There were no observed effects from deletion of the ApoE gene. Feeding with a high fat 'western' diet also had no significant effect on contractility after depolarisation (n = 11, 7, 4, 9, respectively).

Contractility of thoracic aortic rings to a depolarising stimulus was not significantly different between control and $ApoE^{-/-}$ mice fed on a standard chow diet for eight weeks (2.0±0.2mN vs. 2.1±0.2mN). High fat feeding for the same time period did not alter contractility to depolarisation in control (2.0±0.2mN vs. 2.1±0.2mN) or $ApoE^{-/-}$ mice (2.1±0.2mN vs. 2.0±0.1mN).

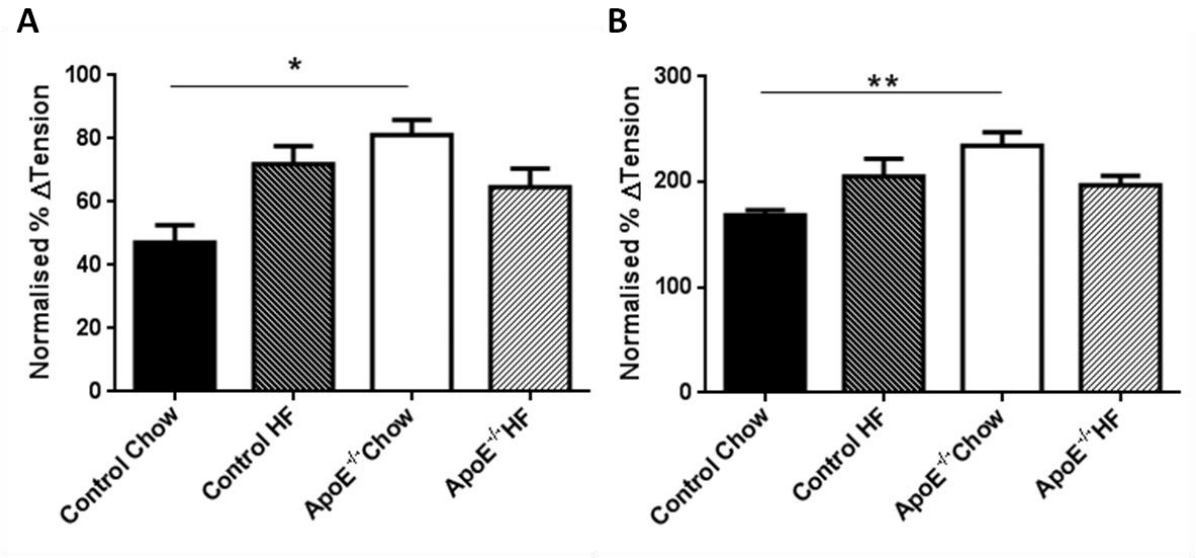

Figure 5.2. The effect of high fat feeding and ApoE gene deletion on contractility of the murine thoracic aorta. When stimulated by agonists to either the α_1-adrenoreceptor (Phenylephrine; **A**) or the 5-HT receptor (Serotonin; **B**) there was a significant increase in contractility in chow-fed ApoE$^{-/-}$ mice when compared to their age, strain and diet matched controls (n = 11,7,11,9, respectively; one-way ANOVA with post hoc Tukey's multiple comparisons test, * $p<0.05$, ** $p<0.01$).

Contractility to the pharmacological agonists phenylephrine and serotonin exhibited a very similar pattern to each other. When arteries from control and ApoE$^{-/-}$ mice were compared after eight weeks feeding on a standard chow diet it was found that, in response to both agonists, the contractility in ApoE$^{-/-}$ mice was significantly increased (phenylephrine: 47.2±5.5% vs. 81.2±4.7%; $p<0.05$. Serotonin: 168.7±4.7% vs. 234.6±12.6%; $p<0.01$). In response to high fat feeding, control mice showed a trend towards increased contractility (Phenylephrine: 47.2±5.5% vs. 71.9±5.80%. Serotonin: 168.7±4.7% vs. 205.3±16.8%), and a trend towards reduced contractility was observed in ApoE$^{-/-}$ mice (Phenylephrine: 81.2±4.7% vs. 64.6±6.0%. Serotonin: 234.6±12.6% vs. 197.0±8.9%). However, these trends were not statistically significant.

In summary, contractility to depolarisation was not altered; however, contractility to both phenylephrine and serotonin was significantly increased in ApoE$^{-/-}$ mice after eight weeks feeding on a standard chow diet. High fat feeding showed a trend towards increasing contractility in control mice but reducing contractility in ApoE$^{-/-}$ mice.

5.2.1.1. Investigating store-operated calcium entry as a mechanism for altered contractility

Store-operated calcium entry has been linked to contractility in other vascular tissues and is affected by cholesterol modulation [187,360]. Intracellular calcium and contractility were measured independently using a protocol to induce store-operated calcium entry through incubation with the SERCA inhibitor cyclopiazonic acid (CPA). Comparisons of the responses in control and ApoE$^{-/-}$ mice were made and also to a vehicle control (DMSO) to confirm an effect of the treatment. Comparisons were made between the basal calcium levels (Figure 5.3), the effect of extracellular calcium removal (Figure 5.4), the direct effect of CPA treatment (Figure 5.5) and the effect of reintroducing extracellular calcium (Figure 5.6).

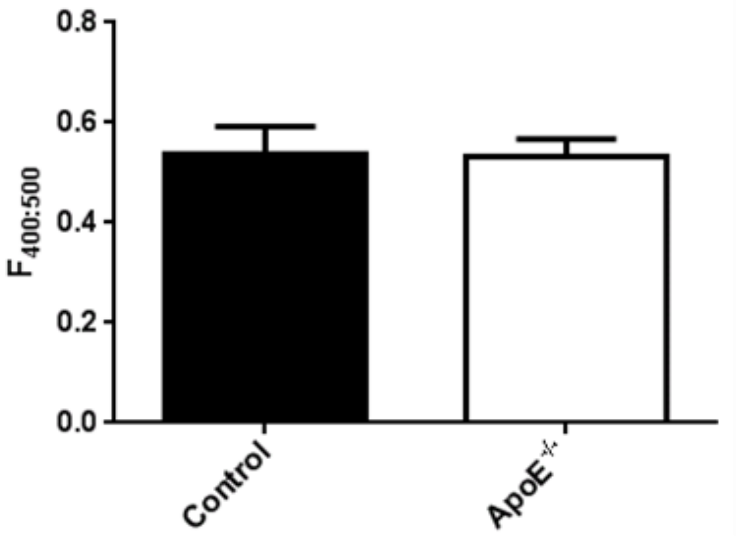

Figure 5.3. The effect of ApoE gene deletion on basal calcium levels. The 405nm:500nm Indo-1 fluorescence ratio, after a 30 minute equilibration period, was compared between control and ApoE$^{-/-}$ mice after eight weeks feeding on a standard chow diet. The ratio sampled at this time was used to measure the baseline level of calcium-sensitive fluorescence. There was no observable difference in the baseline calcium fluorescence between control and ApoE$^{-/-}$ mice (n = 10, 5, respectively).

The baseline autofluorescence corrected ratio was compared between control and ApoE$^{-/-}$ mice after eight weeks feeding on a standard chow diet. There was no significant difference observed between the two groups (0.54±0.06 vs. 0.53±0.04). The removal of extracellular calcium produced a reduction in intracellular calcium in control and ApoE$^{-/-}$ mice but there was no significant difference between the two groups (-0.01±0.08 vs. -0.08±0.008).

Extracellular calcium removal did not cause a significant change in tension in aortic rings from either control or ApoE$^{-/-}$ mice (-0.04±0.01mN vs. -0.04±0.03mN) (Figure 5.4).

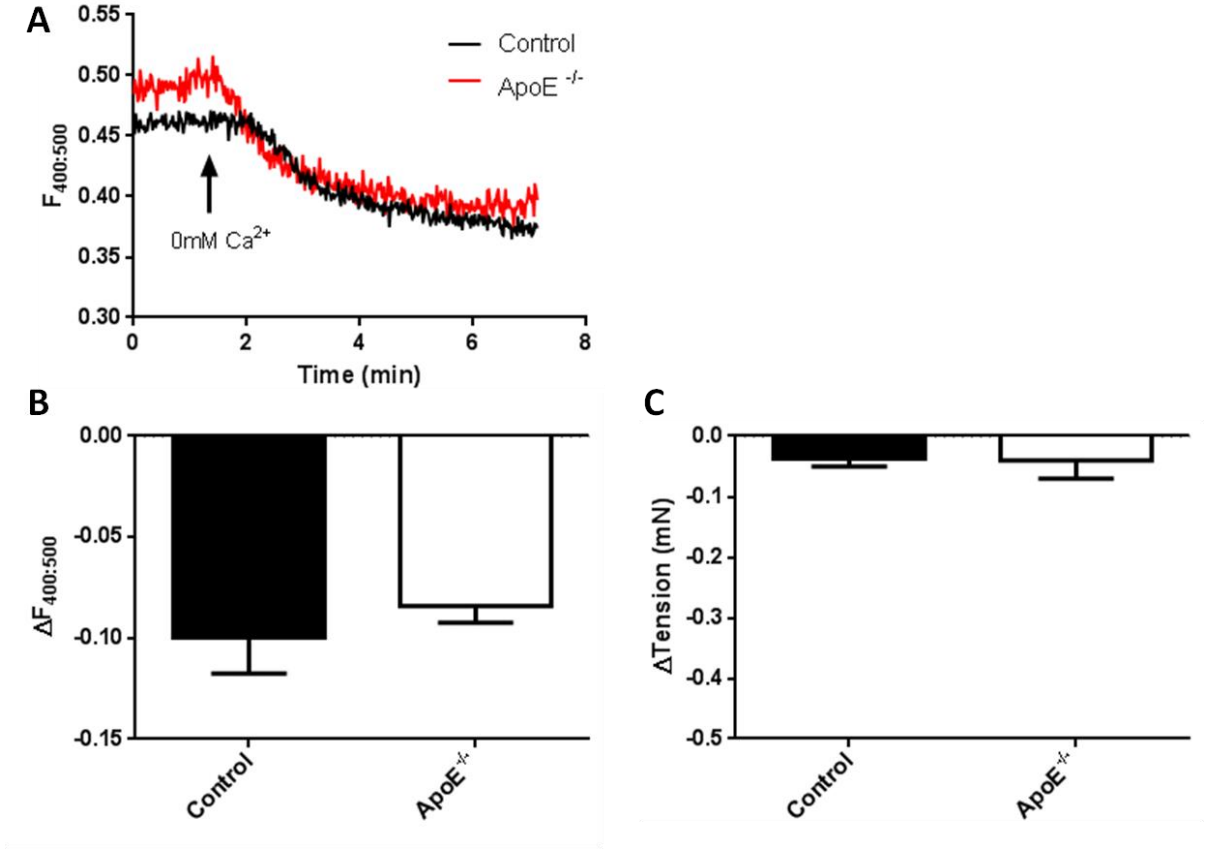

Figure 5.4. The effect of extracellular calcium removal on intracellular calcium and contractility. After equilibrating for 30 minutes, thoracic aortic strips from chow fed C57BL/6 and high fat fed ApoE$^{-/-}$ mice were exposed to a calcium free extracellular solution (2mM EGTA). A drop in the 405:500nm Indo-1 fluorescence ratio was observed that was thought to correlate to the removal of cytosolic calcium. There was no significant difference observed in the ratio decline between control and ApoE$^{-/-}$ mice; as shown by the representative traces (**A**) and the mean data (**B**; n = 7, 3, respectively). In a separate experiment, the same conditions were re-created to assess the effect of cytosolic calcium removal on contractility. In thoracic aortic rings, equilibrated at 5mN resting tension, removal of cytosolic calcium had no significant effect on tension. In addition, there were no differences observed between control and ApoE$^{-/-}$ mice (**D**; n = 7, 5, respectively).

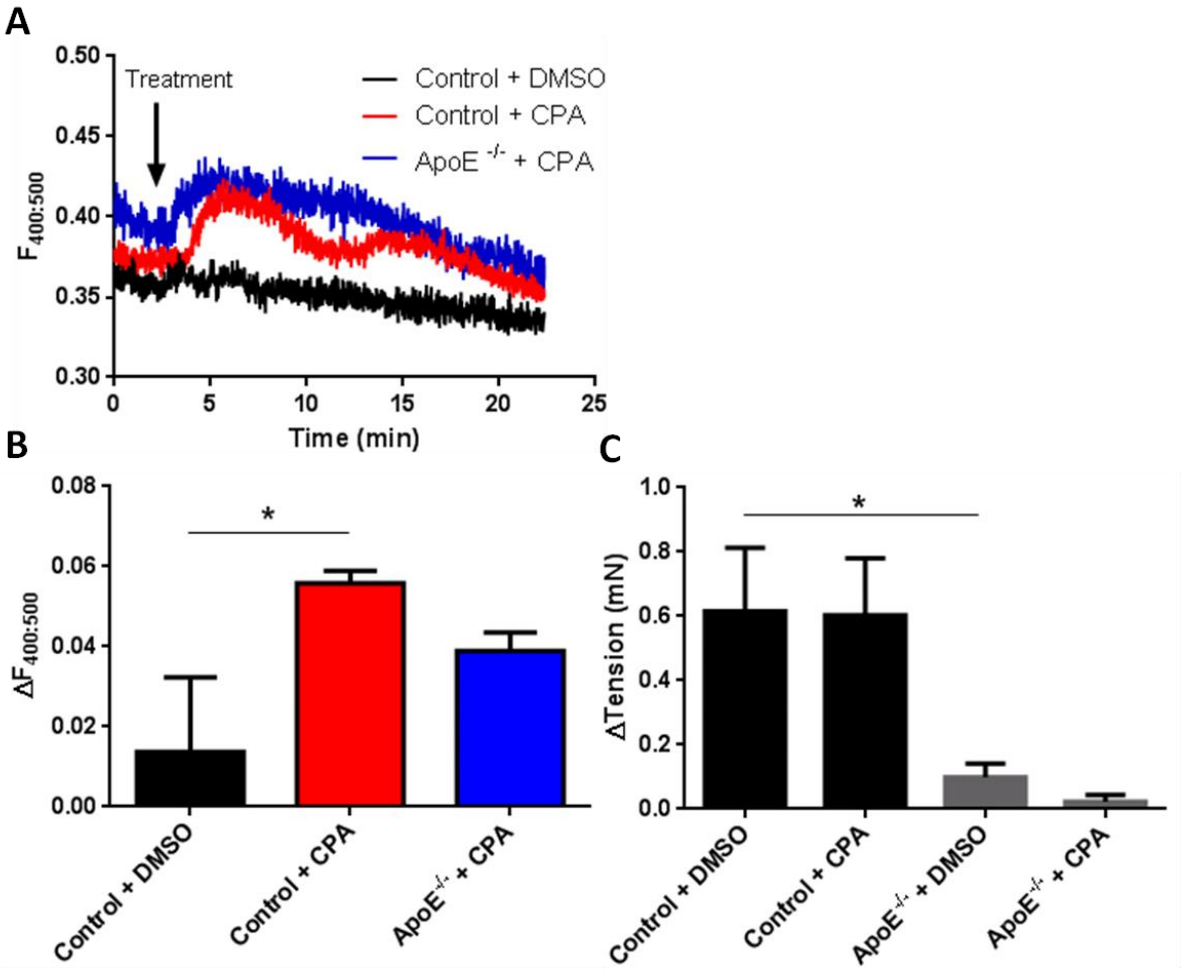

Figure 5.5. The effect of CPA on intracellular calcium and contractility. After depletion of cytoplasmic calcium, by incubation in calcium free solution, the sarcoplasmic stores of thoracic aortic strips from C57BL/6 wild type and high fat fed ApoE$^{-/-}$ mice were emptied through blockade of the SERCA pump with cyclopiazonic acid (CPA;10µM). A transient increase in the 405:500nm Indo-1 fluorescence ratio was observed as shown in the representative traces (**A**). The increase in $[Ca^{2+}]_i$ associated with increased fluorescence was found to be significantly greater in response to CPA over the vehicle control (DMSO) in chow fed C57BL/6 but not ApoE$^{-/-}$ mice (n= 3 per group; one way-ANOVA plus Tukey's multiple comparisons test, * $p<0.05$) (**B**). In a separate experiment employing the same protocol, contractility in response to CPA or the vehicle control was assessed in thoracic aortic rings from both chow fed C57BL/6 and high fat fed ApoE$^{-/-}$ mice (**C**). It was observed that CPA had no significant effect on contractility in the murine thoracic aortae. However, the DMSO vehicle control caused a contractile response in C57BL/6 aortae that was significantly greater than the response elicited in high fat fed ApoE$^{-/-}$ mice (n= 9,3,8,3, respectively; one way-ANOVA plus Tukey's multiple comparisons test, * $p<0.05$).

Cyclopiazonic acid was employed to empty the intracellular calcium stores. A transient increase in $[Ca^{2+}]_i$ was detected in the presence of CPA; the peak rise in the autofluorescence corrected ratio was measured and found to be significantly higher than the DMSO vehicle alone in control animals (0.014±0.018 vs. 0.056±0.003; $p<0.05$). An increase in intracellular calcium was detected in $ApoE^{-/-}$ mice also, however it was not significantly different to the vehicle control (0.056±0.003 vs. 0.039±0.005; p=ns). When the same treatments were applied to aortic rings in a wire myograph there was an increase in tension in control mice to both CPA and the DMSO vehicle alone with no significant difference being found between the two treatments (0.6±0.2mN vs. 0.6±0.2mN; p=ns). The use of the vehicle control was repeated in $ApoE^{-/-}$ mice and the response was found to be significantly lower than in control mice (0.6±0.2mN vs. 0.1±0.04mN; $p<0.05$). There was no significant difference between the DMSO vehicle alone and CPA in $ApoE^{-/-}$ mice (0.1±0.04mN vs. 0.02±0.02mN; p=ns).

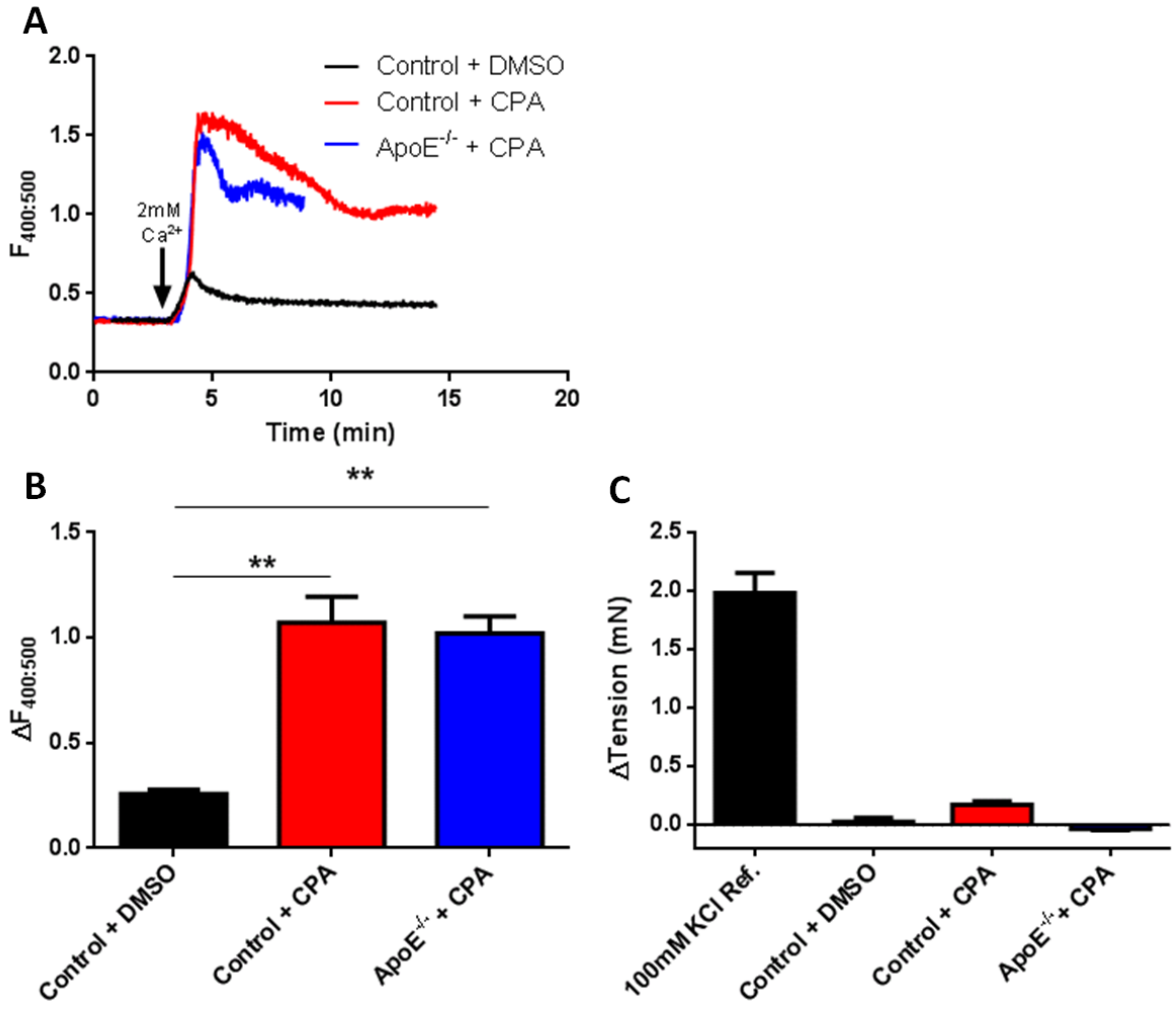

Figure 5.6. The effect of extracellular calcium re-introduction on intracellular calcium and contractility, in the presence of CPA. After depletion of cytoplasmic and sarcoplasmic calcium, extracellular calcium was returned in the continued presence of CPA (10µM) or the vehicle control (DMSO) to induce store-operated calcium entry (SOCE) in thoracic aortic strips from C57BL/6 wild type and high fat fed ApoE$^{-/-}$ mice. A sharp increase in 405:500nm Indo-1 fluorescence ratio was observed immediately after calcium re-introduction (**A)**. This rise was significantly higher in CPA treated tissues compared to vehicle control; however, there was no difference in the peak amplitude between chow fed C57BL/6 and ApoE$^{-/-}$ mice (**B**; n= 3 per group; one way-ANOVA plus Tukey's multiple comparisons test, ** $p<0.01$) In a separate experiment employing the same protocol, contractility in response to calcium re-introduction and stimulation of SOCE was assessed in thoracic aortic rings from both chow fed C57BL/6 and high fat fed ApoE$^{-/-}$ mice (**C**). It was observed that re-introduction of extracellular calcium in the presence of CPA, or the vehicle control, had no significant effect on contractility in the murine thoracic aorta. This was concluded after comparison with the contractile response to 100mM KCl, the previously employed standard.

After incubation with CPA, or the vehicle control, extracellular calcium was returned to induce store-operated calcium entry. A sharp rise in $[Ca^{2+}]_i$ was observed after treatment with CPA but not the DMSO vehicle alone. The plateau phase of this rise was measured in control and ApoE$^{-/-}$ mice and shown to be significantly different from the vehicle alone in both cases

(0.10±0.002 vs. 0.83±0.06, 0.66±0.07, respectively; $p<0.01$). There was no significant difference between control and ApoE$^{-/-}$ mice at either the peak (1.07±0.12 vs. 1.02±0.08) or plateau phase (0.83±0.06 vs. 0.66±0.07) of the rise in $[Ca^{2+}]_i$ after CPA treatment. Returning extracellular calcium after CPA incubation to aortic rings on a wire myograph did not produce a significant change in tension in either control or ApoE$^{-/-}$ mice when compared to the vehicle control alone (0.03±0.04mN vs. 0.2±0.03mN, -0.04±0.01mN, respectively). The overall change in tension was compared qualitatively to the average contraction to depolarisation (100mM KCl Ref.).

In summary, there was no significant difference between the basal cytosolic calcium levels of aortae from control and ApoE$^{-/-}$ mice fed a chow diet for eight weeks. Removal of extracellular calcium lowered $[Ca^{2+}]_i$ equally in control and ApoE$^{-/-}$ mice but did not have an impact on tension. Treatment with CPA, but not the DMSO vehicle alone, caused $[Ca^{2+}]_i$ to rise transiently in both control and ApoE$^{-/-}$ mice. Tension rose significantly higher in response to the DMSO vehicle alone in control compared to ApoE$^{-/-}$ mice but CPA had no significant effect on tension. Stimulation of store-operated calcium entry via re-introduction of extracellular calcium produced a significant rise in $[Ca^{2+}]_i$ in both control and ApoE$^{-/-}$ mice; compared to the DMSO vehicle alone. However, extracellular calcium re-introduction did not have a significant effect on tension.

5.2.2. Vascular relaxation during developmental atherosclerosis

Thoracic aortic rings from C57BL/6 (control) and ApoE$^{-/-}$ mice were constricted with phenylephrine and then exposed to relaxant stimuli that activate endothelial-independent and -dependent mechanisms; sodium nitroprusside (SNP; Figure 5.7.) and acetylcholine (Figure 5.8.), respectively.

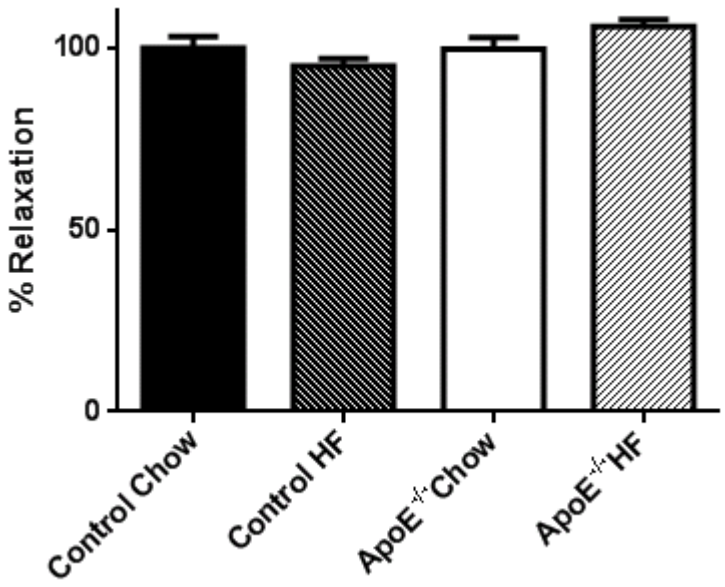

Figure 5.7. The effect of high fat feeding and ApoE gene deletion on endothelial-independent relaxation. Thoracic aortic rings pre-constricted with 10μM phenylephrine were exposed to 10μM sodium nitroprusside (SNP) to stimulate endothelial-independent relaxation. There was no observed impact of high fat feeding or ApoE gene deletion (n = 8,7,4,4).

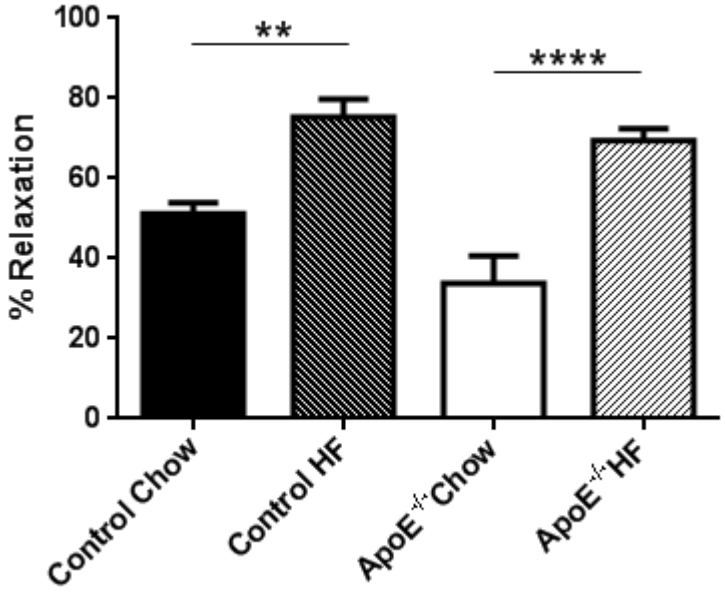

Figure 5.8. The effect of high fat feeding and ApoE deletion on endothelial-dependent relaxation of the murine thoracic aorta. Thoracic aortic rings were pre-constricted with 10μM phenylephrine before being exposed to 10μM acetylcholine to induce endothelial-dependent relaxation. There was no observed impact of the ApoE gene deletion, however, after feeding with a high fat 'western' diet for eight weeks endothelial-dependent relaxation was significantly increased in both control and $ApoE^{-/-}$ mice (n = 14,7,4,7, respectively; one way-ANOVA plus Tukey's multiple comparisons test, ** $p<0.01$, **** $p<0.001$).

When endothelial-dependent relaxation was induced there was a trend towards reduced relaxation in chow fed $ApoE^{-/-}$ mice in comparison to diet matched control mice (33.8±6.9% vs 51.2±2.7%; p=ns), however, this was not shown to be statistically significant. In contrast, feeding for eight weeks on a high fat diet caused a significant increase in endothelial-dependent relaxation in both control (51.2±2.7% vs. 75.3±4.5%, $p<0.05$) and $ApoE^{-/-}$ mice (33.8±6.9% vs. 69.4±3.0%; $p<0.001$).

In order to assess the time course of this change in endothelial-dependent relaxation, $ApoE^{-/-}$ mice were fed for extended time periods and then assessed (Figure 5.8). The significant increase observed after eight weeks high fat feeding, previously described, was lost after 16 weeks feeding with the high fat diet; although there was still a trend towards increased endothelial-dependent relaxation when compared to chow fed $ApoE^{-/-}$ mice (33.8±6.9% vs. 51.6±12.1%). This trend was not observed after further high fat feeding to 26 weeks (33.8±6.9% vs. 33.3±9.3%).

In summary, endothelial-independent relaxation is unaffected by ApoE gene deletion or high fat feeding. In contrast, endothelial-dependent relaxation is not significantly different in chow fed ApoE$^{-/-}$ mice when compared to controls. However, feeding with a high fat 'western' diet for eight weeks causes a significant increase in the level of endothelial-dependent relaxation observed in both control and ApoE$^{-/-}$ mice. This significant increase in endothelial-dependent relaxation is lost after further feeding to 16 weeks in ApoE$^{-/-}$ mice.

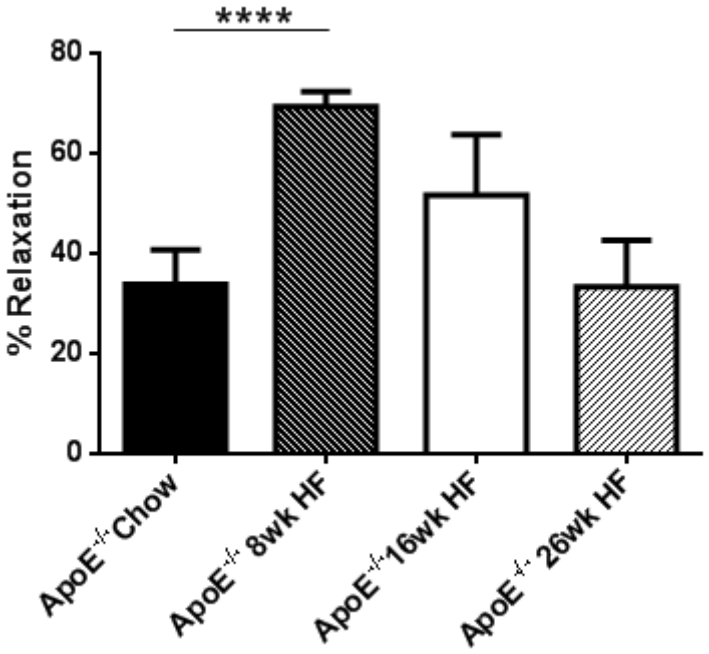

Figure 5.9. The effects of further high fat feeding on endothelial-dependent relaxation in ApoE$^{-/-}$ mice. Aortic rings from ApoE$^{-/-}$ were constricted with phenylephrine (10µM) before being exposed to acetylcholine (10µM) to induce endothelial-dependent relaxation. Mice were fed either a chow diet for eight weeks or a high fat 'western' diet for 8, 26 or 26 weeks. After eight weeks high fat feeding endothelial-dependent relaxation as significantly increased when compared to chow fed ApoE$^{-/-}$ mice. After further feeding to 16 weeks and then 26 weeks, the significant increase in relaxation was no longer observed (n = 4,7,4,5, respectively; one-way ANOVA with post hoc Tukey's multiple comparisons test, **** $p<0.001$).

5.2.2.1. Investigating the mechanism for increased endothelial-dependent relaxation after high fat feeding

The roles of nitric oxide and prostaglandin signalling in the aortae of C57BL/6 (control) mice fed a standard chow diet were isolated through pharmacological inhibition, allowing identification of their individual contribution to relaxation at baseline (Figure 5.10).

Inhibition of both nitric oxide and prostaglandin signalling was then employed on aortic rings from C57BL/6 mice after eight weeks high fat feeding to assess the impact of these relaxant mechanisms on the increased endothelial-dependent relaxation observed at this time point (Figure 5.11).

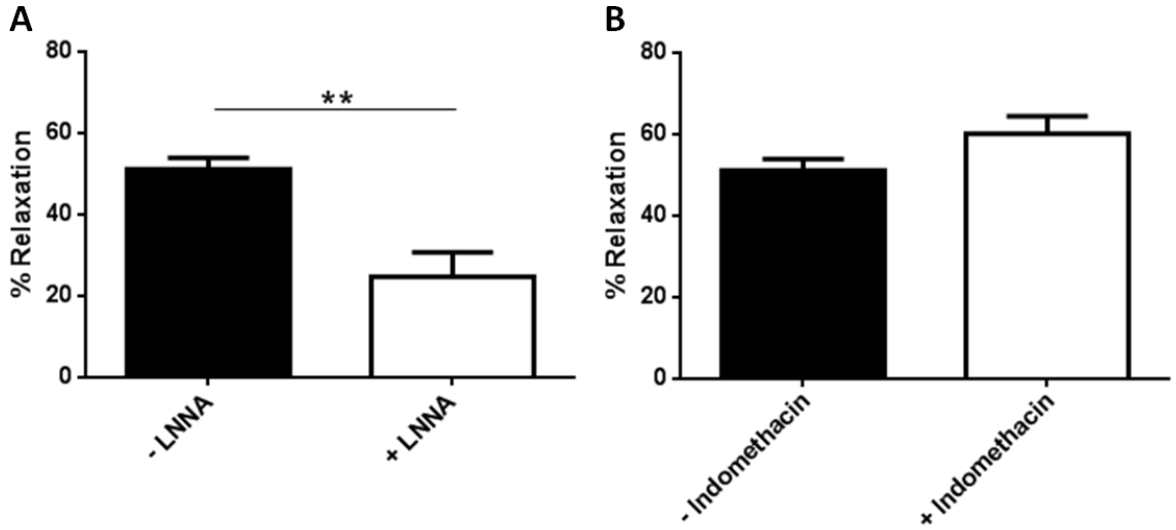

Figure 5.10. The contribution of nitric oxide and prostacyclin signalling to endothelial-dependent relaxation in the C57BL/6 mouse thoracic aorta. Thoracic aortic rings from eight week chow fed C57BL/6 mice were pre-constricted with phenylephrine (10μM) and then exposed to acetylcholine after incubation with either the nitric oxide synthase inhibitor Nω-nitro-L-arginine (LNNA, 50μM; **A**) or the non-specific cyclooxygenase inhibitor indomethacin (10μM; **B**). Endothelial-dependent relaxation was significantly reduced after treatment with LNNA but not indomethacin. These data suggest that nitric oxide, but not prostacyclin, contributes to acetylcholine stimulated endothelial-dependent relaxations in the murine thoracic aorta (n = 15, 4, respectively for both inhibitors; Student's t-test, ** $p<0.01$).

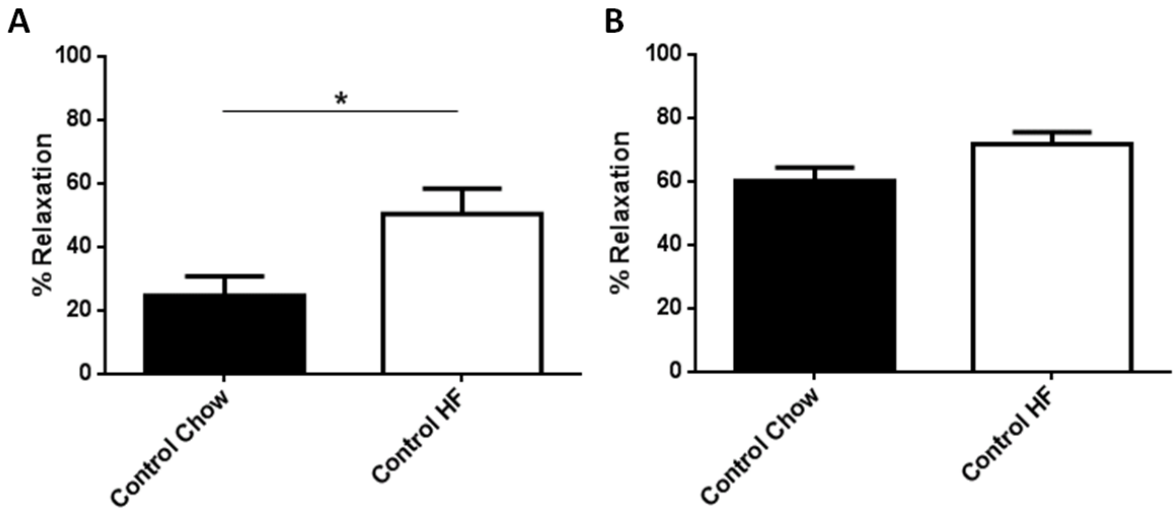

Figure 5.11. The effect of a nitric oxide and prostaglandin inhibition on the increased endothelial-dependent relaxation in response to high fat feeding. Thoracic aortic rings, from chow and high fat diet fed C57BL/6 mice, were pre-constricted with 10μM phenylephrine before being exposed to 10μM acetylcholine to induce endothelial-dependent relaxation. This was conducted in the presence of either the nitric oxide synthase inhibitor Nω-nitro-L-arginine (L-NNA, 50μM; **A**) or the non-specific cyclooxygenase inhibitor indomethacin (10μM; **B**). There was a significantly higher level of relaxation seen in the high fat fed mice after inhibition of nitric oxide production but not in the presence of a cyclooxygenase inhibitor (n = 4 per group; Student's t-test, * $p<0.05$).

Stimulation of endothelial-dependent relaxation produced a significantly smaller relaxation in L-NNA treated control animals fed a chow diet (51.2±2.7% vs. 24.7±6.0%, $p<0.01$). However, there was a significantly larger relaxation observed in high fat fed mice when compared to standard chow fed mice (24.7±6.0% vs. 50.4±8.0%; $p<0.05$). In comparison, inhibition of prostaglandin signalling with indomethacin did not produce a significant change in endothelial-dependent relaxation in chow fed C57BL/6 mice (51.2±2.7% vs. 60.2±4.3). In addition, the significant increase in relaxation after high fat feeding was not observed after treatment with indomethacin when compared to treated control chow fed animals (60.2±4.3% vs. 71.8±3.8%).

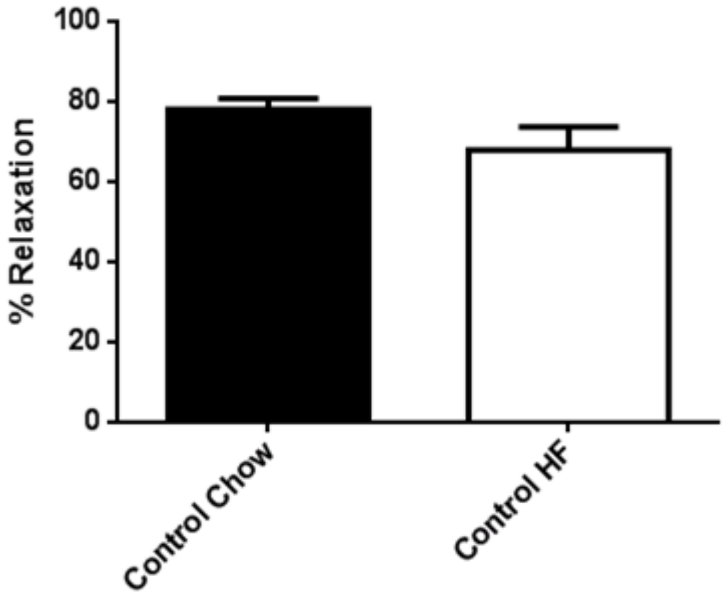

Figure 5.12. The effect of cyclooxygenase-2 inhibition on the increased endothelial-dependent relaxation in response to high fat feeding. After pre-constriction with 10μM phenylephrine, thoracic aortic rings from chow fed and high fat fed C57BL/6 mice were exposed to 10μM acetylcholine in the presence of the specific cyclooxygenase-2 (COX-2) inhibitor Celecoxib (5μM). The blockade of COX-2 was shown to abolish the enhanced endothelial-dependent relaxation seen in response to high fat feeding (n = 4 per group).

Prostaglandin signalling is composed of the actions of two isoforms of the enzyme cyclooxygenase; COX-1 and COX-2. A specific inhibitor of COX-2 signalling, celecoxib, was employed to measure its contribution to the increased endothelial-dependent relaxation observed after high fat feeding. Incubation with celecoxib produced a significant decrease in contractility to phenylephrine, however, there was no significant difference in the contractility between chow fed and high fat fed mice post-treatment (data not shown). It was observed that the previously enhanced endothelial-dependent relaxation in the aortae of animals fed a standard chow or high fat 'western' diet was no longer present after incubation with celecoxib (78.0±2.7% vs. 67.9±5.7%; p=ns).

In summary, blockade of nitric oxide but not prostaglandin signalling significantly reduced endothelial-dependent relaxation in the thoracic aortae of chow fed C57BL/6 mice. After feeding with a high fat 'western' diet for eight weeks significantly increased endothelial-dependent relaxation has been demonstrated to be present in the thoracic aorta after treatment with acetylcholine. Relaxations to acetylcholine remained significantly elevated in the aortae of high fat fed mice in the presence of L-NNA but this enhancement was abolished by incubation with indomethacin and celecoxib, a specific inhibitor of cyclooxygenase-2.

5.3. Discussion

The aim of this chapter was to assess the vascular function of murine thoracic aorta; the effects of feeding with a high fat 'western' diet for eight weeks, in wildtype and $ApoE^{-/-}$ mice, were measured through comparison of responses of *ex vivo* tissues to pharmacological agents. The investigation focussed on contractile and relaxant responses, with observed changes being studied further with the aim of identifying possible cellular mechanisms involved.

5.3.1. Alterations in vascular contractility prior to the development of overt atherosclerosis

Firstly, considering contractility of the murine thoracic aorta, the present study has demonstrated that depolarisation induced contractions, stimulated by direct activation of voltage-sensitive calcium channels, are unaffected by either ApoE gene deletion or high fat diet. This is in agreement with previous data from the present investigation, after modulation of extracellular cholesterol, and also by studies in the aortae of chow fed $ApoE^{-/-}$ mice [186] and coronary arteries of high fat fed pigs [361]. These data suggest that the function of L-type calcium channels is unaffected by hypercholesterolaemia, possibly due to their localisation outside of cholesterol-enriched signalling domains, although this has yet to be confirmed in vascular smooth muscle.

In $ApoE^{-/-}$ mice fed on a chow diet for eight weeks, an increase in maximal contractility to both phenylephrine and serotonin was observed, when compared to age and diet matched wildtype controls. This suggests that deletion of the ApoE gene and/or its role in the development of hypercholesterolaemia is modulating the second messenger cascades associated with receptor mediated contraction, unlike the direct activation induced by depolarisation. Similar results have previously been observed in response to phenylephrine in the $ApoE^{-/-}$ mouse model by Fransen *et al.* (2008) [178]; these authors also showed an increase in the EC_{50} (pD_2) of phenylephrine. An increase in sensitivity to serotonin has been observed in an eight week high fat fed rabbit model, however, there was no observed difference in maximal contractility [172]; suggesting a degree of species dependence for this response. The increase in contractility in chow fed $ApoE^{-/-}$ mice has been suggested to be caused by a

reduction in basal endothelial nitric oxide production; as demonstrated by Kauser *et al.* (2000) [362].

Observation of the same pattern of response after exposure to both phenylephrine and serotonin, agonists acting at different receptors, suggests that the effect is being driven by changes in signalling downstream from the receptor. As previously described, the Gαq-PLC-IP_3 pathway is activated by both agonists employed, and contractions of smooth muscle have been shown to be sensitive to cholesterol modulation [179,295]. Therefore, *in vivo* hypercholesterolaemia was considered as a mechanism for the additional contractility after blockade of nitric oxide signalling, which had been suggested previously to increase the number of plasma membrane bound binding sites for α-adrenoceptor agonists [363]; performed in 28 day hypercholesterolaemic dogs, demonstrating the acute nature of cholesterol modulation. However, considering the present data, although high fat feeding of wildtype mice shows a trend towards increased contractility, the dramatic rise in plasma serum cholesterol after feeding of $ApoE^{-/-}$ mice with a high fat 'western' diet did not produce a concordant increase in contractility to either phenylephrine or serotonin. Therefore a direct link with hypercholesterolaemia is unable to be demonstrated.

In contrast to the previous findings, Agianniotis & Stergiopulos (2012) through biomechanical assessment of the elastic and structural properties of thoracic aortae demonstrated a reduction in the contractile response to phenylephrine in 12 week old chow fed $ApoE^{-/-}$ mice. However, an increase in smooth muscle cell density was also observed, a factor that was attributed by the authors to the process of smooth muscle proliferation and differentiation, although confirmation was not attained [191]. The present investigation also looked to study the effect this early marker of atherosclerotic disease had on vascular function, however, as described in the previous chapter the attempts to identify distinct smooth muscle phenotype populations were unsuccessful. In an attempt to deduce the mechanism of increased contractility observed in the present study, imaging of intracellular calcium, with specific interest in store-operated calcium entry, was performed.

As a driver of smooth muscle cell proliferation [364–367] an increase in $[Ca^{2+}]_i$ at rest in smooth muscle cells was previously observed in 12 week old $ApoE^{-/-}$ mice prior to the development of atherosclerotic disease by Van Assche *et al.* (2007) [186]. However, in the present investigation after feeding on a high fat diet for eight weeks it was found that basal calcium

was not changed in the presence of hypercholesterolaemia and ApoE gene deletion, when compared to wildtype chow fed mice. The contrasting findings reflect the same pattern described previously, where an increase in contractility was observed in ApoE$^{-/-}$ mice fed a chow diet, however high fat feeding did not elicit the same response. An increase in basal $[Ca^{2+}]_i$ was previously observed in cholesterol treated rat vascular smooth muscle cells [183], however, the process of cell culture in which smooth muscle cells switch to a proliferative phenotype has been shown to alter smooth muscle calcium handling, promoting an increase in the $[Ca^{2+}]_i$ which initiates growth and division [67].

The mechanism of the differing responses observed in *ex vivo* ApoE$^{-/-}$ chow and high fat fed tissues is currently unknown and requires further investigation. Two possible contributors that have been identified in the present investigation are phenotypic changes in ApoE$^{-/-}$ mice after feeding on either a chow diet or a high fat western diet for eight weeks; firstly, a significantly greater serum cholesterol concentration in high fat fed ApoE$^{-/-}$ mice and secondly, an increased spleen weight indicative of an increased level of systemic inflammation. As previously discussed, high fat feeding of ApoE$^{-/-}$ mice did not produce a serum cholesterol concentration dependent increase in contractility, therefore demonstrating that there is no direct link to hypercholesterolaemia and suggesting a role for inflammation, which will be discussed further in this chapter.

Store-operated calcium entry (SOCE) is involved in the control of many cellular processes, including proliferation [190] and contraction [368]. The exact mechanism and the channels and signalling proteins involved has been extensively studied, however, firm conclusions have yet to be made [369–373]. The present investigation aimed to assess firstly, the role of SOCE in contraction of the murine thoracic aorta and secondly, the impact of ApoE gene deletion and hypercholesterolaemia on this cellular signalling pathway. SOCE was initiated by depleting thoracic aortic tissues of calcium in the presence of the sarcoplasmic reticulum calcium ATPase (SERCA) blocker, cyclopiazonic acid (CPA), before reintroducing calcium to the extracellular environment and measuring the response. The present investigation has shown that, in the absence of CPA, removal of extracellular calcium was able to reduce the $[Ca^{2+}]_i$ but had no effect on resting tension. There was no difference in either response between chow fed wildtype mice and high fat fed ApoE$^{-/-}$ mice. This supports the previously discussed data where no change in basal $[Ca^{2+}]_i$ was observed in high fat fed ApoE$^{-/-}$ mice compared to chow fed controls. Treatment with CPA has previously been shown to cause contraction in

the mouse thoracic aorta [186] and rat penile arteries [311], dependent on extracellular calcium. The data of the present investigation agree with these studies showing that, although there was a transient rise in $[Ca^{2+}]_i$ due to calcium leak from the sarcoplasmic stores, there was a limited contractile response to CPA in a calcium free environment. The rise in $[Ca^{2+}]_i$ was not significantly different when wild type eight week chow fed mice were compared to $ApoE^{-/-}$ eight week high fat fed mice, reflecting the results observed when $ApoE^{-/-}$ chow fed mice were compared to wild type controls in a previous study [186]. Interpretation of these data, as previously performed [374], enables the conclusion that the sarcoplasmic $[Ca^{2+}]$ is unaffected by ApoE gene deletion and high fat feeding.

In the presence of CPA, extracellular calcium was then re-introduced. As expected a rise in intracellular calcium, SOCE, was observed in both chow fed wild type and high fat fed $ApoE^{-/-}$ mice. Confirmation that this was due to SOCE was provided by the lack of increase in $[Ca^{2+}]_i$ above baseline levels in the presence of the vehicle control only, due to the stores remaining intact. There was no significant difference between the two groups when comparing either the peak or plateau phase of calcium entry. These data are in agreement with a study performed in high fat fed pigs, however, Van Assche *et al.* (2007), using 12 week old chow fed $ApoE^{-/-}$ mice, concluded that SOCE was increased when compared to control [186]. This may suggest an effect of the further increase in hypercholesterolaemia induced by high fat feeding in $ApoE^{-/-}$ mice, employed by the present study. However, it has to be noted that Van Assche *et al.* (2007) included ATP into the SOCE preparation which is able to activate receptor-operated channels [375]. Both store-operated and receptor operated calcium entry have been attributed to the activity of canonical transient receptor potential (TRPC) channels with isoform specificity thought to control the activation of either process [62,68,204]. In the present study only store-dependent channels were activated, therefore, receptor-operated calcium entry induced by ATP may be the reason behind the increase in $[Ca^{2+}]_i$ observed by Van Assche *et al.* (2007) [186].

Previously discussed contractility data has demonstrated that the concentration-response relationship to serum cholesterol in the murine thoracic aorta is not linear. However, it has been demonstrated in rat caudal arteries that removal of membrane cholesterol is able to reduce endothelin-1 contractility via SOCE inhibition [187]. In the present study, however, the re-introduction of 2mM extracellular free calcium did not cause a notable contraction in either chow fed wildtype or high fat fed $ApoE^{-/-}$ mice, in comparison to the mean

depolarisation induced contraction. Although not observed in parallel, a lack of contraction to the rise in $[Ca^{2+}]_i$ was surprising. An explanation for this lack of contraction may lie in the fact that the tissues imaged were prepared with the endothelium maintained intact; confirmed, only in contractility studies, by acetylcholine induced relaxation prior to calcium depletion. The re-introduction of calcium therefore would activate SOCE, a process which can also occur in endothelial cells [376], increasing endothelial as well as vascular smooth muscle $[Ca^{2+}]_i$. An increase in endothelial $[Ca^{2+}]_i$ would activate the Ca^{2+}/Calmodulin dependent eNOS enzyme. Activation of eNOS would stimulate an increase in nitric oxide production [39,377] capable of inhibiting contraction via inhibition of RhoA kinase resulting in calcium sensitisation [378]. This mechanism has not been confirmed and the temporal mechanics involved in nitric oxide signalling need to be considered. A comparison of the present data with current literature was difficult as no evidence was available showing the effects on contractility of calcium re-introduction after complete depletion of calcium.

5.3.2. Alterations in vascular relaxation prior to the development of overt atherosclerosis

Having discussed the contractile responses observed, the focus will now move towards vascular relaxation and the impact of ApoE gene deletion and/or high fat feeding on this process and the mechanisms involved. In agreement with previous investigations the present study has shown that endothelial-independent relaxation, demonstrated through treatment with sodium nitroprusside, was not significantly different between chow fed wildtype and $ApoE^{-/-}$ mice prior to plaque formation [362,379]. Endothelial-independent relaxation also appears to be unaffected after plaque formation; as demonstrated in 13 month old chow fed $ApoE^{-/-}$ mice by Wang *et al.* (2000) [379].

In contrast, endothelial-dependent relaxations have been shown to diminish in response atherosclerotic disease development in humans [380,381]. The role of endothelial dysfunction in atherosclerotic disease has been studied widely in the aorta of the $ApoE^{-/-}$ mouse model, which mimics the endothelial dysfunction observed in humans [175,357,379]; this endothelial dysfunction has been demonstrated to be associated with plaque development, rather than hypercholesterolaemia alone [174]. These data, and that from other studies [176,382], are in agreement with the observations of the present investigation demonstrating that in the thoracic aorta, prior to the development of atherosclerotic plaques, endothelial-dependent

relaxation in response to acetylcholine is unchanged between ApoE$^{-/-}$ and wildtype chow fed mice. However, in the same mouse model, endothelial dysfunction was observed in plaque free coronary arteries [180]. This is possibly due to vascular bed dependent response, however, it may also be explained by the use of a high fat diet for 26 weeks rather than prolonged feeding on a regular chow diet; which in the present study, along with many others [141,262,319], has been shown to greatly exacerbate hypercholesterolaemia in ApoE$^{-/-}$ mice. These results suggest a cholesterol concentration-dependent effect on endothelial relaxation; rather than an age related response (26 week high fat feeding [180] vs. 13 month (56 week) chow feeding [174]). Cholesterol-enriched signalling domains are known to be involved in the regulation of eNOS, with localisation to caveolae and binding to caveolin-1 causing inactivation of the enzyme [189,315,383] . Therefore, this may represent a mechanism for reducing the bioavailability of NO and promoting endothelial dysfunction.

To explore the differential effects between high fat diet fed and chow fed ApoE$^{-/-}$ mice the present investigation explored the effects of high fat feeding after a relatively acute, eight week, feeding period. In addition, the use of high fat diet matched wildtype mice allowed for further analysis of the possibility of concentration-dependent responses to cholesterol. There are no published results currently available observing the effects of endothelial function, in C57BL/6 wildtype or ApoE$^{-/-}$ mice, after an acute feeding period on a high fat 'western' diet. The present investigation has observed that in contrast to the effects of prolonged feeding (26 weeks) of ApoE$^{-/-}$ mice , demonstrated by d'Uscio *et al.* (2001) [180] and others [176,382], eight week high fat feeding enhances endothelial-dependent relaxations to acetylcholine. This result was also mirrored in wildtype C57BL/6 mice fed on a high fat diet; thus, demonstrating that hypercholesterolaemia is not the cause of this unexpected response. In ApoE$^{-/-}$ mice, after further feeding on a high fat diet to 16 and 26 weeks, the increase in endothelial-dependent relaxation was lost. The loss of enhancement suggests either that the acute response to high fat diet activates compensatory mechanisms which counteract the underlying mechanism, however, full characterisation of atherosclerotic disease development in these animals was not carried out, therefore the existence of early atherosclerotic plaque development, not visible without histological examination, may be a contributing factor.

Vascular endothelial-dependent relaxations have three origins; nitric oxide [384], prostacyclin (PGI_2) [47] and EDHF [314]. In the large elastic arteries of mice, investigated in the femoral artery, relaxations are produced primarily by the nitric oxide-dependent signalling pathway

[25]. In the present study, blockade of nitric oxide signalling in the thoracic aorta significantly reduced, but was unable to completely block, the relaxation response to acetylcholine; however, inhibition of prostacyclin with indomethacin had no effect on relaxation in wildtype chow fed C57BL/6 mice. These results suggest a role for EDHF in the murine thoracic aorta response to acetylcholine but require further examination to confirm this observation. In contrast, the increase in endothelial-dependent relaxation, observed in both high fat fed wildtype C57BL/6 and ApoE$^{-/-}$ mice, was still present after blockade of nitric oxide synthase activity but was abolished by prostaglandin signalling inhibition. These results suggest that in response to eight week high fat feeding there is an increase in prostacyclin release from the endothelium which is independent of hypercholesterolaemia.

Increased levels of prostacyclin have been demonstrated previously in humans [385] and in animal models, including ApoE$^{-/-}$ mice [386], when atherosclerotic plaques are present. The formation of prostacyclin is dictated by two isoforms of the cyclooxygenase enzyme, COX-1 and COX-2 [385], however, in addition to prostacyclin, COX-1 is capable of producing a contractile agent, thromboxane A_2. Previously discussed results from the present study have shown that contractility was unaffected by high fat feeding suggesting that COX-1 activity is not affected; in addition, Burleigh *et al*. (2002) [254], (2005) [253], demonstrated that inhibition of COX-2 inhibited atherosclerotic plaque development in LDLR$^{-/-}$ and ApoE$^{-/-}$ mice respectively. Through the use of the COX-2 selective inhibitor celecoxib the present investigation demonstrates that the increase in endothelial-dependent relaxation in response to high fat feeding, in both wildtype C57BL/6 and ApoE$^{-/-}$ mice, is the effect of a COX-2-dependent mechanism; most likely increased production of prostacyclin. This is the first time that the vascular effects of high fat feeding, increasing endothelial-dependent relaxations via COX-2 activity, have been described and evidenced in the thoracic aortae of C57BL/6 and ApoE$^{-/-}$ mice.

5.4. Conclusions

The aim of this chapter was to assess vascular function in murine thoracic aortae prior to development of overt atherosclerotic disease. This was achieved through feeding of atherosclerosis prone ApoE$^{-/-}$ mice on standard chow and high fat diet, along with the often over looked high fat diet matched wildtype controls. The present investigation has demonstrated that contractility to agonists activating the $G\alpha_q$-PLC-IP_3 intracellular pathway

is enhanced in eight week chow fed ApoE$^{-/-}$ mice alone when compared to diet and age matched wildtype C57BL/6 controls. The mechanism for this increased contractile response has been shown to be independent of hypercholesterolaemia and store-operated calcium release. These conclusions compliment and add to the available literature, however, further exploration is required to elucidate the exact mechanism(s) involved.

In contrast, endothelial-dependent acetylcholine induced relaxations were shown to be enhanced in eight week high fat fed wildtype C57BL/6 and ApoE$^{-/-}$ mice, but not chow fed ApoE$^{-/-}$ mice. This again suggests a mechanism independent of hypercholesterolaemia. Further investigation lead to the discovery that enhanced endothelial-dependent relaxations observed after 8 week high fat feeding were transient and sensitive to specific inhibition of cyclooxygenase-2. These findings represent the first evidence for an enhancement of endothelial function in response to high fat feeding in atherosclerosis prone mice. The implications for these observations relate to possibility of masking early signs of vascular dysfunction and also the induction of compensatory mechanisms which may have amplified effects over a longer time course; possibly promoting the development and advancement of atherosclerotic disease.

5.4.1. Summary of conclusions

- **Contractility to phenylephrine and serotonin are increased in eight week chow fed ApoE$^{-/-}$ mice via a yet unknown mechanism that is independent of hypercholesterolaemia and store-operated calcium entry.**

- **High fat feeding for eight weeks causes a COX-2-dependent increase in endothelial-dependent relaxation in C57BL/6 and ApoE$^{-/-}$ mice**

- **When fed on either a chow diet or a high fat diet atherosclerosis prone ApoE$^{-/-}$ mice demonstrate changes in vascular function.**

6. General Discussion

6.1. Discussion

Atherosclerosis is a vascular pathology and in the advanced stages of the disease has been shown to alter vascular function in humans and animal models [174,357,387,388]. It is currently unknown at what stage these changes in vascular function manifest and whether they evolve as the atherosclerotic disease progresses. The overall aim of this thesis was to assess the effects of vascular function on atherosclerotic disease development; prior to the overt presence of atherosclerotic lesions. Studies into the early stages of atherosclerosis are currently limited; difficulties in the clinical translation due to the availability of early atherosclerotic human tissue have to be considered. However, increased knowledge and awareness of the role of vascular function in atherosclerotic disease has lead to diagnostic techniques such as flow-mediated dilation (FMD) and pulse wave velocity (PWV) being employed to predict the extent of disease development [30,31,389,390]. Therefore investigation of vascular function in the early stages of disease progression was performed with the aim of identifying changes that may indicate and possibly contribute to future atherosclerotic disease development.

The exact mechanism behind the initiation of atherosclerotic disease is still unknown; however, one of the primary contributing factors is chronic inflammation. It has been observed that chronic infections of extravascular tissues, such as gingivitis and bronchitis, can stimulate an increase in the levels of circulating inflammatory cytokines [224,391]. This response is thought to result from the activation of the innate immune system upon detection of pathogen-associated molecular patterns (PAMPs) by toll-like receptors (TLRs)[392]. The importance of these receptors in atherosclerotic disease development has been shown by a reduction in atherosclerotic lesion formation after deletion of two isoforms, TLR2 and TLR4 [393,394]. One of the major ligands associated with activation of TLRs is bacterial lipopolysaccharide (LPS, endotoxin). It has been shown that within human atherosclerotic plaques there is evidence of infection with microbes such as *Chlamydia pneumonia* that are able to release LPS and heat-shock proteins therefore perpetuating the inflammatory response [395,396]. The role of inflammation in the development of atherosclerotic disease is therefore an important consideration and the experimental findings in relation to this risk factor will be discussed later in this chapter. In humans, LDL has been shown to increase the sensitivity of cells to LPS increasing the release of inflammatory cytokines [397]. Cholesterol plays a central role in atherosclerotic disease and will therefore be discussed first.

As outlined above atherosclerosis is a multi-factorial disease; however, one of the pre-requisites for the development of atherosclerotic disease is serum cholesterol, an excess of which will exacerbate the rate of development [398]. Initial investigation was conducted to assess the direct effects of cholesterol on *ex vivo* thoracic aortic tissue. The results obtained demonstrated that removal of cholesterol from membranes inhibited contractility to agonists activating the $G\alpha_q$-PLC-IP_3 pathway but not contractions initiated by a depolarising stimulus. Caveolar disruption was observed by Dreja *et al* (2002) [290] after treatment of rat tail arteries with methyl-β-cyclodextrin, therefore, the specific reduction in phenylephrine and serotonin induced contractions demonstrated in the present study supports evidence for the association of $G\alpha_q$-PLC-IP_3 pathway signalling proteins to cholesterol-rich signalling domains [120].

Subsequently, the effect of hypercholesterolaemia, by increasing the extracellular concentration of free cholesterol, was investigated. There was no observed change in vascular contractility after exposure to increased cholesterol; however, endothelial-dependent relaxation was significantly reduced. The mechanism for this alteration in vascular relaxation in response to acute exposure to increased cholesterol is currently unknown. To advance our understanding of vascular function in atherosclerotic disease development an *in vivo* model was necessary to further investigate the actions of chronic hypercholesterolaemia.

The present study employed the $ApoE^{-/-}$ mouse model of hypercholesterolaemia which has, over the last decade, been widely investigated. Comparisons of this *in vivo* model with the human manifestation of atherosclerotic disease have found a high degree of correlation; including, areas of susceptibility to plaque formation [141,399], the appearance of plaque rupture [325] and the cellular composition of plaques [141]. Previous investigations into the effects of the hypercholesterolaemic phenotype of $ApoE^{-/-}$ mice on the vasculature have been conducted in young (3 weeks) [186], adult (12 weeks) [178] and aged (56 weeks) [174] mice fed on a standard chow diet and also in high fat fed mice exhibiting advanced atherosclerotic lesions [382]. It was the aim of the present investigation to further this knowledge through the use of high fat feeding, known to exacerbate hypercholesterolaemia in $ApoE^{-/-}$ mice [262], from weaning through to reaching adulthood (12 weeks [400]). The high fat 'western' diet was also fed to wildtype C57BL/6 mice to allow for assessment of the direct role of high fat feeding in modulation of vascular function.

The multi-faceted nature of atherosclerotic disease, as stated previously, creates difficulties when attempting to demonstrate causal relationships. Therefore, in order to fully describe any changes in vascular function, the phenotype of wildtype C57BL/6 and ApoE$^{-/-}$ mice was investigated focussing on the lipidaemic profile and other known atherosclerotic disease risk factors; inflammation, obesity and diabetes. It was observed that through use of the specific groups in the present study, a gradient of total serum cholesterol concentration was produced after eight weeks feeding in the following manner:

Chow fed C57BL/6 < High fat fed C57BL/6 < Chow fed ApoE$^{-/-}$ < High fat fed ApoE$^{-/-}$

Upon further investigation it was found that deletion of the ApoE gene results in a lower concentration of the anti-atherogenic high-density lipoprotein (HDL). The low concentration of HDL may account in part for the increased susceptibility of ApoE$^{-/-}$ mice to atherosclerosis; a similar pattern of reduced HDL concentration has been observed in humans expressing reduced levels of ApoE [401]. Although not directly measured in the present study, this suggests that a larger proportion of cholesterol will be carried on low-, intermediate low- and very low density lipoproteins (LDL, ILDL, VLDL, respectively) which are liable to become pro-inflammatory through their oxidation [159,402].

Two major co-morbidities associated with hypercholesterolaemia, also indicated in the promotion of an inflammatory phenotype, are obesity [222,403] and type II diabetes [343,391]. The present investigation has shown that high fat feeding produces a significant increase in body weight compared to chow fed mice; however, the deletion of the ApoE gene confers a level of protection against this risk factor. Further investigation showed that this protection was associated with decreased fat deposition, demonstrated in the epididymal fat stores. In addition, perivascular adipose tissue (PVAT) around the thoracic aorta was examined; an increase in PVAT has been identified as an early indicator of obesity and the associated increase in adipocyte size is thought to be the source of increased inflammation [229,241,355]. The data generated during the present investigation have identified that thoracic aortic perivascular adipocytes increase in cell number in response to high fat feeding, however, only in wildtype C57BL/6 mice does high fat feeding cause a significant increase in cell size; in agreement with previous data showing protection against obesity in ApoE$^{-/-}$ mice. The measurement of blood glucose concentrations as an indicator of type II diabetes, another atherosclerosis associated co-morbidity, was also undertaken and was shown to be unaffected

by high fat feeding. Although there was no presence of a diabetic phenotype, compared to blood glucose levels of the db/db mouse model of diabetes [346], there was a significantly lower blood glucose concentration observed in ApoE$^{-/-}$ mice again suggesting a protective role against atherosclerotic co-morbidities conveyed by ApoE. These data would also suggest a protective effect of ApoE gene deletion against inflammation, however, indirect assessment of this risk factor, by comparing spleen weights, demonstrated an increase in systemic inflammation in response to high fat feeding in C57BL/6 and ApoE$^{-/-}$ mice. In support of this observation it has been shown that in humans after a high fat meal circulating levels of LPS are increased; this increase in inflammatory stimulus is thought to derive from the capacity for LPS, from commensal gut bacteria, to be co-transported into the blood along with dietary fats [404].

Assessment of the phenotypic changes associated with early atherosclerosis was successful in identifying an increasing gradient of hypercholesterolaemia across the experimental groups, allowing for correlations to be made to vascular function. There was no indication that high fat feeding induced a diabetic phenotype, however, weight gain was observed in high fat fed mice with an associated, hypercholesterolaemia-independent, increase in systemic inflammation. Therefore, the downstream effects of weight gain and obesity, but not diabetes, were considered in mechanistic investigations of vascular function.

Vascular function was the primary focus of this body of work and was assessed through comparison of the contractile and relaxant capacity of thoracic aortic tissues isolated from each of the previously outlined groups. The aim of these investigations was to assess how the relationship between the vasculature and the combination of factors that lead to atherosclerotic disease development can affect function. The present investigations were performed at a time point prior to the development of overt atherosclerotic plaques to enable a focus on the early pathogenesis. The lack of atherosclerotic plaque formation in the thoracic aorta after eight weeks feeding was confirmed in all groups; although an increase in overall atherosclerotic plaque formation, in the aortic arch and intercostal artery branches, was shown to correlate with the increasing concentrations of cholesterol.

The results of the present investigation have demonstrated that contractility to phenylephrine and serotonin, activators of the $G\alpha_q$-PLC-IP_3 signalling pathway, was enhanced in chow fed ApoE$^{-/-}$ mice only. In contrast, responses to depolarisation were seen to be unaffected in all

groups. Investigation into the effects of early atherosclerotic disease development on vascular relaxation, in mice, has shown no impact on endothelium-independent mechanisms. However, increase in endothelial-dependent relaxation in response to high fat feeding for eight weeks was observed; this increase was shown to be transient and was reduced and then absent completely after further high fat feeding of $ApoE^{-/-}$ mice to 16 and 26 weeks, respectively. These results demonstrate that the present investigation was successful in identifying changes in vascular function prior to the development of overt atherosclerosis in the murine thoracic aorta. A summary of the phenotype analysis and vascular function assessment can be found in Table 2. below. Correlations between these two parts of the study and the subsequent investigations into the possible mechanisms involved in the observed changes in vascular function will now be discussed.

Table 2. A summary of the observed changes induced by high fat feeding and ApoE gene deletion when compared to chow fed wildtype C57BL/6 mice.

Phenotypic Parameter	HF fed C57BL/6	Chow fed ApoE$^{-/-}$	HF fed ApoE$^{-/-}$
Total Cholesterol	–	↑	↑↑
HDL Cholesterol	–	↓	↓
Blood Glucose	↑	↓	↓
Body Weight	↑↑	–	↑
Inflammation	↑	–	↑
Perivascular Adipocyte Size	↑	–	–
Functional Parameter	**HF fed C57BL/6**	**Chow fed ApoE$^{-/-}$**	**HF fed ApoE$^{-/-}$**
Contraction to Depolarisation	–	–	–
Contraction to $G\alpha_q$-PLC-IP_3 agonists	–	↑	–
Endothelial-independent Relaxation	–	–	–
Endothelial-dependent Relaxation	↑	–	↑

6.2. Mechanistic investigations

Investigations into the mechanisms behind the two observed changes in vascular function were conducted and will now be discussed with the additional context of phenotypic alterations recorded in response to high fat feeding and ApoE gene deletion.

6.2.1. Transient increase in endothelial-dependent relaxation

The results from investigations aimed to determine a mechanism of action as to why endothelial-dependent relaxation was transiently increased in response to high fat feeding concluded that it was not due to a modification of nitric oxide signalling. However, the observation of enhanced endothelial-dependent relaxation in high fat fed C57BL/6 and ApoE$^{-/-}$ mice, but not in chow fed ApoE$^{-/-}$ mice, demonstrated that the mechanism was also independent of hypercholesterolaemia. A comparison of the pattern of enhanced endothelial relaxation across the four experimental groups with data demonstrating changes in phenotypic parameters identified two correlating factors (highlighted in red in Table 2.); weight gain, associated with obesity, and an increase in spleen weight, indicative of increased systemic inflammation, were observed only in high fat fed mice.

Therefore, the high fat diet induced inflammation appears to be derived from another source. PVAT has been identified as a possible source of inflammation in atherosclerosis [246] and is associated with weight gain after high fat feeding; eventually manifesting as obesity [241]. Murine thoracic aortic PVAT has been demonstrated to have a similar morphology to brown adipose tissue; adipocytes which are resistant to diet induced inflammation [234]. However, the morphology and classification, brown or white adipose tissue, of PVAT appears to differ between vascular beds in rodents; mesenteric arteries display white adipocytes within the PVAT; liable to transform into a pro-inflammatory phenotype in response to high fat feeding [242,405]. In humans, internal thoracic artery PVAT, removed after coronary artery bypass graft surgery, also show a morphology that is indicative of white adipose tissue [236], however, the differences in PVAT morphology and classification has not been fully investigated in humans to date.

The specific site of fat deposition seems to be important in the relationship to inflammation. A much larger deposition of epididymal fat in high fat diet fed C57BL/6 rather than ApoE$^{-/-}$ mice was not correlated with spleen weight. In addition, ApoE$^{-/-}$ mouse thoracic perivascular

adipocytes appear to be resistant to high fat feeding compared to diet matched C57BL/6 mice. Therefore, a local inflammatory influence of the PVAT in the thoracic aorta is not thought to contribute to the enhanced endothelial-dependent relaxation; however, there appears to be a clear link with systemic inflammation. This inflammation may derive from PVAT in other vascular beds such as the mesentery; as described by Greenstein *et al.* (2009) in high fat fed obese rats [242].

The link between inflammation and the endothelium is predominantly associated with endothelial dysfunction [12,406]; an increase in free radical and superoxide ion formation leading to a reduction in the bioavailability of nitric oxide has been observed in 26 – 29 week high fat fed ApoE$^{-/-}$ mice [175]. However, the present results indicate an enhancement in endothelial-dependent relaxation in response to increased inflammation in the developmental stage of atherosclerosis. As the role of nitric oxide signalling was shown to be unaffected in response to high fat diet, other mechanisms involved in vascular relaxation were considered. In advanced human atherosclerotic disease [407], eight week high fat fed ApoE$^{-/-}$ mice [247] and 12 week chow fed ApoE/LDLR$^{-/-}$ mice increased production of the endothelial-dependent prostanoid relaxing factor prostacyclin has been observed.

The production of prostacyclin is dependent on COX-2 enzyme [408], the expression of which was also shown to be increased in the ApoE$^{-/-}$ mice after eight weeks high fat feeding[247]. COX-2 is not constitutively expressed in vascular tissues but is induced in response to inflammation [251,252]. A link between the activity of the early stages of atherosclerotic disease development was made by Burleigh *et al.* (2005) [253] who showed that selective COX-2 inhibition reduced the extent of atherosclerotic lesion formation in ApoE$^{-/-}$ mice at 16 weeks, this has also been confirmed by other investigators [255]; similar observations were also made in the LDLR$^{-/-}$ mouse model of atherosclerosis [254] demonstrating that the response was not produced through modifications to specific gene deletion. The present investigation has demonstrated an increase in endothelial-dependent relaxation that is sensitive to specific inhibition of COX-2. The transient nature of the enhanced endothelial-dependent relaxations is likely to be linked to the prevalence of atherosclerotic plaques and the temporal development of atherosclerotic disease. The generation of oxidised lipoproteins, primarily oxidised LDL, is closely associated with advanced atherosclerotic plaques[409]. The expression of COX-2 in human macrophages has been shown to be suppressed by oxidised LDL *in vitro* [410]. Therefore as the degree of atherosclerotic disease severity increases the level of COX-2

expression is reduced. This is in agreement with the present results in ApoE$^{-/-}$ mice showing a reduction in the enhanced endothelial-dependent relaxation at 16 weeks high fat feeding and a complete absence after 26 weeks feeding on a high fat diet. An increase in prostacyclin formation, observed in advanced human atherosclerosis, appears to contradict this theory, however, Belton *et al*. (2000) have suggested that in the later stages of atherosclerosis an increase in COX-1 expression is observed and is able to contribute to the production of prostacyclin [385].

An increase in prostacyclin production and COX-2 expression, in response to increased inflammation in the early stages of atherosclerosis, is in agreement with the present data. In the current study, weight gain associated with high fat feeding has been demonstrated to correlate with the increased inflammation. Changes in thoracic aortic endothelial function are not derived from local inflammation in the PVAT, but rather an increase in systemic inflammation. An observed increase in endothelial-dependent relaxation is the first evidence linking the early changes in COX-2 activity to modification of vascular function in the ApoE$^{-/-}$ mouse. In addition, it has been demonstrated that the change in vascular endothelial function is independent of serum cholesterol concentration; however, the enhancement has been shown to be a transient response regulated by the temporal advancement of atherosclerotic disease.

6.2.2. Increased contractility to Gα_q GPCR agonists in ApoE$^{-/-}$ chow fed mice only

The role of cholesterol in the contractility of the murine thoracic aorta to Gα_q GPCR agonists was demonstrated in the present study through *ex vivo* cholesterol depletion with methyl-β-cyclodextrin; this has been confirmed in other animal models [187,301] and other types of smooth muscle [317]. The specific regulation of Gα_q GPCR agonist induced contraction has been attributed to the disruption of the cholesterol enriched signalling domains, caveolae and lipid rafts. Contractility, and the associated intracellular calcium rise, have been shown to increase in response to agonists in the presence of hypercholesterolaemia; demonstrated in *in vitro* cultured vascular smooth muscle cells [183], and *ex vivo* animal [179,181] and human tissue [387]. However, when the pattern of increased contractility, observed only in 12 week old chow fed ApoE$^{-/-}$ mice, was compared to observed changes in phenotype (Table 2. highlighted in blue) there were no direct correlations. The lack of association with increasing serum cholesterol

was in agreement with previous data from the current study after acute exposure to increased cholesterol.

The endothelium is important in the regulation of smooth muscle contraction; therefore, the previously discussed increase in endothelial-dependent relaxation, attributed to inflammation-induced COX-2 activity, may have masked an underlying increase in contractility in high fat fed C57BL/6 and ApoE$^{-/-}$ mice. In both the *db/db* [411] and *ob/ob* [412] mouse models of diabetes, an increase in endothelium-denuded aortic contractility, independent of changes in nitric oxide signalling, was observed. Both investigations showed a reduction in contractility after treatment with the non-specific COX inhibitor, indomethacin; Guo *et al*. (2005) later demonstrated that this reduction in contractility was specific to COX-2 activity [411]. Although inflammation was not directly assessed in the current investigations, the mice exhibited a significant increase in spleen weight; a phenotypic parameter that was associated with an increase in systemic inflammation. In support of the role of inflammation, Qi *et al*. (2007) demonstrated that a COX-2 derived prostanoid was also shown to increase contractility after overnight incubation with lipopolysaccharide in porcine coronary arteries [413]. A modification of the balance between the release of the contractile and relaxant prostanoids, thromboxane A_2 and prostacyclin, respectively, in the pathogenesis of atherosclerosis has been examined by Kobayashi *et al.* (2004) [250]. However, in the present study increased contractility was only observed in chow fed ApoE$^{-/-}$ mice that did not display an increased spleen weight, suggesting systemic inflammation, or perivascular adipocyte hypertrophy, suggesting local inflammation. Therefore, the increase in contractility observed in the present study in ApoE$^{-/-}$ mice is thought to be independent of inflammation.

Tulenko *et al.* (1998) demonstrated, through the use of small angle x-ray diffraction, that there is a linear relationship between vascular smooth muscle plasma membrane cholesterol enrichment and feeding of a high cholesterol diet up to 13 weeks [291]. Cholesterol enrichment increases the plasma membrane bilayer width which can alter the kinetics of membrane bound ion channels and receptors [169]. This lead the current investigation to explore the role of intracellular calcium handling, which is highly regulated by membrane associated channels, pumps and transporters, and has been shown to be affected directly by cholesterol enrichment [184]. Van Assche *et al.* (2007) demonstrated that in 12 week old hypercholesterolaemic, atherosclerotic plaque free ApoE$^{-/-}$ mice, calcium handling was modified in endothelial-denuded sections of thoracic aorta [186]. Specifically, it was observed that vascular smooth

muscle basal calcium was increased in ApoE$^{-/-}$ aortae compared to age matched wildtype controls. This has also been observed in cultured vascular smooth muscle cells enriched with cholesterol [183]. The results of the present investigation, employing eight week high fat fed ApoE$^{-/-}$ mice did not show any change in basal $[Ca^{2+}]_i$; this may represent an effect of the increased serum cholesterol concentration, however, methodological differences may also play a factor. In the present study calcium imaging was conducted on transverse strips of thoracic aortae under nominal tension, with the endothelium intact, whereas an increase in basal calcium was observed in thoracic aortic rings with tension applied to replicate the *in vivo* internal diameter of the thoracic aorta. The differential activation of stretch-sensitive calcium channels [414] and/or the presence of the endothelium may account for the contrasting results.

In addition to basal $[Ca^{2+}]_i$ the present study investigated the effect of high fat feeding and hypercholesterolaemia on SOCE. This mechanism has been shown to contribute to the development of the tonic phase of agonist induced contractions in vascular smooth muscle and is sensitive to cholesterol depletion [187]. The present investigation studied the effects of SOCE on $[Ca^{2+}]_i$ and contractility; performed on separate preparations but using the same protocol. No difference in peak SOCE was demonstrated and only a small contractile response was observed in response to the increase in $[Ca^{2+}]_i$. This was surprising due to the expectation that increased $[Ca^{2+}]_i$ would activate the contractile machinery. However, the calcium imaging rig was not calibrated to allow for calculation of the exact concentrations of $[Ca^{2+}]_i$, therefore, the relative scale of calcium increase was unknown.

The compartmentalisation of calcium signalling may play a role with calcium release being focussed in sub-cellular domains away from the contractile machinery [415]; in the present study global calcium was measured which does not take this into account. In the study performed by Van Assche *et al.* (2007), described previously, the authors demonstrate an increase in SOCE in chow fed hypercholesterolaemic ApoE$^{-/-}$ mice [186]. These data contrast with the present findings; however, comparison of the protocols used to induce SOCE may explain this disparity. The present investigation measured only SOCE after depletion of intracellular stores; observing no change between wildtype and high fat fed ApoE$^{-/-}$ mice. In contrast, the increase in SOCE in chow fed ApoE$^{-/-}$ mice demonstrated by Van Assche *et al.* (2007) was observed in the presence of ATP. Extracellular ATP has been shown to activate receptor-operated cation channels [416]. The divergence in calcium entry in response to store

depletion and receptor activation is through isoform-specific activation of TRPC channels [187,204,371]. This mechanism of calcium entry is stimulated by diacylglycerol (DAG) after $G\alpha_q$ activation [417] and also by another G-protein, $G\alpha_{11}$ [309], which is co-activated by both the α_1-adrenergic receptor [309] and the 5-HT_{2A} receptor [121]; agonists to which increased contractility was observed in the present study. Therefore, an apparent increase of this receptor-dependent component of calcium entry may be involved in the increased contractility observed in response to chow fed $ApoE^{-/-}$ mice; however, this has yet to be evidenced and requires further investigation.

The present investigation has demonstrated directly that contractility is increased in chow fed $ApoE^{-/-}$ mice compared to diet matched wild type C57BL/6 mice, and also high fat diet fed C57BL/6 and $ApoE^{-/-}$ mice. A direct causation was not demonstrated in the present study although evidence suggests this is independent of hypercholesterolaemia and a response to systemic inflammation. It is hypothesised that the mechanism for this increase in contractility to $G\alpha_q$ GPCRs may be linked to an increase in receptor-operated calcium entry through TRPC channels. The increase in contractility observed in the current investigation was observed at an early stage in the development of atherosclerotic disease and may represent a mechanism for future disease progression through vascular smooth muscle cell proliferation. The activation of receptor-activated TRPC channels, in particular TRPC6, has been linked directly to proliferation via increased calcium entry in prostate cancer epithelial cells [418] and also, with specific relevance to the present study, vascular smooth muscle cells [419].

6.3. Conclusions

Overall this body of work has achieved its aims and has presented novel findings exploring the early effects of atherosclerotic risk factors, in particular serum cholesterol levels, on vascular function. It has been demonstrated that removal of cholesterol from vascular membranes selectively inhibits adrenergic and serotonergic contractility but the acute exposure to increased extracellular cholesterol has no demonstrable effect on contractility. In contrast, endothelial-dependent relaxation is significantly decreased in response to acute exposure to increased cholesterol.

Further exploration into the effects of increased cholesterol was conducted using the $ApoE^{-/-}$ mouse model, fed for eight weeks post weaning on either a standard chow or high fat diet, along with age and diet matched wildtype controls. The presented findings have shown for the first time that murine thoracic aortic endothelial-dependent relaxation is transiently enhanced after feeding on a high fat 'western' diet and that this is mediated by a cyclooxygenase-2 dependent mechanism; the expression of which, and thus increased production of relaxant prostacyclin, is thought to be enhanced in response to weight gain associated systemic inflammation. This response was demonstrated to be independent of serum cholesterol concentration.

Finally, this investigation has demonstrated an increase in contractility to adrenergic and serotonergic stimulation in the thoracic aorta of the $ApoE^{-/-}$ mouse. Vascular smooth muscle store-operated calcium entry was investigated as the cause of this increase in agonist induced contractility, however, this calcium entry mechanism has been shown to be unaffected by eight weeks high fat feeding. Therefore, the exact mechanism is yet to be fully elucidated. It is hypothesised that an enhancement of receptor-operated calcium entry may be involved. A chronic increase in activation of receptor-operated calcium channels, leading to promotion of smooth muscle proliferation, may represent an early step in the progression of atherosclerotic disease in the vasculature.

It is hoped that these results, although clinical translation is often difficult when using a murine disease model, may contribute to the understanding of the early changes in vascular function and their association with atherosclerotic risk factors. Observation of these parameters is often the primary method of assessment in highlighting at risk individuals.

Therefore the changes highlighted in the present investigation warrant further investigation to deduce the possibility of their translation into human disease. In addition, evidence demonstrating the hypercholesterolaemic-independent effects of the high fat 'western' diet, after feeding for a relatively short time period, will be a necessary consideration in future studies investigating the role of cholesterol and diet modification on vascular function.

6.3.1. Summary of conclusions

- **Removal of cholesterol from vascular membranes selectively inhibits adrenergic and serotonergic contractility.**

- **Acute exposure to increased extracellular cholesterol did not alter vascular contractility but significantly reduced endothelial-dependent relaxation**

- **Murine thoracic aortic endothelial-dependent relaxation is transiently enhanced after eight weeks feeding on a high fat 'western' diet; mediated by a cyclooxygenase-2 dependent mechanism associated with weight gain and systemic inflammation.**

- **Contractility to adrenergic and serotonergic stimulation in the thoracic aortae of eight week chow fed ApoE$^{-/-}$ mice is increased through a smooth muscle SOCE-independent mechanism.**

6.4. Future work

An expansion of the application of the previously described inhibitors and the introduction of others is important to clarify the COX-2 dependent increase in endothelial-dependent relaxation. The inhibition of nitric oxide synthase with LNNA did not fully inhibit relaxation to acetylcholine; therefore, the use of both LNNA and indomethacin together will be employed to assess the involvement of the endothelium-derived hyperpolarising factor (EDHF). Exploration into the role, if any, of COX-1 in enhanced endothelial-dependent relaxation will be assessed through the use of the specific inhibitor, such as FR122047, individually and also together with celecoxib.

The correlation of increased endothelial-dependent relaxation with weight gain and inflammation will be investigated firstly by assessing the level of macrophage infiltration in the aortic perivascular adipose tissue, a source of inflammatory cytokines and secondly, by exploration of the PVAT morphology in other vascular beds such as the mesentery. The extent of systemic inflammation will be confirmed by measuring the concentration of circulating factors such as TNFα, IL-6 and CRP.

The hypothesis of increased receptor-operated calcium entry contributing to increased contractility in chow fed $ApoE^{-/-}$ mice will not be easy to investigate as there are currently no specific inhibitors available. However, prior to the development of this theory apparatus will be set up to allow for simultaneous measurement of $[Ca^{2+}]_i$ and contractility. Confirmation of the previously described SOCE-independent mechanism will be attempted in thoracic aortic rings that have undergone a stretching protocol to achieve *in vivo* diameter.

7. Appendices

Appendix I – Reagents and consumables

Product	Code	Supplier
General		
Methanol		BDH, Leicestershire, UK
Ethanol		Fisher Scientific, Leicestershire, UK
Sodium Chloride	10241AP	BDH, Leicestershire, UK
Potassium Chloride	10010310	Fisher Scientific, Leicestershire, UK
Magnesium Sulphate	10224680	Fisher Scientific, Leicestershire, UK
HEPES	15630-049	Invitrogen, Paisley, UK
Glucose	10141520	Fisher Scientific, Leicestershire, UK
Calcium Chloride	10050070	Fisher Scientific, Leicestershire, UK
EGTA		BDH, Leicestershire, UK
Manganese chloride	244589	Sigma-Alderich, Poole, UK
Sodium hydroxide		BDH, Leicestershire, UK
Tris base	T1503	Sigma-Alderich, Poole, UK
Tris hydrochloride	T5941	Sigma-Alderich, Poole, UK
Tween – 20	P1379	Sigma-Alderich, Poole, UK
Paraformaldehyde	P6148	Sigma-Alderich, Poole, UK
Triton X-100	X100	Sigma-Alderich, Poole, UK
Animal Husbandry		
Standard rat & mouse chow		B & K Universal, Hull, UK
High fast ‘Western’ Diet	829100	Special diets services, Essex, UK
PCR		
Reddymix PCR mastermix	AB-0575	Thermo-Scientific, Leicestershire, UK
Reaction buffer		Promega, Southampton, UK
Magnesium chloride		Promega, Southampton, UK
0.2ml PCR tubes	1402-8100	Starlab, Milton Keynes, UK
Agarose	MB1200	Melford Labs, Suffolk, UK
Ethidium Bromide	H5041	Promega, Southampton, UK
Loading Buffer	37045	Bioline, London, UK
Hyperladder V	33031	Bioline, London, UK
Primers		Sigma Genosys
Histology/Immunohistochemsitry		
Bovine serum albumin	A7906	Sigma-Alderich, Poole, UK
Hydrogen peroxide	H1009	Sigma-Alderich, Poole, UK
Goat serum	16210-072	Invitrogen, Paisley, UK
Poly-lysine slides	631-0107	VWR International, UK
Coverslips (no.1.5)		SLS, Nottingham, UK
Oil red O powder	00625	Sigma-Alderich, Poole, UK
Triethyl phosphate	538728	Sigma-Alderich, Poole, UK

Product	Code	Supplier
Mayer's Heamatoxyin	H3136	Sigma-Alderich, Poole, UK
Eosin		Sigma-Alderich, Poole, UK
Xylene		Genta Environmental, York, UK
DPX mounting medium	Lamb/DPX.LV	Raymond Lamb, Sussex, UK
Vector red substrate	SK-5100	Vector Labs, Peterborough, UK
DAB	SK-4100	Vector Labs, Peterborough, UK
ABC peroxidase kit	PK-400	Vector Labs, Peterborough, UK
Vectashield	H-1500	Vector Labs, Peterborough, UK

Dissection Equipment

McPherson-Vannas Scissors		World Precision Instruments, UK
Dumont fine forceps No. 5	500232	World Precision Instruments, UK

Myography and Calcium imaging

Phenylephrine	P6126	Sigma-Alderich, Poole, UK
Serotonin	H5923	Sigma-Alderich, Poole, UK
Acetylcholine	A6625	Sigma-Alderich, Poole, UK
Sodium nitroprusside	13451	Sigma-Alderich, Poole, UK
LNNA	N5501	Sigma-Alderich, Poole, UK
CPA	C1530	Sigma-Alderich, Poole, UK
Indo-1 free acid	I1202	Life technologies, UK
Indo-1 AM	I1223	Life Technologies, UK

All Calcium imaging hardware was sourced from Cairn Research, Kent, UK.

Appendix II – Recipes

PCR

1M Tris, pH 8.0 (100ml)
12.1g Tris
Make up to volume with distilled water
pH to 8.0 with HCl

0.5M EDTA (100ml)
14.61g EDTA
Make up to volume with distilled water

10% SDS (100ml)
2.88g Sodium Dodecyl Sulphate
Made up to volume with distilled water

Lysis Buffer (100ml)
5ml 1M Tris pH 8.0 (50mM)
20ml 0.5M EDTA (100mM)
5ml 10% SDS (0.5%)
Make up to volume with distilled water

Tris-EDTA buffer (1 litre)
1.21g Tris
0.37g EDTA
0.5ml Tween
Make up to 1 litre with distilled water
pH to 9.0

Immunohistochemistry and Histology

100mM Tris-HCl, pH 8.2 (100ml)
1.21g Tris-HCl
Make up to volume with distilled water
pH to 8.2 with HCl

Citrate buffer (1 litre)
2.94g tri-sodium citrate
0.5ml Tween
make up to 1 litre with distilled water
pH to 6.0

10x PBS (1 litre)
80g sodium chloride (NaCl)
2g potassium chloride (KCl)
14.4g sodium phosphate (Na_2HPO_4)
2.4g potassium phosphate (KH_2PO_4)
pH to 7.4
make up to 1 litre with distilled water

Oil Red O, 0.5% (50ml)
0.25g Oil Red O powder dissolved in 60% aqueous triethyl phosphate
Filter and use immediately

Myography and calcium imaging

HEPES-PSS, pH 7.4 (5L)
37.1g NaCl (127mM)
2.2g KCl (5.9mM)
1.48g $MgSO_4$ (1.2mM)
11.92g HEPES (10mM)
10.63g Glucose (11.8mM)
1.76g $CaCl_2$ (2.4mM)
Make up to volume with distilled water
pH to 7.4 with NaOH

100mM KCl HEPES-PSS, pH7.4 (1L)
1.92g NaCl (32.9mM)
7.46g KCl (100mM)
0.30g $MgSO_4$ (1.2mM)
2.38g HEPES (10mM)
2.13g Glucose (11.8mM)
0.35g $CaCl_2$ (2.4mM)
Make up to volume with distilled water
pH to 7.4 with NaOH

Calcium free HEPES-PSS (1L)
7.42g NaCl (127mM)
0.44g KCl (5.9mM)
0.30g $MgSO_4$ (1.2mM)
2.38g HEPES (10mM)
2.13g Glucose (11.8mM)
0.76g EGTA (2mM)

20mM MnCl HEPES-PSS, pH 7.4
0.4g MnCl / 100ml HEPES-PSS
pH to 7.4 with NaOH

Appendix III – Antibody Optimisation

Primary Antibody	Primary concentration	Antigen retrieval	Blocking step	Secondary antibody	Secondary concentration
Ms AP-conjugated α-SMA [1A4] (A-5691)	0 1:100 1:200 1:500	1% Triton X-100	10% goat serum	Developed with Vector Red (SK-5100) in 100mM Tris-HCl (25 – 29 minutes)	N/A
Rb smMHCII (ab53219)	0 1:100 1:200 1:400 1:500	Heat mediated – citrate buffer	10% goat serum + 1% BSA	Goat anti-Rabbit TR (ab7088)	1:500 1:500 1:500 1:500 1:500
Rb smMHCII (ab53219)	0 1:50 1:100 1:200 1:500	Heat mediated – citrate buffer	10% goat serum + 1% BSA	Goat anti-Rabbit TR (ab7088)	1:50 1:50 1:50 1:50 1:50
Rb smMHCII (ab53219)	0 1:100 1:200	Heat mediated – citrate buffer	10% goat serum + 1% BSA	Goat anti-Rabbit TR (ab7088)	1:100 1:100 1:100
Rb smMHCII (ab53219)	0 1:100	Heat mediated – citrate buffer + 1% Triton X-100	10% goat serum + 1% BSA	Goat anti-Rabbit Biotinylated (BA-1000)	1:200 1:200
Rb Smoothelin (ab53219)	1:50 1:100 1:200	Heat mediated – citrate buffer	10% goat serum + 1% BSA	Goat anti-Rabbit Biotinylated (BA-1000)	1:200 1:200

Appendix IIII – Images from 26 week high fat 'western' diet fed ApoE$^{-/-}$ mice.

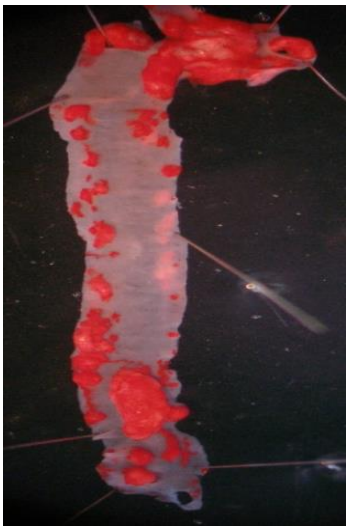

Image 1. *En face* Oil Red O staining of the aorta of an ApoE$^{-/-}$ mouse fed on a high fat 'western' diet for 26 weeks. After prolonged feeding on a high fat diet it can be seen that the build up of lipids within the aorta, indicative of atherosclerotic plaques, is extensive in comparison to after only 8 weeks feeding (c.f. Figure 4.2). Large amounts of staining can be observed in the aortic arch, at the intercostal artery branch points within the thoracic aorta, and also within the abdominal aorta. This time point represents the limit of the duration of high fat feeding available on the current licence.

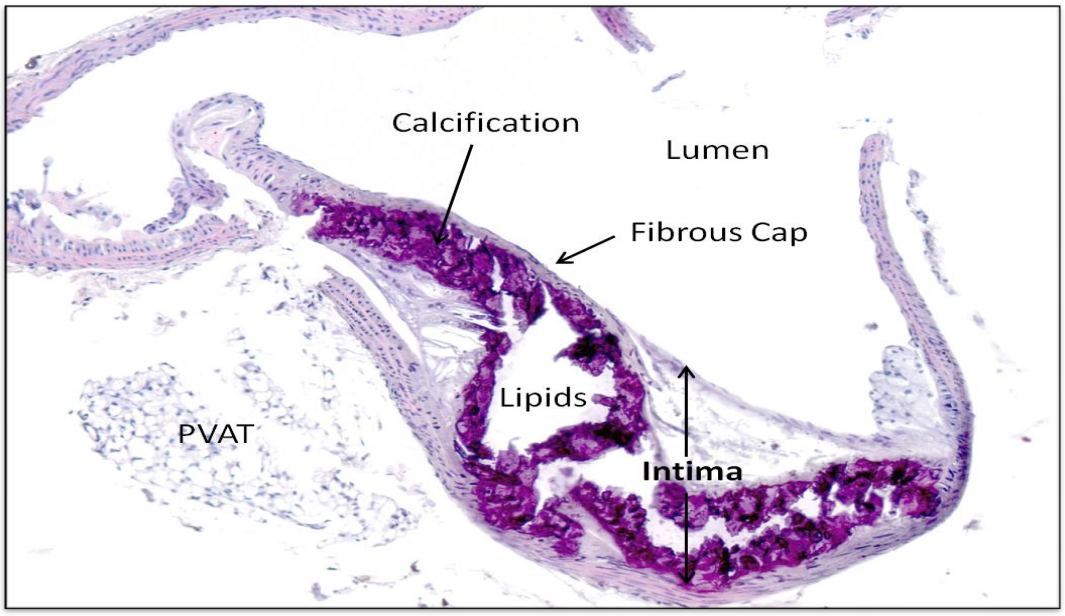

Image 2. Transverse section of the thoracic aorta from an ApoE$^{-/-}$ mouse fed on a high fat 'western' diet for 26 weeks stained with haematoxylin and eosin. This cross-section of the thoracic aorta shows the presence of an advanced atherosclerotic plaque within the thoracic aorta of an ApoE$^{-/-}$ mouse after 26 weeks high fat feeding. The presence of extensive intimal thickening is highlighted as well as the fibrous cap that has formed. Within the plaque the purple crystallisation is calcification and the gaps within the plaque are where lipids that have been removed during tissue processing would exist.

8. Bibliography

1. http://www.heartstats.org. Prevalence of all coronary heart disease. 2010;

2. Okrainec K, Banerjee DK, Eisenberg MJ. Coronary artery disease in the developing world. *Am. Heart J.* [Internet]. 2004; 148:7–15. Available from: http://linkinghub.elsevier.com/retrieve/pii/S0002870304002042?showall=true

3. Douglas G, Channon KM. The pathogenesis of atherosclerosis. *Medicine (Baltimore).* [Internet]. 2010 [cited 2013 Sep 26]; 38:397–402. Available from: http://www.sciencedirect.com/science/article/pii/S1357303910001222

4. Berliner JA, Navab M, Fogelman AM, Frank JS, Demer LL, Edwards PA, Watson AD, Lusis AJ. Atherosclerosis: Basic Mechanisms : Oxidation, Inflammation, and Genetics. *Circulation* [Internet]. 1995; 91:2488–2496. Available from: http://circ.ahajournals.org/cgi/content/abstract/91/9/2488

5. Ku DN, Giddens DP, Zarins CK, Glagov S. Pulsatile flow and atherosclerosis in the human carotid bifurcation. Positive correlation between plaque location and low oscillating shear stress. *Arter. Thromb Vasc Biol* [Internet]. 1985; 5:293–302. Available from: http://atvb.ahajournals.org/cgi/content/abstract/5/3/293

6. Cheng C, Tempel D, van Haperen R, van der Baan A, Grosveld F, Daemen MJAP, Krams R, de Crom R. Atherosclerotic Lesion Size and Vulnerability Are Determined by Patterns of Fluid Shear Stress. *Circulation* [Internet]. 2006; 113:2744–2753. Available from: http://circ.ahajournals.org/cgi/content/abstract/113/23/2744

7. Cibele MP, Simone GR, Jorge Jr. E, Marcos AR. Turbulent blood flow plays an essential localizing role in the development of atherosclerotic lesions in experimentally induced hypercholesterolaemia in rats. *Int. J. Exp. Pathol.* [Internet]. 2008; 89:72–80. Available from: http://dx.doi.org/10.1111/j.1365-2613.2007.00564.x

8. Triggle CR, Samuel SM, Ravishankar S, Marei I, Arunachalam G, Ding H. The endothelium: influencing vascular smooth muscle in many ways. *Can. J. Physiol. Pharmacol.* [Internet]. 2012 [cited 2013 Sep 22]; 90:713–38. Available from: http://www.ncbi.nlm.nih.gov/pubmed/22625870

9. Sima A V, Stancu CS, Simionescu M. Vascular endothelium in atherosclerosis. *Cell Tissue Res.* [Internet]. 2009 [cited 2013 Sep 26]; 335:191–203. Available from: http://www.ncbi.nlm.nih.gov/pubmed/18797930

10. Chatterjee A, Catravas JD. Endothelial nitric oxide (NO) and its pathophysiologic regulation. *Vascul. Pharmacol.* [Internet]. 2008; 49:134–140. Available from: http://www.sciencedirect.com/science/article/B6X3P-4T1FWHV-1/2/08b4960b308409bc187bb02203187a3d

11. Kavurma MM, Tan NY, Bennett MR. Death receptors and their ligands in atherosclerosis. *Arterioscler. Thromb. Vasc. Biol.* [Internet]. 2008 [cited 2013 Sep 26]; 28:1694–702. Available from: http://atvb.ahajournals.org/content/28/10/1694.short

12. Lubrano V, Di Cecco P, Zucchelli GC. Role of superoxide dismutase in vascular inflammation and in coronary artery disease. *Clin. Exp. Med.* [Internet]. 2006 [cited 2013 Sep 17]; 6:84–8. Available from: http://www.ncbi.nlm.nih.gov/pubmed/16820996

13. Spady DK, Wollett LA, Dietschy JM. Regulation of plasma LDL-cholesterol levels by dietary cholesterol and fatty acids. *Annu. Rev. Nutr.* [Internet]. 1993 [cited 2013 Aug 13]; v. 13 p. 3. Available from: http://agris.fao.org/agris-search/search/display.do?f=1994/US/US94040.xml;US9425389

14. Yuan Y, Verna LK, Wang NP, Liao HL, Ma KS, Wang Y, Zhu Y, Stemerman MB. Cholesterol enrichment upregulates intercellular adhesion molecule-1 in human vascular endothelial cells. *Biochim. Biophys. Acta - Mol. Cell Biol. Lipids* [Internet]. 2001 [cited 2013 Aug 13]; 1534:139–148. Available from: http://dx.doi.org/10.1016/S1388-1981(01)00188-3

15. Yoshida T, Owens GK. Molecular Determinants of Vascular Smooth Muscle Cell Diversity. *Circ Res* [Internet]. 2005; 96:280–291. Available from: http://circres.ahajournals.org/cgi/content/abstract/96/3/280

16. Campbell GR, Campbell JH. Smooth muscle phenotypic changes in arterial wall homeostasis: Implications for the pathogenesis of atherosclerosis. *Exp. Mol. Pathol.* [Internet]. 1985; 42:139–162. Available from: http://www.sciencedirect.com/science/article/B6WFB-4C4NSP4-BF/2/63ec65d1ec171687b16cb671f67ebad0

17. Schwartz SM, Campbell GR, Campbell JH. Replication of smooth muscle cells in vascular disease. *Circ Res* [Internet]. 1986; 58:427–444. Available from: http://circres.ahajournals.org/cgi/content/abstract/58/4/427

18. Hadrava V, Tremblay J, Hamet P. Abnormalities in growth characteristics of aortic smooth muscle cells in spontaneously hypertensive rats. *Hypertension* [Internet]. 1989; 13:589–597. Available from: http://hyper.ahajournals.org/cgi/content/abstract/13/6/589

19. Ross R. The pathogenesis of atherosclerosis: a perspective for the 1990s. *Nature* [Internet]. 1993 [cited 2013 Sep 17]; 362:801–9. Available from: http://dx.doi.org/10.1038/362801a0

20. Ross R, Masuda J, Raines EW, Gown AM, Katsuda S, Sasahara M, Malden LT, Masuko H, Sato H. Localization of PDGF-B protein in macrophages in all phases of atherogenesis. *Science (80-.).* [Internet]. 1990; 248:1009–1012. Available from: http://www.sciencemag.org/cgi/content/abstract/248/4958/1009

21. Owens GK, Kumar MS, Wamhoff BR. Molecular Regulation of Vascular Smooth Muscle Cell Differentiation in Development and Disease. *Physiol. Rev.* [Internet]. 2004; 84:767–801. Available from: http://physrev.physiology.org/cgi/content/abstract/84/3/767

22. Ross R. Atherosclerosis -- An Inflammatory Disease. *N Engl J Med* [Internet]. 1999; 340:115–126. Available from: http://content.nejm.org

23. Furchgott RF, Zawadzki J V. The obligatory role of endothelial cells in the relaxation of arterial smooth muscle by acetylcholine. *Nature* [Internet]. 1980; 288:373–376. Available from: http://dx.doi.org/10.1038/288373a0

24. Furchgott RF, Cherry PD, Zawadzki J V, Jothianandan D. Endothelial cells as mediators of vasodilation of arteries. *J Cardiovasc Pharmacol*. 1984; 6 Suppl 2:S336–43.

25. Crauwels HM, Van Hove CE, Herman AG, Bult H. Heterogeneity in relaxation mechanisms in the carotid and the femoral artery of the mouse. *Eur. J. Pharmacol.* [Internet]. 2000 [cited 2013 Sep 13]; 404:341–351. Available from: http://dx.doi.org/10.1016/S0014-2999(00)00619-1

26. Duffy SJ, Tran BT, New G, Tudball RN, Esler MD, Harper RW, Meredith IT. Continuous release of vasodilator prostanoids contributes to regulation of resting forearm blood flow in humans. *Am J Physiol Hear. Circ Physiol* [Internet]. 1998 [cited 2013 Sep 22]; 274:H1174–1183. Available from: http://ajpheart.physiology.org/content/274/4/H1174

27. Duffy SJ, Castle SF, Harper RW, Meredith IT. Contribution of Vasodilator Prostanoids and Nitric Oxide to Resting Flow, Metabolic Vasodilation, and Flow-Mediated Dilation in Human Coronary Circulation. *Circulation* [Internet]. 1999 [cited 2013 Sep 22]; 100:1951–1957. Available from: http://circ.ahajournals.org/content/100/19/1951.short

28. Koller A, Sun D, Kaley G. Role of shear stress and endothelial prostaglandins in flow- and viscosity-induced dilation of arterioles in vitro. *Circ. Res.* [Internet]. 1993 [cited 2013 Sep 22]; 72:1276–1284. Available from: http://circres.ahajournals.org/content/72/6/1276.abstract

29. Koller A, Sun D, Huang A, Kaley G. Corelease of nitric oxide and prostaglandins mediates flow-dependent dilation of rat gracilis muscle arterioles. *Am J Physiol Hear. Circ Physiol* [Internet]. 1994 [cited 2013 Sep 22]; 267:H326–332. Available from: http://ajpheart.physiology.org/content/267/1/H326

30. Yeboah J, Folsom AR, Burke GL, Johnson C, Polak JF, Post W, Lima JA, Crouse JR, Herrington DM. Predictive value of brachial flow-mediated dilation for incident cardiovascular events in a population-based study: the multi-ethnic study of atherosclerosis. *Circulation* [Internet]. 2009 [cited 2013 Sep 15]; 120:502–9. Available from: http://circ.ahajournals.org/content/120/6/502.short

31. Kobayashi K, Akishita M, Yu W, Hashimoto M, Ohni M, Toba K. Interrelationship between non-invasive measurements of atherosclerosis: flow-mediated dilation of brachial artery, carotid intima-media thickness and pulse wave velocity. *Atherosclerosis* [Internet]. 2004 [cited 2013 Sep 15]; 173:13–8. Available from: http://www.atherosclerosis-journal.com/article/S0021-9150(03)00495-7/abstract

32. Pike LJ, Casey L. Localization and Turnover of Phosphatidylinositol 4,5-Bisphosphate in Caveolin-enriched Membrane Domains. *J. Biol. Chem.* [Internet]. 1996; 271:26453–26456. Available from: http://www.jbc.org/cgi/content/abstract/271/43/26453

33. Pike LJ, Miller JM. Cholesterol Depletion Delocalizes Phosphatidylinositol Bisphosphate and Inhibits Hormone-stimulated Phosphatidylinositol Turnover. *J. Biol. Chem.* [Internet]. 1998; 273:22298–22304. Available from: http://www.jbc.org/cgi/content/abstract/273/35/22298

34. Berridge MJ. Inositol trisphosphate and calcium signalling. *Nature* [Internet]. 1993; 361:315–325. Available from: http://dx.doi.org/10.1038/361315a0

35. Sbaa E, Frérart F, Feron O. The Double Regulation of Endothelial Nitric Oxide Synthase by Caveolae and Caveolin: A Paradox Solved Through the Study of Angiogenesis. *Trends Cardiovasc. Med.* [Internet]. 2005; 15:157–162. Available from: http://www.sciencedirect.com/science/article/B6T1D-4H3GWG9-4/2/ac8b877fce46696d92389e01313395dd

36. Krasteva G, Pfeil U, Filip A-M, Lips KS, Kummer W, König P. Caveolin-3 and eNOS colocalize and interact in ciliated airway epithelial cells in the rat. *Int. J. Biochem. Cell Biol.* [Internet]. 2007; 39:615–625. Available from: http://www.sciencedirect.com/science/article/B6TCH-4M762RF-1/2/d511617635146f51cb2ed134a75a5ecc

37. Xu Y, Henning RH, van der Want JJL, van Buiten A, van Gilst WH, Buikema H. Disruption of endothelial caveolae is associated with impairment of both NO- as well as EDHF in acetylcholine-induced relaxation depending on their relative contribution in different vascular beds. *Life Sci.* [Internet]. 2007; 80:1678–1685. Available from: http://www.sciencedirect.com/science/article/B6T99-4MY0MSV-3/2/96be65e88c5be09200536f64ed300f16

38. Shaul PW, Smart EJ, Robinson LJ, German Z, Yuhanna IS, Ying Y, Anderson RGW, Michel T. Acylation Targets Endothelial Nitric-oxide Synthase to Plasmalemmal Caveolae. *J. Biol. Chem.* [Internet]. 1996; 271:6518–6522. Available from: http://www.jbc.org/cgi/content/abstract/271/11/6518

39. Michel JB. Reciprocal Regulation of Endothelial Nitric-oxide Synthase by Ca2+-Calmodulin and Caveolin. *J. Biol. Chem.* [Internet]. 1997 [cited 2013 Aug 19]; 272:15583–15586. Available from: http://www.jbc.org/content/272/25/15583.short

40. Moncada S, Palmer RM, Higgs EA. The discovery of nitric oxide as the endogenous nitrovasodilator. *Hypertension* [Internet]. 1988; 12:365–372. Available from: http://hyper.ahajournals.org/cgi/content/abstract/12/4/365

41. Ignarro LJ. Biosynthesis and Metabolism of Endothelium-Derived Nitric Oxide. 2003 [cited 2013 Sep 22];Available from: http://www.annualreviews.org/doi/abs/10.1146/annurev.pa.30.040190.002535?journalCode=pharmtox

42. Nilius B, Droogmans G. Ion Channels and Their Functional Role in Vascular Endothelium. *Phys. Rev.* [Internet]. 2001; 81:1415–1459. Available from: http://physrev.physiology.org/cgi/content/abstract/81/4/1415

43. Broad LM, Cannon TR, Taylor CW. A non-capacitative pathway activated by arachidonic acid is the major Ca2+ entry mechanism in rat A7r5 smooth muscle cells stimulated with low concentrations of vasopressin. *J. Physiol.* [Internet]. 1999; 517:121–134. Available from: http://jp.physoc.org/cgi/content/abstract/517/1/121

44. Fisslthaler B, Popp R, Kiss L, Potente M, Harder DR, Fleming I, Busse R. Cytochrome P450 2C is an EDHF synthase in coronary arteries. *Nature* [Internet]. 1999; 401:493–497. Available from: http://dx.doi.org/10.1038/46816

45. Fleming I. Cytochrome P450 epoxygenases as EDHF synthase(s). *Pharmacol Res*. 2004; 49:525–533.

46. Gryglewski RJ, Bunting S, Moncada S, Flower RJ, Vane JR. Arterial walls are protected against deposition of platelet thrombi by a substance (prostaglandin X) which they make from prostaglandin endoperoxides. *Prostaglandins* [Internet]. 1976 [cited 2013 Sep 22]; 12:685–713. Available from: http://www.sciencedirect.com/science/article/pii/0090698076900472

47. Siegel G, Schnalke F, Stock G, Grote J. Prostacyclin, endothelium-derived relaxing factor and vasodilatation. *Adv. Prostaglandin. Thromboxane. Leukot. Res.* [Internet]. 1989 [cited 2013 Aug 19]; 19:267–70. Available from: http://www.ncbi.nlm.nih.gov/pubmed/2473608

48. Félétou M. The Endothelium, Part I: Multiple Functions of the Endothelial Cells -- Focus on Endothelium-Derived Vasoactive Mediators. *Colloq. Ser. Integr. Syst. Physiol. From Mol. to Funct.* [Internet]. 2011 [cited 2013 Sep 22]; 3:1–306. Available from: http://europepmc.org/abstract/MED/21850763

49. Dorris SL, Peebles RS. PGI2 as a regulator of inflammatory diseases. *Mediators Inflamm.* [Internet]. 2012 [cited 2013 Sep 22]; 2012:926968. Available from: http://www.pubmedcentral.nih.gov/articlerender.fcgi?artid=3407649&tool=pmcentrez&rendertype=abstract

50. Bolton TB, Gordienko D V, Pucovský V, Parsons S, Povstyan O. Calcium release events in excitation-contraction coupling in smooth muscle. *Novartis Found. Symp.* [Internet]. 2002 [cited 2013 Sep 26]; 246:154–68; discussion 168–73, 221–7. Available from: http://www.ncbi.nlm.nih.gov/pubmed/12164307

51. Marchand A, Abi-Gerges A, Saliba Y, Merlet E, Lompré A-M. Calcium signaling in vascular smooth muscle cells: from physiology to pathology. *Adv. Exp. Med. Biol.* [Internet]. 2012 [cited 2013 Sep 26]; 740:795–810. Available from: http://www.ncbi.nlm.nih.gov/pubmed/22453970

52. Sato K, Tokmakov AA, Iwasaki T, Fukami Y. Tyrosine Kinase-Dependent Activation of Phospholipase Cγ Is Required for Calcium Transient in Xenopus Egg Fertilization. *Dev. Biol.* [Internet]. 2000 [cited 2013 Sep 25]; 224:453–469. Available from: http://www.sciencedirect.com/science/article/pii/S0012160600997823

53. Kelley GG, Kaproth-Joslin KA, Reks SE, Smrcka A V, Wojcikiewicz RJH. G-protein-coupled receptor agonists activate endogenous phospholipase Cepsilon and

phospholipase Cbeta3 in a temporally distinct manner. *J. Biol. Chem.* [Internet]. 2006 [cited 2013 Sep 25]; 281:2639–48. Available from: http://www.jbc.org/content/281/5/2639.short

54. Suh P-G, Park J-I, Manzoli L, Cocco L, Peak JC, Katan M, Fukami K, Kataoka T, Yun S, Ryu SH. Multiple roles of phosphoinositide-specific phospholipase C isozymes. *BMB Rep.* [Internet]. 2008 [cited 2013 Sep 25]; 41:415–34. Available from: http://www.ncbi.nlm.nih.gov/pubmed/18593525

55. Daub H, Wallasch C, Lankenau A, Herrlich A, Ullrich A. Signal characteristics of G protein-transactivated EGF receptor. *EMBO J.* [Internet]. 1997 [cited 2013 Sep 25]; 16:7032–44. Available from: http://dx.doi.org/10.1093/emboj/16.23.7032

56. Berridge MJ. Inositol trisphosphate and calcium signalling mechanisms. *Biochim. Biophys. Acta* [Internet]. 2009 [cited 2013 Sep 26]; 1793:933–40. Available from: http://www.ncbi.nlm.nih.gov/pubmed/19010359

57. Huster M, Frei E, Hofmann F, Wegener JW. A complex of CaV1.2/PKC is involved in muscarinic signaling in smooth muscle. *FASEB J.* [Internet]. 2010; 24:2651–2659. Available from: http://www.fasebj.org/cgi/content/abstract/24/8/2651

58. Dzhura I, Wu Y, Colbran RJ, Balser JR, Anderson ME. Calmodulin kinase determines calcium-dependent facilitation of L-type calcium channels. *Nat Cell Biol* [Internet]. 2000; 2:173–177. Available from: http://dx.doi.org/10.1038/35004052

59. Clapham DE, Runnels LW, Strubing C. The trp ion channel family. *Nat Rev Neurosci* [Internet]. 2001; 2:387–396. Available from: http://dx.doi.org/10.1038/35077544

60. Walker RL, Hume JR, Horowitz B. Differential expression and alternative splicing of TRP channel genes in smooth muscles. *Am J Physiol Cell Physiol* [Internet]. 2001; 280:C1184–1192. Available from: http://ajpcell.physiology.org/cgi/content/abstract/280/5/C1184

61. Inoue R, Jensen LJ, Shi J, Morita H, Nishida M, Honda A, Ito Y. Transient Receptor Potential Channels in Cardiovascular Function and Disease. *Circ Res* [Internet]. 2006; 99:119–131. Available from: http://circres.ahajournals.org/cgi/content/abstract/99/2/119

62. Hofmann T, Obukhov AG, Schaefer M, Harteneck C, Gudermann T, Schultz G. Direct activation of human TRPC6 and TRPC3 channels by diacylglycerol. *Nature* [Internet]. 1999; 397:259–263. Available from: http://dx.doi.org/10.1038/16711

63. Kamouchi M, Philipp S, Flockerzi V, Wissenbach U, Mamin A, Raeymaekers L, Eggermont J, Droogmans G, Nilius B. Properties of heterologously expressed hTRP3 channels in bovine pulmonary artery endothelial cells. *J. Physiol.* [Internet]. 1999; 518:345–358. Available from: http://jp.physoc.org/content/518/2/345.abstract

64. Okada T, Inoue R, Yamazaki K, Maeda A, Kurosaki T, Yamakuni T, Tanaka I, Shimizu S, Ikenaka K, Imoto K, Mori Y. Molecular and Functional Characterization of a Novel Mouse Transient Receptor Potential Protein Homologue TRP7. *J. Biol. Chem.*

[Internet]. 1999; 274:27359–27370. Available from: http://www.jbc.org/content/274/39/27359.abstract

65. Inoue R, Okada T, Onoue H, Hara Y, Shimizu S, Naitoh S, Ito Y, Mori Y. The Transient Receptor Potential Protein Homologue TRP6 Is the Essential Component of Vascular Alpha 1-Adrenoceptor-Activated Ca2+-Permeable Cation Channel. *Circ Res* [Internet]. 2001; 88:325–332. Available from: http://circres.ahajournals.org/cgi/content/abstract/88/3/325

66. Yeromin A V, Zhang SL, Jiang W, Yu Y, Safrina O, Cahalan MD. Molecular identification of the CRAC channel by altered ion selectivity in a mutant of Orai. *Nature* [Internet]. 2006; 443:226–229. Available from: http://dx.doi.org/10.1038/nature05108

67. Berra-Romani R, Mazzocco-Spezzia A, Pulina M V, Golovina VA. Ca2+ handling is altered when arterial myocytes progress from a contractile to a proliferative phenotype in culture. *Am J Physiol Cell Physiol* [Internet]. 2008; 295:C779–790. Available from: http://ajpcell.physiology.org/cgi/content/abstract/295/3/C779

68. Xu S-Z, Beech DJ. TrpC1 Is a Membrane-Spanning Subunit of Store-Operated Ca2+ Channels in Native Vascular Smooth Muscle Cells. *Circ Res* [Internet]. 2001; 88:84–87. Available from: http://circres.ahajournals.org/cgi/content/abstract/88/1/84

69. Beech DJ, Xu SZ, McHugh D, Flemming R. TRPC1 store-operated cationic channel subunit. *Cell Calcium* [Internet]. 2003; 33:433–440. Available from: http://www.sciencedirect.com/science/article/B6WCC-487KHN4-2/2/e930e98a919a653db23ebaa7d92beba2

70. Xu S-Z, Boulay G, Flemming R, Beech DJ. E3-targeted anti-TRPC5 antibody inhibits store-operated calcium entry in freshly isolated pial arterioles. *Am J Physiol Hear. Circ Physiol* [Internet]. 2006; 291:H2653–2659. Available from: http://ajpheart.physiology.org/cgi/content/abstract/291/6/H2653

71. Brock TA, Alexander RW, Ekstein LS, Atkinson WJ, Gimbrone Jr. MA. Angiotensin increases cytosolic free calcium in cultured vascular smooth muscle cells. *Hypertension*. 1985; 7:I105–9.

72. Sato K, Ozaki H, Karaki H. Changes in cytosolic calcium level in vascular smooth muscle strip measured simultaneously with contraction using fluorescent calcium indicator fura 2. *J. Pharmacol. Exp. Ther.* [Internet]. 1988; 246:294–300. Available from: http://jpet.aspetjournals.org/content/246/1/294.abstract

73. Blaustein MP, Golovina VA, Song H, Choate J, Lencesova L, Robinson SW, Wier WG. Organisation of Ca2+ stores in vascular smooth muscle: functional implications. In: 246 NFS, editor. Role of the sarcoplasmic reticulum in smooth muscle. Chichester: Wiley & Sons; 2002. p. 125–141.

74. Szewczyk MM, Davis KA, Samson SE, Simpson F, Rangachari PK, Grover AK. Ca2+-pumps and Na+–Ca2+-exchangers in coronary artery endothelium versus

smooth muscle. *J. Cell. Mol. Med.* [Internet]. 2007; 11:129–138. Available from: http://dx.doi.org/10.1111/j.1582-4934.2007.00010.x

75. Hilgemann DW, Nicoll DA, Philipson KD. Charge movement during Na+ translocation by native and cloned cardiac Na+/Ca2+ exchanger. *Nature* [Internet]. 1991; 352:715–718. Available from: http://dx.doi.org/10.1038/352715a0

76. Blaustein MP, Lederer WJ. Sodium/Calcium Exchange: Its Physiological Implications. *Physiol. Rev.* [Internet]. 1999; 79:763–854. Available from: http://physrev.physiology.org/cgi/content/abstract/79/3/763

77. Moore EDW, Etter EF, Philipson KD, Carrington WA, Fogarty KE, Lifshitz LM, Fay FS. Coupling of the Na+/Ca2+exchanger, Na+/K+ pump and sarcoplasmic reticulum in smooth muscle. *Nature* [Internet]. 1993; 365:657–660. Available from: http://dx.doi.org/10.1038/365657a0

78. Lynch RM, Weber CS, Nullmeyer KD, Moore EDW, Paul RJ. Clearance of store-released Ca2+ by the Na+-Ca2+ exchanger is diminished in aortic smooth muscle from Na+-K+-ATPase {alpha}2-isoform gene-ablated mice. *Am J Physiol Hear. Circ Physiol* [Internet]. 2008; 294:H1407–1416. Available from: http://ajpheart.physiology.org/cgi/content/abstract/294/3/H1407

79. Lytton J, Zarain-Herzberg A, Periasamy M, MacLennan DH. Molecular cloning of the mammalian smooth muscle sarco(endo)plasmic reticulum Ca2+-ATPase. *J. Biol. Chem.* [Internet]. 1989; 264:7059–7065. Available from: http://www.jbc.org/content/264/12/7059.abstract

80. Carafoli E. The Ca2+ pump of the plasma membrane. *J. Biol. Chem.* [Internet]. 1992; 267:2115–2118. Available from: http://www.jbc.org/content/267/4/2115.short

81. Verboomen H, Wuytack F, De Smedt H, Himpens B, Casteels R. Functional difference between SERCA2a and SERCA2b Ca2+ pumps and their modulation by phospholamban. *Biochem J.* 1992; 286 (Pt 2:591–595.

82. Kirichok Y, Krapivinsky G, Clapham DE. The mitochondrial calcium uniporter is a highly selective ion channel. *Nature* [Internet]. 2004 [cited 2013 Sep 18]; 427:360–4. Available from: http://dx.doi.org/10.1038/nature02246

83. Szabadkai G, Duchen MR. Mitochondria: The Hub of Cellular Ca2+ Signaling. *Physiology* [Internet]. 2008; 23:84–94. Available from: http://physiologyonline.physiology.org/cgi/content/abstract/23/2/84

84. Ruegg JC, Paul RJ. Vascular smooth muscle. Calmodulin and cyclic AMP-dependent protein kinase after calcium sensitivity in porcine carotid skinned fibers. *Circ Res* [Internet]. 1982; 50:394–399. Available from: http://circres.ahajournals.org/cgi/content/abstract/50/3/394

85. Karaki H, Sato K, Ozaki H. Different effects of norepinephrine and KCl on the cytosolic Ca2+-tension relationship in vascular smooth muscle of rat aorta. *Eur. J. Pharmacol.* [Internet]. 1988; 151:325–328. Available from:

http://www.sciencedirect.com/science/article/B6T1J-4772VWR-22F/2/b547e4bfee36c8572fdf2a9cec65d444

86. Abe A, Karaki H. Effect of forskolin on cytosolic Ca++ level and contraction in vascular smooth muscle. *J. Pharmacol. Exp. Ther.* [Internet]. 1989; 249:895–900. Available from: http://jpet.aspetjournals.org/content/249/3/895.abstract

87. Himpens B, Somlyo AP. Free-calcium and force transients during depolarization and pharmacomechanical coupling in guinea-pig smooth muscle. *J. Physiol.* [Internet]. 1988; 395:507–530. Available from: http://jp.physoc.org/content/395/1/507.abstract

88. Kitazawa T, Gaylinn BD, Denney GH, Somlyo AP. G-protein-mediated Ca2+ sensitization of smooth muscle contraction through myosin light chain phosphorylation. *J. Biol. Chem.* [Internet]. 1991; 266:1708–1715. Available from: http://www.jbc.org/content/266/3/1708.abstract

89. Gong MC, Fujihara H, Somlyo A V, Somlyo AP. Translocation of rhoA Associated with Ca2+ Sensitization of Smooth Muscle. *J. Biol. Chem.* [Internet]. 1997; 272:10704–10709. Available from: http://www.jbc.org/content/272/16/10704.abstract

90. Taggart MJ, Lee Y-H, Morgan KG. Cellular Redistribution of PKC[alpha], rhoA, and ROK[alpha] Following Smooth Muscle Agonist Stimulation. *Exp. Cell Res.* [Internet]. 1999; 251:92–101. Available from: http://www.sciencedirect.com/science/article/B6WFC-45GMBVP-4W/2/68cce576f5d42fad1385695b00f1d15e

91. Eto M, Kitazawa T, Yazawa M, Mukai H, Ono Y, Brautigan DL. Histamine-induced Vasoconstriction Involves Phosphorylation of a Specific Inhibitor Protein for Myosin Phosphatase by Protein Kinase C Î± and Î´ Isoforms. *J. Biol. Chem.* [Internet]. 2001; 276:29072–29078. Available from: http://www.jbc.org/content/276/31/29072.abstract

92. Woodsome TP, Eto M, Everett A, Brautigan DL, Kitazawa T. Expression of CPI-17 and myosin phosphatase correlates with Ca2+ sensitivity of protein kinase C-induced contraction in rabbit smooth muscle. *J. Physiol.* [Internet]. 2001; 535:553–564. Available from: http://jp.physoc.org/content/535/2/553.abstract

93. Ito M, Nakano T, Erdődi F, Hartshorne D. Myosin phosphatase: Structure, regulation and function. *Mol. Cell. Biochem.* [Internet]. 2004; 259:197–209. Available from: http://dx.doi.org/10.1023/B:MCBI.0000021373.14288.00

94. Tansey MG, Word RA, Hidaka H, Singer HA, Schworer CM, Kamm KE, Stull JT. Phosphorylation of myosin light chain kinase by the multifunctional calmodulin-dependent protein kinase II in smooth muscle cells. *J. Biol. Chem.* [Internet]. 1992; 267:12511–12516. Available from: http://www.jbc.org/content/267/18/12511.abstract

95. Sauzeau V, Le Mellionnec E, Bertoglio J, Scalbert E, Pacaud P, Loirand G. Human Urotensin II-Induced Contraction and Arterial Smooth Muscle Cell Proliferation Are Mediated by RhoA and Rho-Kinase. *Circ. Res.* [Internet]. 2001 [cited 2013 Sep 25]; 88:1102–1104. Available from: http://circres.ahajournals.org/content/88/11/1102.short

96. Yamada E. The fine structure of the gall bladder epithelium of the mouse. *J. Biophys. Biochem. Cytol.* [Internet]. 1955; 1:445–458. Available from: http://jcb.rupress.org/content/1/5/445.abstract

97. Severs NJ. Caveolae: static inpocketings of the plasma membrane, dynamic vesicles or plain artifact? *J Cell Sci* [Internet]. 1988; 90:341–348. Available from: http://jcs.biologists.org

98. Schlegel A, Volonté D, Engelman JA, Galbiati F, Mehta P, Zhang X-L, Scherer PE, Lisanti MP. Crowded Little Caves: Structure and Function of Caveolae. *Cell. Signal.* [Internet]. 1998; 10:457–463. Available from: http://www.sciencedirect.com/science/article/B6T2M-3V3RRJK-2/2/050fc07d25e5e5b6c7dcd209cb13a6a9

99. Anderson RGW. Potocytosis of small molecules and ions by caveolae. *Trends Cell Biol.* [Internet]. 1993; 3:69–72. Available from: http://www.sciencedirect.com/science/article/B6TCX-47GH71W-1T/2/4d5e189a707f50e916e3d14ace04c821

100. Fielding CJ, Fielding PE. Cholesterol and caveolae: structural and functional relationships. *Biochim. Biophys. Acta - Mol. Cell Biol. Lipids* [Internet]. 2000; 1529:210–222. Available from: http://www.sciencedirect.com/science/article/B6VNN-41T1FT7-M/2/7fa134cdf8e6230a049583961b07a396

101. Fielding CJ, Fielding PE. Caveolae and intracellular trafficking of cholesterol. *Adv. Drug Deliv. Rev.* [Internet]. 2001; 49:251–264. Available from: http://www.sciencedirect.com/science/article/B6T3R-43K8DDN-4/2/06800251c28b2b7de58338d234157b1b

102. Pelkmans L, Helenius A. Endocytosis Via Caveolae. *Traffic* [Internet]. 2002; 3:311–320. Available from: http://www.ingentaconnect.com/content/mksg/tra/2002/00000003/00000005/art00001

103. Cohen AW, Hnasko R, Schubert W, Lisanti MP. Role of Caveolae and Caveolins in Health and Disease. *Physiol Rev* [Internet]. 2004; 84:1341–1379. Available from: http://physrev.physiology.org/cgi/content/abstract/84/4/1341

104. Campbell L, Gumbleton M, Ritchie K. Caveolae and the caveolins in human disease. *Adv. Drug Deliv. Rev.* [Internet]. 2001; 49:325–335. Available from: http://www.sciencedirect.com/science/article/B6T3R-43K8DDN-9/2/c0e8c4ca8bf9719eadc71bd5caca3046

105. Rothberg KG, Heuser JE, Donzell WC, Ying Y-S, Glenney JR, Anderson RGW. Caveolin, a protein component of caveolae membrane coats. *Cell* [Internet]. 1992; 68:673–682. Available from: http://www.sciencedirect.com/science/article/B6WSN-4C592WS-64/2/981d7365c36d4f2f6906dff50fe3ac7a

106. Scherer PE, Okamoto T, Chun M, Nishimoto I, Lodish HF, Lisanti MP. Identification, sequence, and expression of caveolin-2 defines a caveolin gene family. *Proc. Natl.*

Acad. Sci. U S A [Internet]. 1996; 93:131–135. Available from: http://www.pnas.org/content/93/1/131.abstract

107. Scherer PE, Tang Z, Chun M, Sargiacomo M, Lodish HF, Lisanti MP. Caveolin Isoforms Differ in Their N-terminal Protein Sequence and Subcellular Distribution. *J. Biol. Chem.* [Internet]. 1995; 270:16395–16401. Available from: http://www.jbc.org/cgi/content/abstract/270/27/16395

108. Tang Z, Scherer PE, Okamoto T, Song K, Chu C, Kohtz DS, Nishimoto I, Lodish HF, Lisanti MP. Molecular Cloning of Caveolin-3, a Novel Member of the Caveolin Gene Family Expressed Predominantly in Muscle. *J. Biol. Chem.* [Internet]. 1996; 271:2255–2261. Available from: http://www.jbc.org/cgi/content/abstract/271/4/2255

109. Fra AM, Williamson E, Simons K, Parton RG. De novo formation of caveolae in lymphocytes by expression of VIP21-caveolin. *Proc. Natl. Acad. Sci. U S A* [Internet]. 1995; 92:8655–8659. Available from: http://www.pnas.org/content/92/19/8655.abstract

110. Galbiati F, VolontÃ© D, Chu JB, Li M, Fine SW, Fu M, Bermudez J, Pedemonte M, Weidenheim KM, Pestell RG, Minetti C, Lisanti MP. Transgenic overexpression of caveolin-3 in skeletal muscle fibers induces a Duchenne-like muscular dystrophy phenotype. *Proc. Natl. Acad. Sci. U S A* [Internet]. 2000; 97:9689–9694. Available from: http://www.pnas.org/content/97/17/9689.abstract

111. Scherer PE, Lewis RY, Volonte D, Engelman JA, Galbiati F, Couet J, Kohtz DS, van Donselaar E, Peters P, Lisanti MP. Cell-type and Tissue-specific Expression of Caveolin-2. Caveolins 1 and 2 Co-localise and Form a Stable Hetero-oligomeric Complex in vivo. *J. Biol. Chem.* [Internet]. 1997; 272:29337–29346. Available from: http://www.jbc.org/cgi/content/abstract/272/46/29337

112. Couet J, Li S, Okamoto T, Ikezu T, Lisanti MP. Identification of Peptide and Protein Ligands for the Caveolin-scaffolding Domain. IMPLICATIONS FOR THE INTERACTION OF CAVEOLIN WITH CAVEOLAE-ASSOCIATED PROTEINS. *J. Biol. Chem.* [Internet]. 1997; 272:6525–6533. Available from: http://www.jbc.org/cgi/content/abstract/272/10/6525

113. Boulanger CM, Morrison KJ, Vanhoutte PM. Mediation by M3-muscarinic receptors of both endothelium-dependent contraction and relaxation to acetylcholine in the aorta of the spontaneously hypertensive rat. *Br J Pharmacol*. 1994; 112:519–524.

114. Tracey WR, Peach MJ. Differential muscarinic receptor mRNA expression by freshly isolated and cultured bovine aortic endothelial cells. *Circ. Res.* [Internet]. 1992; 70:234–240. Available from: http://circres.ahajournals.org/cgi/content/abstract/70/2/234

115. Gosens R, Stelmack GL, Dueck G, Mutawe MM, Hinton M, McNeill KD, Paulson A, Dakshinamurti S, Gerthoffer WT, Thliveris JA, Unruh H, Zaagsma J, Halayko AJ. Caveolae facilitate muscarinic receptor-mediated intracellular Ca2+ mobilization and contraction in airway smooth muscle. *Am. J. Physiol. Lung Physiol.* [Internet]. 2007;

293:L1406–1418. Available from: http://ajplung.physiology.org/cgi/content/abstract/293/6/L1406

116. Feron O, Smith TW, Michel T, Kelly RA. Dynamic Targeting of the Agonist-stimulated m2 Muscarinic Acetylcholine Receptor to Caveolae in Cardiac Myocytes. *J. Biol. Chem.* [Internet]. 1997; 272:17744–17748. Available from: http://www.jbc.org/cgi/content/abstract/272/28/17744

117. Feron O, Han X, Kelly RA. Muscarinic cholinergic signaling in cardiac myocytes: Dynamic targeting of M2AChR to sarcolemmal caveolae and eNOS activation. *Life Sci.* [Internet]. 1999; 64:471–477. Available from: http://www.sciencedirect.com/science/article/B6T99-3W4PNNW-K/2/de8778e3aefceb23c8cfb57a2ec358ab

118. Li S, Okamoto T, Chun M, Sargiacomo M, Casanova JE, Hansen SH, Nishimoto I, Lisanti MP. Evidence for a Regulated Interaction between Heterotrimeric G Proteins and Caveolin. *J. Biol. Chem.* [Internet]. 1995; 270:15693–15701. Available from: http://www.jbc.org/cgi/content/abstract/270/26/15693

119. Pani B, Singh BB. Lipid rafts/caveolae as microdomains of calcium signaling. *Cell Calcium* [Internet]. 2009 [cited 2013 Aug 13]; 45:625–33. Available from: http://dx.doi.org/10.1016/j.ceca.2009.02.009

120. Fujita T. Accumulation of molecules involved in α1-adrenergic signal within caveolae: caveolin expression and the development of cardiac hypertrophy. *Cardiovasc. Res.* [Internet]. 2001 [cited 2013 Aug 16]; 51:709–716. Available from: http://cardiovascres.oxfordjournals.org/content/51/4/709.short

121. Bhatnagar A, Sheffler DJ, Kroeze WK, Compton-Toth B, Roth BL. Caveolin-1 interacts with 5-HT2A serotonin receptors and profoundly modulates the signaling of selected Galphaq-coupled protein receptors. *J. Biol. Chem.* [Internet]. 2004 [cited 2013 Aug 16]; 279:34614–23. Available from: http://www.jbc.org/content/279/33/34614.short

122. Spat A, Ambudkar IS, Bandyopadhyay BC, Liu X, Lockwich TP, Paria B, Ong HL. Functional organization of TRPC-Ca2+ channels and regulation of calcium microdomains. *Cell Calcium* [Internet]. 2006 [cited 2013 Sep 20]; 40:495–504. Available from: http://www.sciencedirect.com/science/article/pii/S014341600600176X

123. Remillard C V, Yuan JX-J. Transient receptor potential channels and caveolin-1: good friends in tight spaces. *Mol. Pharmacol.* [Internet]. 2006 [cited 2013 Sep 20]; 70:1151–4. Available from: http://molpharm.aspetjournals.org/content/70/4/1151.short

124. Cheng H, Lederer WJ, Cannell MB. Calcium sparks: elementary events underlying excitation-contraction coupling in heart muscle. *Science (80-.).* [Internet]. 1993; 262:740–744. Available from: http://www.sciencemag.org/cgi/content/abstract/262/5134/740

125. Nelson MT, Cheng H, Rubart M, Santana LF, Bonev AD, Knot HJ, Lederer WJ. Relaxation of Arterial Smooth Muscle by Calcium Sparks. *Science (80-.).* [Internet]. 1995; 270:633–637. Available from: http://www.sciencemag.org/cgi/content/abstract/270/5236/633

126. Gordienko D V, Greenwood IA, Bolton TB. Direct visualization of sarcoplasmic reticulum regions discharging Ca2+sparks in vascular myocytes. *Cell Calcium* [Internet]. 2001; 29:13–28. Available from: http://www.sciencedirect.com/science/article/B6WCC-45B59DR-2F/2/f8a7ac2805f172e80712068679420a0d

127. Gordienko D V, Bolton TB, Cannell MB. Variability in spontaneous subcellular calcium release in guinea-pig ileum smooth muscle cells. *J. Physiol.* [Internet]. 1998; 507:707–720. Available from: http://jp.physoc.org/content/507/3/707.abstract

128. Brainard AM, Miller AJ, Martens JR, England SK. Maxi-K channels localize to caveolae in human myometrium: a role for an actin-channel-caveolin complex in the regulation of myometrial smooth muscle K+ current. *Am J Physiol Cell Physiol* [Internet]. 2005; 289:C49–57. Available from: http://ajpcell.physiology.org/cgi/content/abstract/289/1/C49

129. Berkefeld H, Sailer CA, Bildl W, Rohde V, Thumfart J-O, Eble S, Klugbauer N, Reisinger E, Bischofberger J, Oliver D, Knaus H-G, Schulte U, Fakler B. BKCa-Cav Channel Complexes Mediate Rapid and Localized Ca2+-Activated K+ Signaling. *Science (80-.).* [Internet]. 2006; 314:615–620. Available from: http://www.sciencemag.org/cgi/content/abstract/314/5799/615

130. Jaggar JH, Stevenson AS, Nelson MT. Voltage dependence of Ca2+ sparks in intact cerebral arteries. *Am J Physiol Cell Physiol* [Internet]. 1998; 274:C1755–1761. Available from: http://ajpcell.physiology.org/cgi/content/abstract/274/6/C1755

131. Jaggar, Wellman, Heppner, Porter, Perez, Gollasch, Kleppisch, Rubart, Stevenson, Lederer, Knot, Bonev, Nelson. Ca2+ channels, ryanodine receptors and Ca2+-activated K+ channels: a functional unit for regulating arterial tone. *Acta Physiol. Scand.* [Internet]. 1998; 164:577–587. Available from: http://dx.doi.org/10.1046/j.1365-201X.1998.00462.x

132. Wray S, Burdyga T. Sarcoplasmic Reticulum Function in Smooth Muscle. *Physiol. Rev.* [Internet]. 2010; 90:113–178. Available from: http://physrev.physiology.org/cgi/content/abstract/90/1/113

133. Santana LF, Navedo MF. Molecular and biophysical mechanisms of Ca2+ sparklets in smooth muscle. *J. Mol. Cell. Cardiol.* [Internet]. 2009 [cited 2013 Sep 26]; 47:436–44. Available from: http://www.pubmedcentral.nih.gov/articlerender.fcgi?artid=2739251&tool=pmcentrez&rendertype=abstract

134. Xiao Q. Genetically Manipulated Models of Atherosclerosis in Mice. *Atherosclerosis* [Internet]. 2001;:15–26. Available from: http://dx.doi.org/10.1385/1-59259-073-X:15

135. Ishibashi S, Perrey S, Chen Z, Osuga J, Shimada M, Ohashi K, Harada K, Yazaki Y, Yamada N. Role of the Low Density Lipoprotein (LDL) Receptor Pathway in the Metabolism of Chylomicron Remnants. *J. Biol. Chem.* [Internet]. 1996; 271:22422–22427. Available from: http://www.jbc.org/content/271/37/22422.abstract

136. Ishibashi S, Brown MS, Goldstein JL, Gerard RD, Hammer RE, Herz J. Hypercholesterolemia in low density lipoprotein receptor knockout mice and its reversal by adenovirus-mediated gene delivery. *J. Clin. Invest.* [Internet]. 1993; 92:883–893. Available from: http://www.jci.org/articles/view/116663

137. Piedrahita JA, Zhang SH, Hagaman JR, Oliver PM, Maeda N. Generation of mice carrying a mutant apolipoprotein E gene inactivated by gene targeting in embryonic stem cells. *Proc. Natl. Acad. Sci. U. S. A.* [Internet]. 1992; 89:4471–4475. Available from: http://www.pnas.org/content/89/10/4471.abstract

138. Plump AS, Smith JD, Hayek T, Aalto-Setälä K, Walsh A, Verstuyft JG, Rubin EM, Breslow JL. Severe hypercholesterolemia and atherosclerosis in apolipoprotein E-deficient mice created by homologous recombination in ES cells. *Cell* [Internet]. 1992; 71:343–353. Available from: http://www.sciencedirect.com/science/article/B6WSN-4C6BN7K-5F/2/650e980e8791d3d2fed44520554a242a

139. Braun A, Trigatti BL, Post MJ, Sato K, Simons M, Edelberg JM, Rosenberg RD, Schrenzel M, Krieger M. Loss of SR-BI expression leads to the early onset of occlusive atherosclerotic coronary artery disease, spontaneous myocardial infarctions, severe cardiac dysfunction, and premature death in apolipoprotein E-deficient mice. *Circ. Res.* [Internet]. 2002 [cited 2013 Aug 19]; 90:270–6. Available from: http://www.ncbi.nlm.nih.gov/pubmed/11861414

140. Zhang SH, Reddick RL, Piedrahita JA, Maeda N. Spontaneous hypercholesterolemia and arterial lesions in mice lacking apolipoprotein E. *Science (80-.).* [Internet]. 1992; 258:468–471. Available from: http://www.sciencemag.org/cgi/content/abstract/258/5081/468

141. Nakashima Y, Plump AS, Raines EW, Breslow JL, Ross R. ApoE-deficient mice develop lesions of all phases of atherosclerosis throughout the arterial tree. *Arter. Thromb.* 1994; 14:133–140.

142. Ohashi R, Mu H, Yao Q, Chen C. Cellular and Molecular Mechanisms of Atherosclerosis with Mouse Models. *Trends Cardiovasc. Med.* [Internet]. 2004; 14:187–190. Available from: http://www.sciencedirect.com/science/article/B6T1D-4CW42GD-4/2/9d7a4a9ac14cad0e4095119a3569ec04

143. Tangirala R, Rubin E, Palinski W. Quantitation of atherosclerosis in murine models: correlation between lesions in the aortic origin and in the entire aorta, and differences in the extent of lesions between sexes in LDL receptor-deficient and apolipoprotein E-deficient mice. *J. Lipid Res.* [Internet]. 1995 [cited 2013 Aug 1]; 36:2320–2328. Available from: http://www.jlr.org/content/36/11/2320.short

144. Zadelaar S, Kleemann R, Verschuren L, de Vries-Van der Weij J, van der Hoorn J, Princen HM, Kooistra T. Mouse Models for Atherosclerosis and Pharmaceutical

Modifiers. *Arter. Thromb Vasc Biol* [Internet]. 2007; 27:1706–1721. Available from: http://atvb.ahajournals.org/cgi/content/abstract/27/8/1706

145. Schreyer SA, Vick C, Lystig TC, Mystkowski P, LeBoeuf RC. LDL receptor but not apolipoprotein E deficiency increases diet-induced obesity and diabetes in mice. *Am J Physiol Endocrinol Metab* [Internet]. 2002 [cited 2013 Aug 28]; 282:E207–214. Available from: http://ajpendo.physiology.org/content/282/1/E207

146. Schreyer SA, Lystig TC, Vick CM, LeBoeuf RC. Mice deficient in apolipoprotein E but not LDL receptors are resistant to accelerated atherosclerosis associated with obesity. *Atherosclerosis* [Internet]. 2003 [cited 2013 Aug 12]; 171:49–55. Available from: http://dx.doi.org/10.1016/j.atherosclerosis.2003.07.010

147. Fruchart J, Ailhaud G. Apolipoprotein A-containing lipoprotein particles: physiological role, quantification, and clinical significance. *Clin. Chem.* [Internet]. 1992 [cited 2013 Nov 20]; 38:793–797. Available from: http://www.clinchem.org/content/38/6/793.short

148. Yokoyama S. Apolipoprotein-mediated cellular cholesterol efflux. *Biochim. Biophys. Acta* [Internet]. 1998 [cited 2013 Nov 20]; 1392:1–15. Available from: http://www.ncbi.nlm.nih.gov/pubmed/9593801

149. Jonas A. Lecithin cholesterol acyltransferase. *Biochim. Biophys. Acta - Mol. Cell Biol. Lipids* [Internet]. 2000 [cited 2013 Nov 20]; 1529:245–256. Available from: http://www.sciencedirect.com/science/article/pii/S1388198100001530

150. Barbaras R, Puchois P, Fruchart J-C, Ailhaud G. Cholesterol efflux from cultured adipose cells is mediated by LpAI particles but not by LpAI:AII particles. *Biochem. Biophys. Res. Commun.* [Internet]. 1987 [cited 2013 Nov 20]; 142:63–69. Available from: http://www.sciencedirect.com/science/article/pii/0006291X87904517

151. Benn M. Apolipoprotein B levels, APOB alleles, and risk of ischemic cardiovascular disease in the general population, a review. *Atherosclerosis* [Internet]. 2009 [cited 2013 Nov 20]; 206:17–30. Available from: http://www.sciencedirect.com/science/article/pii/S0021915009000136

152. Aguie GA, Rader DJ, Clavey V, Traber MG, Torpier G, Kayden HJ, Fruchart JC, Brewer HB, Castro G. Lipoproteins containing apolipoprotein B isolated from patients with abetalipoproteinemia and homozygous hypobetalipoproteinemia: identification and characterization. *Atherosclerosis* [Internet]. 1995 [cited 2013 Nov 20]; 118:183–191. Available from: http://www.sciencedirect.com/science/article/pii/002191509505605X

153. LaRosa JC, Levy RI, Herbert P, Lux SE, Fredrickson DS. A specific apoprotein activator for lipoprotein lipase. *Biochem. Biophys. Res. Commun.* [Internet]. 1970 [cited 2013 Nov 20]; 41:57–62. Available from: http://www.sciencedirect.com/science/article/pii/0006291X70904687

154. Wang CS, McConathy WJ, Kloer HU, Alaupovic P. Modulation of lipoprotein lipase activity by apolipoproteins. Effect of apolipoprotein C-III. *J. Clin. Invest.* [Internet].

1985 [cited 2013 Nov 20]; 75:384–90. Available from: http://www.pubmedcentral.nih.gov/articlerender.fcgi?artid=423500&tool=pmcentrez&rendertype=abstract

155. Quarfordt SH, Michalopoulos G, Schirmer B. The effect of human C apolipoproteins on the in vitro hepatic metabolism of triglyceride emulsions in the rat. *J. Biol. Chem.* [Internet]. 1982 [cited 2013 Nov 20]; 257:14642–7. Available from: http://www.ncbi.nlm.nih.gov/pubmed/7174660

156. Bolanos-Garcia VM, Miguel RN. On the structure and function of apolipoproteins: more than a family of lipid-binding proteins. *Prog. Biophys. Mol. Biol.* [Internet]. 2003 [cited 2013 Nov 20]; 83:47–68. Available from: http://www.sciencedirect.com/science/article/pii/S0079610703000282

157. Hatters DM, Peters-Libeu CA, Weisgraber KH. Apolipoprotein E structure: insights into function. *Trends Biochem. Sci.* [Internet]. 2006 [cited 2013 Nov 20]; 31:445–454. Available from: http://www.sciencedirect.com/science/article/pii/S0968000406001708

158. Miyata M, Smith JD. Apolipoprotein E allele-specific antioxidant activity and effects on cytotoxicity by oxidative insults and beta-amyloid peptides. *Nat. Genet.* [Internet]. 1996 [cited 2013 Nov 20]; 14:55–61. Available from: http://dx.doi.org/10.1038/ng0996-55

159. Zhou X, Paulsson G, Stemme S, Hansson GK. Hypercholesterolemia is associated with a T helper (Th) 1/Th2 switch of the autoimmune response in atherosclerotic apo E-knockout mice. *J. Clin. Invest.* [Internet]. 1998 [cited 2013 Sep 12]; 101:1717–25. Available from: http://www.pubmedcentral.nih.gov/articlerender.fcgi?artid=508754&tool=pmcentrez&rendertype=abstract

160. Ishigami M. Apolipoprotein E Inhibits Platelet-derived Growth Factor-induced Vascular Smooth Muscle Cell Migration and Proliferation by Suppressing Signal Transduction and Preventing Cell Entry to G1 Phase. *J. Biol. Chem.* [Internet]. 1998 [cited 2013 Nov 20]; 273:20156–20161. Available from: http://www.jbc.org/content/273/32/20156.short

161. Taylor F, Huffman MD, Macedo AF, Moore THM, Burke M, Davey Smith G, Ward K, Ebrahim S. Statins for the primary prevention of cardiovascular disease. *Cochrane database Syst. Rev.* [Internet]. 2013 [cited 2013 Aug 12]; 1:CD004816. Available from: http://www.ncbi.nlm.nih.gov/pubmed/23440795

162. Goldstein JL, Brown MS. The LDL receptor. *Arterioscler. Thromb. Vasc. Biol.* [Internet]. 2009 [cited 2013 Nov 19]; 29:431–8. Available from: http://atvb.ahajournals.org/content/29/4/431.short

163. Trigatti BL, Krieger M, Rigotti A. Influence of the HDL receptor SR-BI on lipoprotein metabolism and atherosclerosis. *Arterioscler. Thromb. Vasc. Biol.* [Internet]. 2003 [cited 2013 Nov 19]; 23:1732–8. Available from: http://atvb.ahajournals.org/content/23/10/1732.short

164. Drobnik W, Lindenthal B, Lieser B, Ritter M, Weber TC, Liebisch G, Giesa U, Igel M, Borsukova H, Büchler C, Fung–Leung WP, Bergmann K Von, Schmitz G. ATP-binding cassette transporter A1 (ABCA1) affects total body sterol metabolism. *Gastroenterology* [Internet]. 2001 [cited 2013 Nov 19]; 120:1203–1211. Available from: http://www.sciencedirect.com/science/article/pii/S0016508501139405

165. Dikkers A, Tietge U-J. Biliary cholesterol secretion: more than a simple ABC. *World J. Gastroenterol.* [Internet]. 2010 [cited 2013 Nov 19]; 16:5936–45. Available from: http://www.pubmedcentral.nih.gov/articlerender.fcgi?artid=3007110&tool=pmcentrez&rendertype=abstract

166. Tulenko TN, Chen M, Mason PE, Mason RP. Physical effects of cholesterol on arterial smooth muscle membranes: evidence of immiscible cholesterol domains and alterations in bilayer width during atherogenesis. *J. Lipid Res.* [Internet]. 1998; 39:947–956. Available from: http://www.jlr.org/cgi/content/abstract/39/5/947

167. Chen M, Preston Mason R, Tulenko TN. Atherosclerosis alters the composition, structure and function of arterial smooth muscle cell plasma membranes. *Biochim. Biophys. Acta - Mol. Basis Dis.* [Internet]. 1995 [cited 2013 Aug 14]; 1272:101–112. Available from: http://dx.doi.org/10.1016/0925-4439(95)00073-D

168. Hong WC, Amara SG. Membrane cholesterol modulates the outward facing conformation of the dopamine transporter and alters cocaine binding. *J. Biol. Chem.* [Internet]. 2010 [cited 2013 Jun 3]; 285:32616–26. Available from: http://www.jbc.org/content/285/42/32616.short

169. Tulenko TN, Bialecki R, Gleason M, D'Angelo G. Ion channels, membrane lipids and cholesterol: a role for membrane lipid domains in arterial function. *Prog. Clin. Biol. Res.* [Internet]. 1990 [cited 2013 Aug 16]; 334:187–203. Available from: http://www.ncbi.nlm.nih.gov/pubmed/1689856

170. Grayson TH, Chadha PS, Bertrand PP, Chen H, Morris MJ, Senadheera S, Murphy T V, Sandow SL. Increased caveolae density and caveolin-1 expression accompany impaired NO-mediated vasorelaxation in diet-induced obesity. *Histochem. Cell Biol.* [Internet]. 2013 [cited 2013 Sep 20]; 139:309–21. Available from: http://www.ncbi.nlm.nih.gov/pubmed/23007290

171. Azadzoi KM, Saenz de Tejada I. Hypercholesterolemia impairs endothelium-dependent relaxation of rabbit corpus cavernosum smooth muscle. *J. Urol.* [Internet]. 1991 [cited 2013 Aug 19]; 146:238–40. Available from: http://europepmc.org/abstract/MED/2056597

172. Verbeuren TJ, Jordaens FH, Zonnekeyn LL, Van Hove CE, Coene MC, Herman AG. Effect of hypercholesterolemia on vascular reactivity in the rabbit. I. Endothelium-dependent and endothelium-independent contractions and relaxations in isolated arteries of control and hypercholesterolemic rabbits. *Circ. Res.* [Internet]. 1986 [cited 2013 Aug 19]; 58:552–564. Available from: http://circres.ahajournals.org/content/58/4/552.short

173. Weisbrod RM, Griswold MC, Du Y, Bolotina VM, Cohen RA. Reduced Responsiveness of Hypercholesterolemic Rabbit Aortic Smooth Muscle Cells to Nitric Oxide. *Arterioscler. Thromb. Vasc. Biol.* [Internet]. 1997 [cited 2013 Aug 14]; 17:394–402. Available from: http://atvb.ahajournals.org/content/17/2/394.abstract

174. Crauwels H. Plaque-associated endothelial dysfunction in apolipoprotein E-deficient mice on a regular diet. Effect of human apolipoprotein AI. *Cardiovasc. Res.* [Internet]. 2003 [cited 2013 Sep 4]; 59:189–199. Available from: http://cardiovascres.oxfordjournals.org/content/59/1/189.short

175. d'Uscio L V., Baker TA, Mantilla CB, Smith L, Weiler D, Sieck GC, Katusic ZS. Mechanism of Endothelial Dysfunction in Apolipoprotein E-Deficient Mice. *Arterioscler. Thromb. Vasc. Biol.* [Internet]. 2001 [cited 2013 Jul 22]; 21:1017–1022. Available from: http://atvb.ahajournals.org/content/21/6/1017.short

176. Yaghoubi M, Oliver-Krasinski J, Cayatte AJ, Cohen RA. Decreased Sensitivity to Nitric Oxide in the Aorta of Severely Hypercholesterolemic Apolipoprotein E-Deficient Mice. *J. Cardiovasc. Pharmacol.* [Internet]. 2000; 36:751–757. Available from: http://journals.lww.com/cardiovascularpharm/Fulltext/2000/12000/Decreased_Sensitivity_to_Nitric_Oxide_in_the_Aorta.10.aspx

177. Van Langen J, Fransen P, Van Hove CE, Schrijvers DM, Martinet W, De Meyer GRY, Bult H. Selective loss of basal but not receptor-stimulated relaxation by endothelial nitric oxide synthase after isolation of the mouse aorta. *Eur. J. Pharmacol.* [Internet]. 2012 [cited 2013 Aug 19]; 696:111–9. Available from: http://dx.doi.org/10.1016/j.ejphar.2012.09.016

178. Fransen P, Van Assche T, Guns P-J, Van Hove CE, De Keulenaer GW, Herman AG, Bult H. Endothelial function in aorta segments of apolipoprotein E-deficient mice before development of atherosclerotic lesions. *Pflugers Arch.* [Internet]. 2008 [cited 2013 Aug 20]; 455:811–8. Available from: http://www.ncbi.nlm.nih.gov/pubmed/17899169

179. Broderick R, Bialecki R, Tulenko TN. Cholesterol-induced changes in rabbit arterial smooth muscle sensitivity to adrenergic stimulation. *Am J Physiol Hear. Circ Physiol* [Internet]. 1989 [cited 2013 Aug 14]; 257:H170–178. Available from: http://ajpheart.physiology.org/content/257/1/H170

180. d'Uscio L V., Smith LA, Katusic ZS. Hypercholesterolemia Impairs Endothelium-Dependent Relaxations in Common Carotid Arteries of Apolipoprotein E-Deficient Mice. *Stroke* [Internet]. 2001 [cited 2013 Aug 13]; 32:2658–2664. Available from: http://stroke.ahajournals.org/content/32/11/2658.short

181. Heistad DD, Armstrong ML, Marcus ML, Piegors DJ, Mark AL. Augmented responses to vasoconstrictor stimuli in hypercholesterolemic and atherosclerotic monkeys. *Circ. Res.* [Internet]. 1984 [cited 2013 Aug 14]; 54:711–718. Available from: http://circres.ahajournals.org/content/54/6/711.short

182. Ibengwe JK, Suzuki H. Changes in mechanical responses of vascular smooth muscles to acetylcholine, noradrenaline and high-potassium solution in hypercholesterolemic rabbits. *Br. J. Pharmacol.* [Internet]. 1986; 87:395–402. Available from: http://ukpmc.ac.uk/abstract/MED/3955307

183. Bialecki RA, Tulenko TN, Colucci WS. Cholesterol enrichment increases basal and agonist-stimulated calcium influx in rat vascular smooth muscle cells. *J. Clin. Invest.* [Internet]. 1991 [cited 2013 Aug 13]; 88:1894–900. Available from: http://www.pubmedcentral.nih.gov/articlerender.fcgi?artid=295758&tool=pmcentrez&rendertype=abstract

184. Bialecki RA, Tulenko TN. Excess membrane cholesterol alters calcium channels in arterial smooth muscle. *Am J Physiol Cell Physiol* [Internet]. 1989 [cited 2013 Aug 13]; 257:C306–314. Available from: http://ajpcell.physiology.org/content/257/2/C306

185. Gleason MM, Medow MS, Tulenko TN. Excess membrane cholesterol alters calcium movements, cytosolic calcium levels, and membrane fluidity in arterial smooth muscle cells. *Circ. Res.* [Internet]. 1991 [cited 2013 Aug 8]; 69:216–227. Available from: http://circres.ahajournals.org/content/69/1/216.short

186. Van Assche T, Fransen P, Guns PJ, Herman AG, Bult H. Altered Ca2+ handling of smooth muscle cells in aorta of apolipoprotein E-deficient mice before development of atherosclerotic lesions. *Cell Calcium* [Internet]. 2007; 41:295–302. Available from: http://www.sciencedirect.com/science/article/B6WCC-4M04F1C-1/2/36e88e1761e412ab9d4e4886e58b469a

187. Bergdahl A, Gomez MF, Dreja K, Xu S-Z, Adner M, Beech DJ, Broman J, Hellstrand P, Sward K. Cholesterol Depletion Impairs Vascular Reactivity to Endothelin-1 by Reducing Store-Operated Ca2+ Entry Dependent on TRPC1. *Circ Res* [Internet]. 2003; 93:839–847. Available from: http://circres.ahajournals.org/cgi/content/abstract/93/9/839

188. Feron O, Dessy C, Moniotte S, Desager JP, Balligand JL. Hypercholesterolemia decreases nitric oxide production by promoting the interaction of caveolin and endothelial nitric oxide synthase. *J Clin Invest*. 1999; 103:897–905.

189. Belhassen L. Endothelial Nitric Oxide Synthase Targeting to Caveolae. SPECIFIC INTERACTIONS WITH CAVEOLIN ISOFORMS IN CARDIAC MYOCYTES AND ENDOTHELIAL CELLS. *J. Biol. Chem.* [Internet]. 1996 [cited 2013 Aug 19]; 271:22810–22814. Available from: http://www.jbc.org/content/271/37/22810.short

190. Golovina VA. Cell proliferation is associated with enhanced capacitative Ca2+ entry in human arterial myocytes. *Am J Physiol Cell Physiol* [Internet]. 1999; 277:C343–349. Available from: http://ajpcell.physiology.org/cgi/content/abstract/277/2/C343

191. Agianniotis A, Stergiopulos N. Wall properties of the apolipoprotein E-deficient mouse aorta. *Atherosclerosis* [Internet]. 2012 [cited 2013 Jul 16]; 223:314–20. Available from: http://dx.doi.org/10.1016/j.atherosclerosis.2012.06.014

192. Berridge MJ. Calcium signalling remodelling and disease. *Biochem. Soc. Trans.* [Internet]. 2012 [cited 2013 Sep 26]; 40:297–309. Available from: http://www.ncbi.nlm.nih.gov/pubmed/22435804

193. House S, Potier M, Bisaillon J, Singer H, Trebak M. The non-excitable smooth muscle: Calcium signaling and phenotypic switching during vascular disease. *Pflügers Arch. Eur. J. Physiol.* [Internet]. 2008; 456:769–785. Available from: http://dx.doi.org/10.1007/s00424-008-0491-8

194. Gollasch M, Haase H, Ried C, Lindschau C, Morano I, Luft FC, Haller H. L-type calcium channel expression depends on the differentiated state of vascular smooth muscle cells. *FASEB J.* [Internet]. 1998; 12:593–601. Available from: http://www.fasebj.org/cgi/content/abstract/12/7/593

195. Wamhoff BR, Bowles DK, McDonald OG, Sinha S, Somlyo AP, Somlyo A V, Owens GK. L-type Voltage-Gated Ca2+ Channels Modulate Expression of Smooth Muscle Differentiation Marker Genes via a Rho Kinase/Myocardin/SRF-Dependent Mechanism. *Circ Res* [Internet]. 2004; 95:406–414. Available from: http://circres.ahajournals.org/cgi/content/abstract/95/4/406

196. Rodman DM, Reese K, Harral J, Fouty B, Wu S, West J, Hoedt-Miller M, Tada Y, Li K-X, Cool C, Fagan K, Cribbs L. Low-Voltage-Activated (T-Type) Calcium Channels Control Proliferation of Human Pulmonary Artery Myocytes. *Circ Res* [Internet]. 2005; 96:864–872. Available from: http://circres.ahajournals.org/cgi/content/abstract/96/8/864

197. Bryant HJ, Harder DR, Pamnani MB, Haddy FJ. In vivo membrane potentials of smooth muscle cells in the caudal artery of the rat. *Am J Physiol Cell Physiol* [Internet]. 1985; 249:C78–83. Available from: http://ajpcell.physiology.org/cgi/content/abstract/249/1/C78

198. Gollasch M, Nelson MT. Voltage-Dependent Ca2+ Channels in Arterial Smooth Muscle Cells. *Kidney Blood Press. Res.* [Internet]. 1997; 20:355–371. Available from: http://www.karger.com/DOI/10.1159/000174250

199. Kuga T, Shimokawa H, Hirakawa Y, Kadokami Y, Arai Y, Fukumoto Y, Kuwata K, Kozai T, Egashira K, Takeshita A. Increased Expression of L-Type Calcium Channels in Vascular Smooth Muscle Cells at Spastic Site in a Porcine Model of Coronary Artery Spasm. *J. Cardiovasc. Pharmacol.* [Internet]. 2000; 35:822–828. Available from: http://journals.lww.com/cardiovascularpharm/Fulltext/2000/05000/Increased_Expression_of_L_Type_Calcium_Channels_in.21.aspx

200. Vallot O, Combettes L, Jourdon P, Inamo J, Marty I, Claret M, Lompre A-M. Intracellular Ca2+ Handling in Vascular Smooth Muscle Cells Is Affected by Proliferation. *Arter. Thromb Vasc Biol* [Internet]. 2000; 20:1225–1235. Available from: http://atvb.ahajournals.org/cgi/content/abstract/20/5/1225

201. Quignard J-F, Harricane M-C, Menard C, Lory P, Nargeot J, Capron L, Mornet D, Richard S. Transient down-regulation of L-type Ca2+ channel and dystrophin

expression after balloon injury in rat aortic cells. *Cardiovasc. Res.* [Internet]. 2001; 49:177–188. Available from: http://cardiovascres.oxfordjournals.org/content/49/1/177.abstract

202. Ihara E, Hirano K, Hirano M, Nishimura J, Nawata H, Kanaide H. Mechanism of down-regulation of L-type Ca2+ channel in the proliferating smooth muscle cells of rat aorta. *J. Cell. Biochem.* [Internet]. 2002; 87:242–251. Available from: http://dx.doi.org/10.1002/jcb.10295

203. Golovina VA, Platoshyn O, Bailey CL, Wang J, Limsuwan A, Sweeney M, Rubin LJ, Yuan JXJ. Upregulated TRP and enhanced capacitative Ca2+ entry in human pulmonary artery myocytes during proliferation. *Am J Physiol Hear. Circ Physiol* [Internet]. 2001; 280:H746–755. Available from: http://ajpheart.physiology.org/cgi/content/abstract/280/2/H746

204. Bergdahl A, Gomez MF, Wihlborg A-K, Erlinge D, Eyjolfson A, Xu S-Z, Beech DJ, Dreja K, Hellstrand P. Plasticity of TRPC expression in arterial smooth muscle: correlation with store-operated Ca2+ entry. *Am J Physiol Cell Physiol* [Internet]. 2005; 288:C872–880. Available from: http://ajpcell.physiology.org/cgi/content/abstract/288/4/C872

205. Kumar B, Dreja K, Shah SS, Cheong A, Xu SZ, Sukumar P, Naylor J, Forte A, Cipollaro M, McHugh D, Kingston PA, Heagerty AM, Munsch CM, Bergdahl A, Hultgardh-Nilsson A, Gomez MF, Porter KE, Hellstrand P, Beech DJ. Upregulated TRPC1 Channel in Vascular Injury In Vivo and Its Role in Human Neointimal Hyperplasia. *Circ Res* [Internet]. 2006; 98:557–563. Available from: http://circres.ahajournals.org/cgi/content/abstract/98/4/557

206. Rossi D, Sorrentino V. Molecular genetics of ryanodine receptors Ca2+-release channels. *Cell Calcium* [Internet]. 2002; 32:307–319. Available from: http://www.sciencedirect.com/science/article/B6WCC-47DM7NH-7/2/f0c32904ea844e80de8c439b0749c88f

207. Jaggar JH, Porter VA, Lederer WJ, Nelson MT. Calcium sparks in smooth muscle. *Am J Physiol Cell Physiol* [Internet]. 2000; 278:C235–256. Available from: http://ajpcell.physiology.org/cgi/content/abstract/278/2/C235

208. Miyatake R, Furukawa A, Matsushita M, Iwahashi K, Nakamura K, Ichikawa Y, Suwaki H. Tissue-specific alternative splicing of mouse brain type ryanodine receptor/calcium release channel mRNA. *FEBS Lett.* [Internet]. 1996; 395:123–126. Available from: http://www.sciencedirect.com/science/article/B6T36-497C8B7-2V/2/fa1ff088f384738eb681bb894a742c0d

209. Wilkerson MK, Heppner TJ, Bonev AD, Nelson MT. Inositol trisphosphate receptor calcium release is required for cerebral artery smooth muscle cell proliferation. *Am J Physiol Hear. Circ Physiol* [Internet]. 2006; 290:H240–247. Available from: http://ajpheart.physiology.org/cgi/content/abstract/290/1/H240

210. House SJ, Singer HA. CaMKII-{delta} Isoform Regulation of Neointima Formation After Vascular Injury. *Arter. Thromb Vasc Biol* [Internet]. 2008; 28:441–447. Available from: http://atvb.ahajournals.org/cgi/content/abstract/28/3/441

211. Wang Y, Chen J, Wang Y, Taylor CW, Hirata Y, Hagiwara H, Mikoshiba K, Toyo-oka T, Omata M, Sakaki Y. Crucial Role of Type 1, but Not Type 3, Inositol 1,4,5-Trisphosphate (IP3) Receptors in IP3-Induced Ca2+ Release, Capacitative Ca2+ Entry, and Proliferation of A7r5 Vascular Smooth Muscle Cells. *Circ Res* [Internet]. 2001; 88:202–209. Available from: http://circres.ahajournals.org/cgi/content/abstract/88/2/202

212. Afroze T, Hussain M. Cell Cycle Dependent Regulation of Intracellular Calcium Concentration in Vascular Smooth Muscle Cells: A Potential Target for Drug Therapy. *Curr. Drug Targets - Cardiovasc. Hematol. Disord.* [Internet]. 2001; 1:23–40. Available from: http://www.ingentaconnect.com/content/ben/cdtchd/2001/00000001/00000001/art00003

213. Lipskaia L, del Monte F, Capiod T, Yacoubi S, Hadri L, Hours M, Hajjar RJ, Lompre A-M. Sarco/Endoplasmic Reticulum Ca2+-ATPase Gene Transfer Reduces Vascular Smooth Muscle Cell Proliferation and Neointima Formation in the Rat. *Circ Res* [Internet]. 2005; 97:488–495. Available from: http://circres.ahajournals.org/cgi/content/abstract/97/5/488

214. Abramowitz J, Aydemir-Koksoy A, Helgason T, Jemelka S, Odebunmi T, Seidel CL, Allen JC. Expression of Plasma Membrane Calcium ATPases in Phenotypically Distinct Canine Vascular Smooth Muscle Cells. *J. Mol. Cell. Cardiol.* [Internet]. 2000; 32:777–789. Available from: http://www.sciencedirect.com/science/article/B6WK6-45F4V9M-3J/2/9d3b8b30c29e7d18aba584e1bb3e7cfe

215. Neylon CB, Lang RJ, Fu Y, Bobik A, Reinhart PH. Molecular Cloning and Characterization of the Intermediate-Conductance Ca2+-Activated K+ Channel in Vascular Smooth Muscle : Relationship Between KCa Channel Diversity and Smooth Muscle Cell Function. *Circ Res* [Internet]. 1999; 85:e33–43. Available from: http://circres.ahajournals.org/cgi/content/abstract/85/9/e33

216. Neylon CB. Potassium channels and vascular proliferation. *Vascul. Pharmacol.* [Internet]. 2002; 38:35–41. Available from: http://www.sciencedirect.com/science/article/B6X3P-47C9JMK-5/2/3c0c3d76aad26069c89657c4f63eb742

217. Kohler R, Wulff H, Eichler I, Kneifel M, Neumann D, Knorr A, Grgic I, Kampfe D, Si H, Wibawa J, Real R, Borner K, Brakemeier S, Orzechowski H-D, Reusch H-P, Paul M, Chandy KG, Hoyer J. Blockade of the Intermediate-Conductance Calcium-Activated Potassium Channel as a New Therapeutic Strategy for Restenosis. *Circulation* [Internet]. 2003; 108:1119–1125. Available from: http://circ.ahajournals.org/cgi/content/abstract/108/9/1119

218. Schworer CM, Rothblum LI, Thekkumkara TJ, Singer HA. Identification of novel isoforms of the delta subunit of Ca2+/calmodulin-dependent protein kinase II.

Differential expression in rat brain and aorta. *J. Biol. Chem.* [Internet]. 1993; 268:14443–14449. Available from: http://www.jbc.org/content/268/19/14443.abstract

219. Pfleiderer PJ, Lu KK, Crow MT, Keller RS, Singer HA. Modulation of vascular smooth muscle cell migration by calcium/ calmodulin-dependent protein kinase II-{delta}2. *Am J Physiol Cell Physiol* [Internet]. 2004; 286:C1238–1245. Available from: http://ajpcell.physiology.org/cgi/content/abstract/286/6/C1238

220. Ginnan R, Singer HA. PKC-{delta}-dependent pathways contribute to PDGF-stimulated ERK1/2 activation in vascular smooth muscle. *Am J Physiol Cell Physiol* [Internet]. 2005; 288:C1193–1201. Available from: http://ajpcell.physiology.org/cgi/content/abstract/288/6/C1193

221. House SJ, Ginnan RG, Armstrong SE, Singer HA. Calcium/calmodulin-dependent protein kinase II-{delta} isoform regulation of vascular smooth muscle cell proliferation. *Am J Physiol Cell Physiol* [Internet]. 2007; 292:C2276–2287. Available from: http://ajpcell.physiology.org/cgi/content/abstract/292/6/C2276

222. McGill HC. Obesity Accelerates the Progression of Coronary Atherosclerosis in Young Men. *Circulation* [Internet]. 2002 [cited 2013 Sep 16]; 105:2712–2718. Available from: http://circ.ahajournals.org/content/105/23/2712.short

223. Smith SR, Lovejoy JC, Greenway F, Ryan D, deJonge L, de la Bretonne J, Volafova J, Bray GA. Contributions of total body fat, abdominal subcutaneous adipose tissue compartments, and visceral adipose tissue to the metabolic complications of obesity [Internet]. Metabolism. 2001 [cited 2013 Sep 22]; 50:425–435. Available from: http://www.sciencedirect.com/science/article/pii/S0026049501719865

224. Libby P. Inflammation and Atherosclerosis. *Circulation* [Internet]. 2002 [cited 2013 Nov 8]; 105:1135–1143. Available from: http://circ.ahajournals.org/content/105/9/1135.short

225. Ridker PM, Rifai N, Stampfer MJ, Hennekens CH. Plasma Concentration of Interleukin-6 and the Risk of Future Myocardial Infarction Among Apparently Healthy Men. *Circulation* [Internet]. 2000 [cited 2013 Nov 10]; 101:1767–1772. Available from: http://circ.ahajournals.org/content/101/15/1767.abstract

226. Ridker PM, Rifai N, Pfeffer M, Sacks F, Lepage S, Braunwald E. Elevation of Tumor Necrosis Factor- and Increased Risk of Recurrent Coronary Events After Myocardial Infarction. *Circulation* [Internet]. 2000 [cited 2013 Nov 20]; 101:2149–2153. Available from: http://circ.ahajournals.org/content/101/18/2149.short

227. Ridker PM, Cushman M, Stampfer MJ, Tracy RP, Hennekens CH. Inflammation, aspirin, and the risk of cardiovascular disease in apparently healthy men. *N. Engl. J. Med.* [Internet]. 1997 [cited 2013 Nov 7]; 336:973–9. Available from: http://www.ncbi.nlm.nih.gov/pubmed/9077376

228. Ridker PM, Hennekens CH, Buring JE, Rifai N. C-reactive protein and other markers of inflammation in the prediction of cardiovascular disease in women. *N. Engl. J. Med.*

[Internet]. 2000 [cited 2013 Nov 7]; 342:836–43. Available from: http://www.ncbi.nlm.nih.gov/pubmed/10733371

229. Chang L, Milton H, Eitzman DT, Chen YE. Paradoxical Roles of Perivascular Adipose Tissue in Atherosclerosis and Hypertension. *Circ. J.* [Internet]. 2013 [cited 2013 Aug 15]; 77:11–18. Available from: http://europepmc.org/abstract/MED/23207957

230. Szasz T, Webb RC. Perivascular adipose tissue: more than just structural support. *Clin. Sci. (Lond).* [Internet]. 2012 [cited 2013 Sep 26]; 122:1–12. Available from: http://www.ncbi.nlm.nih.gov/pubmed/21910690

231. Tiraby C, Langin D. Conversion from white to brown adipocytes: a strategy for the control of fat mass? *Trends Endocrinol. Metab.* [Internet]. 2003 [cited 2013 Sep 26]; 14:439–441. Available from: http://www.cell.com/trends/endocrinology-metabolism/fulltext/S1043-2760(03)00216-9

232. Verhagen SN, Visseren FLJ. Perivascular adipose tissue as a cause of atherosclerosis. *Atherosclerosis* [Internet]. 2011 [cited 2013 Sep 20]; 214:3–10. Available from: http://www.ncbi.nlm.nih.gov/pubmed/20646709

233. Lehman SJ, Massaro JM, Schlett CL, O'Donnell CJ, Hoffmann U, Fox CS. Peri-aortic fat, cardiovascular disease risk factors, and aortic calcification: the Framingham Heart Study. *Atherosclerosis* [Internet]. 2010 [cited 2013 Sep 26]; 210:656–61. Available from: http://www.pubmedcentral.nih.gov/articlerender.fcgi?artid=2878932&tool=pmcentrez&rendertype=abstract

234. Fitzgibbons TP, Kogan S, Aouadi M, Hendricks GM, Straubhaar J, Czech MP. Similarity of mouse perivascular and brown adipose tissues and their resistance to diet-induced inflammation. *Am. J. Physiol. Heart Circ. Physiol.* [Internet]. 2011 [cited 2013 Aug 28]; 301:H1425–37. Available from: http://ajpheart.physiology.org/content/301/4/H1425

235. Desreumaux*,‡ P, Ernst§ O, Geboes‖ K, Gambiez¶ L, Berrebi# D, Müller-Alouf‡ H, Hafraoui* S, Emilie** D, Ectors‖ N, Peuchmaur# M, Cortot* A, Capron‡ M, Auwerx‡‡ J, Colombel* J-F. Inflammatory alterations in mesenteric adipose tissue in Crohn's disease. *Gastroenterology* [Internet]. 1999 [cited 2013 Sep 26]; 117:73–81. Available from: http://www.sciencedirect.com/science/article/pii/S0016508599705524

236. Gao Y-J, Zeng Z, Teoh K, Sharma AM, Abouzahr L, Cybulsky I, Lamy A, Semelhago L, Lee RMKW. Perivascular adipose tissue modulates vascular function in the human internal thoracic artery. *J. Thorac. Cardiovasc. Surg.* [Internet]. 2005 [cited 2013 Aug 29]; 130:1130–6. Available from: http://dx.doi.org/10.1016/j.jtcvs.2005.05.028

237. Kassam SI, Lu C, Buckley N, Lee RMKW. The mechanisms of propofol-induced vascular relaxation and modulation by perivascular adipose tissue and endothelium. *Anesth. Analg.* [Internet]. 2011 [cited 2013 Sep 22]; 112:1339–45. Available from: http://www.anesthesia-analgesia.org/content/112/6/1339.short

238. Gao Y-J, Lee RMKW. Hydrogen peroxide is an endothelium-dependent contracting factor in rat renal artery. *Br. J. Pharmacol.* [Internet]. 2005 [cited 2013 Sep 22]; 146:1061–8. Available from: http://www.pubmedcentral.nih.gov/articlerender.fcgi?artid=1751245&tool=pmcentrez&rendertype=abstract

239. Gu P, Xu A. Interplay between adipose tissue and blood vessels in obesity and vascular dysfunction. *Rev. Endocr. Metab. Disord.* [Internet]. 2013 [cited 2013 Sep 22]; 14:49–58. Available from: http://www.ncbi.nlm.nih.gov/pubmed/23283583

240. Zhu W, Cheng KKY, Vanhoutte PM, Lam KSL, Xu A. Vascular effects of adiponectin: molecular mechanisms and potential therapeutic intervention. *Clin. Sci. (Lond).* [Internet]. 2008 [cited 2013 Sep 26]; 114:361–74. Available from: http://www.ncbi.nlm.nih.gov/pubmed/18230060

241. Chatterjee TK, Stoll LL, Denning GM, Harrelson A, Blomkalns AL, Idelman G, Rothenberg FG, Neltner B, Romig-Martin SA, Dickson EW, Rudich S, Weintraub NL. Proinflammatory phenotype of perivascular adipocytes: influence of high-fat feeding. *Circ. Res.* [Internet]. 2009 [cited 2013 Aug 29]; 104:541–9. Available from: http://circres.ahajournals.org/content/104/4/541.short

242. Greenstein AS, Khavandi K, Withers SB, Sonoyama K, Clancy O, Jeziorska M, Laing I, Yates AP, Pemberton PW, Malik RA, Heagerty AM. Local inflammation and hypoxia abolish the protective anticontractile properties of perivascular fat in obese patients. *Circulation* [Internet]. 2009 [cited 2013 Aug 29]; 119:1661–70. Available from: http://circ.ahajournals.org/content/119/12/1661.short

243. Ketonen J, Shi J, Martonen E, Mervaala E. Periadventitial Adipose Tissue Promotes Endothelial Dysfunction via Oxidative Stress in Diet-Induced Obese C57Bl/6 Mice. *Circ. J.* [Internet]. 2010 [cited 2013 Sep 23]; 74:1479–1487. Available from: http://europepmc.org/abstract/MED/20526041

244. Gao Y-J, Takemori K, Su L-Y, An W-S, Lu C, Sharma AM, Lee RMKW. Perivascular adipose tissue promotes vasoconstriction: the role of superoxide anion. *Cardiovasc. Res.* [Internet]. 2006 [cited 2013 Sep 26]; 71:363–73. Available from: http://cardiovascres.oxfordjournals.org/content/71/2/363.short

245. Ma L, Ma S, He H, Yang D, Chen X, Luo Z, Liu D, Zhu Z. Perivascular fat-mediated vascular dysfunction and remodeling through the AMPK/mTOR pathway in high-fat diet-induced obese rats. *Hypertens. Res.* [Internet]. 2010 [cited 2013 Sep 17]; 33:446–53. Available from: http://dx.doi.org/10.1038/hr.2010.11

246. Sandra NV, Frank LJV. Perivascular adipose tissue as a cause of atherosclerosis. *Atherosclerosis* [Internet]. 2010; 214:3–10. Available from: http://linkinghub.elsevier.com/retrieve/pii/S0021915010004120?showall=true

247. Belton OA, Duffy A, Toomey S, Fitzgerald DJ. Cyclooxygenase isoforms and platelet vessel wall interactions in the apolipoprotein E knockout mouse model of atherosclerosis. *Circulation* [Internet]. 2003 [cited 2013 Sep 18]; 108:3017–23. Available from: http://circ.ahajournals.org/content/108/24/3017.short

248. Traupe T, Lang M, Goettsch W, Münter K, Morawietz H, Vetter W, Barton M. Obesity increases prostanoid-mediated vasoconstriction and vascular thromboxane receptor gene expression. *J. Hypertens.* [Internet]. 2002; 20:2239–2245. Available from: http://journals.lww.com/jhypertension/Fulltext/2002/11000/Obesity_increases_prostanoid_mediated.24.aspx

249. Praticò D, Tillmann C, Zhang ZB, Li H, FitzGerald GA. Acceleration of atherogenesis by COX-1-dependent prostanoid formation in low density lipoprotein receptor knockout mice. *Proc. Natl. Acad. Sci. U. S. A.* [Internet]. 2001 [cited 2013 Sep 23]; 98:3358–63. Available from: http://www.pnas.org/content/98/6/3358.short

250. Kobayashi T, Tahara Y, Matsumoto M, Iguchi M, Sano H, Murayama T, Arai H, Oida H, Yurugi-Kobayashi T, Yamashita JK, Katagiri H, Majima M, Yokode M, Kita T, Narumiya S. Roles of thromboxane A(2) and prostacyclin in the development of atherosclerosis in apoE-deficient mice. *J. Clin. Invest.* [Internet]. 2004 [cited 2013 Sep 23]; 114:784–94. Available from: http://www.jci.org/articles/view/21446

251. Simon LS. Role and regulation of cyclooxygenase-2 during inflammation. *Am. J. Med.* [Internet]. 1999 [cited 2013 Sep 18]; 106:37S–42S. Available from: http://www.sciencedirect.com/science/article/pii/S0002934399001151

252. Seibert K, Masferrer JL. Role of inducible cyclooxygenase (COX-2) in inflammation. *Receptor* [Internet]. 1994 [cited 2013 Sep 18]; 4:17–23. Available from: http://www.ncbi.nlm.nih.gov/pubmed/8038702

253. Burleigh ME, Babaev VR, Yancey PG, Major AS, McCaleb JL, Oates JA, Morrow JD, Fazio S, Linton MF. Cyclooxygenase-2 promotes early atherosclerotic lesion formation in ApoE-deficient and C57BL/6 mice. *J. Mol. Cell. Cardiol.* [Internet]. 2005 [cited 2013 Aug 8]; 39:443–52. Available from: http://dx.doi.org/10.1016/j.yjmcc.2005.06.011

254. Burleigh ME. Cyclooxygenase-2 Promotes Early Atherosclerotic Lesion Formation in LDL Receptor-Deficient Mice. *Circulation* [Internet]. 2002 [cited 2013 Aug 1]; 105:1816–1823. Available from: http://circ.ahajournals.org/content/105/15/1816.short

255. Jacob S, Laury-Kleintop L, Lanza-Jacoby S. The select cyclooxygenase-2 inhibitor celecoxib reduced the extent of atherosclerosis in apo E-/- mice. *J. Surg. Res.* [Internet]. 2008 [cited 2013 Sep 13]; 146:135–42. Available from: http://dx.doi.org/10.1016/j.jss.2007.04.040

256. Egan KM, Lawson JA, Fries S, Koller B, Rader DJ, Smyth EM, Fitzgerald GA. COX-2-derived prostacyclin confers atheroprotection on female mice. *Science* [Internet]. 2004 [cited 2013 Sep 12]; 306:1954–7. Available from: http://www.sciencemag.org/content/306/5703/1954.abstract

257. Jüni P, Nartey L, Reichenbach S, Sterchi R, Dieppe PA, Egger M. Risk of cardiovascular events and rofecoxib: cumulative meta-analysis. *Lancet* [Internet]. 2004 [cited 2013 Sep 23]; 364:2021–2029. Available from: http://www.sciencedirect.com/science/article/pii/S0140673604175144

258. Shimano H, Ohsuga J, Shimada M, Namba Y, Gotoda T, Harada K, Katsuki M, Yazaki Y, Yamada N. Inhibition of diet-induced atheroma formation in transgenic mice expressing apolipoprotein E in the arterial wall. *J. Clin. Invest.* [Internet]. 1995 [cited 2013 Aug 28]; 95:469–76. Available from: http://www.pubmedcentral.nih.gov/articlerender.fcgi?artid=295491&tool=pmcentrez&rendertype=abstract

259. Jiang F, Gibson AP, Dusting GJ. Endothelial dysfunction induced by oxidized low-density lipoproteins in isolated mouse aorta: a comparison with apolipoprotein-E deficient mice. *Eur. J. Pharmacol.* [Internet]. 2001 [cited 2013 Aug 19]; 424:141–149. Available from: http://dx.doi.org/10.1016/S0014-2999(01)01140-2

260. Ali K, Middleton M, Puré E, Rader DJ. Apolipoprotein E suppresses the type I inflammatory response in vivo. *Circ. Res.* [Internet]. 2005 [cited 2013 Aug 29]; 97:922–7. Available from: http://circres.ahajournals.org/content/97/9/922.short

261. Björkbacka H, Kunjathoor V V, Moore KJ, Koehn S, Ordija CM, Lee MA, Means T, Halmen K, Luster AD, Golenbock DT, Freeman MW. Reduced atherosclerosis in MyD88-null mice links elevated serum cholesterol levels to activation of innate immunity signaling pathways. *Nat. Med.* [Internet]. 2004 [cited 2013 Nov 10]; 10:416–21. Available from: http://dx.doi.org/10.1038/nm1008

262. Plump AS, Smith JD, Hayek T, Aalto-Setälä K, Walsh A, Verstuyft JG, Rubin EM, Breslow JL. Severe hypercholesterolemia and atherosclerosis in apolipoprotein E-deficient mice created by homologous recombination in ES cells. *Cell* [Internet]. 1992 [cited 2013 Aug 21]; 71:343–353. Available from: http://dx.doi.org/10.1016/0092-8674(92)90362-G

263. Johnson J, Carson K, Williams H, Karanam S, Newby A, Angelini G, George S, Jackson C. Plaque Rupture After Short Periods of Fat Feeding in the Apolipoprotein E-Knockout Mouse: Model Characterization and Effects of Pravastatin Treatment. *Circulation* [Internet]. 2005; 111:1422–1430. Available from: http://circ.ahajournals.org/cgi/content/abstract/111/11/1422

264. Harrison B, Leazenby C, Halldorsdottir S. Accuracy of the CONTOUR® blood glucose monitoring system. *J. Diabetes Sci. Technol.* [Internet]. 2011 [cited 2013 Jul 18]; 5:1009–13. Available from: http://europepmc.org/articles/PMC3192609/?report=abstract

265. Sullivan D, Kruijswijk Z, West C, Kohlmeier M, Katan M. Determination of serum triglycerides by an accurate enzymatic method not affected by free glycerol. *Clin. Chem.* [Internet]. 1985 [cited 2013 Jul 18]; 31:1227–1228. Available from: http://www.clinchem.org/content/31/7/1227.short

266. Allain CC, Poon LS, Chan CSG, Richmond W, Fu PC. Enzymatic Determination of Total Serum Cholesterol. *Clin. Chem.* [Internet]. 1974 [cited 2013 Jul 18]; 20:470–475. Available from: http://www.clinchem.org/content/20/4/470.short

267. Menys VC, Liu Y, Mackness MI, Caslake MJ, Kwok S, Durrington PN. Measurement of plasma small-dense LDL concentration by a simplified ultracentrifugation

procedure and immunoassay of apolipoprotein B. *Clin. Chim. Acta* [Internet]. 2003 [cited 2013 Jul 18]; 334:95–106. Available from: http://dx.doi.org/10.1016/S0009-8981(03)00231-6

268. Mackness B, Davies GK, Turkie W, Lee E, Roberts DH, Hill E, Roberts C, Durrington PN, Mackness MI. Paraoxonase Status in Coronary Heart Disease: Are Activity and Concentration More Important Than Genotype? *Arterioscler. Thromb. Vasc. Biol.* [Internet]. 2001 [cited 2013 Jul 18]; 21:1451–1457. Available from: http://atvb.ahajournals.org/content/21/9/1451.short

269. Judkins CP, Sobey CG, Dang TT, Miller AA, Dusting GJ, Drummond GR. NADPH-induced contractions of mouse aorta do not involve NADPH oxidase: a role for P2X receptors. *J. Pharmacol. Exp. Ther.* [Internet]. 2006 [cited 2013 Jul 16]; 317:644–50. Available from: http://jpet.aspetjournals.org/content/317/2/644.short

270. LAWRENCE RN, DUNN WR, WILSON VG. Endothelium-dependent Relaxation in Response to Ethanol in the Porcine Isolated Pulmonary Artery. *J. Pharm. Pharmacol.* [Internet]. 1998 [cited 2013 Jul 16]; 50:885–890. Available from: http://doi.wiley.com/10.1111/j.2042-7158.1998.tb04004.x

271. Al-Shalmani S, Suri S, Hughes DA, Kroon PA, Needs PW, Taylor MA, Tribolo S, Wilson VG. Quercetin and its principal metabolites, but not myricetin, oppose lipopolysaccharide-induced hyporesponsiveness of the porcine isolated coronary artery. *Br. J. Pharmacol.* [Internet]. 2011 [cited 2013 Jul 16]; 162:1485–97. Available from: http://www.pubmedcentral.nih.gov/articlerender.fcgi?artid=3057287&tool=pmcentrez&rendertype=abstract

272. Suri S, Liu XH, Rayment S, Hughes DA, Kroon PA, Needs PW, Taylor MA, Tribolo S, Wilson VG. Quercetin and its major metabolites selectively modulate cyclic GMP-dependent relaxations and associated tolerance in pig isolated coronary artery. *Br. J. Pharmacol.* [Internet]. 2010 [cited 2013 Jul 16]; 159:566–75. Available from: http://www.pubmedcentral.nih.gov/articlerender.fcgi?artid=2828021&tool=pmcentrez&rendertype=abstract

273. Bowles DK, Heaps CL, Turk JR, Maddali KK, Price EM. Hypercholesterolemia inhibits L-type calcium current in coronary macro-, not microcirculation. *J Appl Physiol* [Internet]. 2004; 96:2240–2248. Available from: http://jap.physiology.org/cgi/content/abstract/96/6/2240

274. Otter D, Austin C. Mechanisms of hypoxic vasodilatation of isolated rat mesenteric arteries: a comparison with metabolic inhibition. *J. Physiol.* [Internet]. 1999 [cited 2013 Sep 26]; 516 (Pt 1:249–59. Available from: http://www.pubmedcentral.nih.gov/articlerender.fcgi?artid=2269207&tool=pmcentrez&rendertype=abstract

275. Absi M, Burnham MP, Weston AH, Harno E, Rogers M, Edwards G. Effects of methyl [beta]-cyclodextrin on EDHF responses in pig and rat arteries; association between SKCa channels and caveolin-rich domains. *Br J Pharmacol* [Internet]. 2007; 151:332–340. Available from: http://dx.doi.org/10.1038/sj.bjp.0707222

276. Zygmunt PM, Hogestatt ED. Role of potassium channels in endothelium-dependent relaxation resistant to nitroarginine in the rat hepatic artery. *Br J Pharmacol*. 1996; 117:1600–1606.

277. Jerde TJ, Calamon-Dixon JL, Bjorling DE, Nakada SY. Celecoxib inhibits ureteral contractility and prostanoid release. *Urology* [Internet]. 2005 [cited 2013 Sep 26]; 65:185–190. Available from: http://www.sciencedirect.com/science/article/pii/S0090429504010544

278. Grynkiewicz G, Poenie M, Tsien RY. A new generation of Ca2+ indicators with greatly improved fluorescence properties. *J. Biol. Chem.* [Internet]. 1985; 260:3440–3450. Available from: http://www.jbc.org/content/260/6/3440.abstract

279. Paddle BM. A cytoplasmic component of pyridine nucleotide fluorescence in rat diaphragm: evidence from comparisons with flavoprotein fluorescence. *Pfl*[illegible]*gers Arch. Eur. J. Physiol.* [Internet]. 1985 [cited 2013 Jul 18]; 404:326–331. Available from: http://link.springer.com/10.1007/BF00585343

280. Sick TJ, Rosenthal M. Indo-1 measurements of intracellular free calcium in the hippocampal slice: complications of labile NADH fluorescence. *J. Neurosci. Methods* [Internet]. 1989 [cited 2013 Jul 18]; 28:125–132. Available from: http://dx.doi.org/10.1016/0165-0270(89)90017-4

281. Taggart MJ, Sheader EA, Walker SD, Naderali EK, Moore S, Wray S. External alkalinization decreases intracellular Ca++ and spontaneous contractions in pregnant rat myometrium. *Am. J. Obstet. Gynecol.* [Internet]. 1997 [cited 2013 Jul 18]; 177:959–963. Available from: http://dx.doi.org/10.1016/S0002-9378(97)70301-6

282. Austin C, Wray S. The effects of extracellular pH and calcium change on force and intracellular calcium in rat vascular smooth muscle. *J. Physiol.* [Internet]. 1995; 488:281–291. Available from: http://jp.physoc.org/content/488/Pt_2/281.abstract

283. Lückhoff A. Measuring cytosolic free calcium concentration in endothelial cells with indo-1: The pitfall of using the ratio of two fluorescence intensities recorded at different wavelengths. *Cell Calcium* [Internet]. 1986; 7:233–248. Available from: http://www.sciencedirect.com/science/article/B6WCC-4C0CVM3-88/2/ef09637ab08e048904311c5d88cb92ae

284. Hove-Madsen L, Bers DM. Indo-1 binding to protein in permeabilized ventricular myocytes alters its spectral and Ca binding properties. *Biophys. J.* [Internet]. 1992 [cited 2013 Jun 20]; 63:89–97. Available from: http://dx.doi.org/10.1016/S0006-3495(92)81597-7

285. Simons K. How Cells Handle Cholesterol. *Science (80-.).* [Internet]. 2000 [cited 2013 Aug 8]; 290:1721–1726. Available from: http://www.sciencemag.org/content/290/5497/1721.long

286. Lingwood D, Simons K. Lipid rafts as a membrane-organizing principle. *Science* [Internet]. 2010 [cited 2013 Aug 7]; 327:46–50. Available from: http://www.sciencemag.org/content/327/5961/46.short

287. Kahn MB, Boesze-Battaglia K, Stepp DW, Petrov A, Huang Y, Mason RP, Tulenko TN. Influence of serum cholesterol on atherogenesis and intimal hyperplasia after angioplasty: inhibition by amlodipine. *Am J Physiol Hear. Circ Physiol* [Internet]. 2005; 288:H591–600. Available from: http://ajpheart.physiology.org/cgi/content/abstract/288/2/H591

288. Suo J, Ferrara DE, Sorescu D, Guldberg RE, Taylor WR, Giddens DP. Hemodynamic shear stresses in mouse aortas: implications for atherogenesis. *Arterioscler. Thromb. Vasc. Biol.* [Internet]. 2007 [cited 2013 Aug 13]; 27:346–51. Available from: http://atvb.ahajournals.org/content/27/2/346.short

289. Passerini AG, Shi C, Francesco NM, Chuan P, Manduchi E, Grant GR, Stoeckert CJ, Karanian JW, Wray-Cahen D, Pritchard WF, Davies PF. Regional determinants of arterial endothelial phenotype dominate the impact of gender or short-term exposure to a high-fat diet. *Biochem. Biophys. Res. Commun.* [Internet]. 2005 [cited 2013 Aug 16]; 332:142–8. Available from: http://dx.doi.org/10.1016/j.bbrc.2005.04.103

290. Dreja K. Cholesterol Depletion Disrupts Caveolae and Differentially Impairs Agonist-Induced Arterial Contraction. *Arterioscler. Thromb. Vasc. Biol.* [Internet]. 2002 [cited 2013 Aug 13]; 22:1267–1272. Available from: http://atvb.ahajournals.org/content/22/8/1267.short

291. Tulenko TN, Chen M, Mason PE, Mason RP. Physical effects of cholesterol on arterial smooth muscle membranes: evidence of immiscible cholesterol domains and alterations in bilayer width during atherogenesis. *J. Lipid Res.* [Internet]. 1998 [cited 2013 Aug 13]; 39:947–956. Available from: http://www.jlr.org/content/39/5/947.short

292. Pomerantz KB, Hajjar DP, Levi R, Gross SS. Cholesterol enrichment of arterial smooth muscle cells upregulates cytokine-induced nitric oxide synthesis. *Biochem. Biophys. Res. Commun.* [Internet]. 1993 [cited 2013 Aug 13]; 191:103–9. Available from: http://dx.doi.org/10.1006/bbrc.1993.1190

293. Simons K, Ehehalt R. Cholesterol, lipid rafts, and disease. *J. Clin. Invest.* [Internet]. 2002 [cited 2013 Aug 13]; 110:597–603. Available from: http://www.jci.org/articles/view/16390

294. Simons K, Toomre D. Lipid rafts and signal transduction. *Nat. Rev. Mol. Cell Biol.* [Internet]. 2000 [cited 2013 Aug 13]; 1:31–9. Available from: http://dx.doi.org/10.1038/35036052

295. Babiychuk EB, Smith RD, Burdyga T, Babiychuk VS, Wray S, Draeger A. Membrane cholesterol regulates smooth muscle phasic contraction. *J. Membr. Biol.* [Internet]. 2004 [cited 2013 Aug 15]; 198:95–101. Available from: http://www.ncbi.nlm.nih.gov/pubmed/15138749

296. Rajendran L, Simons K. Lipid rafts and membrane dynamics. *J. Cell Sci.* [Internet]. 2005; 118:1099–1102. Available from: http://www.ncbi.nlm.nih.gov/pubmed/15764592

297. Armstrong CL, Marquardt D, Dies H, Kučerka N, Yamani Z, Harroun TA, Katsaras J, Shi A-C, Rheinstädter MC. The Observation of Highly Ordered Domains in Membranes with Cholesterol. *PLoS One* [Internet]. 2013 [cited 2013 Aug 13]; 8:e66162. Available from: http://www.pubmedcentral.nih.gov/articlerender.fcgi?artid=3688844&tool=pmcentrez&rendertype=abstract

298. Sones WR, Davis AJ, Leblanc N, Greenwood IA. Cholesterol depletion alters amplitude and pharmacology of vascular calcium-activated chloride channels. *Cardiovasc. Res.* [Internet]. 2010 [cited 2013 Aug 13]; 87:476–84. Available from: http://cardiovascres.oxfordjournals.org/content/87/3/476.short

299. Christian A, Haynes M, Phillips M, Rothblat G. Use of cyclodextrins for manipulating cellular cholesterol content. *J. Lipid Res.* [Internet]. 1997 [cited 2013 Aug 13]; 38:2264–2272. Available from: http://www.jlr.org/content/38/11/2264.short

300. Dolmetsch RE, Lewis RS, Goodnow CC, Healy JI. Differential activation of transcription factors induced by Ca2+ response amplitude and duration. *Nature* [Internet]. 1997; 386:855–858. Available from: http://dx.doi.org/10.1038/386855a0

301. Cristofaro V, Peters CA, Yalla S V, Sullivan MP. Smooth muscle caveolae differentially regulate specific agonist induced bladder contractions. *Neurourol. Urodyn.* [Internet]. 2007 [cited 2013 Aug 16]; 26:71–80. Available from: http://www.ncbi.nlm.nih.gov/pubmed/17123298

302. Prendergast C, Quayle J, Burdyga T, Wray S. Cholesterol depletion alters coronary artery myocyte Ca2+ signalling in a stimulus-specific manner. *Cell Calcium* [Internet]. 2010; 47:84–91. Available from: http://www.sciencedirect.com/science/article/B6WCC-4XYB433-2/2/e9002826f311a4de18452255263a18fe

303. Lohn M, Furstenau M, Sagach V, Elger M, Schulze W, Luft FC, Haller H, Gollasch M. Ignition of Calcium Sparks in Arterial and Cardiac Muscle Through Caveolae. *Circ. Res.* [Internet]. 2000 [cited 2013 Aug 16]; 87:1034–1039. Available from: http://circres.ahajournals.org/content/87/11/1034.short

304. Balijepalli RC, Foell JD, Hall DD, Hell JW, Kamp TJ. Localization of cardiac L-type Ca(2+) channels to a caveolar macromolecular signaling complex is required for beta(2)-adrenergic regulation. *Proc. Natl. Acad. Sci. U. S. A.* [Internet]. 2006 [cited 2013 Aug 16]; 103:7500–5. Available from: http://www.pnas.org/content/103/19/7500.short

305. Martin GR, Humphrey PPA. Receptors for 5-Hydroxytryptamine: Current perspectives on classification and nomenclature. *Neuropharmacology* [Internet]. 1994 [cited 2013 Aug 16]; 33:261–273. Available from: http://dx.doi.org/10.1016/0028-3908(94)90058-2

306. Muramatsu I, Ohmura T, Kigoshi S, Hashimoto S, Oshita M. Pharmacological subclassification of α1-adrenoceptors in vascular smooth muscle. *Br. J. Pharmacol.*

[Internet]. 1990 [cited 2013 Aug 16]; 99:197–201. Available from: http://doi.wiley.com/10.1111/j.1476-5381.1990.tb14678.x

307. Cohen M, Fuller R, Wiley K. Evidence for 5-HT2 receptors mediating contraction in vascular smooth muscle. *J. Pharmacol. Exp. Ther.* [Internet]. 1981 [cited 2013 Aug 16]; 218:421–425. Available from: http://jpet.aspetjournals.org/content/218/2/421.extract

308. Knight AR, Misra A, Quirk K, Benwell K, Revell D, Kennett G, Bickerdike M. Pharmacological characterisation of the agonist radioligand binding site of 5-HT(2A), 5-HT(2B) and 5-HT(2C) receptors. *Naunyn. Schmiedebergs. Arch. Pharmacol.* [Internet]. 2004 [cited 2013 Aug 16]; 370:114–23. Available from: http://www.ncbi.nlm.nih.gov/pubmed/15322733

309. Kalkbrenner F. Distinct Functions of Gq and G11 Proteins in Coupling alpha 1-Adrenoreceptors to Ca2+ Release and Ca2+ Entry in Rat Portal Vein Myocytes. *J. Biol. Chem.* [Internet]. 1997 [cited 2013 Aug 16]; 272:5261–5268. Available from: http://www.jbc.org/content/272/8/5261.short

310. Wilson SM, Mason HS, Ng LC, Montague S, Johnston L, Nicholson N, Mansfield S, Hume JR. Role of basal extracellular Ca2+ entry during 5-HT-induced vasoconstriction of canine pulmonary arteries. *Br. J. Pharmacol.* [Internet]. 2005 [cited 2013 Aug 16]; 144:252–64. Available from: http://www.pubmedcentral.nih.gov/articlerender.fcgi?artid=1575999&tool=pmcentrez&rendertype=abstract

311. Villalba N, Stankevicius E, Garcia-Sacristán A, Simonsen U, Prieto D. Contribution of both Ca2+ entry and Ca2+ sensitization to the alpha1-adrenergic vasoconstriction of rat penile small arteries. *Am. J. Physiol. Heart Circ. Physiol.* [Internet]. 2007 [cited 2013 Aug 16]; 292:H1157–69. Available from: http://ajpheart.physiology.org/content/292/2/H1157

312. Darblade B. Alteration of plasmalemmal caveolae mimics endothelial dysfunction observed in atheromatous rabbit aorta. *Cardiovasc. Res.* [Internet]. 2001 [cited 2013 Aug 13]; 50:566–576. Available from: http://cardiovascres.oxfordjournals.org/content/50/3/566.short

313. Moncada S, Palmer R, Higgs E. Nitric oxide: physiology, pathophysiology, and pharmacology. *Pharmacol. Rev.* [Internet]. 1991 [cited 2013 Aug 19]; 43:109–142. Available from: http://pharmrev.aspetjournals.org/content/43/2/109.extract

314. Félétou M, Vanhoutte PM. The third pathway: endothelium-dependent hyperpolarization. *J. Physiol. Pharmacol.* [Internet]. 1999 [cited 2013 Aug 19]; 50:525–34. Available from: http://www.ncbi.nlm.nih.gov/pubmed/10639003

315. Dessy C, Feron O, Balligand J-L. The regulation of endothelial nitric oxide synthase by caveolin: a paradigm validated in vivo and shared by the "endothelium-derived hyperpolarizing factor". *Pflugers Arch.* [Internet]. 2010 [cited 2013 Aug 19]; 459:817–27. Available from: http://www.ncbi.nlm.nih.gov/pubmed/20339866

316. Blair A. Oxidized Low Density Lipoprotein Displaces Endothelial Nitric-oxide Synthase (eNOS) from Plasmalemmal Caveolae and Impairs eNOS Activation. *J. Biol. Chem.* [Internet]. 1999 [cited 2013 Aug 19]; 274:32512–32519. Available from: http://www.jbc.org/content/274/45/32512.short

317. Smith RD, Babiychuk EB, Noble K, Draeger A, Wray S. Increased cholesterol decreases uterine activity: functional effects of cholesterol alteration in pregnant rat myometrium. *Am. J. Physiol. Cell Physiol.* [Internet]. 2005 [cited 2013 Aug 11]; 288:C982–8. Available from: http://ajpcell.physiology.org/content/288/5/C982

318. Shimokawa H, Tomoike H, Nabeyama S, Yamamoto H, Araki H, Nakamura M, Ishii Y, Tanaka K. Coronary artery spasm induced in atherosclerotic miniature swine. *Science (80-.).* [Internet]. 1983 [cited 2013 Aug 14]; 221:560–562. Available from: http://www.sciencemag.org/content/221/4610/560.short

319. Meir KS, Leitersdorf E. Atherosclerosis in the apolipoprotein-E-deficient mouse: a decade of progress. *Arterioscler. Thromb. Vasc. Biol.* [Internet]. 2004 [cited 2013 Aug 7]; 24:1006–14. Available from: http://atvb.ahajournals.org/content/24/6/1006.short

320. Shore B, Shore V, Salel A, Mason D, Zelis R. An apolipoprotein preferentially enriched in cholesteryl ester-rich very low density lipoproteins. *Biochem. Biophys. Res. Commun.* [Internet]. 1974 [cited 2013 Aug 21]; 58:1–7. Available from: http://dx.doi.org/10.1016/0006-291X(74)90882-1

321. Rosenfeld ME, Averill MM, Bennett BJ, Schwartz SM. Progression and disruption of advanced atherosclerotic plaques in murine models. *Curr. Drug Targets* [Internet]. 2008 [cited 2013 Aug 21]; 9:210–6. Available from: http://www.pubmedcentral.nih.gov/articlerender.fcgi?artid=2942086&tool=pmcentrez&rendertype=abstract

322. Doran AC, Meller N, McNamara CA. Role of smooth muscle cells in the initiation and early progression of atherosclerosis. *Arterioscler. Thromb. Vasc. Biol.* [Internet]. 2008 [cited 2013 Aug 7]; 28:812–9. Available from: http://atvb.ahajournals.org/content/28/5/812.short

323. Baribault H, Penner J, Iozzo R V, Wilson-Heiner M. Colorectal hyperplasia and inflammation in keratin 8-deficient FVB/N mice. *Genes Dev.* [Internet]. 1994 [cited 2013 Aug 29]; 8:2964–2973. Available from: http://genesdev.cshlp.org/content/8/24/2964.short

324. Skurk T, Alberti-Huber C, Herder C, Hauner H. Relationship between adipocyte size and adipokine expression and secretion. *J. Clin. Endocrinol. Metab.* [Internet]. 2007 [cited 2013 Aug 29]; 92:1023–33. Available from: http://jcem.endojournals.org/content/92/3/1023.short

325. Johnson JL, Jackson CL. Atherosclerotic plaque rupture in the apolipoprotein E knockout mouse. *Atherosclerosis* [Internet]. 2001; 154:399–406. Available from: http://www.sciencedirect.com/science/article/B6T12-4292GSY-J/2/5d5cfe8a4c447c0a8017f7b59b238d47

326. Tunick PA, Kronzon I. Atheromas of the thoracic aorta: clinical and therapeutic update. *J. Am. Coll. Cardiol.* [Internet]. 2000 [cited 2013 Aug 28]; 35:545–554. Available from: http://content.onlinejacc.org/article.aspx?articleid=1126276

327. Ferrari E, Vidal R, Chevallier T, Baudouy M. Atherosclerosis of the thoracic aorta and aortic debris as a marker of poor prognosis: benefit of oral anticoagulants. *J. Am. Coll. Cardiol.* [Internet]. 1999 [cited 2013 Aug 28]; 33:1317–1322. Available from: http://content.onlinejacc.org/article.aspx?articleid=1125694

328. Rabkin SW, Mathewson FAL, Hsu P-H. Relation of body weight to development of ischemic heart disease in a cohort of young north American men after a 26 year observation period: The manitoba study. *Am. J. Cardiol.* [Internet]. 1977 [cited 2013 Aug 28]; 39:452–458. Available from: http://dx.doi.org/10.1016/S0002-9149(77)80104-5

329. Braun A, Trigatti BL, Post MJ, Sato K, Simons M, Edelberg JM, Rosenberg RD, Schrenzel M, Krieger M. Loss of SR-BI Expression Leads to the Early Onset of Occlusive Atherosclerotic Coronary Artery Disease, Spontaneous Myocardial Infarctions, Severe Cardiac Dysfunction, and Premature Death in Apolipoprotein E-Deficient Mice. *Circ Res* [Internet]. 2002; 90:270–276. Available from: http://circres.ahajournals.org/cgi/content/abstract/90/3/270

330. Schreyer SA, Vick C, Lystig TC, Mystkowski P, LeBoeuf RC. LDL receptor but not apolipoprotein E deficiency increases diet-induced obesity and diabetes in mice. *Am. J. Physiol. Endocrinol. Metab.* [Internet]. 2002 [cited 2013 Aug 28]; 282:E207–14. Available from: http://www.ncbi.nlm.nih.gov/pubmed/11739102

331. Drechsler M, Megens RTA, van Zandvoort M, Weber C, Soehnlein O. Hyperlipidemia-Triggered Neutrophilia Promotes Early Atherosclerosis. *Circulation* [Internet]. 2010; 122:1837–1845. Available from: http://circ.ahajournals.org/cgi/content/abstract/122/18/1837

332. Besler C, Lüscher TF, Landmesser U. Molecular mechanisms of vascular effects of High-density lipoprotein: alterations in cardiovascular disease. *EMBO Mol. Med.* [Internet]. 2012 [cited 2013 Aug 29]; 4:251–68. Available from: http://www.pubmedcentral.nih.gov/articlerender.fcgi?artid=3376856&tool=pmcentrez&rendertype=abstract

333. Mineo C, Shaul PW. Novel biological functions of high-density lipoprotein cholesterol. *Circ. Res.* [Internet]. 2012 [cited 2013 Aug 11]; 111:1079–90. Available from: http://circres.ahajournals.org/content/111/8/1079.long

334. Mensink RP, Zock PL, Kester AD, Katan MB. Effects of dietary fatty acids and carbohydrates on the ratio of serum total to HDL cholesterol and on serum lipids and apolipoproteins: a meta-analysis of 60 controlled trials. *Am J Clin Nutr* [Internet]. 2003 [cited 2013 Aug 29]; 77:1146–1155. Available from: http://ajcn.nutrition.org/content/77/5/1146.short

335. White CR, Datta G, Zhang Z, Gupta H, Garber DW, Mishra VK, Palgunachari MN, Handattu SP, Chaddha M, Anantharamaiah GM. HDL therapy for cardiovascular

diseases: the road to HDL mimetics. *Curr. Atheroscler. Rep.* [Internet]. 2008 [cited 2013 Aug 29]; 10:405–412. Available from: http://link.springer.com/10.1007/s11883-008-0063-6

336. Pal M, Pillarisetti S. HDL Elevators and Mimetics - Emerging Therapies for Atherosclerosis. *Cardiovasc. Hematol. Agents Med. Chem.* [Internet]. 2007 [cited 2013 Aug 29]; 5:55–66. Available from: http://www.ingentaconnect.com/content/ben/chamc/2007/00000005/00000001/art00006

337. Plump AS, Scott CJ, Breslow JL. Human apolipoprotein A-I gene expression increases high density lipoprotein and suppresses atherosclerosis in the apolipoprotein E-deficient mouse. *Proc. Natl. Acad. Sci.* [Internet]. 1994 [cited 2013 Aug 29]; 91:9607–9611. Available from: http://www.pnas.org/content/91/20/9607.short

338. PAIGEN B, MORROW A, BRANDON C, MITCHELL D, HOLMES P. Variation in susceptibility to atherosclerosis among inbred strains of mice. *Atherosclerosis* [Internet]. 1985 [cited 2013 Aug 29]; 57:65–73. Available from: http://dx.doi.org/10.1016/0021-9150(85)90138-8

339. Paigen B, Morrow A, Holmes PA, Mitchell D, Williams RA. Quantitative assessment of atherosclerotic lesions in mice. *Atherosclerosis* [Internet]. 1987; 68:231–240. Available from: http://linkinghub.elsevier.com/retrieve/pii/0021915087902024?showall=true

340. Schultz JR, Verstuyft JG, Gong EL, Nichols A V, Rubin EM. Protein composition determines the anti-atherogenic properties of HDL in transgenic mice. *Nature* [Internet]. 1993 [cited 2013 Aug 29]; 365:762–4. Available from: http://www.nature.com/nature/journal/v365/n6448/pdf/365762a0.pdf

341. Klotzsch S, McNamara J. Triglyceride measurements: a review of methods and interferences. *Clin. Chem.* [Internet]. 1990 [cited 2013 Aug 28]; 36:1605–1613. Available from: http://www.clinchem.org/content/36/9/1605.short

342. Beckman JA. Diabetes and Atherosclerosis<SUBTITLE>Epidemiology, Pathophysiology, and Management</SUBTITLE>. *JAMA* [Internet]. 2002 [cited 2013 Aug 29]; 287:2570. Available from: http://jama.jamanetwork.com/article.aspx?articleid=194930

343. Pyörälä K, Laakso M, Uusitupa M. Diabetes and atherosclerosis: An epidemiologic view. *Diabetes / Metab. Rev.* [Internet]. 1987 [cited 2013 Aug 29]; 3:463–524. Available from: http://doi.wiley.com/10.1002/dmr.5610030206

344. Stout R. Diabetes and atherosclerosis. *Biomed. Pharmacother.* [Internet]. 1993 [cited 2013 Aug 29]; 47:1–2. Available from: http://dx.doi.org/10.1016/0753-3322(93)90029-K

345. Chen H, Charlat O, Tartaglia LA, Woolf EA, Weng X, Ellis SJ, Lakey ND, Culpepper J, More KJ, Breitbart RE, Duyk GM, Tepper RI, Morgenstern JP. Evidence That the Diabetes Gene Encodes the Leptin Receptor: Identification of a Mutation in the Leptin

Receptor Gene in db/db Mice. *Cell* [Internet]. 1996 [cited 2013 Aug 29]; 84:491–495. Available from: http://dx.doi.org/10.1016/S0092-8674(00)81294-5

346. Kobayashi K, Forte TM, Taniguchi S, Ishida BY, Oka K, Chan L. The db/db mouse, a model for diabetic dyslipidemia: Molecular characterization and effects of western diet feeding. *Metabolism* [Internet]. 2000 [cited 2013 Aug 21]; 49:22–31. Available from: http://dx.doi.org/10.1016/S0026-0495(00)90588-2

347. Belke DD, Swanson EA, Dillmann WH. Decreased Sarcoplasmic Reticulum Activity and Contractility in Diabetic db/db Mouse Heart. *Diabetes* [Internet]. 2004 [cited 2013 Aug 29]; 53:3201–3208. Available from: http://diabetes.diabetesjournals.org/content/53/12/3201.short

348. Montero-Vega MT. The Inflammatory Process Underlying Atherosclerosis. *Crit. Rev. Immunol.* [Internet]. 2012 [cited 2013 Aug 13]; 32:373–462. Available from: http://www.dl.begellhouse.com/journals/2ff21abf44b19838,6cc7a19267e8eaba,023c57a37f1bbfda.html

349. Fletcher DS, Widmer WR, Luell S, Christen A, Orevillo C, Shah S, Visco D. Therapeutic Administration of a Selective Inhibitor of Nitric Oxide Synthase Does Not Ameliorate the Chronic Inflammation and Tissue Damage Associated with Adjuvant-Induced Arthritis in Rats. *J. Pharmacol. Exp. Ther.* [Internet]. 1998 [cited 2013 Aug 29]; 284:714–721. Available from: http://jpet.aspetjournals.org/content/284/2/714.short

350. Armour KJ, Armour KE, Van 't Hof RJ, Reid DM, Wei X-Q, Liew FY, Ralston SH. Activation of the inducible nitric oxide synthase pathway contributes to inflammation-induced osteoporosis by suppressing bone formation and causing osteoblast apoptosis. *Arthritis Rheum.* [Internet]. 2001 [cited 2013 Aug 29]; 44:2790–2796. Available from: http://doi.wiley.com/10.1002/1529-0131%28200112%2944%3A12%3C2790%3A%3AAID-ART466%3E3.0.CO%3B2-X

351. Christensen SR, Shupe J, Nickerson K, Kashgarian M, Flavell RA, Shlomchik MJ. Toll-like receptor 7 and TLR9 dictate autoantibody specificity and have opposing inflammatory and regulatory roles in a murine model of lupus. *Immunity* [Internet]. 2006 [cited 2013 Aug 9]; 25:417–28. Available from: http://dx.doi.org/10.1016/j.immuni.2006.07.013

352. Lynch JR, Tang W, Wang H, Vitek MP, Bennett ER, Sullivan PM, Warner DS, Laskowitz DT. APOE genotype and an ApoE-mimetic peptide modify the systemic and central nervous system inflammatory response. *J. Biol. Chem.* [Internet]. 2003 [cited 2013 Aug 29]; 278:48529–33. Available from: http://www.jbc.org/content/278/49/48529.short

353. Jofre-Monseny L, Minihane A-M, Rimbach G. Impact of apoE genotype on oxidative stress, inflammation and disease risk. *Mol. Nutr. Food Res.* [Internet]. 2008 [cited 2013 Aug 29]; 52:131–45. Available from: http://www.ncbi.nlm.nih.gov/pubmed/18203129

354. Marchesi C, Ebrahimian T, Angulo O, Paradis P, Schiffrin EL. Endothelial nitric oxide synthase uncoupling and perivascular adipose oxidative stress and inflammation contribute to vascular dysfunction in a rodent model of metabolic syndrome. *Hypertension* [Internet]. 2009 [cited 2013 Aug 12]; 54:1384–92. Available from: http://hyper.ahajournals.org/content/54/6/1384.short

355. Bays HE, González-Campoy JM, Bray GA, Kitabchi AE, Bergman DA, Schorr AB, Rodbard HW, Henry RR. Pathogenic potential of adipose tissue and metabolic consequences of adipocyte hypertrophy and increased visceral adiposity. *Expert Rev. Cardiovasc. Ther.* [Internet]. 2008 [cited 2013 Aug 27]; 6:343–68. Available from: http://www.expert-reviews.com/doi/abs/10.1586/14779072.6.3.343

356. Kyselovic J, Martinka P, Batova Z, Gazova A, Godfraind T. Calcium Channel Blocker Inhibits Western-Type Diet-Evoked Atherosclerosis Development in ApoE-Deficient Mice. *J. Pharmacol. Exp. Ther.* [Internet]. 2005; 315:320–328. Available from: http://jpet.aspetjournals.org/content/315/1/320.abstract

357. Landmesser U, Hornig B, Drexler H. Endothelial function: a critical determinant in atherosclerosis? *Circulation* [Internet]. 2004 [cited 2013 Jun 3]; 109:II27–33. Available from: http://circ.ahajournals.org/content/109/21_suppl_1/II-27.short

358. Napoli C, de Nigris F, Williams-Ignarro S, Pignalosa O, Sica V, Ignarro LJ. Nitric oxide and atherosclerosis: An update. *Nitric Oxide* [Internet]. 2006; 15:265–279. Available from: http://www.sciencedirect.com/science/article/B6WNT-4JR41BJ-1/2/4eb64f316e647765dc1df27eb53eb183

359. Blankenberg S, Barbaux S, Tiret L. Adhesion molecules and atherosclerosis. *Atherosclerosis* [Internet]. 2003 [cited 2013 Sep 3]; 170:191–203. Available from: http://dx.doi.org/10.1016/S0021-9150(03)00097-2

360. Watanabe H, Murakami M, Ohba T, Takahashi Y, Ito H. TRP channel and cardiovascular disease. *Pharmacol. Ther.* [Internet]. 2008; 118:337–351. Available from: http://www.sciencedirect.com/science/article/B6TBG-4S80XCF-1/2/7b17c9156f8d8ba29689f1e4b18247c4

361. Hill BJ., Price EM, Dixon JL, Sturek M. Increased calcium buffering in coronary smooth muscle cells from diabetic dyslipidemic pigs. *Atherosclerosis* [Internet]. 2003 [cited 2013 Sep 12]; 167:15–23. Available from: http://dx.doi.org/10.1016/S0021-9150(02)00381-7

362. Kauser K, da Cunha V, Fitch R, Mallari C, Rubanyi GM. Role of endogenous nitric oxide in progression of atherosclerosis in apolipoprotein E-deficient mice. *Am J Physiol Hear. Circ Physiol* [Internet]. 2000 [cited 2013 Sep 9]; 278:H1679–1685. Available from: http://ajpheart.physiology.org/content/278/5/H1679.full-text.pdf+html

363. Rosendorff C, Hoffman JI, Verrier ED, Rouleau J, Boerboom LE. Cholesterol potentiates the coronary artery response to norepinephrine in anesthetized and conscious dogs. *Circ. Res.* [Internet]. 1981 [cited 2013 Aug 14]; 48:320–329. Available from: http://circres.ahajournals.org/content/48/3/320.short

364. Sunagawa M. Involvement of Ca2+ channel activity in proliferation of vascular smooth muscle cells. *Pathophysiology* [Internet]. 2010; 17:101–108. Available from: http://www.sciencedirect.com/science/article/B6TBB-4WGJKJM-1/2/6c5cce7f918d8843fc741dadeee4d9b8

365. Husain M, Jiang L, See V, Bein K, Simons M, Alper SL, Rosenberg RD. Regulation of vascular smooth muscle cell proliferation by plasma membrane Ca(2+)-ATPase. *Am J Physiol Cell Physiol* [Internet]. 1997; 272:C1947–1959. Available from: http://ajpcell.physiology.org/cgi/content/abstract/272/6/C1947

366. Nagel DJ, Aizawa T, Jeon K-I, Liu W, Mohan A, Wei H, Miano JM, Florio VA, Gao P, Korshunov VA, Berk BC, Yan C. Role of Nuclear Ca2+/Calmodulin-Stimulated Phosphodiesterase 1A in Vascular Smooth Muscle Cell Growth and Survival. *Circ Res* [Internet]. 2006; 98:777–784. Available from: http://circres.ahajournals.org/cgi/content/abstract/98/6/777

367. Berridge MJ. Calcium signalling and cell proliferation. *Bioessays*. 1995; 17:491–500.

368. Vaca L. SOCIC: the store-operated calcium influx complex. *Cell Calcium* [Internet]. 2010 [cited 2013 Aug 13]; 47:199–209. Available from: http://dx.doi.org/10.1016/j.ceca.2010.01.002

369. Parekh AB, Putney Jr. JW. Store-Operated Calcium Channels. *Physiol. Rev.* [Internet]. 2005; 85:757–810. Available from: http://physrev.physiology.org/cgi/content/abstract/85/2/757

370. Putney JW. Recent breakthroughs in the molecular mechanism of capacitative calcium entry (with thoughts on how we got here). *Cell Calcium* [Internet]. 2007 [cited 2013 Aug 21]; 42:103–10. Available from: http://dx.doi.org/10.1016/j.ceca.2007.01.011

371. Wang Y, Deng X, Hewavitharana T, Soboloff J, Gill DL. Stim, ORAI and TRPC channels in the control of calcium entry signals in smooth muscle. *Clin. Exp. Pharmacol. Physiol.* [Internet]. 2008 [cited 2013 Aug 12]; 35:1127–33. Available from: http://www.pubmedcentral.nih.gov/articlerender.fcgi?artid=3601895&tool=pmcentrez&rendertype=abstract

372. Hewavitharana T, Deng X, Soboloff J, Gill DL. Role of STIM and Orai proteins in the store-operated calcium signaling pathway. *Cell Calcium* [Internet]. 2007 [cited 2013 Aug 20]; 42:173–82. Available from: http://dx.doi.org/10.1016/j.ceca.2007.03.009

373. Soboloff J, Spassova MA, Dziadek MA, Gill DL. Calcium signals mediated by STIM and Orai proteins--a new paradigm in inter-organelle communication. *Biochim. Biophys. Acta* [Internet]. 2006 [cited 2013 Sep 11]; 1763:1161–8. Available from: http://dx.doi.org/10.1016/j.bbamcr.2006.09.023

374. Schmidt T, Zaib F, Samson SE, Kwan C-Y, Grover AK. Peroxynitrite resistance of sarco/endoplasmic reticulum Ca2+ pump in pig coronary artery endothelium and smooth muscle. *Cell Calcium* [Internet]. 2004 [cited 2013 Aug 19]; 36:77–82. Available from: http://dx.doi.org/10.1016/j.ceca.2003.12.002

375. Benham CD, Tsien RW. A novel receptor-operated Ca2+-permeable channel activated by ATP in smooth muscle. *Nature* [Internet]. 1987 [cited 2013 Sep 12]; 328:275–8. Available from: http://dx.doi.org/10.1038/328275a0

376. Abdullaev IF, Bisaillon JM, Potier M, Gonzalez JC, Motiani RK, Trebak M. Stim1 and Orai1 mediate CRAC currents and store-operated calcium entry important for endothelial cell proliferation. *Circ. Res.* [Internet]. 2008 [cited 2013 Aug 19]; 103:1289–99. Available from: http://circres.ahajournals.org/content/103/11/1289.short

377. Sessa WC. eNOS at a glance. *J. Cell Sci.* [Internet]. 2004 [cited 2013 Aug 27]; 117:2427–9. Available from: http://jcs.biologists.org/content/117/12/2427.short

378. Chitaley K. Nitric Oxide Induces Dilation of Rat Aorta via Inhibition of Rho-Kinase Signaling. *Hypertension* [Internet]. 2002 [cited 2013 Sep 12]; 39:438–442. Available from: http://hyper.ahajournals.org/content/39/2/438.short

379. Wang Y-X, Halks-Miller M, Vergona R, Sullivan ME, Fitch R, Mallari C, Martin-McNulty B, da Cunha V, Freay A, Rubanyi GM, Kauser K. Increased aortic stiffness assessed by pulse wave velocity in apolipoprotein E-deficient mice. *Am J Physiol Hear. Circ Physiol* [Internet]. 2000 [cited 2013 Sep 13]; 278:H428–434. Available from: http://ajpheart.physiology.org/content/278/2/H428.full-text.pdf+html

380. Choi B-J, Prasad A, Gulati R, Best PJ, Lennon RJ, Barsness GW, Lerman LO, Lerman A. Coronary endothelial dysfunction in patients with early coronary artery disease is associated with the increase in intravascular lipid core plaque. *Eur. Heart J.* [Internet]. 2013 [cited 2013 Sep 13]; 34:2047–54. Available from: http://eurheartj.oxfordjournals.org/content/early/2013/04/06/eurheartj.eht132.short

381. Zeiher AM, Drexler H, Wollschlager H, Just H. Modulation of coronary vasomotor tone in humans. Progressive endothelial dysfunction with different early stages of coronary atherosclerosis. *Circulation* [Internet]. 1991 [cited 2013 Sep 13]; 83:391–401. Available from: http://circ.ahajournals.org/content/83/2/391.short

382. Deckert V, Lizard G, Duverger N, Athias A, Palleau V, Emmanuel F, Moisant M, Gambert P, Lallemant C, Lagrost L. Impairment of Endothelium-Dependent Arterial Relaxation By High-Fat Feeding in ApoE-Deficient Mice : Toward Normalization By Human ApoA-I Expression. *Circulation* [Internet]. 1999 [cited 2013 Sep 13]; 100:1230–1235. Available from: http://circ.ahajournals.org/content/100/11/1230.short

383. Shah V, Toruner M, Haddad F, Cadelina G, Papapetropoulos A, Choo K, Sessa WC, Groszmann RJ. Impaired endothelial nitric oxide synthase activity associated with enhanced caveolin binding in experimental cirrhosis in the rat. *Gastroenterology* [Internet]. 1999 [cited 2013 Aug 19]; 117:1222–1228. Available from: http://dx.doi.org/10.1016/S0016-5085(99)70408-7

384. Ignarro LJ. Endothelium-Derived Relaxing Factor Produced and Released from Artery and Vein is Nitric Oxide. *Proc. Natl. Acad. Sci.* [Internet]. 1987 [cited 2013 Sep 13]; 84:9265–9269. Available from: http://www.pnas.org/content/84/24/9265.short

385. Belton O, Byrne D, Kearney D, Leahy A, Fitzgerald DJ. Cyclooxygenase-1 and -2-Dependent Prostacyclin Formation in Patients With Atherosclerosis. *Circulation* [Internet]. 2000 [cited 2013 Sep 13]; 102:840–845. Available from: http://circ.ahajournals.org/content/102/8/840.short

386. McClelland S, Gawaz M, Kennerknecht E, Konrad CSI, Sauer S, Schuerzinger K, Massberg S, Fitzgerald DJ, Belton O. Contribution of cyclooxygenase-1 to thromboxane formation, platelet-vessel wall interactions and atherosclerosis in the ApoE null mouse. *Atherosclerosis* [Internet]. 2009 [cited 2013 Sep 13]; 202:84–91. Available from: http://dx.doi.org/10.1016/j.atherosclerosis.2008.04.016

387. Berkenboom G, Unger P, Fontaine J. Atherosclerosis and Responses of Human Isolated Coronary Arteries to Endothelium-Dependent and -Independent Vasodilators. *J. Cardiovasc. Pharmacol.* [Internet]. 1989; 14:S35–39. Available from: http://journals.lww.com/cardiovascularpharm/Fulltext/1989/06152/Atherosclerosis_and_Responses_of_Human_Isolated.7.aspx

388. Yang R, Powell-Braxton L, Ogaoawara AK, Dybdal N, Bunting S, Ohneda O, Jin H. Hypertension and Endothelial Dysfunction in Apolipoprotein E Knockout Mice. *Arterioscler. Thromb. Vasc. Biol.* [Internet]. 1999 [cited 2013 Jul 22]; 19:2762–2768. Available from: http://atvb.ahajournals.org/content/19/11/2762.short

389. Yamashina A, Tomiyama H, Arai T, Hirose K, Koji Y, Hirayama Y, Yamamoto Y, Hori S. Brachial-ankle pulse wave velocity as a marker of atherosclerotic vascular damage and cardiovascular risk. *Hypertens. Res.* [Internet]. 2003 [cited 2013 Sep 15]; 26:615–22. Available from: http://www.ncbi.nlm.nih.gov/pubmed/14567500

390. Blacher J, Asmar R, Djane S, London GM, Safar ME. Aortic Pulse Wave Velocity as a Marker of Cardiovascular Risk in Hypertensive Patients. *Hypertension* [Internet]. 1999 [cited 2013 Aug 12]; 33:1111–1117. Available from: http://hyper.ahajournals.org/content/33/5/1111.short

391. Carallo C, Fortunato L, de Franceschi MS, Irace C, Tripolino C, Cristofaro MG, Giudice M, Gnasso A. Periodontal disease and carotid atherosclerosis: Are hemodynamic forces a link? *Atherosclerosis* [Internet]. 2010; 213:263–267. Available from: http://www.sciencedirect.com/science/article/B6T12-50N38PS-1/2/860e71f824a4f752846be0e49c3355cd

392. Erridge C. The Roles of Pathogen-Associated Molecular Patterns in Atherosclerosis. *Trends Cardiovasc. Med.* [Internet]. 2008 [cited 2013 Nov 21]; 18:52–56. Available from: http://www.sciencedirect.com/science/article/pii/S1050173807002599

393. Michelsen KS, Wong MH, Shah PK, Zhang W, Yano J, Doherty TM, Akira S, Rajavashisth TB, Arditi M. Lack of Toll-like receptor 4 or myeloid differentiation factor 88 reduces atherosclerosis and alters plaque phenotype in mice deficient in apolipoprotein E. *Proc. Natl. Acad. Sci. U. S. A.* [Internet]. 2004 [cited 2013 Nov 21]; 101:10679–84. Available from: http://www.pubmedcentral.nih.gov/articlerender.fcgi?artid=489994&tool=pmcentrez&rendertype=abstract

394. Mullick AE, Tobias PS, Curtiss LK. Modulation of atherosclerosis in mice by Toll-like receptor 2. *J. Clin. Invest.* [Internet]. 2005 [cited 2013 Nov 21]; 115:3149–56. Available from: http://www.jci.org/articles/view/25482

395. Libby P, Egan D, Skarlatos S. Roles of Infectious Agents in Atherosclerosis and Restenosis: An Assessment of the Evidence and Need for Future Research. *Circulation* [Internet]. 1997 [cited 2013 Nov 21]; 96:4095–4103. Available from: http://circ.ahajournals.org/content/96/11/4095.short

396. Kol A, Bourcier T, Lichtman AH, Libby P. Chlamydial and human heat shock protein 60s activate human vascular endothelium, smooth muscle cells, and macrophages. *J. Clin. Invest.* [Internet]. 1999 [cited 2013 Nov 21]; 103:571–7. Available from: http://www.jci.org/articles/view/5310

397. Netea MG. Native LDL potentiate TNFalpha and IL-8 production by human mononuclear cells. *J. Lipid Res.* [Internet]. 2002 [cited 2013 Nov 21]; 43:1065–1071. Available from: http://www.jlr.org/content/43/7/1065.short

398. Berenson GS, Srinivasan SR, Bao W, Newman WP, Tracy RE, Wattigney WA. Association between multiple cardiovascular risk factors and atherosclerosis in children and young adults. The Bogalusa Heart Study. *N. Engl. J. Med.* [Internet]. 1998 [cited 2013 Sep 27]; 338:1650–6. Available from: http://www.ncbi.nlm.nih.gov/pubmed/9614255

399. Tangirala RK, Rubin EM, Palinski W. Quantitation of atherosclerosis in murine models: correlation between lesions in the aortic origin and in the entire aorta, and differences in the extent of lesions between sexes in LDL receptor-deficient and apolipoprotein E-deficient mice. *J. Lipid Res.* [Internet]. 1995; 36:2320–2328. Available from: http://www.jlr.org/cgi/content/abstract/36/11/2320

400. Tamashiro KLK, Wakayama T, Yamazaki Y, Akutsu H, Woods SC, Kondo S, Yanagimachi R, Sakai RR. Phenotype of cloned mice: development, behavior, and physiology. *Exp. Biol. Med. (Maywood).* [Internet]. 2003 [cited 2013 Sep 16]; 228:1193–200. Available from: http://ebm.sagepub.com/content/228/10/1193.full

401. Dallongeville J, Lussier-Cacan S, Davignon J. Modulation of plasma triglyceride levels by apoE phenotype: a meta- analysis. *J. Lipid Res.* [Internet]. 1992 [cited 2013 Sep 16]; 33:447–454. Available from: http://www.jlr.org/content/33/4/447.short

402. Palinski W, Ord VA, Plump AS, Breslow JL, Steinberg D, Witztum JL. ApoE-deficient mice are a model of lipoprotein oxidation in atherogenesis. Demonstration of oxidation-specific epitopes in lesions and high titers of autoantibodies to malondialdehyde-lysine in serum. *Arter. Thromb*. 1994; 14:605–616.

403. Keaney JF, Larson MG, Vasan RS, Wilson PWF, Lipinska I, Corey D, Massaro JM, Sutherland P, Vita JA, Benjamin EJ. Obesity and systemic oxidative stress: clinical correlates of oxidative stress in the Framingham Study. *Arterioscler. Thromb. Vasc. Biol.* [Internet]. 2003 [cited 2013 Sep 16]; 23:434–9. Available from: http://atvb.ahajournals.org/content/23/3/434.short

404. Erridge C, Attina T, Spickett CM, Webb DJ. A high-fat meal induces low-grade endotoxemia: evidence of a novel mechanism of postprandial inflammation. *Am J Clin Nutr* [Internet]. 2007 [cited 2013 Nov 21]; 86:1286–1292. Available from: http://ajcn.nutrition.org/content/86/5/1286.short

405. Lu C, Su L-Y, Lee RMKW, Gao Y-J. Mechanisms for perivascular adipose tissue-mediated potentiation of vascular contraction to perivascular neuronal stimulation: The role of adipocyte-derived angiotensin II. *Eur. J. Pharmacol.* [Internet]. 2010 [cited 2013 Sep 16]; 634:107–112. Available from: http://www.sciencedirect.com/science/article/pii/S0014299910000890

406. Sinisalo J, Paronen J, Mattila K., Syrjälä M, Alfthan G, Palosuo T, Nieminen M., Vaarala O. Relation of inflammation to vascular function in patients with coronary heart disease. *Atherosclerosis* [Internet]. 2000 [cited 2013 Sep 17]; 149:403–411. Available from: http://www.sciencedirect.com/science/article/pii/S0021915099003330

407. FitzGerald GA, Smith B, Pedersen AK, Brash AR. Increased prostacyclin biosynthesis in patients with severe atherosclerosis and platelet activation. *N. Engl. J. Med.* [Internet]. 1984 [cited 2013 Sep 18]; 310:1065–8. Available from: http://www.ncbi.nlm.nih.gov/pubmed/6231483

408. Ricciotti E, Yu Y, Grosser T, Fitzgerald GA. COX-2, the dominant source of prostacyclin. *Proc. Natl. Acad. Sci. U. S. A.* [Internet]. 2013 [cited 2013 Sep 18]; 110:E183. Available from: http://www.pubmedcentral.nih.gov/articlerender.fcgi?artid=3549068&tool=pmcentrez&rendertype=abstract

409. Nishi K. Oxidized LDL in Carotid Plaques and Plasma Associates With Plaque Instability. *Arterioscler. Thromb. Vasc. Biol.* [Internet]. 2002 [cited 2013 Sep 18]; 22:1649–1654. Available from: http://atvb.ahajournals.org/content/22/10/1649.short

410. Eligini S, Colli S, Basso F, Sironi L, Tremoli E. Oxidized Low Density Lipoprotein Suppresses Expression of Inducible Cyclooxygenase in Human Macrophages. *Arterioscler. Thromb. Vasc. Biol.* [Internet]. 1999 [cited 2013 Sep 18]; 19:1719–1725. Available from: http://atvb.ahajournals.org/content/19/7/1719.short

411. Guo Z, Su W, Allen S, Pang H, Daugherty A, Smart E, Gong MC. COX-2 up-regulation and vascular smooth muscle contractile hyperreactivity in spontaneous diabetic db/db mice. *Cardiovasc. Res.* [Internet]. 2005 [cited 2013 Sep 18]; 67:723–35. Available from: http://cardiovascres.oxfordjournals.org/content/67/4/723.short

412. Okon EB, Szado T, Laher I, McManus B, van Breemen C. Augmented contractile response of vascular smooth muscle in a diabetic mouse model. *J. Vasc. Res.* [Internet]. 2004 [cited 2013 Sep 18]; 40:520–30. Available from: http://www.karger.com/Article/FullText/75238

413. Qi W, Wei JX, Dorairaj I, Mahajan RP, Wilson VG. Evidence that a prostanoid produced by cyclo-oxygenase-2 enhances contractile responses of the porcine isolated coronary artery following exposure to lipopolysaccharide. *Br. J. Anaesth.* [Internet].

2007 [cited 2013 Sep 18]; 98:323–30. Available from: http://bja.oxfordjournals.org/content/98/3/323.short

414. Ji G. Stretch-induced Calcium Release in Smooth Muscle. *J. Gen. Physiol.* [Internet]. 2002 [cited 2013 Sep 18]; 119:533–544. Available from: http://jgp.rupress.org/content/119/6/533.full

415. Bootman MD, Lipp P, Berridge MJ. The organisation and functions of local Ca2+ signals. *J Cell Sci* [Internet]. 2001; 114:2213–2222. Available from: http://jcs.biologists.org/cgi/content/abstract/114/12/2213

416. Sasaki T, Gallacher DV. Extracellular ATP activates receptor-operated cation channels in mouse lacrimal acinar cells to promote calcium influx in the absence of phosphoinositide metabolism [Internet]. FEBS Lett. 1990 [cited 2013 Sep 20]; 264:130–134. Available from: http://www.sciencedirect.com/science/article/pii/001457939080782E

417. Thebault S, Roudbaraki M, Sydorenko V, Shuba Y, Lemonnier L, Slomianny C, Dewailly E, Bonnal J-L, Mauroy B, Skryma R, Prevarskaya N. Alpha1-adrenergic receptors activate Ca(2+)-permeable cationic channels in prostate cancer epithelial cells. *J. Clin. Invest.* [Internet]. 2003 [cited 2013 Sep 20]; 111:1691–701. Available from: http://www.jci.org/articles/view/16293

418. Thebault S, Flourakis M, Vanoverberghe K, Vandermoere F, Roudbaraki M, Lehen'kyi V, Slomianny C, Beck B, Mariot P, Bonnal J-L, Mauroy B, Shuba Y, Capiod T, Skryma R, Prevarskaya N. Differential role of transient receptor potential channels in Ca2+ entry and proliferation of prostate cancer epithelial cells. *Cancer Res.* [Internet]. 2006 [cited 2013 Sep 20]; 66:2038–47. Available from: http://cancerres.aacrjournals.org/content/66/4/2038.short

419. Yu Y, Sweeney M, Zhang S, Platoshyn O, Landsberg J, Rothman A, Yuan JX-J. PDGF stimulates pulmonary vascular smooth muscle cell proliferation by upregulating TRPC6 expression. *Am. J. Physiol. Cell Physiol.* [Internet]. 2003 [cited 2013 Sep 20]; 284:C316–30. Available from: http://ajpcell.physiology.org/content/284/2/C316